ParisTech
INSTITUT DES SCIENCES ET TECHNOLOGIES
PARIS INSTITUTE OF TECHNOLOGY

MINES ParisTech

Ecole doctorale n° 432: Sciences des Métiers de l'ingénieur

Doctorat ParisTech

T H È S E

pour obtenir le grade de docteur délivré par

l'École nationale supérieure des mines de Paris

Spécialité « Mathématique et Automatique »

présentée et soutenue publiquement par

Delphine BRESCH-PIETRI

le 17 décembre 2012

Commande robuste de systèmes à retard variable. Contributions théoriques et applications au contrôle moteur.

Directeur de thèse : **Nicolas PETIT**
Co-encadrement de la thèse : **Jonathan CHAUVIN**

Jury

M. Jean-Michel CORON, Professeur, Lab. JL. Lions, UPMC	Président
M. Miroslav KRSTIC, Professeur, UC San Diego	Rapporteur
M. Michel SORINE, Directeur de Recherche, INRIA	Rapporteur
M. Wilfrid PERRUQUETTI, Professeur, LAGIS, INRIA	Examinateur
M. Olivier SENAME, Professeur, ENSE3, GIPSA-Lab	Examinateur
M. Nicolas PETIT, Professeur, CAS, MINES ParisTech	Examinateur
M. Jonathan CHAUVIN, Docteur, IFPEn	Examinateur

MINES ParisTech
Centre Automatique et Systèmes, Unité Mathématiques et Systèmes
60 boulevard Saint-Michel, 75006 Paris

THÈSE

ParisTech
INSTITUT DES SCIENCES ET TECHNOLOGIES
PARIS INSTITUTE OF TECHNOLOGY

MINES ParisTech

ParisTech

PhD T H E S I S

to obtain the Doctor's degree from

École nationale supérieure des Mines de Paris

Specialty "Mathematics and Control"

defended in public by

Delphine BRESCH-PIETRI

December 17th, 2012

Robust control of variable time-delay systems. Theoretical contributions and applications to engine control.

Advisor: **Nicolas PETIT**
Supervisor: **Jonathan CHAUVIN**

Committee

M. Jean-Michel CORON, Professor, Lab. J-L. Lions, UPMC	Chair
M. Miroslav KRSTIC, Professor, UC San Diego	Referee
M. Michel SORINE, Directeur de Recherche, INRIA	Referee
M. Wilfrid PERRUQUETTI, Professor, LAGIS, INRIA	Examiner
M. Olivier SENAME, Professor, ENSE3, GIPSA-Lab	Examiner
M. Nicolas PETIT, Professor, CAS, MINES ParisTech	Examiner
M. Jonathan CHAUVIN, Doctor, IFPEn	Examiner

MINES ParisTech
Centre Automatique et Systèmes, Unité Mathématiques et Systèmes
60 boulevard Saint-Michel, 75006 Paris

THÈSE

Résumé

Cette thèse étudie la compensation robuste d'un retard de commande affectant un système dynamique. Pour répondre aux besoins du domaine applicatif du contrôle moteur, nous étudions d'un point de vue théorique des lois de contrôle par prédiction, dans les cas de retards incertains et de retards variables, et présentons des résultats de convergence asymptotique.

Dans une première partie, nous proposons une méthodologie générale d'adaptation du retard, à même de traiter également d'autres incertitudes par une analyse de Lyapunov-Krasovskii. Cette analyse est obtenue grâce à une technique d'ajout de dérivateur récemment proposée dans la littérature et exploitant une modélisation du retard sous forme d'une équation à paramètres distribués.

Dans une seconde partie, nous établissons des conditions sur les variations admissibles du retard assurant la stabilité du système boucle fermée. Nous nous intéressons tout particulièrement à une famille de retards dépendant de la commande (retard de transport). Des résultats de stabilité inspirés de l'ingalité Halanay sont utilisés pour formuler une condition de petit gain permettant une compensation robuste. Des exemples illustratifs ainsi que des résultats expérimentaux au banc moteur soulignent la compatibilité de ces lois de contrôle avec les impératifs du temps réel ainsi que les mérites de cette approche.

Mots-clefs

Systèmes à retard, systèmes à paramètres distribués, contrôle moteur, ajout de dérivateur, control adaptatif, analyse de Lyapunov, contrôle robuste, équations différentielles à retard

---

Abstract

This thesis addresses the general problem of robust compensation of input delays. Motivated by engine applications, we theoretically study prediction-based control laws for uncertain delays and time-varying delays. Results of asymptotic convergence are obtained.

In a first part, a general delay-adaptive scheme is proposed to handle uncertainties, through a Lyapunov-Krasovskii analysis induced by a backstepping transformation (applied to a transport equation) recently introduced in the literature.

In a second part, conditions to handle delay variability are established. A particular class of input-dependent delay is considered (transport). Halanay-like stability results serve to formulate a small-gain condition guaranteeing robust compensation. Illustrative examples and experimental results obtained on a test bench assess the implementability of the proposed control laws and highlight the merits of the approach.

Keywords

Time-delay systems, distributed parameter systems, engine control, backstepping, adaptive control, Lyapunov design, robust control, delay differential equations

Remerciements

En tout premier lieu, je souhaite remercier mes encadrants de thèse, Nicolas Petit et Jonathan Chauvin. Nicolas, pour l'intérêt et l'enthousiasme toujours incessants dont il fait preuve face aux idées et travaux qui lui sont soumis, pour m'avoir fait confiance, pour ne m'avoir jamais lâché la main, pour m'avoir conseillée sans cesse pendant ces trois (cinq ?) ans. Jonathan, pour m'avoir poussée devant les difficultés et l'expérimental, pour m'avoir forcée à ne pas refuser l'obstacle et pour s'être démené pour que la campagne d'essais au banc 23 voie le jour. Merci à tous les deux pour votre patience et vos encouragements, j'ai beaucoup appris pendant cette thèse et surtout à votre contact.

Je remercie également Gilles Cordes ainsi que le reste du département Contrôle, Signal et Système à IFP Energies nouvelles pour m'avoir accueillie pendant ces trois ans. Je vais regretter les échanges autour de la machine Lavazza. Un remerciement tout particulier à ceux qui ont été mes co-bureaux pendant la plus grande partie de ces trois ans, Wissam et Thomas. J'étais contente de vous retrouver le matin et de partager journée et travaux avec vous.

Un merci également à l'ensemble du Centre Automatique et Systèmes de MINES ParisTech, permanents et doctorants, qui constitue un lieu de travail et de stimulation intellectuelle inégalable. Je voudrais en particulier adresser tous mes remerciements à Laurent Praly pour l'appui et les conseils qu'il m'a accordés ces derniers mois et l'intérêt qu'il a toujours montré à mes travaux.

Je tiens à remercier Miroslav Krstic et Michel Sorine, qui m'ont fait l'honneur d'accepter d'être les rapporteurs de cette thèse. Merci également à Jean-Michel Coron, Olivier Séname et Wilfrid Perruquetti d'avoir participé à mon jury de soutenance. Vos questions et commentaires m'ont aidée à améliorer ce manuscrit et m'ont fourni de nouvelles pistes de travail.

Un merci aux amis qui ont été là, volontaires ou non, pour me remonter le moral et m'écouter au quotidien. Je pense à Pierrine, Flore, Guillaume, Florent, Lionel, Marianne, Anne-Lise...

Enfin, je voudrais remercier mes parents. Non pas pour cette thèse, qui doit leur paraître bien obscure et criblée de signes énigmatiques, mais pour m'avoir autant poussée, m'avoir donné le goût d'apprendre et l'envie de m'améliorer. C'est à vous que je dois d'être là et de pouvoir écrire ces lignes.

Contents

Chapter 1

Introduction : handling the variability of delays to unblock a performance bottleneck

The general problem under consideration in this thesis is the robust compensation of input delays in control systems. For decades, the occurrence of a delay has been identified as a source of performance losses of closed-loop control design. Indeed, to reach acceptable levels of robustness, it is necessary to decrease the feedback gains, that in turn lowers the tracking and disturbance rejection capabilities.

When the delay is sufficiently large so that it can not be neglected in the control synthesis, a natural question is its compensation. Ideally, delay compensation by a prediction of the future system state should allow, after a finite time, to obtain the same performance as for the corresponding delay-free system.

In this manuscript, we are interested into automotive Spark-Ignited engines, in which delays are ubiquitous. Indeed, flow transportations (fresh air, burned gas) and the numerous loops involved in engine architecture naturally result into transport delay. Furthermore, for cost reasons, only a few sensors are embedded in commercial-line engines, resulting into delayed measurement in addition to communication lags. Finally, delays also originate from the inherent distributed nature of post-treatment devices. All these delays are varying and uncertain.

Prediction-based techniques are difficult to apply in this context, because these methods are well known to provide little robustness to delay uncertainties and compensation is not easy to obtain for time-varying delays. However, the potential performance improvements motivates to address these issues.

In this thesis, two problems are tackled by *a robust compensation approach*. By robust compensation, we refer to a prediction-based control law, which does not exactly compensate the input delay but still provides asymptotic convergence. This thesis is then divided in two parts, pictured in Figure 1.1.

Part I. This part focuses on the case of constant but uncertain input delay. A general method to design a prediction-based control law aiming at robustly compensating the input delay is proposed. It follows and develops a recent overture to conduct a Lyapunov-Krasovskii analysis of prediction-based control. This method uses a transport partial differential equation representation of the delay, together with a backstepping transformation, and sets up a delay-adaptive scheme. The scheme is compliant with various other

components the control may need to handle system specificities. In addition, the proposed control strategy is shown to ensure closed-loop system stability for a large number of delay update laws.

The infinite-dimensional tools that are used in this general adaptive scheme are first presented in a dedicated introduction, before focusing, in Chapter 3, on plant parameter adaptation. In Chapter 4, we study admissible delay on-line update laws, before introducing an output feedback design in Chapter 5. In Chapter 6, we propose a disturbance rejection strategy. Each of these designs is illustrated by simulation examples of two different systems: one open-loop unstable plant and a stable but very slow plant. These two examples aim at highlighting the different merits of the proposed control strategy.

From a bird's eye view, the results stated in these parts can be summarized as follows: robust compensation is achieved provided that the estimation errors made while computing the state prediction are small enough. Besides, the delay estimate used for this prediction has to vary sufficiently slowly.

Finally, in Chapter 7, the versatility of the proposed approach is underlined by experimental results obtained on test-bench for the Fuel-to-Air Ratio regulation in Spark-Ignited engines. Various combinations of the proposed elements are declined, to illustrate the vast class of possible problems this methodology can handle.

Part II. This part focuses on the case of time-varying input delays. Particular attention is paid to a given model of transport delay, which implicitly defines the delay as the lower-bound of a positive integral. The relevance of this model is illustrated by numerous examples of flow processes, most of them related to engines. The practical interest of this model and its compliance with on line requirements are highlighted by experiments conducted on test bench for the estimation of the burned gas rate for Spark-Ignited engines.

This class of transport delay, together with the engine context elements presented earlier, motivate the need to design a delay compensation methodology for time-varying delays. Indeed, the existing tools require a prediction of the system state on a varying time interval, the length of which matches the future variations of the delay. When these variations are not known or not available, e.g. when the time dependency is related to an exogenous variable (flow, ...), this cannot be achieved.

In this thesis, we propose to use the current value of the delay as prediction horizon and show that robust compensation is achieved provided that the delay variations are sufficiently slow. Besides, in the case of an input-dependent delay defined by the aforementioned transport delay model, this requirement is ensured by a small gain condition on the feedback gain, which provides insight into the nature of the interconnection between the control and the delay variations. This result is obtained using delay differential equation stability results inspired from the Halanay inequality.

This part is organized as follows. In Chapter 8, the previously mentioned model of transport delay, relating the delay to past values of given variables, is presented. Various examples are given. Then, in Chapter 9, practical use of this model is proposed, to estimate the transport delay occurring for a low-pressure exhaust burned gas recirculation loop on a spark-ignited engine. The delay is analytically determined by the ideal gas low fed with measurements from temperature and pressure sensors located along the line. Extensive experimental results obtained on test bench stress the relevance of this model. In Chapter 10, robust compensation of a general time-varying delay is designed, requiring that the delay variations are sufficiently slow. This condition is then further studied in the

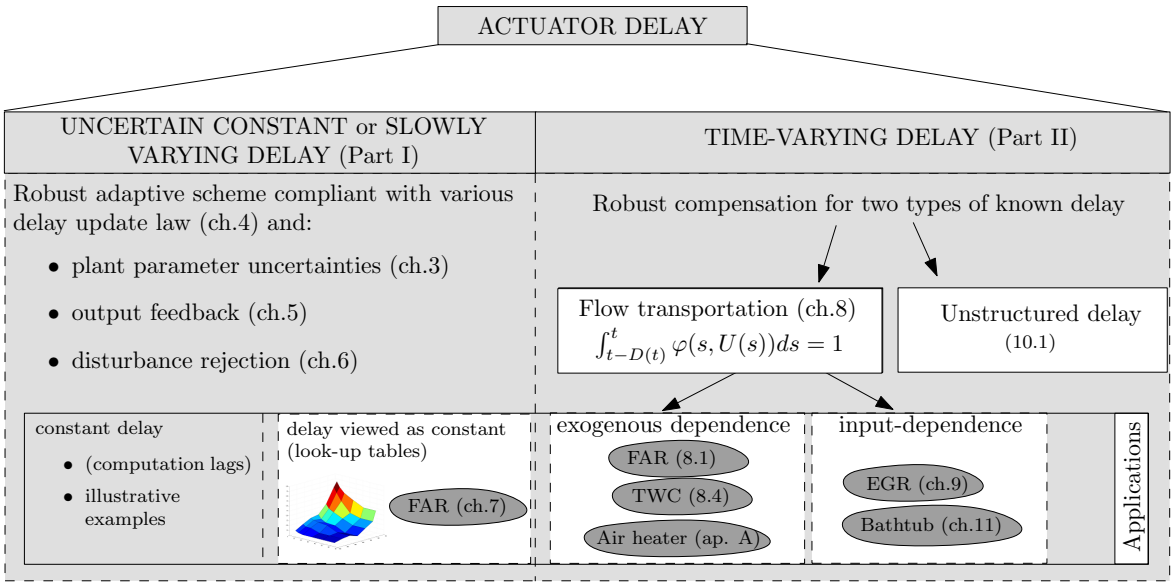

Figure 1.1: The problem addressed in this thesis.

particular case of input-dependent delay belonging to the considered transport delay class and finally related to a small gain condition, provided stabilization of the plant is still achieved. The merits of this result is then illustrated on a well-known time delay system, the temperature regulation of a shower (or bathtub). Chapter 11 briefly introduces the system under consideration and presents simulation results highlighting the benefits of the designed robust compensation approach for input-dependent input delay.

The works presented in this thesis have been the subject of the following publications:

- Journals

  1. D. Bresch-Pietri, J. Chauvin, and N. Petit, "*Adaptive control scheme for uncertain time-delay systems*", in Automatica, Vol. 48, Issue 8, pp.1536-1552, 2012

- Conference

  1. D. Bresch-Pietri, T. Leroy, J. Chauvin and N. Petit, "*Practical delay modeling of externally recirculated burned gas fraction for Spark-Ignited Engines*", to appear in the Proc. of the 11th Workshop on Time Delay Systems 2013
  2. D. Bresch-Pietri, T. Leroy, J. Chauvin and N. Petit, "*Contrôle de la recirculation de gaz brûlés pour un moteur essence suralimenté*", in Proc. of the Conférence Internationale Française d'Automatique 2012, Invited Session *Time-delay systems: applications and theoretical advances*
  3. D. Bresch-Pietri, J. Chauvin, and N. Petit,"*Invoking Halanay inequality to conclude on closed-loop stability of processes with input-varying delay*", in Proc. of the 10-th IFAC Workshop on Time Delay Systems 2012

4. D. Bresch-Pietri, J. Chauvin, and N. Petit,"*Prediction-based feedback control of a class of processes with input-varying delay*", in Proc. of the American Control Conference 2012
5. D. Bresch-Pietri, T. Leroy, J. Chauvin, and N. Petit,"*Prediction-based trajectory tracking of External Gas Recirculation for turbocharged SI engines*", in Proc. of the American Control Conference 2012
6. D. Bresch-Pietri, J. Chauvin, and N. Petit, "*Output feedback control of time delay systems with adaptation of delay estimate*", in Proc. of the 2011 IFAC World Congress
7. D. Bresch-Pietri, J. Chauvin, and N. Petit, "*Adaptive backstepping for uncertain systems with time-delay on-line update laws*", in Proc. of the American Control Conference 2011
8. D. Bresch-Pietri, J. Chauvin, and N. Petit, "*Adaptive backstepping controller for uncertain systems with unknown input time-Delay. Application to SI engines*", in Proc. of the 49th IEEE Conf. on Decision and Control 2010

Introduction : maîtriser les variations de retards pour pallier les pertes de performance

Cette thèse étudie la compensation robuste d'un retard de commande affectant un système dynamique. Depuis des décennies, l'apparition d'un retard a été diagnostiquée comme une cause majeure de dégradation des performances d'un système boucle fermée. En effet, pour obtenir un niveau satisfaisant de robustesse, il est alors nécessaire de diminuer l'amplitude des gains de rétroaction, ce qui, en conséquence, diminue également les performances en asservissement et en rejet de perturbations.

Quand le retard de commande est trop grand pour pouvoir être négligé lors du développement des lois de commande, on cherche tout naturellement à le compenser. Idéalement, cela permettrait, par une prédiction de l'état futur du système, d'obtenir, après un temps fini, des performances similaires à celles du système non-retardé correspondant.

Dans ce manuscrit, nous considérons des sous-systèmes de moteurs thermiques essence, dans lesquels les retards sont omniprésents. En effet, les flux de matière en jeu (gaz frais ou brûlés) et les nombreux circuits de canalisations présents sur un moteur thermique impliquent intrinsèquement un retard de transport. De plus, pour des raisons de coût, peu de capteurs sont embarqués sur des moteurs série ; en conséquence, les signaux mesurés sont souvent retardés, ce à quoi il faut ajouter le retard inhérent à la chaîne d'acquisition des données. Enfin, la nature distribuée des systèmes de post-traitement utilisés dans la ligne d'échappement génèrent également un retard de transport. Tous ces retards sont variables et incertains.

Les techniques usuelles de compensation par prédiction sont difficilement applicables dans un tel contexte, du fait de leur grande sensibilité aux erreurs d'estimation du retard et de la complexité de leur extension au retard variable. Cependant, du fait des gains de performances qu'elles peuvent susciter, il est utile d'étudier ces deux cas de figure et de fournir des solutions correspondantes.

Dans cette thèse, ces deux problèmes sont abordés par une approche de compensation robuste. Nous entendons par compensation robuste, une loi de contrôle exploitant une prédiction, ne compensant pas exactement le retard mais préservant la convergence asymptotique. Cette thèse s'articule donc naturellement en deux parties, comme représenté en Figure 1.2.

Part I. Cette partie aborde le cas d'un retard de commande constant, mais incertain. Une méthodologie générale de développement de lois de prédiction réalisant une compensation robuste d'un retard d'entrée y est proposée. Cette méthode poursuit et étend des travaux récents ayant permis une analyse de Lyapunov-Krasovskii des lois de contrôle

par prédiction. Ces travaux s'appuient sur la représentation du retard par une équation différentielle partielle de transport, ainsi que sur une transformation backstepping du contrôle distribué correspondant, et fondent les prémisses d'un schéma d'adaptation du retard. La méthodologie obtenue est compatible avec diverses autres difficultés que le système peut présenter et permet, de plus, l'utilisation d'une large gamme de lois d'adaptation du retard.

Les outils de dimension infinie utilisés dans cette méthodologie générale d'adaptation sont d'abord présentés individuellement en introduction, avant de détailler l'adaptation aux paramètres incertains du systèmes dans le Chapitre 3. Puis, dans le Chapitre 4, nous étudions les lois admissibles d'adaptation du retard, avant de nous concentrer sur la régulation de sortie dans le Chapitre 5. Dans le Chapter 6, nous proposons une stratégie de rejet de perturbations. Chaque loi de contrôle est illustrée par des simulations ; deux exemples de dynamique sont considérés, l'une instable en boucle ouverte et l'autre stable mais présentant un temps de réponse conséquent, pour souligner les différents mérites de notre approche.

D'une façon générale, les différents résultats présentés dans cette partie stipulent que le retard est bien compensé de façon robuste sous réserve que les erreurs d'estimation réalisées lors du calcul de la prédiction sont suffisamment faibles. De plus, les variations de l'estimation du retard utilisée lors de cette prédiction doivent être suffisamment lentes.

Enfin, dans le Chapitre 7, la polyvalence de notre approche est mise en exergue par des résultats expérimentaux obtenus sur banc moteur pour la régulation de la richesse sur moteur essence. Différentes combinaisons des éléments présentés précédemment sont déclinées, afin d'illustrer la vaste classe de problèmes que notre méthodologie permet de traiter.

Part II. Cette partie aborde le cas d'un retard variable dans le temps et accorde une attention particulière à une famille de retards de transport, pour laquelle le retard est modélisé sous forme de borne inférieure d'une équation intégrale implicite, d'intégrande positive. La validité de ce modèle est soulignée par de nombreux exemples de dynamique de flux, la plupart liés au domaine du contrôle moteur. L'intérêt pratique de ce modèle et sa compatibilité avec les exigences temps-réel sont illustrés par des essais réalisés au banc moteur pour l'estimation boucle ouverte du taux de gaz brûlés admission d'un moteur essence.

Cette famille de retards de transport, ainsi que les spécificités du domaine du contrôle moteur évoquées ci-dessus, expliquent que nous cherchions à développer une méthodologie de compensation pour un retard variable. En effet, les outils existants nécessitent une prédiction de l'état du système sur un horizon temporel variable, dont la longueur dépend des variations futures du retard. Lorsque ces variations ne sont pas connues ou pas obtensibles, par exemple lorsque le retard dépendent implicitement du temps comme fonction de variables exogènes (flux,...), cette longueur ne peut pas être déterminée.

Dans cette thèse, nous proposons d'utiliser la valeur courante du retard comme horizon de prédiction et prouvons que le retard est alors compensé de façon robuste pourvu que ses variations soient suffisamment lentes au cours du temps. De plus, dans le cas d'un retard dépendant de la commande et défini par l'équation intégrale de transport susmentionnée, nous montrons qu'une condition suffisante pour cela est une condition de petit gain portant sur le gain de rétroaction. Ce résultat est obtenu grâce à des propriétés de stabilité d'équations différentielles à retard, obtenues par analyse de la dépendance implicite entre commande et variations du retard.

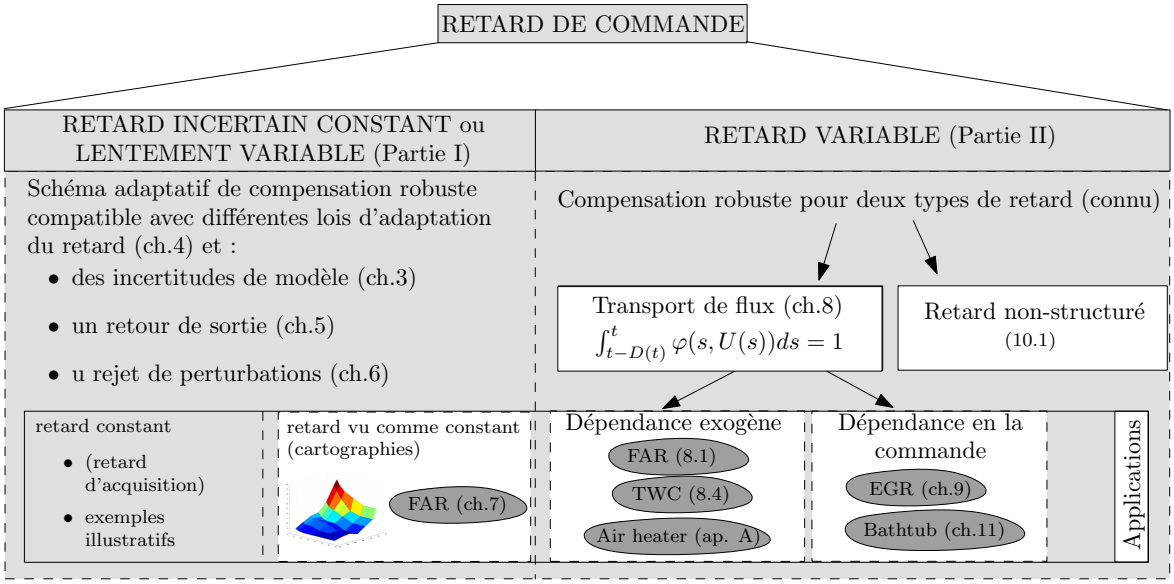

Figure 1.2: Le problème considéré dans cette thèse.

Cette partie du manuscrit est organisée comme suit. Le Chapitre 8 présente le modèle de retarde de transport évoqué ci-dessus, exprimant le retard en fonction de l'historique des commandes. Puis, dans le Chapitre 9, une utilisation pratique de ce modèle est exposée, afin d'estimer le retard de transport présent dans la dynamique d'un système de recirculation basse-pression de gaz brûlés pour moteur essence. Le retard est calculé analytiquement par l'intermédiaire de la loi des gaz parfaits et à l'aide de mesures ponctuelles de températures et pressions le long de la ligne admission. De nombreux essais sur banc moteur soulignent l'intérêt et la pertinence de notre modèle. Le chapitre 10 présente une approche de compensation robuste d'un retard variable, sous réserve que les variations de ce dernier soient suffisamment lentes. L'étude de cette condition est complétée dans le cas particulier d'un retard dépendant de la commande et appartenant à la famille de retard de transport considéré et conduit à une condition finale de petit gain, sous laquelle la stabilisation du système est assurée. Enfin, ce résultat est ensuite illustré sur un exemple classique des systèmes à retard, celui de la douche (ou du bain); le chapitre 11 présente brièvement ce système, puis les résultats de simulation obtenus qui soulignent les nombreux avantages en termes de performance de notre approche par compensation robuste pour retard dépendant de la commande.

Les travaux présentés dans ce manuscrit ont fait l'objet des publications suivantes :

- Journaux internationaux avec comité de lecture

  1. D. Bresch-Pietri, J. Chauvin, and N. Petit, "*Adaptive control scheme for uncertain time-delay systems*", in Automatica, Vol. 48, Issue 8, pp.1536-1552, 2012

- Conférences internationales avec comité de lecture

  1. D. Bresch-Pietri, T. Leroy, J. Chauvin and N. Petit, "*Practical delay modeling of externally recirculated burned gas fraction for Spark-Ignited Engines*", to

appear in the Proc. of the 11th Workshop on Time Delay Systems 2013

2. D. Bresch-Pietri, T. Leroy, J. Chauvin and N. Petit, "*Contrôle de la recirculation de gaz brûlés pour un moteur essence suralimenté*", in Proc. of the Conférence Internationale Française d'Automatique 2012, Invited Session *Time-delay systems: applications and theoretical advances*
3. D. Bresch-Pietri, J. Chauvin, and N. Petit,"*Invoking Halanay inequality to conclude on closed-loop stability of processes with input-varying delay*", in Proc. of the 10-th IFAC Workshop on Time Delay Systems 2012
4. D. Bresch-Pietri, J. Chauvin, and N. Petit,"*Prediction-based feedback control of a class of processes with input-varying delay*", in Proc. of the American Control Conference 2012
5. D. Bresch-Pietri, T. Leroy, J. Chauvin, and N. Petit,"*Prediction-based trajectory tracking of External Gas Recirculation for turbocharged SI engines*", in Proc. of the American Control Conference 2012
6. D. Bresch-Pietri, J. Chauvin, and N. Petit, "*Output feedback control of time delay systems with adaptation of delay estimate*", in Proc. of the 2011 IFAC World Congress
7. D. Bresch-Pietri, J. Chauvin, and N. Petit, "*Adaptive backstepping for uncertain systems with time-delay on-line update laws*", in Proc. of the American Control Conference 2011
8. D. Bresch-Pietri, J. Chauvin, and N. Petit, "*Adaptive backstepping controller for uncertain systems with unknown input time-Delay. Application to SI engines*", in Proc. of the 49th IEEE Conf. on Decision and Control 2010

‘

Chapter 2

A quick tour of state prediction for input delay systems

Chapitre 2 – Un rapide tour d'horizon des techniques de prédiction pour systèmes à entrée retardée. *Ce chapitre introduit brièvement les technique de contrôle utilisant une prédiction d'état et aborde leur sensibilité aux erreurs d'estimation du retard. Nous cherchons ici à donner des éléments de contexte sur le contrôle des systèmes à entrée retardée pour situer la contribution de cette thèse. Deux pans se dessinent clairement, l'un concernant un schéma adaptatif pour retard constant mais incertain et l'autre la compensation robuste d'un retard de commande variable. Enfin, ce chapitre contient une présentation des outils de dimension infinie récemment développés dans la littérature et utilisés dans ce manuscrit pour développer une analyse de Lyapunov-Krasovskii des lois de contrôle par prédiction considérées.*

Contents

Introduction

This first chapter contains a short description of state prediction control techniques and a discussion of their sensitivity to delay uncertainties. For sake of simplicity, we address only stabilization problems and leaves out open-loop and motion planning techniques. The subject under discussion here is well-established and widely described in the literature. The aim here is not to provide an exhaustive panorama of results but simply to introduce some background information on control of input delay systems and implementation considerations. These elements are necessary to situate the contribution of this thesis. For more details, interested readers are referred to recent monographs on this topic ([Zhong 06, Michiels 07, Krstic 09a, Watanabe 96]).

We first sketch the principles behind the method by gathering some early results published in the 1970s.

2.1 Compensation of a (known) constant input delay: Smith Predictor and its modifications

Consider a constant lag D that delays the input of a continuous linear time-invariant (LTI) dynamic system

$$\dot{X}(t) = AX(t) + BU(t - D) \tag{2.1}$$

The basic idea of state prediction is to *compensate* the time delay D by generating a control law that enables one to directly reason on the corresponding delay-free case. The prediction control law

$$U(t) = KX(t + D) \tag{2.2}$$

guarantees that, after D units of time, the closed-loop system simply writes without delay

$$\dot{X}(t) = (A + BK)X(t) \tag{2.3}$$

Thus, after a non-reducible time-lag of D, the transient *performances do not depend anymore on the delay*, which is compensated by the prediction.

Illustrative example

To emphasize the merits of this technique, consider the scalar open-loop unstable plant $\dot{x} = x + u(t - D)$. The transient performance of the previous control law is compared to a simple proportional controller using the same feedback gain in Figure 2.1. The system is not initially at equilibrium, with $x(0) = 1$ and, for $-D \leq t \leq 0$, $u(t) = 1$. This results into an initial state increase.

When the delay is significantly smaller than the system time constant, the two controllers act similarly (see Figure 2.1(a) with $D = 0.05$ s). However, the benefits of the prediction-based control law become visible when the delay is increased (see Figure 2.1(b) with $D = 0.5$ s), as the proportional controller performance substantially worsen. In particular, one can note that the exponential decrease obtained after D units of time with

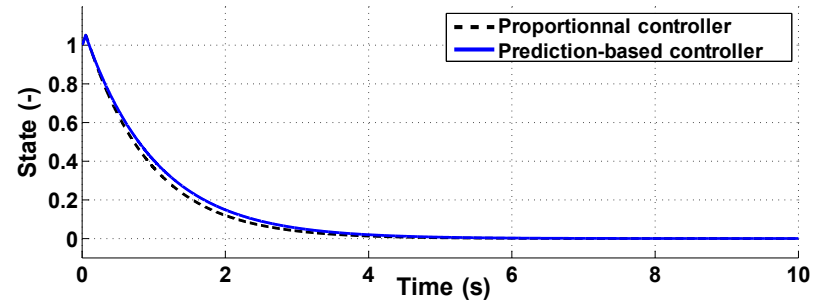

(a) With a constant input delay $D = 0.05$ s

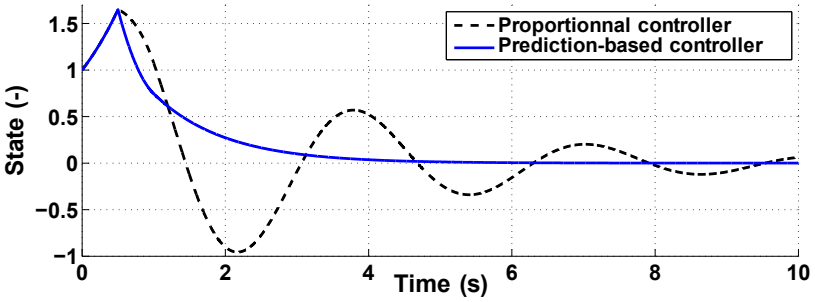

(b) With a constant input delay $D = 0.5$ s

Figure 2.1: Simulation results of the closed loop system consisting in the scalar plant $\dot{x} = x + u(t - D)$ and, respectively, a proportional controller or a prediction-based controller. The two controllers employ the same feedback gain $K = -2$. Two scenarii with different delays are considered.

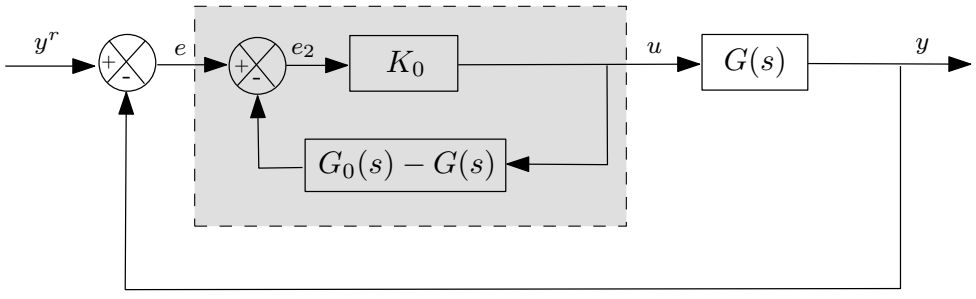

Figure 2.2: The Smith Predictor controller (in the gray box) for a stable transfer function $G(s) = G_0(s)e^{-Ds}$ with G_0 rational. The internal loop of the controller generates a signal $e_2 = y^r - G_0(s)u$ where $G_0(s)u$ is the output of the delay-free system, i.e. the prediction of the output over a time horizon D. The actual Smith Predictor control law is then $u = K_0 e_2 = K_0(y^r - y(t + D))$ where $-K_0$ is a stabilizing gain for the delay-free system.

the prediction-based controller has the exact same rate in both cases. This is because the performance resulting from the delay compensation (2.3) are, by construction, delay-independent.

The prediction control method was first introduced by O. J. Smith in 1957 in the frequency-domain for Single-Input-Single-Output (SISO) and open-loop stable systems [Smith 57], [Smith 59]. The Smith Predictor originally proposed[1] is pictured in Figure 2.2. The corresponding state-space extension described above was only conceived two decades later, almost simultaneously, by Manitius and Olbrot [Manitius 79] and Kwon and Pearson [Kwon 80] under the name of Finite Spectrum Assignment (FSA)[2] and by Artstein [Artstein 82] as Model Reduction.

2.1.1 Finite spectrum assignment or model reduction

By definition, a delayed differential equation has an infinite spectrum [Hale 71]. The name FSA highlights the fact that using a state prediction leads to a closed-loop system with a finite spectrum and that this spectrum can be freely assigned. On the contrary, a linear state feedback controller $u(t) = Kx(t)$ would result into an infinite spectrum as the closed-loop dynamics would be $\dot{X} = AX(t) + BX(t-D)$. This is the meaning of the following theorem [3].

Theorem 1. *(FSA, Manitius and Olbrot [1979]) The spectrum of the closed-loop system*

$$\begin{aligned} \dot{X}(t) =& AX(t) + BU(t-D) \\ U(t) =& KX(t+D) = K\left[e^{AD}X(t) + \int_t^{t+D} e^{A(t+D-s)}BU(s-D)ds\right] \end{aligned} \tag{2.4}$$

coincides with the spectrum of the matrix $A + BK$. Moreover, assuming controllability (resp. stabilizability) of the pair (A, B) the spectrum of the above closed-loop system can be placed at any preassigned self-conjugate set of n points in the complex plan (resp. the unstable eigenvalues of A can be arbitrarily shifted) by a suitable choice of the matrix K.

Equivalently, and more closely to the Smith predictor approach, one can understand this result by directly considering the predicted system state at time $t + D$

$$P(t) = X(t+D) = e^{AD}X(t) + \int_t^{t+D} e^{A(t+D-s)}BU(s-D)ds$$

which is governed by the following *free-of-delay* dynamics

$$\dot{P}(t) = AP(t) + BU(t)$$

This transformation is known as *model reduction*. It is straightforward to compute a classical state feedback, provided that the pair (A, B) is controllable, in the form

$$U(t) = KP(t) \tag{2.5}$$

[1] Several other versions exist, e.g. to improve performance in case of model mismatch or to reject disturbances.

[2] The results presented in [Manitius 79] deal with a slightly different type of system of type $\dot{x}(t) = Ax(t) + B_0u(t) + B_1u(t-D)$. For sake of clarity, we present here a modified version of these results for $B_0 = 0$.

[3] Similar results were obtained for the more general class of distributed delays, which input delays are a particular class of.

The strong similarities between the two design frameworks (FSA and model reduction) explain why the two approaches are classically presented together, often even without any distinction. However, the underlying principles are radically different:

- FSA is inherently an *eigenvalue-based approach* that focuses on the characteristic equation of the closed-loop system.
- model reduction is a functional analysis result which uses the operator

$$\mathcal{L} : (X_t, U_t) \in \mathcal{C}^0([-D, 0])^2 \mapsto e^{AD} X_t(0) + \int_{-D}^{0} e^{-As} B U_t(s) ds$$

  where $X_t(.)$ and $U_t(.)$ are functions defined on the interval $[-D, 0]$ by $X_t(s) = X(t + s)$ and $U_t(s) = U(t + s)$ for $s \in [-D, 0]$. Equivalence between the original system and the predicted one is based on the properties of this mapping to ensure stabilization for the original system.

From these elements, a significant number of improvements and modifications were proposed and resulted in various control laws that are called *prediction-based control laws*. Interested readers are referred to [Palmor 96] for examples.

We now focus on the resulting control law (2.4) or, equivalently, (2.5).

2.1.2 A distributed control law

The feedback law (2.4) can be interpreted as the result of the variation-of-constants formula, starting at time t, over a time-window of length D. For LTI systems, this prediction can be made explicitly.

At first sight, choice of the prediction-based control law $u(t) = Kx(t+D)$ might seem non-implementable. However, a simple change of time leads to

$$\begin{aligned} U(t) =& K \left[e^{AD} X(t) + \int_{t}^{t+D} e^{A(t+D-s)} B U(s - D) ds \right] \\ =& K \left[e^{AD} X(t) + \int_{t-D}^{t} e^{A(t-s)} B U(s) ds \right] \end{aligned} \tag{2.6}$$

which is actually an implementable feedback law, as only past values of the input are involved in the calculation of the integral. To be more precise, this last expression defines a Volterra integral equation of the second kind (see [Polyanin 07]) of kernel $K(t - s) = \exp^{A(t-s)} B$ and the feedback law is properly defined by this implicit relation.

Owing to the integral term $\int_{t-D}^{t} e^{A(t-s)} B U(s) ds$, which can be viewed as a distributed delay, this input is infinite-dimensional. As a result, the dimension of the spectrum of the closed-loop system has only been reduced at the expense of the dimension of the definition set of the input. This integral term is also the main source of practical difficulties.

Two issues arise when considering the implementation of this control law and often lead to a performance bottleneck.

First, exact knowledge of the delay D is required. This issue has been highlighted since the seminal work of Smith and is one of the essential purposes of this thesis. We detail this below.

Second, discretization of the integral in (2.6) to implement the feedback law may yield to instability. such integral is widely used throughout this thesis, so we provide some further details regarding this issue.

Implementation of the integral

Use of a quadratic rule to approximate the integral yields the discrete form

$$U(t) = K\left[e^{AD}X(t) + \sum_{i\in\mathcal{I}_n} h_i e^{A\theta_i} BU(t-\theta_i)\right] \tag{2.7}$$

where $\mathcal{I}_n$ is a finite sequence of sets of length (h_i) mapping the interval $[-D, 0]$ and the scalars θ_i depend on the integration rule selected. The effect of the implementation (2.7) on stability was fist investigated by Van Assche and co-workers in [Van Assche 99]. Interestingly and non-intuitively, they have shown that the closed-loop system consisting of (2.1) and the discretized control law (2.7) may be unstable for *arbitrarily large values of* n.

This striking fact was analyzed using eigenvalue considerations. When the theoretical control law (2.4) is replaced by the approximated form (2.7), the finite spectrum property is lost. Indeed, the corresponding closed-loop system is then a point-wise delayed differential equation that potentially possesses an infinite number of characteristic roots, like any time-delay system. While improving the approximation accuracy (by making n larger), some of the characteristic roots tend to those of the exact closed-loop system, while others tend to infinity. Depending on the discretization method, unstable characteristic roots may appear and some of them may tend to infinity while staying on the right half-plane. If this is the case, instability occurs even for n arbitrarily large.

Van Assche et al. pointed out this mechanism on an example [Van Assche 99]. By comparing three classical constant-step integration methods, the authors stressed the importance of the choice of the integration rule.

Alternatively, a necessary and sufficient stability condition that does not depend on the discrete integration scheme was provided by Michiels et al. [Michiels 03]. Yet, this condition is only obtained at the expense of severe restrictions on the feasible feedback gain which involve the value of the delay. As a result, in [Mondié 03], a modification of the control law was proposed, by adding a low-pass filter to relax this condition. To avoid numerical instabilities, particular attention of these considerations is required when using a prediction-based feedback approach. In this thesis, following the comforting results presented in [Van Assche 99], a trapezoidal approximation is systematically used to implement the proposed control strategies.

2.1.3 Sensitivity to delay uncertainties

A well-known fact about prediction-based techniques is that they may suffer from being sensitive to delay mismatch (and, to a lesser extent, to plant parameters uncertainties) [Palmor 80]. Numerous works investigated the robustness of predictor-based controllers to such mismatch. Most were devoted to the derivation of an upper-bound of admissible delay mismatch preserving stability, based on analysis in the frequency-domain [Smith 59], [Owens 82] [Adam 00], [Mondié 01], [Niculescu 01], [Zhong 06].

The main idea of these methods can be summarized as follows. Consider a system with n states and m inputs. First, define a mismatch Δ between the actual delay D and

the one used for prediction $D_0 = D - \Delta$. The control law can be written as

$$U(t) = K\left[e^{A(D-\Delta)}X(t) + \int_{t-D+\Delta}^{t} e^{A(t-\xi)}BU(\xi)\right]d\xi$$

and is described in the frequency domain by

$$[I_m - K(sI - A)^{-1}(I - e^{-(D-\Delta)(sI-A)})B]U(s) = Ke^{A(D-\Delta)}X(s)$$

After taking the Laplace transform of (2.1), the closed-loop characteristic matrix can be expressed as

$$M_{char} = \begin{pmatrix} sI - A & -Be^{-Ds} \\ -Ke^{A(D-\Delta)} & I_m - K(sI - A)^{-1}(I - e^{-(D-\Delta)(sI-A)})B \end{pmatrix}$$

It is then possible to study the resulting characteristic roots and to determine a maximum admissible value of the error Δ, depending on the feedback gain K and on the system dynamics.

However, this approach cannot be naturally extended when the delay estimate is varying over time (e.g. in an attempt to improve the prediction capabilities), because no frequency-domain tool can capture the variations of $D_0(t)$ in a refined manner.

2.1.4 Extension to a broader class of systems

Predictor strategies can be extended to more general dynamics than the relatively simple but tutorial plant (2.1). We describe these briefly.

Linear time-varying (LTV) systems

By introducing the transition matrix $\Phi(t, s)$ of the homogeneous LTV dynamics $\dot{X}(t) = A(t)X$

$$\frac{\partial \Phi}{\partial t}(t, s) = A(t)\Phi(t, s)\,, \quad \phi(t, t) = I$$

the prediction-based control law becomes

$$U(t) = K\left[\Phi(t, t + D)X(t) + \int_{t}^{t+D} \Phi(s, t + D)B(s)U(s - D)ds\right]$$

Even if this expression is not explicit, it is implementable provided that the values of B over the time-interval $[t, t + D]$ are known. More details can be found in [Artstein 82].

Nonlinear systems

Non-linear versions of the original Smith predictors were developed quite early for processes [Kravaris 89], [Henson 94]. However, generalization of prediction techniques to more general classes of systems was only proposed recently [Krstic 09a]. The class of nonlinear systems considered is the one of forward complete systems (i.e. non-linear systems that do not escape in finite time for any finite control law or initial conditions [Angeli 99]) of the form

$$\dot{X}(t) = f(X(t), U(t - D))$$

for which a continuous control law $\kappa(X)$ is known such that the delay-free system $\dot{X} = f(X, \kappa(X))$ is globally asymptotically stable. Compensation of the delay is then achieved via the prediction-based control law

$$\begin{aligned} U(t) =& \kappa(P(t)) \\ P(t) =& X(0) + \int_t^{t+D} f(X(s), U(s-D))ds = X(0) + \int_{t-D}^{t} f(P(s), U(s))ds \end{aligned}$$

Again, this control law is implicit but computable.

2.2 Compensation of a time-varying delay

Extension of the prediction to the case of time-varying delays is rather intuitive. The key is to calculate the prediction over a non-constant time window, accounting for future variations of the delay. These elements were introduced by Nihtila [Nihtila 91], who considered the following linear system

$$\dot{X}(t) = AX(t) + Bu(\eta(t)), \quad \eta(t) = t - D(t) \tag{2.8}$$

For mathematical well-posedness, the time-varying delay is assumed to satisfy the following properties:

- the delay function D is differentiable
- the delay D is bounded: $0 \leq D(t) \leq D_{max}, t \geq 0$ with $D_{max} > 0$.
- the time-derivative of D is strictly upper-bounded by one, $\dot{D}(t) \leq 1 - \delta, \quad \delta > 0$

This last property ensures that the time derivative of the function η is strictly positive, as $\dot{\eta} = 1 - \dot{D}$. Consequently, the causality of system (2.8) is guaranteed: as η is a strictly increasing function, there is no flashback in the input history. Furthermore, under this assumption, the function η is invertible and one can consider $r(t) = \eta^{-1}(t)$.

To obtain a delay-free closed loop system, prediction techniques aim at obtaining $U(\eta(t)) = KX(t)$, which naturally results here into the control law

$$U(t) = KX(r(t)) \tag{2.9}$$

which can be reformulated as

$$\begin{aligned} U(t) =& K\left[e^{A(r(t)-t)}X(t) + \int_t^{r(t)} e^{A(r(t)-s)}BU(\eta(s))ds\right] \\ =& K\left[e^{A(r(t)-t)}X(t) + \int_{t-D(t)}^{t} e^{A(r(t)-r(s))}BU(s)\frac{ds}{1-\dot{D}(r(s))}\right] \end{aligned} \tag{2.10}$$

Remark 1. *To illustrate the discussion above, consider the case of a constant delay $D > 0$. The inverse of the function η is then simply $r(t) = 1 + D$, which yields $\dot{r} = 0$. Thus,* (2.10) *can be rewritten as* (2.6)*.*

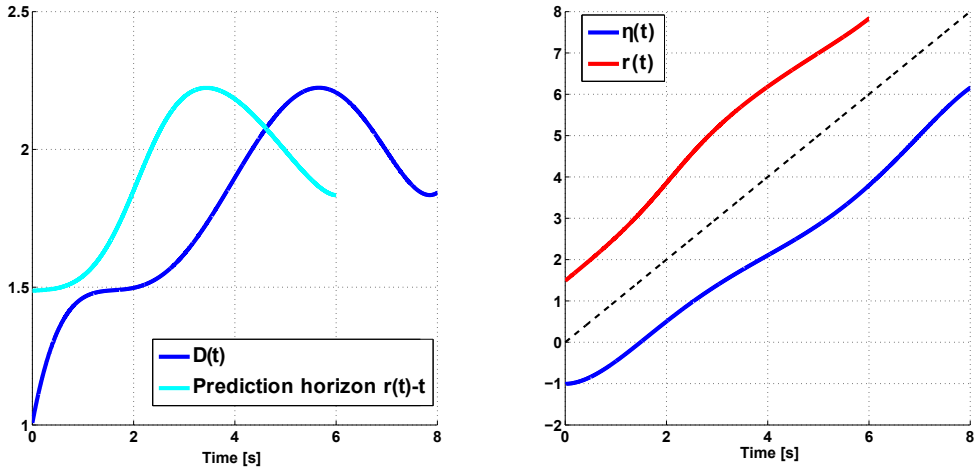

Figure 2.3: Example of the delay evolution function (in blue, on the left-hand side figure) and of the corresponding delay-related functions. In the right-hand panel, the delayed function $\eta = t - D(t)$ is plotted along with its inverse $r = \eta^{-1}$. As this inverse is computed from the original function, it is not available at all times.

Remark 2. *Again, for the sake of clarity, consider the feedback law* $U(t) = KX(t+D(t))$ *that one might be tempted to apply by directly following the approach of the constant delay case. Then the closed-loop systems can be rewritten as*

$$\dot{X}(t) = AX(t) + BU(t - D(t)) = AX(t) + BKX(t \underbrace{-D(t) + D(t - D(t))}_{\neq 0 \text{ in general}})$$

The appearance of the term $D(t) - D(t - D(t))$ *highlights the fact that the delay has changed between the time the input was computed,* $t - D(t)$*, and the time it reaches the system,* t*. As a result, the future variations of the delay have to be taken into account to compensate the delay.*

The various elements presented above are summarized in Figure 2.3 for a given delay variation.

One point of crucial importance, in particular for implementation, is the calculation of $r(t)$. This involves future values of the delay, which may not be available.

Witrant proposed a methodology to compute this horizon when a model of the delay is available [Witrant 05] and Bekiaris-Liberis et al. proposed another approach for state-dependent delay with joint convergence analysis [Bekiaris-Liberis 12].

2.3 Open questions related to input delay systems and compensation

As a summary of the elements presented above, one can notice the importance of the following issues.

1. for constant input delays : the delay mismatches have been identified has a major source of performance losses. Even if operational calculus methods exist to evaluate the maximal admissible mismatch preserving stability, *no result is available today on asymptotic stabilization using (time-varying) delay update laws used in prediction-based feedbacks*. Second, even if several works considered the on-line identification of either the delay or the parameters, *simultaneous adaptation of delay and plant parameters remains to be done*.

2. for time-varying input delays : exact compensation of time-varying delay requires to anticipate the future variations of the delay, which can only be performed when delay time-variations are known. *The case of unknown (even if structured) delay variations remains to be addressed*. Second, it is also worth noticing that delay compensation does not naturally extend to the case of input-dependent delay. This case arises in many transport phenomena, but has never been studied theoretically. Therefore, *robust compensation of input-varying input delay is an open problem*.

These are the problems this manuscript focuses on. A large part of our work relies on an overture that was recently proposed to design a systematic Lyapunov methodology for input delay system. We now describe these tools.

2.4 Transport representation and backstepping approach

Recently, in the case of a single input (i.e. U scalar), Krstic interpreted (2.6) as the result of a backstepping transformation that allows one to use systematic Lyapunov tools to analyze the stability of input delay systems [Krstic 08a].

Let us introduce a transport representation of the delay phenomenon by defining a distributed input $u(x,t) = U(t + D(x-1))$ for $x \in [0,1]$. This actuator satisfies the following partial differential equation (PDE)

$$\left\{ \begin{array}{rcl} Du_t(x,t) & = & u_x(x,t) \\ u(1,t) & = & U(t) \\ u(0,t) & = & U(t-D) \end{array} \right. \tag{2.11}$$

This convective/first-order hyperbolic PDE is simply a propagation equation with a speed $1/D$, having boundary condition $U(t)$ at $x = 1$. It is represented in Figure 2.4. With this formalism, the LTI system (2.1) can be expressed as

$$\left\{ \begin{array}{rcl} \dot{X}(t) & = & AX(t) + Bu(0,t) \\ Du_t(x,t) & = & u_x(x,t) \\ u(1,t) & = & U(t) \end{array} \right. \tag{2.12}$$

(2.12) represents an ordinary differential equation (ODE) cascaded with a PDE driven by the input U at its boundary. When the boundary $U(t)$ is chosen as the stabilizing prediction-based control law (2.6), this coupling is stable, and even exponentially stable after a finite-time (D units of time).

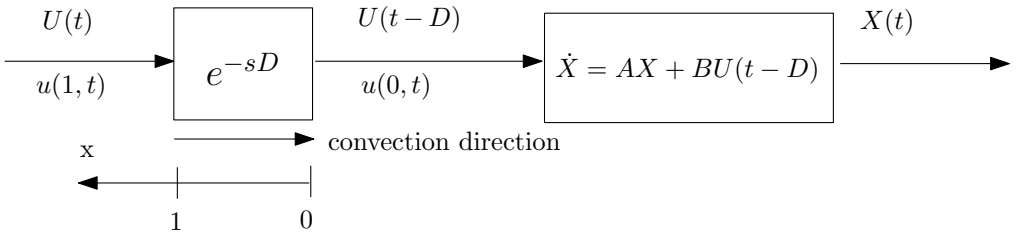

Figure 2.4: Representation of the plant with a transport equation accounting for the delay.

2.4.1 Backstepping transformation

To emphasize the exponential stability resulting from delay compensation, one may choose to modify the distributed input and to design a transformed actuator $w(.,t)$ satisfying the target system

$$\left\{\begin{array}{rcl} \dot{X}(t) &=& (A+BK)X(t)+Bw(0,t) \\ Dw_t(x,t) &=& w_x(x,t) \\ w(1,t) &=& 0 \end{array}\right. \tag{2.13}$$

Indeed, if such a transformation can be performed, one can observe that the transformed actuator value is zero in finite time and, after D units of time, exponential convergence of the plant is ensured by the nominal design (i.e. the Hurwitz matrix $A+BK$).

Following this idea, a natural modified distributed actuator, which satisfies the same transport PDE with propagation speed $1/D$, is

$$\begin{aligned} w(x,t) =& u(x,t) - KX(t+Dx) \\ =& u(x,t) - Ke^{ADx}X(t) - K\int_t^{t+Dx} e^{A(t+Dx-s)}BU(s-D)ds \\ =& u(x,t) - Ke^{ADx}X(t) - K\int_0^x e^{AD(x-y)}Bu(y,t)dy \end{aligned} \tag{2.14}$$

Then, in particular, the boundary condition of (2.13) can be used to obtain the original control law generating this delay compensation, i.e.

$$U(t) = u(1,t) = w(1,t) + KX(t+D) = KX(t+D)$$

which is indeed the prediction-based law (2.2). Due to the boundary condition, one can now complete a corresponding Lyapunov analysis, which, so far, had never been designed for prediction-based control laws[4].

2.4.2 Lyapunov-Krasovskii analysis

To illustrate the last point, consider the Lyapunov-Krasovskii functional

$$\Gamma(t) = X(t)^TPX(t) + b\int_{t-D}^t U(s)^2ds = X(t)^TPX(t) + bD\int_0^1 u(s)^2ds$$

[4]This is not the case for state delay systems or memoryless proportional controllers that may be used for input delays (in a robustness spirit in the case of small delay), see [Malisoff 09].

which may be shown, using (2.14), to be equivalent to

$$V(t) = X(t)^T P X(t) + bD \int_0^1 (1+x) w(x,t)^2 dx$$

Taking a time derivative of the last functional and using (2.13) jointly with integration by parts, one obtains

$$\begin{aligned}
\dot{V}(t) =& - X(t)^T Q X(t) + 2X(t)^T PBw(0,t) + 2b \int_0^1 (1+x) w(x,t) w_x(x,t) dx \\
=& - X(t)^T Q X(t) + 2X(t)^T PBw(0,t) + \left[b(1+x) w(x,t)^2 \right]_0^1 - b \int_0^1 w(x,t)^2 dx \\
\leq& - \frac{\lambda_{min}(Q)}{2} |X(t)|^2 - \left(b - \frac{2}{\lambda_{min}(Q)} |PB|^2 \right) w(0,t)^2 - b \left\| w(t) \right\|^2 \\
\leq& - \min \left\{ \frac{\lambda_{min}(Q)}{2}, b \right\} \left(|X(t)|^2 + \left\| w(t) \right\|^2 \right)
\end{aligned}$$

by choosing $b \geq \frac{2}{\lambda_{min}(Q)} |PB|^2$. Successive use of the equivalence between V and $|\tilde{X}|^2 + \|w(t)\|^2$ and between V and Γ gives the existence of strictly positive constants R and ρ such that

$$\forall t \geq 0 \, , \Gamma(t) \leq R \Gamma(0) e^{-\rho t}$$

Comparing this approach to the ones presented in Section 2.1, this last methodology only provides an alternative proof of stabilization of (2.1) while using a predictor-based control. Nevertheless, this technique presents two major advantages:

- the transport PDE characterizing the distributed input $u(x,t)$ introduces a linear parametrization of the delay, which is compliant with adaptive control design as highlighted in [Ioannou 96].
- the transformed state of the actuator $w(x,t)$ is designed to fulfill the boundary condition $w(1,t) = 0$, which is of particular interest in Lyapunov analysis as it represents a stabilizing effect on a diffusion phenomenon. Consequently, this transport PDE representation of the delay, reformulated with a backstepping transformation, equips the designer with a tool for Lyapunov-Krasovskii analysis compliant with a delay-adaptation framework.

2.5 Organization of the thesis/ Presentation of the contributions

The tools presented above are the main ones used in this thesis to address the open problems listed in Section 2.3. Following this list, this manuscript is naturally divided in two parts.

Part I focuses on the case of a *constant but uncertain input delay*. Exploiting the certainty equivalence principle, the backstepping tools introduced earlier are employed to propose a generic adaptive framework for input delay systems. This approach is then illustrated by experimental results obtained on test-bench for the Fuel-to-Air Ratio regulation in Spark-Ignited engines.

Part II focuses on the case of *time-varying input delays* and, among them, on *an input-dependent input delay*. Robust compensation of these two classes is addressed by combining the previous Lyapunov tools with Delay Differential Equation (DDE) stability results. Special care is taken for a class of transport delays, often involved in flow processes, modeled by an implicit integral. Relevance of this model is illustrated by experiments conducted at test bench on an Exhaust Gas Recirculation system for Spark-Ignited engines. The strategy is then illustrated on a well-known delay-system case study, the temperature regulation of a shower/bathtub.

By *robust* compensation, we refer to a prediction-based control law, inspired from the elements presented above in this chapter, which does not exactly compensate the input delay but still provides asymptotic convergence of the plant considered. The reasons for not compensating exactly the delay are either delay uncertainties or delay variations.

Part I

Adaptive control scheme for uncertain systems with constant input delay

Introduction

In this part, the general problem of equilibrium regulation of (potentially unstable) linear systems with an uncertain input delay is addressed. To fulfill this objective, the new predictor-based technique proposed lately in [Krstic 08a] and [Krstic 08b] and described in Chapter 2 is used.

Here, this methodology is pursued for an uncertain delay and an implementable form of the resulting controller is developed, that potentially uses an on-line delay estimate. In the spirit of [Bresch-Pietri 10], we use a backstepping boundary control corresponding to a transport PDE with an estimated propagation speed accounting for delay estimation. This transformation still allows to use the systematic Lyapunov tools presented previously, to design robust stabilization and adaptation.

Different classical control issues are considered in this part, jointly with delay uncertainty. Each increases the complexity of the controller design. For pedagogical reasons, these issues are addressed separately, in dedicated chapters (Chapters 3–6) in which the merits of each corresponding robust input delay compensation are illustrated by simulations results. Of course, various combinations of the elements presented in this part are possible. Examples of practical use of the proposed general methodology are then given on an (Spark Ignited) engine control problem, and illustrated experimentally.

Problem Statement

In this part of the thesis, we consider a potentially open-loop unstable LTI input delay system of the form

$$\begin{cases} \dot{X}(t) = A(\theta)X(t) + B(\theta)[U(t-D) + d] \\ Y(t) = CX(t) \end{cases} \tag{2.15}$$

where $Y \in \mathbb{R}^m$, $X \in \mathbb{R}^n$ and U is a scalar input. $D > 0$ is an unknown (potentially long) constant delay, d is a constant input disturbance and the system matrix $A(\theta)$ and the input vector $B(\theta)$ are linearly parameterized under the form

$$A(\theta) = A_0 + \sum_{i=1}^{p} A_i\theta_i \quad \text{and} \quad B(\theta) = B_0 + \sum_{i=1}^{p} B_i\theta_i\,, \tag{2.16}$$

where θ is a constant parameter belonging to a convex closed set $\Pi = \{\theta \in \Pi | \mathcal{P}(\theta) \leq 0\}$ included in $\mathbb{R}^p$, where $\mathcal{P} : \mathbb{R}^p \to \mathbb{R}$ is a smooth convex function.

The control objective is to have system (2.15) *track a given constant set point* Y^r *via a robust compensation approach, despite uncertainties for the delay* D. The control also has to deal with several other difficulties that may be encountered: (i) uncertainty in the plant parameter θ; (ii) unmeasured state X of the plant; and (iii) unknown input disturbance d.

Several assumptions are formulated following [Bresch-Pietri 09] that apply throughout subsequent chapters. The first two ensure that the problem is well-posed, while the fourth is useful for the Lyapunov analysis.

Assumption 1. *The set* Π *is known and bounded. An upper bound* $\bar{D}$ *and a lower bound* $\underline{D} > 0$ *of the delay* D *are known.*

Assumption 2. *For a given set point* Y^r*, there exist known functions* $X^r(\theta)$ *and* $U^r(\theta)$ *that are continuously differentiable in the parameter* $\theta \in \Pi$ *and that satisfy, for all* $\theta \in \Pi$*,*

$$0 = A(\theta)X^r(\theta) + B(\theta)U^r(\theta) \tag{2.17}$$
$$Y^r = CX^r(\theta) \tag{2.18}$$

Assumption 3. *The pair* $(A(\theta), B(\theta))$ *is controllable for every* $\theta \in \Pi$ *and there exists a triple of vector/matrix functions* $(K(\theta), P(\theta), Q(\theta))$ *such that, for all* $\theta \in \Pi$*,*
i) $P(\theta)$ *and* $Q(\theta)$ *are positive definite and symmetric ;*
ii) the following Lyapunov equation is satisfied

$$P(\theta)(A + BK)(\theta) + (A + BK)(\theta)^T P(\theta) = -Q(\theta)$$

iii) $(K, P) \in C^1(\Pi)^2$ *and* $Q \in C^0(\Pi)$*.*

Assumption 4. *The following quantities are well-defined*

$$\underline{\lambda} = \inf_{\theta\in\Pi} \min\left\{\lambda_{\min}(P(\theta)), \lambda_{\min}(Q(\theta))\right\}$$
$$\overline{\lambda} = \sup_{\theta\in\Pi} \lambda_{\max}(P(\theta))$$

Only one of these assumptions is restrictive: Assumption 3 requires the equivalent delay-free form of the system (2.15) to be controllable. This is a reasonable assumption to guarantee the possibility of regulation about the constant reference Y^r. As a final remark, we wish to stress that neither the reference U^r considered, nor the state reference X^r depend on time or delay, because the reference Y^r is constant. This point is important in the control design.

Adaptive methodology principle and organization of the chapters

As detailed in Chapter 2, when delay, plant and disturbance are perfectly known and system state is fully-measured, the following controller compensates for the delay and achieves exponential stabilization of system (2.15) after D units of time[5]

$$U(t) = KX(t + D) - d = K\left[e^{AD}X(t) + \int_{t-D}^{t} e^{A(t-s)}BU(s)ds\right] - d \tag{2.19}$$

In the following, applying the certainty equivalence principle ([Ioannou 96, Landau 98]), we decline different versions of this controller (2.19) to tackle each difficulty listed above. The aim here is to develop a prediction-based control law stabilizing the plant output to the set-point Y^r, corresponding to the equilibrium $(X^r(.), U^r(.))$ defined in Assumption 2.

To analyze the robustness of the resulting control law and to design delay adaptation, we aim at exploiting the cascaded ODE-PDE representation introduced in Chapter 2,

[5]The only difference here is the presence of the term d, counteracting the input bias in (2.15).

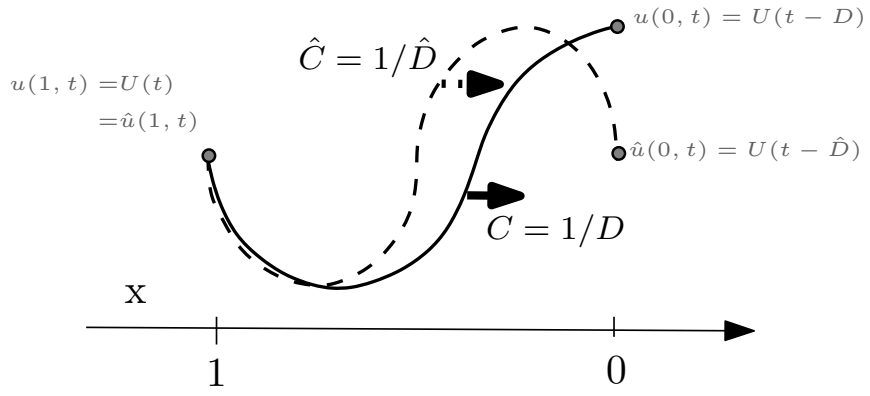

Figure 2.5: Transport representation of the waiting line at a speed of $C = 1/D$, and the estimate for a constant but overestimated delay $\hat{D} > D$ corresponding to an underestimated propagation speed $\hat{C} = 1/\hat{D}$.

together with corresponding backstepping elements. The key element of this framework is the distributed input $u(x,t) = U(t + D(x-1))$, for $x \in [0,1]$. When, the full actuator state is known (i.e. the past values of the input over an interval of length equal to the delay), the systematic adaptive control design proposed in [Bresch-Pietri 09] for an unknown actuator delay can be applied.

Unfortunately, because the propagation speed $1/D$ is uncertain, even if the applied input $U(t)$ is fully known, one cannot deduce the value of $u(x,t)$ for each $x \in [0,1]$ from it. Consequently, if this distributed input is not measured (which is seldom the case in applications, especially as this variable is infinite-dimensional), one cannot directly apply this strategy. Yet, it is still possible to introduce an estimate of the actuator state and to design the infinite-dimensional elements corresponding to this estimate.

Distributed input estimate and backstepping transformation

Let us define an estimate of the distributed input as $\hat{u}(x,t) = U(t + \hat{D}(t)(x-1))$, for $x \in [0,1]$. This variable is obtained naturally by replacing the delay appearing in the definition of $u(.,t)$ by an estimate $\hat{D}$, potentially time-varying. This estimate satisfies the following transport equation

$$\hat{D}(t)\hat{u}_t(x,t) = \hat{u}_x(x,t) + \dot{\hat{D}}(t)(x-1)\hat{u}_x(x,t) \tag{2.20}$$

$$\hat{u}(1,t) = U(t) \tag{2.21}$$

in which the propagation speed is time- and spatially-varying. This distributed input estimate is represented in Figure 2.5 for a constant delay estimate and is a key point in the control design.

By considering the original backstepping transformation (2.14) in Chapter 2, a natural choice for the backstepping transformation corresponding to the previous distributed input estimate is

$$\hat{w}(x,t) = \hat{u}(x,t) - KX_P(t + \hat{D}(t)x) \tag{2.22}$$

where $X_P(t_0)$ represents a system state prediction at time t_0 computed using the delay estimate $\hat{D}(t)$ (and, potentially, using additional estimates depending on the arising issues).

The transformed actuator state satisfies

$$\begin{cases} \hat{D}(t)\hat{w}_t(x,t) = & \hat{w}_x(x,t) + \dot{\hat{D}}(t)(x-1)\hat{w}_x(x,t) + \psi(x,t) \\ \hat{w}(1,t) = & 0 \end{cases} \tag{2.23}$$

where ψ aggregates the different terms that may arise due to potential erroneous estimates when calculating the prediction.

This last equation can be seen as a transport phenomena, similar to the one of the estimate (2.20), but impacted by a distributed source term ψ. The unforced transport PDE is naturally stable because of its zero boundary condition, and one can guess that the same is true for the forced case for both significantly small source term and delay estimate variations. These are the considerations that are rigorously obtained in the next chapters.

These elements above have been presented in the paper [Bresch-Pietri 10] and form the basis of the methodology proposed in this part of the thesis. They are represented as gray blocks in Figure 2.6.

Organization of the chapters

In the following, besides delay uncertainties, a series of classic issues in the filed of linear automatic control is considered: model uncertainties, disturbance rejection and partial state measurement. In addition to the distributed input estimate presented above, each of the aforementioned regulation issues requires introduction of specific elements. For clarity, these difficulties are therefore addressed separately in the following chapters.

For each issue, a dedicated implementable solution is proposed and theoretically studied via a formal proof of convergence, that stresses the role of the various adaptation and feedback components. Even if each situation represents a different technical challenge, a common structure guides the convergence proofs detailed in each chapter. To facilitate reading and comprehension, we provide it here:

1. definition of a backstepping transformation $w(.,t)$ of the actuator state, compliant with the general form (2.22) and based on the certainty equivalence principle, to obtain the null boundary condition $w(1,t) = 0$;

2. definition of a Lyapunov equation, involving a suitable set of error variables and alternative spatial integral norms of some of them;

3. derivation of the corresponding differential error equations (one of them being of form (2.23));

4. a time derivative of the Lyapunov equation and integration by parts to create negative upper-bounding terms; and

5. bounding of the remaining positive error terms using Young's and Cauchy-Schwartz's inequality.

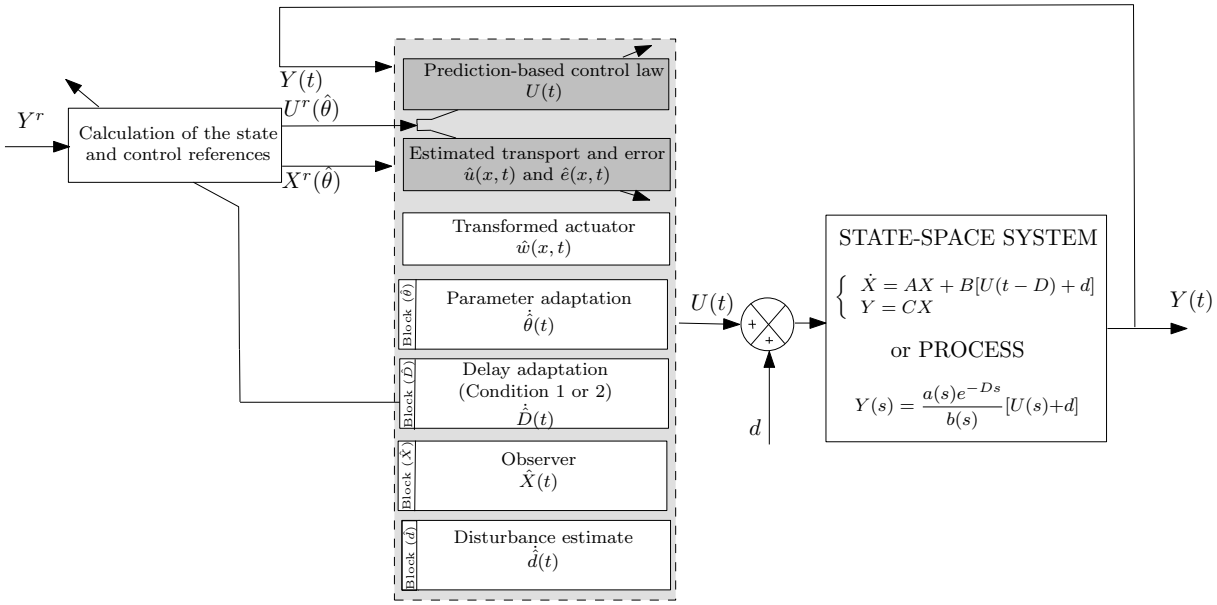

Figure 2.6: The proposed adaptive control scheme. The closed-loop algorithm still uses a prediction-based control law jointly with distributed parameters, i.e. the estimated waiting line (gray; Section I). According to the context, a combination of the remaining blocks (in white), namely a parameter estimate update law (Chapter 3), a delay estimate update law (Chapter 4), a system state observer (Chapter 5) or a disturbance estimate (Chapter 6), can be applied. This may also require computation of the transformed state of the actuator.

Table 2.1: Comparison of the presented results and the corresponding elements of proof.

Problem under consideration	Error variables in Lyapunov analysis	Main technicality in the Lyapunov analysis	Solution	CV
Parameter adaptation (Block $(\hat{\theta})$)	$\tilde{X}, \tilde{e}, \hat{w}, \hat{w}_x, \tilde{\theta}$	creation of error variables (completion of non-vanishing terms)	introduction of a parameter update law	lo. & as.
Delay adaptation (Block $(\hat{D})$)	$\tilde{X}, \tilde{e}, \hat{w}, \hat{w}_x, \tilde{D}$	bounding of $\lvert\dot{\hat{D}}(t)\rvert$	Conditions 1 and 2	lo. & as.
Observer (Block $(\hat{X})$)	$\tilde{X}, \Delta\hat{X}, \tilde{e}, \hat{w}, \hat{w}_x$	extra state variable	study of an extra Lyapunov equation	gl. & exp.
Disturbance estimate (Block $(\hat{d})$)	$\tilde{X}, \tilde{e}_0, \hat{w}_0, \hat{w}_{0,x}, \tilde{d}$	additive disturbance estimate in the control law	incorporation of a double integral term in the functional	gl. & as.

(Abbreviations: CV, convergence; lo., local; gl., global; as. asymptotic; exp., exponential.)

Choice of the variables set in (2) and the bounding realized in (5) are the most elaborate parts. In particular, the last point is different in each of the contexts and chapters because of the specific difficulties listed in Table 2.1. This table also aims at facilitating the reading and comparison of the following chapters.

Corresponding controller elements designed in the following chapters are represented as white blocks in Figure 2.6. Elements in the gray blocks, which are not problem-specific, have been presented in the previous section.

The goal of this part is to present a unified framework of these various techniques, for sake of comparisons of their merits and limitations in the light of their mathematical analysis. In view of application, the interested reader and the practitioner can simply make its own selection to address a vast class of possible problems. We illustrate this point in the last chapter by detailing experiments that were conducted on a test-bench to control the Fuel-to-Air Ratio of a Spark-Ignited engine.

This part is organized as follows. In Chapter 3, we focus on plant parameter adaptation. In Chapter 4, we study admissible delay on-line adaptation scheme, before introducing an output feedback design in Chapter 5. In Chapter 6, we propose a disturbance rejection strategy. Each of these designs is illustrated by simulation examples of two different systems: one open-loop unstable plant and a stable but very slow plant. These two examples highlight the merits of the proposed control strategy. Finally, in Chapter 7, the versatility of the proposed approach is underlined by experiments covering various cases.

Chapter 3

Control strategy with parameter adaptation

Chapitre 3 – Stratégie de contrôle avec adaptation aux incertitudes de modèle. *Ce chapitre présente une loi de compensation robuste du retard (incertain) avec adaptation aux paramètres inconnus de dynamique. Les résultats locaux de convergence asymptotique obtenus sont illustrés en simulation sur un système instable.*

Contents

This chapter addresses the case of plant parameters adaptation despite uncertainties on the delay, which yields to the consideration of the plant

$$\begin{cases} \dot{X}(t) = A(\theta)X(t) + B(\theta)U(t-D) \\ Y(t) = CX(t) \end{cases} \tag{3.1}$$

where, compared to (2.15) we consider the input disturbance d as known and, more conveniently, equal to zero and the system state X as measured. In (3.1), the plant parameter θ and the delay D are uncertain.

Several works on the frequency-domain (see [Palmor 96] and more recently [Evesque 03], [Niculescu 03]) have dealt with an adaptive framework for input delay systems. Yet, a few have simultaneously considered delay uncertainties and most controllers are not prediction-based and do not aim to compensate the delay effect. Some time-domain approaches (lately, [Zhou 09]) have also been proposed, but the same drawbacks apply.

Here, to achieve regulation despite the uncertainties, we introduce two estimates of the delay D and the plant parameter θ. For clarity, no particular effort is made to update the delay estimate, which is kept constant[1].

3.1 Controller design

Consider the error variables used below

$$\begin{aligned} \tilde{X}(t) =& X(t) - X^r(\hat{\theta}) \\ e(x,t) = u(x,t) - U^r(\hat{\theta}), \quad \hat{e}(x,t) =& \hat{u}(x,t) - U^r(\hat{\theta}), \quad \tilde{e}(x,t) = u(x,t) - \hat{u}(x,t) \end{aligned}$$

in which $\tilde{X}$ represents the tracking error, $e(.,t)$ and $\hat{e}(.,t)$ are the distributed input tracking errors, and $\tilde{e}(.,t)$ is the distributed input estimation error. These are the variables used to represent the overall system state.

Applying the certainty equivalence principle from the general prediction-based feedback (2.19), we apply the control law

$$U(t) = U^r(\hat{\theta}) - K(\hat{\theta})X^r(\hat{\theta}) + K(\hat{\theta})\left[e^{A(\hat{\theta})\hat{D}}X(t) + \hat{D}\int_0^1 e^{A(\hat{\theta})\hat{D}(1-x)}B(\hat{\theta})\hat{u}(x,t)dx\right] \quad (3.2)$$

and define the transformed state of the distributed input estimate $\hat{e}$ by the following Volterra integral equation of the second kind

$$\hat{w}(x,t) = \hat{e}(x,t) - \hat{D}\int_0^x K(\hat{\theta})e^{A(\hat{\theta})\hat{D}(x-y)}B(\hat{\theta})\hat{e}(y,t)dy - K(\hat{\theta})e^{A(\hat{\theta})\hat{D}x}\tilde{X}(t) \quad (3.3)$$

The parameter update law chosen is

$$\dot{\hat{\theta}}(t) = \gamma_\theta \mathrm{Proj}_\Pi(\tau_\theta(t)) \quad (3.4)$$

with

$$\begin{cases} \tau_{\theta,i}(t) = h(t) \times (A_i X(t) + B_i U^r(\hat{\theta})) & (3.5) \\ h(t) = \dfrac{\tilde{X}(t)^T P(\hat{\theta})}{b_2} - \hat{D}K(\hat{\theta})\displaystyle\int_0^1 (1+x)\left[\hat{w}(x,t) + A(\hat{\theta})\hat{D}\hat{w}_x(x,t)\right]e^{A(\hat{\theta})\hat{D}x}dx & (3.6) \end{cases}$$

and $\gamma_\theta > 0$, $1 \le i \le p$. In addition, the matrix P is the one considered in Assumption 3, the constant b_2 is chosen such that $b_2 \ge 8\sup_{\theta\in\Pi}|PB(\theta)|^2/\underline{\lambda}$ and Proj_Π is the standard projector operator onto the convex set Π

$$\mathrm{Proj}_\Pi\{\tau_\theta\} = \tau_\theta \begin{cases} I, & \hat{\theta} \in \mathring{\Pi} \text{ or } \nabla_{\hat{\theta}}\mathcal{P}^T\tau_\theta \le 0 \\ I - \frac{\nabla_{\hat{\theta}}\mathcal{P}\nabla_{\hat{\theta}}\mathcal{P}^T}{\nabla_{\hat{\theta}}\mathcal{P}^T\nabla_{\hat{\theta}}\mathcal{P}}, & \hat{\theta} \in \partial\Pi \text{ and } \nabla_{\hat{\theta}}\mathcal{P}^T\tau_\theta > 0 \end{cases} \quad (3.7)$$

Theorem 3.1.1

Consider the closed-loop system consisting of (3.1)*, the control law* (3.2) *and the update law defined by* (3.4)–(3.6)*. Define the functional*

$$\Gamma(t) = |\tilde{X}(t)| + \|e(t)\|^2 + \|\hat{e}(t)\|^2 + \|\hat{e}_x(t)\|^2 + \tilde{\theta}(t)^2 \quad (3.8)$$

[1] i.e. $\dot{\hat{D}}(t) = 0$, which trivially satisfies either Condition 1 or Condition 2 defined later in Chapter 4. Delay adaptation is addressed specifically in Chapter 4.

Then there exists $\gamma^* > 0$, $\delta^* > 0$, $R > 0$ and $\rho > 0$ such that, provided the initial state $(\tilde{X}(0), e_0, \hat{e}_0, \hat{e}_{x,0}, \tilde{\theta}(0))$ is such that $\Gamma(0) < \rho$, if $|\tilde{D}| < \delta^*$ and if $\gamma_\theta < \gamma^*$, then

$$\forall t \geq 0 \quad \Gamma(t) \leq R\Gamma(0)\,, \tag{3.9}$$

$$\lim_{t\to\infty} Y(t) = Y^r\,, \quad \lim_{t\to\infty} \tilde{X}(t) = 0 \quad \textit{and} \quad \lim_{t\to\infty} [U(t) - U^r(\hat{\theta})] = 0 \tag{3.10}$$

Before proving this theorem, a few comments can be made. First, Theorem 3.1.1 introduces a functional Γ that can be understood as an evaluation of both convergence and estimation errors. In particular, note the presence of the spatial derivative of the estimate queue $\hat{e}_x$ in the statement. This quantity is involved in the state variable dynamics presented below as a result of the estimation of the distributed input.

The stated results are only asymptotic and local; in other words, they require that each of the state variables is initially sufficiently close to its corresponding set-point (namely, X^r, U^r and the unknown θ). This is the meaning of the condition $\Gamma(0) < \rho$. The delay estimate also needs to be sufficiently close to the true (uncertain) delay, which can be interpreted as robustness to a delay mismatch.

The main particularity of the above statement lies in introduction of the parameter update law (3.4)–(3.6) based on the projector (3.7). This operator, commonly found in adaptive schemes [Ioannou 96], is typical of a Lyapunov adaptive design, which is here possible here because of the backstepping transformation (3.3), as shown in the following. Note that the update gain of the parameter estimate has to be upper-bounded to be compliant with the control design.

Finally, and contrary to the controllers designed in the following, the backstepping transformation appears explicitly in the control design and is not only an element of proof. This is because of the adaptive Lyapunov design of the parameter update law.

3.2 Convergence analysis

3.2.1 Error variable dynamics and Lyapunov analysis

To take advantage of the backstepping transformation (designed to fulfill the boundary condition $\hat{w}(1,t) = 0$ from the control law (3.2)), instead of Γ, we use an alternative functional, which is the Lyapunov-Krasovskii functional we consider from now on,

$$\begin{aligned} V(t) =& \tilde{X}(t)^T P(\hat{\theta})\tilde{X}(t) + b_1 D \int_0^1 (1+x)\tilde{e}(x,t)^2 dx + b_2 \hat{D} \int_0^1 (1+x)\hat{w}(x,t)dx \\ &+ b_2 \hat{D} \int_0^1 (1+x)\hat{w}_x(x,t)dx + b_2 |\tilde{\theta}(t)|^2/\gamma_\theta \end{aligned}$$

where b_1 and b_2 are positive constants. The boundary conditions of the set $(\tilde{e}, \hat{w}, \hat{w}_x)$ can easily be obtained via integrations by parts, involving the factor $(1+x)$ under the integrals, to create upper-bounding negative terms. Before working with this functional, we consider the dynamics of the variables involved using (3.3) and its inverse transformation

$$\hat{e}(x,t) = \hat{w}(x,t) + K(\hat{\theta})\hat{D} \int_0^x e^{(A+BK)(\hat{\theta})(x-y)} B(\hat{\theta})\hat{w}(y,t)dy + K(\hat{\theta}) e^{(A+BK)(\hat{\theta})\hat{D}x} \tilde{X}(t) \tag{3.11}$$

which yields

$$\dot{\tilde{X}}(t) = (A+BK)(\hat{\theta})\tilde{X}(t) + B(\hat{\theta})\hat{w}(0,t) + B(\hat{\theta})\tilde{e}(0,t) + \tilde{A}X(t) + \tilde{B}u(0,t) - \frac{\partial X^r}{\partial \hat{\theta}}\dot{\hat{\theta}}(t) \tag{3.12}$$

$$\begin{cases} D\tilde{e}_t(x,t) = \tilde{e}_x(x,t) - \tilde{D}(t)f(x,t) \\ \quad \tilde{e}(1,t) = 0 \end{cases}$$

$$\begin{cases} \hat{D}\hat{w}_t(x,t) = \hat{w}_x(x,t) - \hat{D}\dot{\hat{\theta}}(t)^T g(x,t) - \hat{D}\tilde{\theta}(t)^T g_0(x,t) - \hat{D}K(\hat{\theta})e^{A(\hat{\theta})\hat{D}x}B(\hat{\theta})\tilde{e}(0,t) \\ \hat{w}(1,t) = 0 \end{cases} \tag{3.13}$$

$$\begin{cases} \hat{D}\hat{w}_{xt}(x,t) = \hat{w}_{xx}(x,t) - \hat{D}\dot{\hat{\theta}}(t)^T g_x(x,t) - \hat{D}\tilde{\theta}(t)^T g_{0,x}(x,t) \\ \qquad\qquad -\hat{D}^2 KA(\hat{\theta})e^{A(\hat{\theta})\hat{D}x}B(\hat{\theta})\tilde{e}(0,t) & (3.14) \\ \hat{w}_x(1,t) = \hat{D}\dot{\hat{\theta}}(t)^T g(1,t) + \hat{D}\tilde{\theta}(t)^T g_0(1,t) + \hat{D}K(\hat{\theta})e^{A(\hat{\theta})\hat{D}}B(\hat{\theta})\tilde{e}(0,t) & (3.15) \end{cases}$$

where $\tilde{A} = \sum_{i=1}^{p} A_i\tilde{\theta}_i(t)$, $\tilde{B} = \sum_{i=1}^{p} B_i\tilde{\theta}_i(t)$ and f, g and g_0 are defined as

$$\begin{aligned}
f(x,t) =& \frac{\hat{w}_x(x,t)}{\hat{D}} + KB(\hat{\theta})\hat{w}(x,t) + \hat{D}\int_0^x K(A+BK)(\hat{\theta})e^{(A+BK)(\hat{\theta})\hat{D}(x-y)}B(\hat{\theta})\hat{w}(y,t)dy \\
&+ K(A+BK)(\hat{\theta})e^{(A+BK)(\hat{\theta})\hat{D}x}\tilde{X}(t) \\
g_{0,i}(x,t) =& K(\hat{\theta})e^{A(\hat{\theta})\hat{D}x}(A_iX(t) + B_iu(0,t)) \\
g_i(x,t) =& \hat{D}\int_0^x \hat{w}(y,t)\left[\left(\frac{\partial K}{\partial\hat{\theta}_i} + K(\hat{\theta})A_i\hat{D}(x-y)\right)e^{A(\hat{\theta})\hat{D}(x-y)}B(\hat{\theta}) + K(\hat{\theta})e^{A(\hat{\theta})\hat{D}(x-y)}B_i\right. \\
&+\hat{D}\int_y^x\left[\left(\frac{\partial K}{\partial\hat{\theta}_i} + K(\hat{\theta})A_i\hat{D}(x-\xi)\right)e^{A(\hat{\theta})\hat{D}(x-\xi)}B(\hat{\theta}) + K(\hat{\theta})e^{A(\hat{\theta})\hat{D}(x-\xi)}B_i\right] \\
&\left.K(\hat{\theta})e^{(A+BK)(\hat{\theta})\hat{D}(\xi-y)}B(\hat{\theta})d\xi\right]dy - \hat{D}\int_0^x K(\hat{\theta})e^{A(\hat{\theta})\hat{D}(x-y)}B(\hat{\theta})\frac{dU^r}{d\hat{\theta}_i}(\hat{\theta})dy \\
&- K(\hat{\theta})e^{A(\hat{\theta})\hat{D}x}\frac{\partial X^r}{\partial\hat{\theta}_i} + \frac{dU^r}{d\hat{\theta}_i}(\hat{\theta}) \\
&+\left(\hat{D}\int_0^x\left(\left[\frac{\partial K}{\partial\hat{\theta}_i} + K(\hat{\theta})A_i\hat{D}(x-y)\right]e^{A(\hat{\theta})\hat{D}(x-y)}B(\hat{\theta}) + K(\hat{\theta})e^{A(\hat{\theta})\hat{D}(x-y)}B_i\right)\right. \\
&\left.\times\, K(\hat{\theta})e^{(A+BK)(\hat{\theta})\hat{D}y}dy + \left[\frac{\partial K}{\partial\hat{\theta}_i} + K(\hat{\theta})A_i\hat{D}x\right]e^{A(\hat{\theta})\hat{D}x}\right)\tilde{X}(t)
\end{aligned}$$

Taking a time derivative of V, after suitable integration by parts and using the update law (3.4)-(3.6), one obtains

$$\begin{aligned}
\dot{V}(t) \leq & -(\underline{\lambda}|\tilde{X}(t)| + b_1\tilde{e}(0,t)^2 + b_1\left\|\tilde{e}(t)\right\|^2 + b_2\hat{w}(0,t)^2 + b_2\left\|\hat{w}(t)\right\|^2 + b_2\left\|\hat{w}_x(t)\right\|^2) \\
& + 2|\dot{\hat{\theta}}(t)|\left|P(\hat{\theta})\frac{\partial X^r}{\partial\hat{\theta}}\right||\tilde{X}(t)| + 2b_2|h(t)||\tilde{B}||\tilde{e}(0,t) + \hat{w}(0,t) + K(\hat{\theta})\tilde{X}(t)| \\
& + 2|\tilde{X}(t)^T PB(\hat{\theta})(\hat{w}(0,t) + \tilde{e}(0,t))| + 2b_1|\tilde{D}|\int_0^1 (1+x)|\tilde{e}(x,t)||f(x,t)|dx \\
& + b_2\Big(2\hat{D}|\dot{\hat{\theta}}(t)|\int_0^1 (1+x)|\hat{w}(x,t)||g(x,t)|dx \\
& + 2\hat{D}|\tilde{e}(0,t)|\int_0^1 (1+x)|\hat{w}(x,t)||K(\hat{\theta})e^{A(\hat{\theta})\hat{D}x}B(\hat{\theta})|dx\Big) \\
& + b_2\Big(2\hat{D}|\dot{\hat{\theta}}(t)|\int_0^1 (1+x)|\hat{w}_x(x,t)||g_x(x,t)|dx \\
& + 2\hat{D}^2|\tilde{e}(0,t)|\int_0^1 (1+x)|\hat{w}_x(x,t)||KA(\hat{\theta})e^{A(\hat{\theta})\hat{D}x}B(\hat{\theta})|dx\Big) \\
& + 2b_2\hat{w}_x(1,t)^2 + \sum_{i=1}^{p}|\dot{\hat{\theta}}_i(t)|\left\|\frac{\partial P}{\partial\hat{\theta}_i}\right\|_\infty |\tilde{X}(t)|^2
\end{aligned}$$

Furthermore, applying Young's inequality, Cauchy-Schwartz's inequality and Agmon's inequality $\hat{w}(0,t)^2 \leq 4\left\|\hat{w}_x(t)\right\|^2$ (with the help of the fact that $\hat{w}(1,t)^2 = 0$), one can obtain the inequalities below. The positive constants $M_1, \ldots, M_{10}$ are independent on initial conditions and the functional V_0 is defined as $V_0(t) = |\tilde{X}(t)|^2 + \left\|\tilde{e}(t)\right\|^2 + \left\|\hat{w}(t)\right\|^2 + \left\|\hat{w}_x(t)\right\|^2$.

$$\begin{aligned}
2|h(t)||\tilde{B}||\tilde{e}(0,t) + \hat{w}(0,t) + K(\hat{\theta})\tilde{X}(t)| \quad &\leq \quad M_1|\tilde{\theta}(t)|\left(V_0(t) + \tilde{e}(0,t)^2\right) \\
2|\tilde{X}(t)^T PB(\hat{\theta})(\hat{w}(0,t) + \tilde{e}(0,t))| \quad &\leq \quad \frac{\lambda}{2}|\tilde{X}(t)|^2 + \frac{4\left\|PB\right\|_\infty^2}{\underline{\lambda}}(\hat{w}(0,t)^2 + \tilde{e}(0,t)^2) \\
2\int_0^1 (1+x)|\tilde{e}(x,t)||f(x,t)|dx \quad &\leq \quad M_2V_0(t) \\
2\hat{D}\int_0^1 (1+x)|\hat{w}(x,t)||g(x,t)|dx \quad &\leq \quad M_3\left(V_0(t) + \left\|\hat{w}(t)\right\|\right) \\
2\hat{D}|\tilde{e}(0,t)|\int_0^1 (1+x)|\hat{w}(x,t)||K(\hat{\theta})e^{A(\hat{\theta})\hat{D}x}B(\hat{\theta})|dx \quad &\leq \quad M_4\tilde{e}(0,t)^2 + \left\|\hat{w}(t)\right\|^2/2 \\
2\hat{D}\int_0^1 (1+x)|\hat{w}(x,t)||g_x(x,t)|dx \quad &\leq \quad M_5V_0(t) \\
2\hat{D}^2|\tilde{e}(0,t)|\int_0^1 (1+x)|\hat{w}_x(x,t)||KA(\hat{\theta})e^{A(\hat{\theta})\hat{D}x}B(\hat{\theta})|dx \quad &\leq \quad M_6\tilde{e}(0,t)^2 + \left\|\hat{w}_x(t)\right\|^2/2 \\
2\hat{w}_x(1,t)^2 \quad &\leq \quad M_7|\dot{\hat{\theta}}(t)|^2\left(V_0(t)+1\right) + M_8\tilde{e}(0,t)^2 + M_9|\tilde{\theta}(t)|^2\left(|\tilde{X}(t)|^2 + \left\|\hat{w}_x(t)\right\|^2\right)
\end{aligned} \tag{3.16}$$

$$|\dot{\hat{\theta}}(t)| \quad \leq \quad \gamma_\theta M_{10}(V_0(t) + |\tilde{X}(t)| + \left\|\hat{w}(t)\right\| + \left\|\hat{w}_x(t)\right\|) \tag{3.17}$$

With these inequalities, by choosing $b_{2,2} \geq \frac{8\|PB\|_\infty^2}{\underline{\lambda}}$ and defining $M_{11} = 2\left\|P\partial X^r/\partial\hat{\theta}\right\|_\infty$ and $M_0 = p\max_{1\leq i\leq p}\left\|\partial P/\partial\hat{\theta}_i\right\|_\infty$, the previous inequality yields

$$\begin{aligned}\dot{V}(t) \leq & -\frac{\lambda}{2}|\tilde{X}(t)|^2 - b_1\left\|\tilde{e}(t)\right\|^2 - \frac{b_2}{2}\hat{w}(0,t)^2 - \frac{b_2}{2}\left\|\hat{w}(t)\right\|^2 - \frac{b_2}{2}\left\|\hat{w}_x(t)\right\|^2 + M_0|\dot{\hat{\theta}}(t)||\tilde{X}(t)|^2 \\ & + M_{11}|\dot{\hat{\theta}}||\tilde{X}(t)| - \left(b_1 - b_2\left(\frac{1}{2} + M_1|\tilde{\theta}(t)| + M_4 + M_6 + M_8\right)\right)\tilde{e}(0,t)^2 \\ & + (b_2M_1|\tilde{\theta}(t)| + b_1|\tilde{D}|M_2)V_0(t) + b_2|\dot{\hat{\theta}}(t)|\Big(M_3\left(V_0(t) + \|\hat{w}(t)\|\right) + M_5\left(V_0(t) + \|\hat{w}_x(t)\|\right)\Big) \\ & + b_2M_7|\dot{\hat{\theta}}(t)|^2\left(V_0(t)+1\right) + b_2M_9|\tilde{\theta}(t)|^2V_0(t)\end{aligned}$$

To obtain a negative definite expression, we choose $b_1 > b_2(1/2 + 2M_1\left\|\theta\right\|_\infty + M_4 + M_6 + M_8)$ and define $\eta = \min\left\{\underline{\lambda}/2, b_1, b_2/2\right\}$. Then, using (3.17), Young's inequality $|\tilde{\theta}(t)| \leq \frac{\epsilon_2}{2} + \frac{1}{2\epsilon_2}(V_2(t) - \eta_2V_0(t))$, involving $\epsilon_2 > 0$, yields

$$\begin{aligned}\dot{V}(t) \leq & -\left[\eta - b_1M_2|\tilde{D}| - \gamma_\theta n_1(\gamma_\theta) - b_2(M_1 + 2M_9\left\|\theta\right\|_\infty)\left(\frac{\epsilon_2}{2} + \frac{1}{2\epsilon_2}V_2(t)\right)\right]V_0(t) \\ & - \left[\frac{\eta_2 b_{2,2}}{2\epsilon_2}(M_1 + 2M_9\left\|\theta\right\|_\infty) - \gamma_\theta n_2(\gamma_\theta) - 5M_7\gamma_\theta M_{10}V_0(t)\right]V_0(t)^2 \qquad (3.18)\end{aligned}$$

where the function n_1 and n_2 are defined as $n_1(\gamma_\theta) = 2M_{10}(M_0 + 3M_{11} + 4M_3 + 4M_5 + 4\gamma_\theta M_7M_{10})$ and $n_2(\gamma_\theta) = M_{10}(M0 + 2M_{11} + 5M_3 + 5M_5 + 13M_7\gamma_\theta M_{10})$. Consequently, if the delay estimate error satisfies $|\tilde{D}(t)| < \frac{\eta}{b_1M_2}$, choosing the update gain γ_θ and the parameter ϵ_2 such that

$$\begin{aligned}\gamma_\theta < & \gamma^* = \min\left\{1, \frac{\eta - b_1M_2|\tilde{D}|}{n_1(1)}\right\} \qquad (3.19)\\ \epsilon_2 < & \min\left\{\frac{2(\eta - b_1M_2|\tilde{D}| - \gamma_\theta n_1(\gamma_\theta))}{b_2(M_1 + 2M_9\left\|\theta\right\|_\infty^2)}, \frac{\eta_2 b_2}{2\gamma_\theta n_2(\gamma_\theta)}(M_1 + 2M_9\left\|\theta\right\|_\infty)\right\}\end{aligned}$$

and restricting the initial condition to

$$V(0) \leq \min\left\{\epsilon_2\left[2\frac{\eta - b_1M_2|\tilde{D}| - \gamma_\theta n_1(\gamma_\theta)}{b_2(M_1 + 2M_9\left\|\theta\right\|_\infty^2)} - \epsilon_2\right], \eta_2\frac{\eta_2 b_2(M_1 + 2M_9\left\|\theta\right\|_\infty) - 2\epsilon_2\gamma_\theta n_2(\gamma_\theta)}{10\epsilon_2M_7\gamma_\theta M_{10}}\right\} \qquad (3.20)$$

one finally obtains two non-negative functions μ_1 and μ_2 such that

$$\dot{V}(t) \leq -\mu_1(t)V_0(t) - \mu_2(t)V_0(t)^2 \qquad (3.21)$$

and consequently

$$\forall t \geq 0\,, \quad V(t) \leq V(0) \qquad (3.22)$$

3.2.2 Equivalence and convergence result

To obtain the stability result stated in Theorem 3.1.1, one can prove the equivalence of the two functionals V and Γ, that is, the existence of $(a,b) \in {\mathbb{R}_+^*}^2$ such that

$aV_1(t) \leq \Gamma_1(t) \leq bV_1(t)$, for $t \geq 0$. First, considering (3.3) and its inverse (3.11) and applying Young's inequality, one can establish the following inequalities

$$\|\hat{e}(t)\|^2 \leq r_1|\tilde{X}(t)|^2 + r_2\|\hat{w}(t)\|^2 \tag{3.23}$$
$$\|\hat{e}_x(t)\|^2 \leq r_3|\tilde{X}(t)|^2 + r_4\|\hat{w}(t)\|^2 + r_5\|\hat{w}_x(t)\|^2 \tag{3.24}$$
$$\|\hat{w}(t)\|^2 \leq s_1|\tilde{X}(t)|^2 + s_2\|\hat{e}(t)\|^2 \tag{3.25}$$
$$\|\hat{w}_x(t)\|^2 \leq s_3|\tilde{X}(t)|^2 + s_4\|\hat{e}(t)\|^2 + s_5\|\hat{e}_x(t)\|^2 \tag{3.26}$$

where $r_1, r_2, r_3, r_4, r_5, s_1, s_2, s_3, s_4$ and s_5 are positive constants. From this, one directly obtains

$$\begin{aligned}\Gamma(t) \leq& |\tilde{X}(t)|^2 + 2\|\tilde{e}(t)\|^2 + 3\|\hat{e}(t)\|^2 + \|\hat{e}_x(t)\|^2 + \tilde{\theta}^2(t)\\ \leq& \frac{\max\{1+3r_1+r_3, 3r_2+r_4, r_5, 2\}}{\min\{\underline{\lambda}, b_1 D, b_2\underline{D}, b_2/\gamma_\theta\}} V(t)\\ V(t) \leq& \max\left\{\bar{\lambda} + 2s_1b_1\bar{D} + 2s_3b_2\bar{D}, 2s_5b_2\bar{D}, 4b_1D + 2s_2b_1\bar{D} + 2s_4b_2\bar{D}, b_2/\gamma_\theta\right\}\Gamma(t)\end{aligned}$$

This gives the desired stability property (3.9), with $R = b/a$.

We conclude using Barbalat's Lemma on the variables $|\tilde{X}(t)|$ and $\tilde{U}(t)$. By integrating (3.21) from 0 to $+\infty$, it is straightforward to show that both signals are square integrable. Then, consider the following equations

$$\begin{aligned}\frac{d|\tilde{X}(t)|^2}{dt} =& 2\tilde{X}(t)\left(A(\theta)X(t) + B(\theta)u(0,t) - \frac{\partial X^r}{\partial\hat{\theta}}\dot{\hat{\theta}}\right)\\ \frac{d\tilde{U}(t)^2}{dt} =& 2\tilde{U}(t)\left(K(\hat{\theta})e^{A(\hat{\theta})\hat{D}}\dot{\tilde{X}}(t) + \sum_{i=1}^{p}\dot{\hat{\theta}}_i(t)G_i(t) + H_0(t)\right)\end{aligned}$$

where

$$\begin{aligned}G_i(t) =& \frac{\partial K}{\partial\hat{\theta}_i}\left[e^{A(\hat{\theta})\hat{D}}\tilde{X}(t) + \hat{D}\int_0^1 e^{A(\hat{\theta})\hat{D}(1-y)}B(\hat{\theta})\hat{e}(y,t)dy\right]\\ &+ K(\hat{\theta})\left[\hat{D}A_i e^{A(\hat{\theta})\hat{D}}\tilde{X}(t) + \hat{D}\int_0^1 e^{A(\hat{\theta})\hat{D}(1-y)}(A_i\hat{D}(1-y)B(\hat{\theta}) + B_i)\hat{e}(y,t)dy\right.\\ &\left.- \hat{D}\int_0^1 e^{A(\hat{\theta})\hat{D}(1-y)}B(\hat{\theta})\frac{dU^r}{d\hat{\theta}_i}(\hat{\theta})dy\right]\\ H_0(t) =& K(\hat{\theta})\int_0^1 e^{A(\hat{\theta})\hat{D}(1-y)}B(\hat{\theta})\hat{e}_x(y,t)dy\end{aligned}$$

From (3.22), it follows that $|\tilde{X}(t)|, \|\tilde{e}(t)\|$, $\|\hat{w}(t)\|$ and $\|\hat{w}_x(t)\|$ are uniformly bounded. Then, with (3.23), we obtain the uniform boundedness of $\|\hat{e}(t)\|$ and, consequently, of $\|\hat{u}(t)\|$. With (4.2), we conclude that $U(t)$ is uniformly bounded, and, therefore, that $u(0,t) = U(t-D)$ is bounded for $t \geq \bar{D}$. Using the projection operator properties, one can deduce that $G_1, \ldots, G_p$ and H_0 are uniformly bounded for $t \geq \max\left\{D, \hat{D}\right\}$. Finally, from (3.4)–(3.6), one obtains the uniform boundedness of $\dot{\hat{\theta}}_i$ for $1 \leq i \leq p$. It is therefore easy to conclude that both $d|\tilde{X}(t)|^2/dt$ and $d\tilde{U}(t)^2/dt$ are uniformly bounded for $t \geq \max\left\{D, \hat{D}\right\}$. Consequently, one obtains, with Barbalat's Lemma, that $\tilde{X}(t) \to 0$ and $\tilde{U}(t) \to 0$ as $t \to \infty$.

3.2.3 Main specificity of the proof and other comments

The essence of the proof is based on the backstepping transformation of the actuator state. As shown in Section 2.4.2, this transformation facilitates use of a class of Lyapunov-Krasovskii techniques taking advantage of the particular null boundary condition. These tools are then particularly useful for analysis of the closed-loop stability.

Contrary to the following chapters, this backstepping transformation is more than an analysis tool here. The present proof uses an actual Lyapunov design of the parameter update law and consequently the transformed distributed input explicitly appears in the update law (3.6).

In detail, the $(\tilde{X}, \hat{w}, \hat{w}_x)$ dynamics (3.12), (3.13), (3.14) introduce bilinear terms of the form $\tilde{\theta}_i(t)(A_iX(t) + B_iu(0,t))$ (for $1 \leq i \leq p$). Because of the presence of the unknown term $u(0,t)$, it is impossible to exactly cancel these terms via the parameter update law, which itself appears in the time-derivative as a sum of terms $\tilde{\theta}_i\tau_{\theta,i}$. However, one can still create vanishing terms, namely $e(0,t)$, by incorporating the control reference $U^r(\hat{\theta})$ in the parameter update law, as in (3.5). Because these terms arise in the three dynamics, $\tilde{X}, \hat{w}(.,t)$ and $\hat{w}_x(.,t)$ appear in the definition of h in (3.6). In other words, the function h aggregates all the terms appearing as factors of $\tilde{\theta}$ in the error variable dynamics.

A point worth noting is that the creation of vanishing terms cannot be directly applied to a non-constant trajectory. Indeed, in this context, the reference distributed input $u^r(x,t,\hat{\theta})$ depends explicitly on time and space. Then the quantity $u^r(0,t,\hat{\theta})$ is unknown and cannot be used in the parameter update law as done above.

One parameter estimation error term also occurs in $\hat{w}_x(1,t)^2$, as (3.15) points it out. Its quadratic form is inconsistent with a Lyapunov design. Consequently, its treatment requires introduction of the intermediate function V_0 and a constraint on the initial condition. Treatment of the delay estimation error $\tilde{D}$ directly yields the condition stated in Theorem 3.1.1.

The main calculation difficulty is due to cubic terms because of the quantity $\hat{w}_x(1,t)^2$. Various bounds can be used to express these in polynomial form in the V_0 variables. The bounds presented in (3.18) have been relatively roughly chosen. Consequently, the proposed expression for the bound for the update gain γ^* (3.19) and for the initial condition (3.20) are not the least conservative ones.

3.3 Illustrative example

In this section, to illustrate the merits, the practical interest and the feasibility of the proposed adaptive control scheme, we consider an open-loop unstable systems of order three with an unknown time delay, as originally proposed in [Huang 95] and [Huang 97]

$$Y(s) = \frac{e^{-0.5s}}{(5s-1)(2s+1)(0.5s+1)}U(s)$$

Control is designed to regulate the system around the set-point $Y^r = 1$. We compare the simulation results obtained for both the PID proposed in [Huang 95] and the control strategy proposed in [Huang 97], called a three-element controller in the following.

3.3.1 State-space representation

The controller proposed in [Huang 97] was designed specifically for a first- and second-order-delayed unstable plant. Consequently, for control purposes, the authors used the effective following approximation of the plant

$$Y(s) \approx \frac{e^{-0.939s}}{(5s-1)(2.07s+1)}U(s) = \frac{e^{-Ds}}{(as-1)(Ts+1)}U(s)$$

The stable part of the transfer function is here approximated by a first-order plus delay plant, using a closed-loop identification technique and a least mean-square optimization in the frequency domain. Huang and Chen searched for controller settings using this approximated model, so we consider the same model for comparison and consider the plant parameters as uncertain (with a 10% uncertainty interval).

Our first step is derivation of a state-space realization of this transfer function. To match the previous framework, we choose the following realization

$$\dot{X}(t) = \begin{pmatrix} 0 & \frac{1}{aT} \\ 1 & \frac{a-T}{aT} \end{pmatrix} X(t) + \begin{pmatrix} \frac{1}{aT} \\ 0 \end{pmatrix} U(t-D) \tag{3.27}$$

$$Y(t) = (0 \quad 1)X(t) \tag{3.28}$$

This formulation is consistent with the linear parametrization form (2.16), with the parameter $\theta = \frac{1}{aT}(1 \quad a-T)^T \in \mathbb{R}^2$ and the matrices

$$A(\theta) = \begin{pmatrix} 0 & \theta_1 \\ 1 & \theta_2 \end{pmatrix} = A_0 + A_1\theta_1 + A_2\theta_2 \quad B(\theta) = \begin{pmatrix} \theta_1 \\ 0 \end{pmatrix} = B_1\theta_1$$

We focus on the reference corresponding to the output set point Y^rn which can be simply determined as

$$X^r(\theta) = \begin{bmatrix} -\theta_2 \\ 1 \end{bmatrix} Y^r \quad \text{and} \quad U^r(\theta) = -Y^r$$

We consider that the plant (3.27) is fully measured.

3.3.2 Control law with parameter adaptation

The delay D is uncertain but is known to belong to the interval $[\underline{D}, \bar{D}] = [0.8, 1.1]$. Its estimate is taken as $\hat{D} = 1$.

Considering a 10% error interval on the parameters a and T yields a definition of the convex set $\Pi = [0.05, 0.15] \times [0.2, 0.4]$ for the parameter θ.

The closed-loop system (3.1), the control law (3.2) and the update law are defined through (3.4)–(3.6) with

$$\begin{aligned} \tau_{\theta,1}(t) &= h(t) \times (A_1X(t) - B_1Y^r) \\ \tau_{\theta,2}(t) &= h(t) \times A_2X(t) \end{aligned}$$

The integrals in (3.2) and (3.6) are calculated with a trapezoidal discretization scheme.

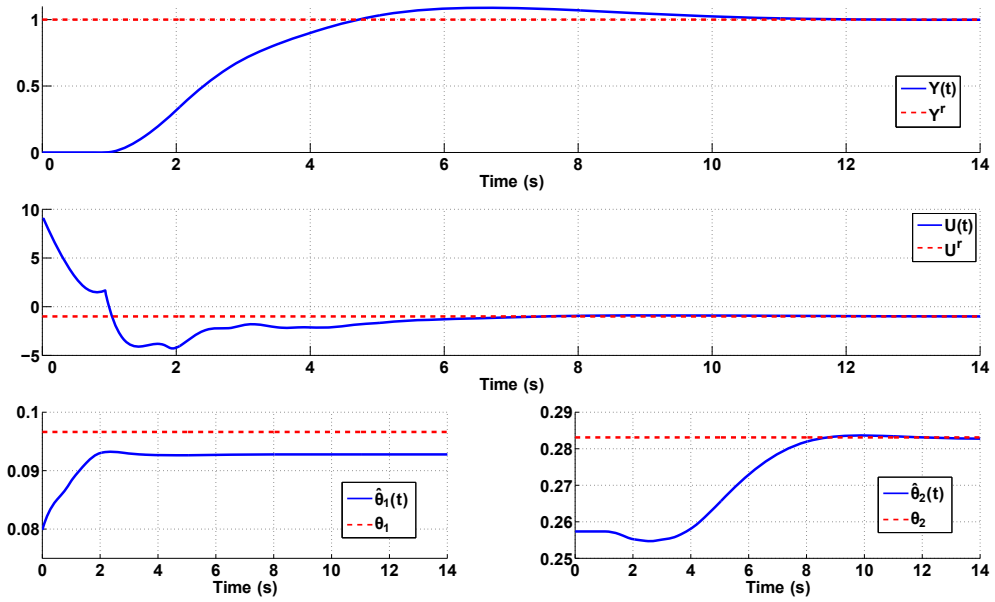

Figure 3.1: Simulation results for control of system (3.27) starting from $X(0) = [0 \quad 0]^T$, $u(.,0) = 0$ and $\hat{\theta}(0) = [0.08 \quad 0.258]$. The constant delay estimate is $\hat{D} = 1$. The controller gain $K(\hat{\theta})$ is chosen according to an LQR criterion and the update gain is chosen as $\gamma_\theta = 10^{-4}$.

Table 3.1: Performances in tracking for the different controllers : Integral Absolute Error (IAE) and 5% time-response.

	Proposed strategy	Three-elements controller	PID
IAE [-]	2.77	3.04	5.37
$T_{5\%}$	8	8.02	14.81

Simulation results are reported in Figure 3.1 for $\hat{\theta}(0) = [0.08 \quad 0.258]$ and an unknown plant parameter of $\theta = [0.097 \quad 0.28]$ which represents an error of approximately 15%. In general, the performance of the controller is consistent with the properties stated in Theorem 3.1.1. The slight overshoot observed during the transient at approximately 4-5 s is due to the parameter adaptation lag.

When convergence of the system state and control is eventually achieved (approx. 12s), the estimate $\hat{\theta}(t)$ also converges, which is expected from the update law (3.4)–(3.6). Nevertheless, a multiparameter estimation is not obtained, as is well-known in adaptive control [Ioannou 96]. In particular, $\tilde{\theta}_2(t)$ converges to zero for the considered system, but $\tilde{\theta}_1(t)$ does not. This is consistent with the dynamics given above. By examining (2.17)–(2.18) in Assumption 2 and comparing it to the plant (3.27) jointly with the convergence result of Theorem 3.1.1, one can infer the convergence of $\hat{\theta}_2$ to θ_2, but not of $\hat{\theta}_1$.

Table 3.1 shows that this control strategy compares favorably to the PID and the alternative feedback law proposed in [Huang 97]. Furthermore, it is worth noting that the performances obtained here are not the best achievable, as the controller was not tuned for speed convergence but was merely used to illustrate the mechanism.

Chapter 4

Control strategy with an online time-delay update law

Chapitre 4 – Stratégie de contrôle avec adaptation en ligne de l'estimation du retard. *Dans ce chapitre, l'intégration d'une loi d'évolution du retard estimé dans la stratégie de commande est étudiée, ainsi que son impact sur la stabilité en boucle fermée. On montre qu'une large gamme de loi d'adaptation peut être considérée, sous réserve que les variations de l'estimation soient suffisamment lentes. Ce résultat local est illustré en simulation pour une loi particulière d'adaptation inspirée de méthodes d'identification/optimisation.*

Contents

This chapter focuses on derivation of a delay estimate and its integration in the proposed general prediction-based control law. We consider the plant

$$\begin{cases} \dot{X}(t) = AX(t) + BU(t-D) \\ Y(t) = X(t) \end{cases} \tag{4.1}$$

where, compared to (2.15), we consider the plant and the input disturbance d as perfectly known (more conveniently, $d = 0$) and the system state X as fully-measured.

As shown below, a Lyapunov-based synthesis of the delay update law in the spirit of [Bresch-Pietri 09] is not possible without the knowledge of the distributed input u. Instead, to improve the delay estimation, one can use an optimization-based update law (e.g. gradient methods) or exploit some knowledge about delay stochastic properties in the sense of the methods presented in [O'Dwyer 00]. These techniques are shown here to be compliant with the proposed adaptive control scheme, but at the expense of extra assumptions bearing on the delay initial estimate (required to be close enough to the unknown delay value).

This is the main result of this chapter, based on Conditions 1 and 2, presented below which cover relatively large classes of delay update laws.

4.1 Controller design

Following (2.19) and the certainty equivalence principle, we use the control law

$$U(t) = U^r - KX^r + K\hat{D}(t)\int_0^1 e^{A\hat{D}(t)(1-x)}B\hat{u}(x,t)dx + Ke^{A\hat{D}(t)}X(t) \tag{4.2}$$

where the update law for the delay estimate is characterized by one of the following growth conditions expressed in terms of the error variables

$$\tilde{X}(t) = X(t) - X^r\,, \quad e(x,t) = u(x,t) - U^r\,, \quad \hat{e}(x,t) = \hat{u}(x,t) - U^r$$
$$\tilde{e}(x,t) = u(x,t) - \hat{u}(x,t)$$

Condition 1. *There exist positive constants $\gamma_D > 0$ and $M > 0$ such that*

$$\dot{\hat{D}}(t) = \gamma_D \mathrm{Proj}_{[\underline{D},\bar{D}]}\{\tau_D(t)\}$$
$$|\tau_D(t)| \leq M\left(|\tilde{X}(t)|^2 + \|e(t)\|^2 + \|\hat{e}(t)\|^2 + \|\hat{e}_x(t)\|^2\right)$$

where $Proj_{[\underline{D},\bar{D}]}$ is the standard projection operator on the interval $[\underline{D},\bar{D}]$.

Condition 2. *There exists positive constants $\gamma_D > 0$ and $M > 0$ such that*

$$\dot{\hat{D}}(t) = \gamma_D \mathrm{Proj}_{[\underline{D},\bar{D}]}\{\tau_D(t)\}$$
$$\forall t \geq 0, \quad \tau_D(t)\tilde{D}(t) \geq 0 \quad \textit{and} \quad |\tau_D(t)| \leq M$$

where $Proj_{[\underline{D},\bar{D}]}$ is the standard projection operator on the interval $[\underline{D},\bar{D}]$.

The following result was described in a less general form in [Bresch-Pietri 10]. The main difference is the form of delay update law used: int the latter case, only one particular law is proposed[1], whereas both Condition 1 and Condition 2 allow considerations of a large number of laws.

[1]This particular delay update law originates from the case in which the (infinite) state of the transport PDE is known, applying the certainty equivalence principle. In the case of regulation, this update law can be expressed as

$$\tau_D(t) = -\int_0^1 (1+x)\hat{w}(x,t)Ke^{A\hat{D}(t)x}dx\left[A\tilde{X}(t) + B\hat{e}(0,t)\right]$$

which satisfies Condition 1.

Theorem 4.1.1

Consider the closed-loop system consisting of (4.1)*, the control law* (4.2)*, the actuator state estimate* (2.20)–(2.21) *and a delay update law satisfying either Condition 1 or Condition 2. Define*

$$\Gamma(t) = |\tilde{X}(t)|^2 + \|e(t)\|^2 + \|\hat{e}(t)\|^2 + \|\hat{e}_x(t)\|^2 + \tilde{D}(t)^2$$

Then there exist $\gamma^* > 0$, $R > 0$ *and* $\rho > 0$ *such that if* $0 < \gamma_D < \gamma^*$ *and if the initial state satisfies* $\Gamma(0) < \rho$*, then*

$$\forall t \geq 0, \quad \Gamma(t) \leq R\Gamma(0) \tag{4.3}$$

$$Y(t) \underset{t\to\infty}{\to} Y^r, \qquad X(t) \underset{t\to\infty}{\to} X^r \quad \text{and} \qquad U(t) \underset{t\to\infty}{\to} U^r \tag{4.4}$$

From a comparison of this result to Theorem 3.1.1, several remarks can be made. First, it is evident that similar tools are introduced to formulate the two statements. The functional Γ also evaluates the system state, but, as expected, the delay estimation error is included in the functional in place of the parameter.

Theorem 4.1.1 states an asymptotic and local result, as the functional Γ has to be small enough initially.

Condition 1 allows updating of the delay estimate while preserving stability. This condition cannot be checked directly, as some of the signals involved in the upper bound are unavailable. For strict implementability, an alternative constructive choice could be to satisfy the more restrictive assumption $\tau_D(t) \leq M\left(|\tilde{X}(t)| + \|\hat{e}(t)\|^2 + \|\hat{e}_x(t)\|^2\right)$. Conversely, Condition 2 allows consideration of sharper update laws provided that they improve in the estimation, which is consistent with numerous delay identification techniques [O'Dwyer 00].

Use of an online time-delay update-law that satisfies Condition 2 should allow identification of the unknown delay and thus facilitate larger leeway for control (i.e. advanced feedforward strategies). In this context, Condition 1 would then ensure that small computational errors in the delay update law do not jeopardize the stability of the controller. For both cases, Theorem 4.1.1 requires this delay update law to be slow enough ($\gamma_D < \gamma^*$) to guarantee that it does not negatively affect the controller.

4.2 Convergence analysis

4.2.1 Error dynamics and Lyapunov analysis

Following the main steps summarized in Table 2.1, in the following we use a backstepping transformation of the actuator state that satisfies a Volterra integral equation of the second kind,

$$\hat{w}(x,t) = \hat{e}(x,t) - K\hat{D}(t)\int_0^x e^{A\hat{D}(t)(x-y)}B\hat{e}(y,t)dy - Ke^{A\hat{D}(t)x}\tilde{X}(t) \tag{4.5}$$

together with the inverse transformation

$$\hat{e}(x,t) = \hat{w}(x,t) + K\hat{D}(t)\int_0^x e^{(A+BK)\hat{D}(t)(x-y)}B\hat{w}(y,t)dy + Ke^{(A+BK)\hat{D}(t)x}\tilde{X}(t) \tag{4.6}$$

designed to fulfill the boundary condition $\hat{w}(1,t) = 0$ for control law (4.2). This motivates the definition of the following candidate functional

$$\begin{aligned} V(t) =& \tilde{X}(t)^T P\tilde{X}(t) + b_1 D\int_0^1 (1+x)\tilde{e}(x,t)^2 dx \\ &+ b_2\hat{D}(t)\int_0^1 (1+x)\hat{w}(x,t)^2 dx + b_2\hat{D}(t)\int_0^1 (1+x)\hat{w}_x(x,t)^2 dx + \tilde{D}(t)^2 \end{aligned} \tag{4.7}$$

where P is defined in Assumption 3 and b_1 and b_2 are positive coefficients.

First, consider the dynamics of the variables involved in (4.7), which can be written, using (4.5) and (4.6), as

$$\dot{\tilde{X}}(t) = (A+BK)\tilde{X}(t) + B\tilde{e}(0,t) + B\hat{w}(0,t) \tag{4.8}$$

$$\begin{cases} D\tilde{e}_t(x,t) = \tilde{e}_x(x,t) - \tilde{D}(t)f(x,t) - \dot{\hat{D}}(t)D(x-1)f(x,t) \\ \tilde{e}(1,t) = 0 \end{cases} \tag{4.9}$$

$$\begin{cases} \hat{D}(t)\hat{w}_t(x,t) = \hat{w}_x(x,t) - \hat{D}(t)\dot{\hat{D}}(t)g(x,t) - \hat{D}(t)Ke^{A\hat{D}(t)x}B\tilde{e}(0,t) \\ \hat{w}(1,t) = 0 \end{cases} \tag{4.10}$$

$$\begin{cases} \hat{D}(t)\hat{w}_{xt}(x,t) = \hat{w}_{xx}(x,t) - \hat{D}(t)\dot{\hat{D}}(t)g_x(x,t) - \hat{D}(t)^2 KAe^{A\hat{D}(t)x}B\tilde{e}(0,t) \\ \hat{w}_x(1,t) = \hat{D}(t)\dot{\hat{D}}(t)g(1,t) + \hat{D}(t)Ke^{A\hat{D}(t)}B\tilde{e}(0,t) \end{cases} \tag{4.11}$$

where the functions f and g can be expressed, according to (4.5) and (4.6), using the set of variables $(\tilde{e}, \hat{w}, \hat{w}_x)$ as follows

$$\begin{aligned} f(x,t) =& \frac{\hat{w}_x(x,t)}{\hat{D}(t)} + KB\hat{w}(x,t) + K(A+BK)e^{(A+BK)\hat{D}(t)x}\tilde{X}(t) \\ &+ \hat{D}(t)\int_0^x K(A+BK)e^{(A+BK)\hat{D}(t)(x-y)}B\hat{w}(y,t)dy \\ g(x,t) =& (1-x)f(x,t) + \hat{D}(t)K\int_0^x e^{A\hat{D}(t)(x-y)}B(y-1)f(y,t)dy + KAxe^{A\hat{D}(t)x}\tilde{X}(t) \\ &+ \int_0^x K(I + A\hat{D}(t)(x-y))e^{A\hat{D}(t)(x-y)}B\Big[\hat{w}(y,t) + \hat{D}(t)\int_0^y Ke^{(A+BK)\hat{D}(t)(y-\xi)}B\hat{w}(\xi,t)d\xi \\ &+ Ke^{(A+BK)\hat{D}(t)y}\tilde{X}(t)\Big] \end{aligned}$$

Taking a time derivative of V and using suitable integrations by parts, one obtains from

the dynamic equations (4.8)-(4.11)

$$\begin{aligned}\dot{V}(t) = &-\tilde{X}(t)^T Q\tilde{X}(t) + 2\tilde{X}(t)^T PB\left[\tilde{e}(0,t)+\hat{w}(0,t)\right] + b_1\Big(- \|\tilde{e}(t)\|^2 - \tilde{e}(0,t)^2 \\ &- 2\tilde{D}(t)\int_0^1 (1+x)f(x,t)\tilde{e}(x,t)dx + 2\dot{\hat{D}}(t)D\int_0^1 (1-x^2)f(x,t)\tilde{e}(x,t)dx\Big) \\ &+ b_2\Big(- \|\hat{w}(t)\|^2 - \hat{w}(0,t)^2 - 2\hat{D}(t)\dot{\hat{D}}(t)\int_0^1 (1+x)g(x,t)\hat{w}(x,t)dx \\ &- 2\hat{D}(t)\int_0^1 (1+x)Ke^{A\hat{D}(t)x}B\tilde{e}(0,t)\hat{w}(x,t)dx\Big) + b_2\left(2\hat{w}_x(1,t)^2 - \hat{w}_x(0,t)^2 - \|\hat{w}_x(t)\|^2\right. \\ &\left.-2\hat{D}(t)\dot{\hat{D}}(t)\int_0^1 (1+x)g_x(x,t)\hat{w}_x(x,t)dx - 2\hat{D}(t)^2\int_0^1 (1+x)KAe^{A\hat{D}(t)x}B\tilde{e}(0,t)\hat{w}_x(x,t)dx\right) \\ &+ b_2\dot{\hat{D}}(t)\int_0^1 (1+x)[\hat{w}(x,t)^2+\hat{w}_x(x,t)^2]dx - 2\tilde{D}(t)\dot{\hat{D}}(t)\end{aligned}$$

The magnitude of the resulting non-negative terms can be bounded. Indeed, using Young and Cauchy-Schwartz inequalities, one can obtain the following inequalities, where $M_1,\ldots,M_6$ are positive constants independent of the initial conditions,

$$\begin{aligned}2\tilde{X}(t)^T PB\left[\tilde{e}(0,t)+\hat{w}(0,t)\right] &\leq \frac{\lambda_{min}(Q)}{2}|\tilde{X}(t)|^2 + \frac{4\|PB\|^2}{\lambda_{min}(Q)}(\tilde{e}(0,t)^2+\hat{w}(0,t)^2) \\ 2\int_0^1 (1+x)|f(x,t)\tilde{e}(x,t)|dx &\leq M_1\left(|\tilde{X}(t)|^2+\|\tilde{e}(t)\|^2+\|\hat{w}(t)\|^2+\|\hat{w}_x(t)\|^2\right) \\ 2\int_0^1 (1-x^2)|f(x,t)\tilde{e}(x,t)|dx &\leq M_1\left(|\tilde{X}(t)|^2+\|\tilde{e}(t)\|^2+\|\hat{w}(t)\|^2+\|\hat{w}_x(t)\|^2\right) \\ 2\hat{D}(t)\int_0^1 (1+x)|g(x,t)\hat{w}(x,t)|dx &\leq M_2\left(|\tilde{X}(t)|^2+\|\hat{w}(t)\|^2+\|\hat{w}_x(t)\|^2\right) \\ 2\hat{D}(t)\int_0^1 (1+x)\left|Ke^{A\hat{D}(t)x}B\tilde{e}(0,t)\hat{w}(x,t)\right|dx &\leq M_3\tilde{e}(0,t)^2+\|\hat{w}(t)\|^2/2 \\ 2\hat{w}_x(1,t)^2 &\leq M_4\left(\dot{\hat{D}}(t)^2\left(|\tilde{X}(t)|^2+\|\hat{w}(t)\|^2+\|\hat{w}_x(t)\|^2\right)+\tilde{e}(0,t)^2\right) \\ 2\hat{D}(t)\int_0^1 (1+x)|g_x(x,t)\hat{w}_x(x,t)|dx &\leq M_5\left(|\tilde{X}(t)|^2+\|\hat{w}(t)\|^2+\|\hat{w}_x(t)\|^2+\hat{w}_x(0,t)^2\right) \\ 2\hat{D}(t)^2\int_0^1 (1+x)\left|KAe^{A\hat{D}(t)x}B\tilde{e}(0,t)\hat{w}_x(x,t)\right|dx &\leq M_6\tilde{e}(0,t)^2+\|\hat{w}_x(t)\|^2/2\end{aligned}$$

Consequently, if one defines $V_0(t) = |\tilde{X}(t)|^2+\|\tilde{e}(t)\|^2+\|\hat{w}(t)\|^2+\|\hat{w}_x(t)\|^2$, the previous ineequality yields

$$\begin{aligned}\dot{V}(t) \leq &-\frac{\lambda_{min}(Q)}{2}|\tilde{X}(t)|^2 - b_1\|\tilde{e}(t)\|^2 - \frac{b_2}{2}\|\hat{w}(t)\|^2 - \frac{b_2}{2}\|\hat{w}_x(t)\|^2 \\ &- \left(b_2 - \frac{4\|PB\|^2}{\lambda_{min}(Q)}\right)\hat{w}(0,t)^2 - \left(b_1 - \frac{4\|PB\|^2}{\lambda_{min}(Q)} - b_2M_3 - b_2M_4 - b_2M_6\right)\tilde{e}(0,t)^2 \\ &+ \left(b_1|\tilde{D}(t)|M_1 + b_1\bar{D}|\dot{\hat{D}}(t)|M_1 + b_2|\dot{\hat{D}}(t)|M_2 + b_2M_4\dot{\hat{D}}(t)^2 + b_2M_5|\dot{\hat{D}}(t)| + 2b_2|\dot{\hat{D}}(t)|\right)V_0(t) \\ &- 2\tilde{D}(t)\dot{\hat{D}}(t) - b_2\left(1-|\dot{\hat{D}}(t)|M_5\right)\hat{w}_x(0,t)^2 \qquad (4.12)\end{aligned}$$

Conveniently, to make the terms in $\tilde{e}(0,t)^2$ and $\hat{w}(0,t)^2$ vanish, one can choose constant coefficients b_1 and b_2 such that $b_2 = \frac{8\|PB\|^2}{\lambda_{min}(Q)}$ and $b_1 > b_2\left(\frac{1}{2} + M_3 + M_4 + M_6\right)$ The techniques for treating the remaining non-negative terms slightly depend on whether Condition 1 or Condition 2 is satisfied. We now distinguish the two cases.

4.2.2 Delay update law satisfying Condition 1

First, considering (4.5)-(4.6) and applying Young's inequality, one can establish the following inequalities

$$\|\hat{e}(t)\|^2 \leq r_1|\tilde{X}(t)|^2 + r_2\|\hat{w}(t)\|^2 \tag{4.13}$$

$$\|\hat{e}_x(t)\|^2 \leq r_3|\tilde{X}(t)|^2 + r_4\|\hat{w}(t)\|^2 + r_5\|\hat{w}_x(t)\|^2 \tag{4.14}$$

$$\|\hat{w}(t)\|^2 \leq s_1|\tilde{X}(t)|^2 + s_2\|\hat{e}(t)\|^2 \tag{4.15}$$

$$\|\hat{w}_x(t)\|^2 \leq s_3|\tilde{X}(t)|^2 + s_4\|\hat{e}(t)\|^2 + s_5\|\hat{e}_x(t)\|^2 \tag{4.16}$$

where $r_1, r_2, r_3, r_4, r_5, s_1, s_2, s_3, s_4$ and s_5 are positive constants. Using (4.13) and (4.14), Condition 1 (with $M > 0$) can be reformulated as

$$|\dot{\hat{D}}(t)| \leq \gamma_D M V_0(t)$$

which, with $\eta = \min\{\lambda_{min}(Q)/2, b_1, b_2/2\}$, yields

$$\dot{V}(t) \leq -\left(\eta - b_1|\tilde{D}(t)|M_1 - 2|\tilde{D}(t)|\gamma_D M\right)V_0(t) + \gamma_D M\left(b_2M_2 + b_1\bar{D}M_1 + b_2M_5 + 2b_2\right)V_0(t)^2$$
$$+ b_2M_4\gamma_D^2M^2V_0(t)^3 - b_2\left(1 - \gamma_D M V_0(t)M_5\right)\hat{w}_x(0,t)^2$$

Furthermore, we use the following bound, where $\epsilon_1 > 0$,

$$|\tilde{D}(t)| \leq \frac{\epsilon_1}{2} + \frac{1}{2\epsilon_1}\left(V(t) - \eta V_0(t)\right) \tag{4.17}$$

and obtain

$$\dot{V}(t) \leq -\left(\eta - (b_1M_1 + 2\gamma_D M)\left(\frac{\epsilon_1}{2} + \frac{V(t)}{2\epsilon_1}\right)\right)V_0(t) - b_2\left(1 - \gamma_D M V_0(t)M_5\right)\hat{w}_x(0,t)^2$$
$$-\left((b_1M_1 + 2\gamma_D M_1)\frac{\eta}{2\epsilon_1} - \gamma_D M(b_2M_2 + b_1\bar{D}M_1 + b_2M_5 + 2b_2) - b_2M_4\gamma_D^2M^2V_0(t)\right)V_0(t)^2$$

By choosing ϵ_1 such that

$$\epsilon_1 < \min\left\{\frac{2\eta}{b_1M_1 + 2\gamma_D M}, \frac{\eta(b_1M + 2\gamma_D M)}{2\gamma_D M(b_2M_2 + b_1\bar{D}M_1 + b_2M_5 + 2b_2)}\right\}$$

and restricting the initial condition to

$$V(0) < \min\left\{\epsilon_1\left(\frac{2\eta}{b_1M_1 + 2\gamma_D M} - \epsilon_1\right),\right.$$
$$\left.\frac{\eta}{b_2M_4\gamma_D^2M^2}\left((b_1M_1 + 2\gamma_D M)\frac{\eta}{2\epsilon_1} - \gamma_D M(b_2M_2 + b_1\bar{D}M_1 + b_2M_5 + 2b_2)\right), \frac{\eta}{\gamma_D M M_5}\right\}$$

we conclude that there exist non-negative functions μ_1 and μ_2 such that

$$\dot{V}(t) \leq -\mu_1(t)V_0(t) - \mu_2(t)V_0(t)^2 \tag{4.18}$$

and finally

$$\forall t \geq 0\,, \quad V(t) \leq V(0) \tag{4.19}$$

This gives the conclusion.

4.2.3 Delay update law satisfying Condition 2

Inequality (4.12), together with (4.17), gives

$$\begin{aligned}\dot{V}(t) \leq &- \left(\eta - b_1 M_1 \left(\frac{\epsilon_1}{2} + \frac{V(t)}{2\epsilon_1}\right) - \gamma_D M(b_1 \bar{D} M_1 + b_2(M_2 + \gamma_D M M_4 + M_5 + 2))\right) V_0(t) \\ &- b_2 \left(1 - \gamma_D M M_5\right) \hat{w}_x(0,t)^2\end{aligned}$$

Consequently, by choosing the delay update gain γ_D and the parameter ϵ_1 such that

$$\begin{aligned}\gamma_D <& \min\left\{\frac{\eta}{M(b_1\bar{D}M_1 + b_2(M_2 + MM_4 + M_5 + 2))}, \frac{1}{MM_5}, 1\right\} \\ \frac{\epsilon_1}{2} <& \frac{\eta - \gamma_D M(b_1\bar{D}M_1 + b_2(M_2 + \gamma_D M M_4 + M_5 + 2))}{b_1 M_1 + 2\gamma_D M}\end{aligned}$$

and restricting the initial condition to satisfy

$$V(0) < 2\epsilon_1 \left(\frac{\eta - \gamma_D M b_1 \bar{D} M_1}{b_1 M_1} - \frac{\epsilon_1}{2} + \frac{\gamma_D M b_2(M_2 + \gamma_D M M_4 + M_5 + 2)}{b_1 M_1}\right)$$

one finally obtains

$$\dot{V}(t) \leq - \mu(t) V_0(t) \tag{4.20}$$

where μ is a non-negative function. Consequently,

$$\forall t \geq 0\,, \quad V(t) \leq V(0) \tag{4.21}$$

This gives the conclusion.

4.2.4 Equivalence and convergence result

Stability results for the Lyapunov function V have been provided in (4.19) and (4.21) respectively. In view of the proof of Theorem 4.1.1, as previously, we now show the equivalence of the two functionals V and Γ.

Using (4.13)-(4.16), one directly obtains this property as follows

$$\begin{aligned}\Gamma(t) \leq& |\tilde{X}(t)|^2 + 2\left\|\tilde{e}(t)\right\|^2 + 3\left\|\hat{e}(t)\right\|^2 + \left\|\hat{e}_x(t)\right\|^2 + \tilde{D}(t)^2 \\ \leq& \frac{\max\left\{1 + 3r_1 + r_3, 3r_2 + r_4, r_5, 2\right\}}{\min\left\{\lambda_{min}(P), b_1 D, b_2 \underline{D}, 1\right\}} V(t) \\ V(t) \leq& \max\left\{\lambda_{max}(P) + 2s_1 b_1 \bar{D} + 2s_3 b_2 \bar{D}, 4b_1 D + 2s_2 b_1 \bar{D} + 2s_4 b_2 \bar{D}, 2s_5 b_2 \bar{D}, 1\right\} \Gamma(t)\end{aligned}$$

This gives the desired stability property (4.3) with $R = b/a$.

We can now conclude the proof of Theorem 4.1.1, by applying Barbalat's Lemma to the variables $|\tilde{X}(t)|^2$ and $\tilde{U}(t)^2$. Integrating (4.18) and (4.20) from 0 to $+\infty$, we can directly conclude that both quantities are integrable. Furthermore, from (4.8), one has

$$\frac{d|\tilde{X}(t)|^2}{dt} = 2\tilde{X}(t)^T((A + BK)\tilde{X}(t) + B\tilde{e}(0,t) + B\hat{w}(0,t))$$

From (4.19) or (4.21), it follows that $|\tilde{X}(t)|, \|\tilde{e}(t)\|$, $\|\hat{w}(t)\|$ and $\|\hat{w}_x(t)\|$ are uniformly bounded. Then, according to (4.13), we obtain the uniform boundedness of $\|\hat{e}(t)\|$ and

consequently of $\|\hat{u}(t)\|$. From (4.2), we conclude that $U(t)$ is uniformly bounded, and therefore that $\tilde{e}(0,t) = U(t-D) - U(t-\hat{D}(t))$ is bounded for $t \geq \bar{D}$. Furthermore, from the definition (4.5), we obtain the uniform boundedness of $\hat{w}(0,t)$ for $t \geq \bar{D}$ and of $d(|\tilde{X}(t)|^2)/dt$ for $t \geq \bar{D}$. Finally, using Barbalat's lemma, we conclude that $\tilde{X}(t) \to 0$ as $t \to \infty$.

Similarly, from (4.2), one can obtain

$$\frac{d\tilde{U}(t)^2}{dt} = 2\tilde{U}(t)\left(Ke^{A\hat{D}(t)}\dot{\tilde{X}}(t) + \hat{D}(t)G_0(t) + H_0(t)\right)$$

with

$$\begin{aligned} G_0(t) =& K\left[e^{A\hat{D}(t)}A\tilde{X}(t) + \int_0^1 e^{A\hat{D}(y)(1-y)}B(y-1)\hat{e}_x(y,t)dy\right. \\ &\left. + \int_0^1 (I + A\hat{D}(t)(1-y))e^{A\hat{D}(t)(1-y)}B\hat{e}(y,t)dy\right] \\ H_0(t) =& K\int_0^1 e^{A\hat{D}(t)(1-y)}B\hat{e}_x(y,t)dy \end{aligned}$$

Using (4.14), we deduce from above that $\|\hat{e}_x(t)\|$ is uniformly bounded. Therefore, it is straightforward to obtain the uniform boundedness of G_0 and H_0 and the one of $d\tilde{U}(t)^2/dt$, using Assumption 1 and the previous arguments. Then, applying Barbalat's Lemma, we conclude the $\tilde{U}(t) \to 0$ as $t \to \infty$. This concludes the proof of Theorem 4.1.1.

4.2.5 Main specificity of the proof of Theorem 4.1.1 and other comments

The transformed state of the actuator plays a key role in the Lyapunov analysis and in the emergence of negative bounding terms in particular. However, compared to the proof presented in the previous chapter, this backstepping transformation is only a generic tool for studying stability and does not play any constructive role in the control design.

Here, the main difficulties stem from treatment of the delay update law $\dot{\hat{D}}(t)$ and the delay estimate error $\tilde{D}(t)$. These two difficulties arise from the same fact: the dynamics of $\tilde{e}$ results in a bilinear term in $\dot{V}$, namely a $\tilde{D}(t)\tilde{e}(.,t)$, that is difficult to handle in a Lyapunov design [Ioannou 06]; this has been used in previous studies in which this term is linear, as it was assumed that $\tilde{e}(.,t)$ is measured [Bresch-Pietri 09, Krstic 09b]. The first difficulty is addressed by the formulation of Condition 1 and Condition 2. The second one implies both the definition of the intermediate functional V_0 and the restriction imposed on the initial condition. Furthermore, a direct consequence is the necessity to invoke Barbalat's Lemma to transform the stability (4.3) into the asymptotic convergence (4.4).

4.3 Illustrative example

We consider the same illustrative example as in Chapter 3 in which the following open-loop unstable system under state-space representation was considered

$$\dot{X}(t) = \begin{pmatrix} 0 & \frac{1}{aT} \\ 1 & \frac{a-T}{aT} \end{pmatrix} X(t) + \begin{pmatrix} \frac{k}{aT} \\ 0 \end{pmatrix} U(t-D) \tag{4.22}$$

$$Y(t) = (0 \quad 1)X(t) \tag{4.23}$$

where a and T positive parameters and the time value of the time-delay $D = 0.939$ is unknown, but is supposed to belong to the known interval $[\underline{D}, \bar{D}] = [0.8, 1.1]$.

4.3.1 Delay update law design

We focus here on the design of a particular delay update law satisfying Condition (2). For this, we define the cost function

$$\begin{aligned}&\phi : [0, +\infty) \times [\underline{D}, \bar{D}] \to \mathbb{R},\\ &\quad (t, \hat{D}) \mapsto |X_P(t, \hat{D}) - X(t)|^2 = \left| e^{A(t-\hat{D})} X(\hat{D}) + \int_{\hat{D}}^{t} e^{A(t-s)} BU(s - \hat{D}) ds - X(t) \right|^2\end{aligned}$$

where $X_P(t, \hat{D})$ is a $(t - \hat{D})-$units of time ahead prediction of the system state, using $X(\hat{D})$ as the initial condition and assuming that the actual delay value is $\hat{D}(t)$. Then, using a steepest descent algorithm, one can take

$$\begin{aligned}\tau_D(t) =& -\gamma_D (X_P(t, \hat{D}) - X(t)) \times \frac{\partial X_P}{\partial \hat{D}}(t, \hat{D}) \\ \frac{\partial X_P}{\partial \hat{D}} =& e^{At} BU(0) - BU(t - \hat{D}) - \int_{\hat{D}}^{t} A e^{A(t-\tau)} BU(\tau - \hat{D}) d\tau\end{aligned} \tag{4.24}$$

where these expressions are directly implementable.

This choice is based on comparison of two versions of a signal, one (measured) corresponding to the unknown delay D and another computed with a prediction using the controlled delay $\hat{D}(t)$. The descent algorithm provides an accurate estimation of the unknown delay provided that the initial delay estimate is sufficiently close to the true value. In particular, this condition, which is compliant with the one stated in Theorem 4.1.1, guarantees that no extraneous local minimum interferes with the minimization process.

4.3.2 Simulation results

Simulation results are reported in Figure 4.1. The tracked trajectory is a periodic signal, with the period set to highlight transient behaviors. It is evident that the delay estimate eventually converges to the unknown delay. The most visible improvements in the estimation occur immediately after step changes in the reference signal. This is consistent with the update law, as the cost function shows the most significant gradient at these instants. This identification extends the possibilities for regulation, as accurate tracking of any time-varying smooth trajectory is then achievable.

In general, the performance of the controller is consistent with the properties stated in Theorem 4.1.1.

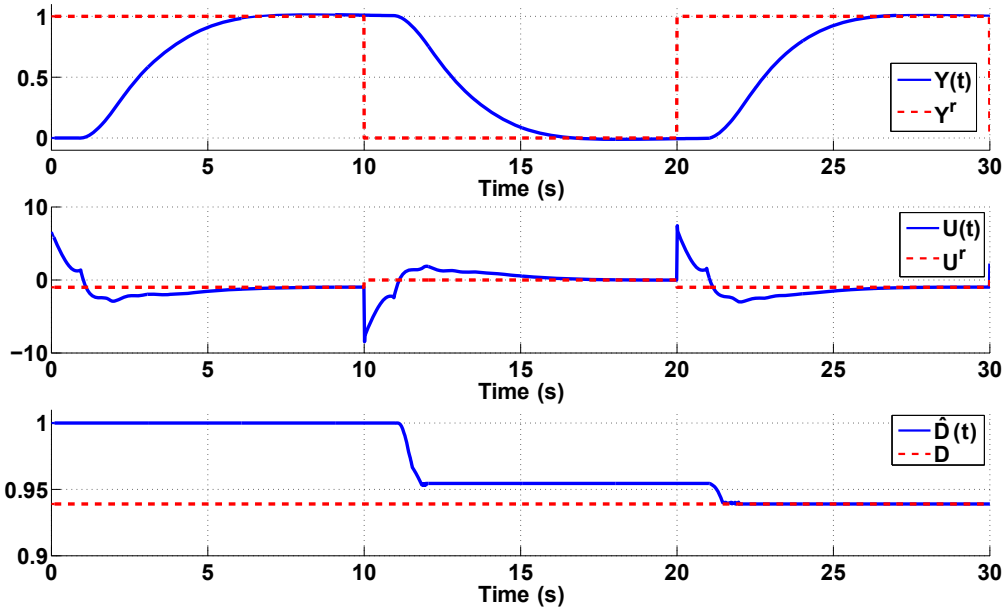

Figure 4.1: Simulation results for control of system (4.22), starting from $X(0) = [0 \quad 0]^T$, $u(.,0) = 0$ and $\hat{D}(0) = 1$. The gradient-based delay update law (4.24) is used, with $\gamma_D = 50$ and the controller gain K is chosen according to an LQR criterion.

Chapter 5

Output feedback strategy

Chapitre 5 – Stratégie de retour de sortie. *L'extension d'une loi de contrôle par prédiction au retour de sortie est réalisée dans ce chapitre. Les résultats de convergence obtenus ici sont globaux et exponentiels, sous réserve que l'erreur d'estimation du retard de commande soit suffisamment faible. Nous illustrons les performances de cette loi de contrôle sur un système de réchauffeur dont la dynamique (stable) a fait l'objet de tests d'identification sur banc moteur.*

Contents

In this chapter, we consider the more general case of partial measurement of the system state X and design an output feedback version of the prediction-based controller. The plant considered here is

$$\begin{cases} \dot{X}(t) = AX(t) + BU(t-D) \\ Y(t) = CX(t) \end{cases} \tag{5.1}$$

where, compared to (2.15), we consider the plant as known (and certain) and the input disturbance d known and, more conveniently, equal to zero. The output dimension m is supposed to be strictly inferior to the state dimension n.

The control design we propose originates from the delay-compensation observer form previously described in [Klamka 82] [Watanabe 81] and incorporates modifications corresponding to the presence of an input in the plant.

5.1 Controller design

First, using the estimate waiting line introduced in (2.20)–(2.21), we define the following observer for the system state

$$\dot{\hat{X}}(t) = A\hat{X}(t) + B\hat{u}(0,t) - L(Y(t) - C\hat{X}(t)) \tag{5.2}$$

where the vector gain L is defined through the following additional assumption.

Assumption 5. *The pair (A, C) is observable and $L \in \mathbb{R}^{n\times m}$ is a stabilizing gain.*

Applying the certainty equivalence principle, we use the control law

$$U(t) = U^r - KX^r + K\left[e^{A\hat{D}}\hat{X}(t) + \hat{D}\int_0^1 e^{A\hat{D}(1-y)}B\hat{u}(y,t)dy\right] \tag{5.3}$$

and introduce several error variables,

$$\Delta X(t) = X(t) - X^r\,,\ \Delta\hat{X}(t) = \hat{X}(t) - X^r\,,\ \tilde{X}(t) = X(t) - \hat{X}(t)$$

Theorem 5.1.1

Consider the closed-loop system, consisting of (5.1), the plant estimate (5.2) and the control law (5.3). Define

$$\Gamma(t) = |\Delta X(t)|^2 + |\Delta\hat{X}(t)|^2 + \|e(t)\|^2 + \|\hat{e}(t)\|^2 + \|\hat{e}_x(t)\|^2 \tag{5.4}$$

Then there exist $\delta^* > 0$, $R > 0$ and $\rho > 0$ such that, if $|\tilde{D}| < \delta^*$, then for any initial conditions one has

$$\forall t \geq 0, \quad \Gamma(t) \leq R\Gamma(0)e^{-\rho t} \tag{5.5}$$

and, consequently, $Y(t) \to Y^r$ and $\tilde{X}(t) \to 0$ as $t \to \infty$.

Again, the statement comprises a functional Γ that evaluates the overall system. The functional contains the state observation error.

Compared to the previous chapters, two main differences should be noted: the convergence is now global (provided that the delay estimate is chosen close enough to the uncertain delay, which can be understood here as robustness to delay mismatch) and exponential. The reasons for these differences are detailed above.

5.2 Convergence analysis

5.2.1 Error dynamics and Lyapunov analysis

Following similar lines to the proof of the previous results (summarized in Table 2.1), we define the following candidate Lyapunov functional

$$V(t) = \Delta\hat{X}(t)^T P_1 \Delta\hat{X}(t) + b_0\tilde{X}(t)P_2\tilde{X}(t) + b_1 D\int_0^1 (1+x)\tilde{e}(x,t)^2 dx$$
$$+ b_2\hat{D}\int_0^1 (1+x)[\hat{w}(x,t)^2 + \hat{w}_x(x,t)^2]dx \tag{5.6}$$

where b_0, b_1 and b_2 are positive coefficients, $(P_1, Q_1) = (P, Q)$ is defined in Assumption 3 and the symmetric definite matrix P_2 satisfies the following Lyapunov equation, with Q_2 a given symmetric definite positive matrix,

$$P_2(A + LC) + (A + LC)^T P_2 = - Q_2 \tag{5.7}$$

The transformed state of the actuator is then defined through the following Volterra integral equation of the second kind

$$\hat{w}(x,t) = \hat{e}(x,t) - \hat{D} \int_0^x K e^{A\hat{D}(x-y)} B \hat{e}(y,t) dy - K e^{A\hat{D}x} \Delta \hat{X}(t) \tag{5.8}$$

which satisfies the boundary property $\hat{w}(1,t) = 0$, taking into account the control law (5.3). First, we consider this transformation jointly with its inverse to obtain the dynamics of the variables in (5.6)

$$\begin{aligned}
&\dot{\tilde{X}}(t) = (A + LC)\tilde{X}(t) + B\tilde{e}(0,t) \\
&\frac{d\Delta\hat{X}}{dt} = (A + BK)\Delta\hat{X}(t) + B\hat{w}(0,t) - LC\tilde{X}(t) \\
&\begin{cases} D\tilde{e}(x,t) = \tilde{e}_x(x,t) - \tilde{D} f(x,t) \\ \tilde{e}(1,t) = 0 \end{cases} \\
&\begin{cases} \hat{D}\hat{w}_t(x,t) = \hat{w}_x(x,t) + \hat{D} K e^{A\hat{D}x} LC\tilde{X}(t) \\ \hat{w}(1,t) = 0 \end{cases} \\
&\begin{cases} \hat{D}\hat{w}_{xt}(x,t) = \hat{w}_{xx}(x,t) + \hat{D}^2 K A e^{A\hat{D}x} LC\tilde{X}(t) \\ \hat{w}_x(1,t) = - \hat{D} K e^{A\hat{D}} LC\tilde{X}(t) \end{cases}
\end{aligned}$$

where the function f can be expressed in terms of $(\hat{w}, \hat{w}_x)$ in the form

$$\begin{aligned}
f(x,t) = &\frac{\hat{w}_x(x,t)}{\hat{D}} + KB\hat{w}(x,t) + K(A + BK)e^{(A+BK)\hat{D}x}\Delta\hat{X}(t) \\
&+ \hat{D}\int_0^x K(A + BK)e^{(A+BK)\hat{D}(x-y)} B\hat{w}(y,t)dy
\end{aligned}$$

Taking a time derivative of V and using suitable integrations by parts, one obtains

$$\begin{aligned}
\dot{V}(t) = &- \Delta\hat{X}(t)^T Q_1 \Delta\hat{X}(t) + 2\Delta\hat{X}(t)^T P_1 B\hat{w}(0,t) - 2\Delta\hat{X}(t)^T P_1 LC\tilde{X}(t) \\
&+ b_0 \left(-\tilde{X}(t)^T Q_2 \tilde{X}(t) + 2\tilde{X}(t) P_2 B\tilde{e}(0,t) \right) \\
&+ b_1 \left(- \|\tilde{e}(t)\|^2 - \tilde{e}(0,t)^2 - 2\tilde{D}\int_0^1 (1+x)\tilde{e}(x,t) f(x,t) dx \right) \\
&+ b_2 \left(- \|\hat{w}(t)\|^2 - \hat{w}(0,t)^2 + 2\hat{D}\int_0^1 (1+x)\hat{w}(x,t) K e^{A\hat{D}x} LC\tilde{X}(t) dx \right) \\
&+ b_2 \left(2\hat{w}_x(1,t)^2 - \hat{w}_x(0,t)^2 - \|\hat{w}_x(t)\|^2 + 2\hat{D}^2 \int_0^1 (1+x)\hat{w}_x(x,t) K A e^{A\hat{D}x} LC\tilde{X}(t) dx \right)
\end{aligned}$$

Choosing $b_2 \geq 4|P_1B|^2/\lambda_1$, $b_0 \geq 16\frac{|P_1LC|^2}{\lambda_1\lambda_2}$, one gets

$$\begin{aligned}\dot{V}(t) \leq & -\frac{\lambda_1}{4}|\Delta\hat{X}(t)|^2 - \frac{b_0\lambda_2}{4}|\tilde{X}(t)|^2 - b_1\left\|\tilde{e}(t)\right\|^2 - \left(b_1 - \frac{2|P_2B|^2}{\lambda_2 b_0}\right)\tilde{e}(0,t)^2 - b_2\left\|\hat{w}(t)\right\|^2 \\ & - \frac{b_2}{2}\hat{w}(0,t)^2 + 2b_2\hat{w}_x(1,t)^2 - b_2\left\|\hat{w}_x\right\|^2 - b_2\hat{w}_x(0,t)^2 + 2b_1|\tilde{D}|\int_0^1(1+x)|\tilde{e}(x,t)||f(x,t)|dx \\ & + 2b_2\hat{D}\int_0^1(1+x)|Ke^{A\hat{D}x}LC\tilde{X}(t)\hat{w}(x,t)|dx \\ & + 2b_2\hat{D}(t)^2\int_0^1(1+x)|KAe^{A\hat{D}(t)x}LC\tilde{X}(t)\hat{w}_x(x,t)|dx\end{aligned}$$

Applying Young's and Cauchy-Schwartz's inequalities, one can show that there exist positive constants M_1, M_2, M_3 and M_4 that are independent on initial conditions such that

$$\begin{aligned}2\int_0^1(1+x)|\tilde{e}(x,t)||f(x,t)|dx &\leq M_1\left(|\Delta\hat{X}(t)|^2 + \left\|\tilde{e}(t)\right\|^2 + \left\|\hat{w}(t)\right\|^2 + \left\|\hat{w}_x(t)\right\|^2\right) \\ 2\hat{D}\int_0^1(1+x)|Ke^{A\hat{D}x}LC\hat{w}(x,t)dx| &\leq M_2|\tilde{X}(t)|^2 + \left\|\hat{w}(t)\right\|^2/2 \\ 2\hat{w}_x(1,t)^2 &\leq M_3|\tilde{X}(t)|^2 \\ 2\hat{D}^2\int_0^1(1+x)|KAe^{A\hat{D}x}LC\hat{w}_x(x,t)|dx &\leq M_4|\tilde{X}(t)|^2 + \left\|\hat{w}_x(t)\right\|^2/2\end{aligned}$$

One can use the last inequalities to bound the resulting positive terms in the last expression of $\dot{V}$. By choosing $b_1 \geq \frac{2|P_2B|^2}{\lambda_2 b_0}$ and $b_0 \geq \frac{8b_2}{\lambda_2}(M_2 + M_3 + M_4)$, we define the quantities

$$\begin{aligned}V_0(t) =& |\Delta\hat{X}(t)|^2 + |\tilde{X}(t)|^2 + \left\|\tilde{e}(t)\right\|^2 + \left\|\hat{w}(t)\right\|^2 + \left\|\hat{w}_x(t)\right\|^2 \\ \eta =& \min\{\lambda_1/4, b_0\lambda_2/8, b_1, b_2/2\}\end{aligned} \tag{5.9}$$

and obtain

$$\dot{V}(t) \leq -\left(\eta - b_1M_1|\tilde{D}|\right)V_0(t)$$

Consequently, if we assume $\tilde{D} < \frac{\eta}{2b_1M_1} = \delta^*$, we can finally conclude that

$$\dot{V}(t) \leq -\frac{\eta}{2}V_0(t) \leq -\frac{\eta V(t)}{2\max\left\{\lambda_{max}(P_1), b_0\lambda_{max}(P_2), 2b_1D, 2b_2\hat{D}\right\}}$$

This establishes the existence of $\rho > 0$ such that

$$\forall t \geq 0\,, \quad V(t) \leq V(0)e^{-\rho t} \tag{5.10}$$

This concludes the proof of Theorem 5.1.1.

5.2.2 Equivalence and convergence

In view of obtaining the exponential stability result stated in Theorem 5.1.1, we prove that the two functionals Γ and V are equivalent, in other words that there exist $a > 0$

and $b > 0$ such that $\forall t \geq 0, aV(t) \leq \Gamma(t) \leq bV(t)$. This is straightforward and follows the same lines as in Chapters 3 and 4. Then, using (5.10), one directly obtains

$$\Gamma(t) \leq bV(t) \leq bV(0)e^{-\rho t} \leq \frac{b}{a}\Gamma(0)e^{-\rho t}$$

which gives the desired exponential convergence result with $R = b/a$. This concludes the proof of Theorem 5.1.1 without the need to invoke Barbalat's Lemma, as was done earlier, because the Lyapunov analysis directly provides asymptotic stability.

5.2.3 Main specificity and other comments

The main challenge in this chapter has been the introduction of a second error variable to account for the state estimation error. This additional variable is treated in the proof according to the dedicated Lyapunov equation (5.7), highlighting the stability of its internal dynamics.

In fact, this stability is directly related to the global and exponential convergence of the overall system. In the previous chapters and the following one, the existence of estimation error variables, which were impossible to compensate, motivated the definition of a "truncated" functional V_0 to express a restriction on the initial condition. The resulting bound on the time derivative of the Lyapunov functional then appears as a function of this truncated functional, which cannot be directly compared to the original Lyapunov one. Nevertheless, in the present case, there are no such terms because the state estimation error is asymptotically stable. Therefore, the intermediate functional V_0 defined in (5.9) does not need to be truncated and is directly equivalent to the Lyapunov functional V.

5.3 Illustration : control of an air heater

For illustration, we present an automotive engine control problem. The system considered is an air heater that uses electrical resistance of power ϕ to heat the intake air. As shown in Appendix A, thermal exchange between the air and the electrical device can be efficiently represented by an asymptotically stable third-order plus delay transfer function

$$G(s) = \frac{K_H(T_z s + 1)}{a_3 s^3 + a_2 s^2 + a_1 s + 1} e^{-Ds} \tag{5.11}$$

In practice, the delay varies due to both transport phenomena and communication lags. This variability is treated here as an uncertainty. Furthermore, as mentioned in Appendix A, the plant parameters may be subject to large variations. However, careful identification of the gain is possible. Then, because the plant is asymptotically stable for every value of the parameters, updating of the parameters in the control design is not necessary. Therefore, for clarity, we consider the plant as perfectly known.

The control objective is to have the output of the system (air temperature) reach a set-point T_{ref} as fast as possible. The described context motivates the use of the proposed prediction-based approach. Because of the third-order dynamics and the fact that only the outlet temperature of the gas is measured, an observer design is clearly necessary if one desires to reach good performances.

5.3.1 State-space representation

We consider a canonical state-space realization of the previous process using the three-dimensional state

$$X = \begin{pmatrix} Y(t) \\ \dot{Y}(t) \\ \ddot{Y}(t) - K_H \frac{T_z}{a_3} u \end{pmatrix}$$

and define the corresponding dynamics matrices

$$A = \begin{pmatrix} 0 & 1 & 0 \\ 0 & 0 & 1 \\ -\frac{1}{a_3} & -\frac{a_1}{a_3} & -\frac{a_2}{a_3} \end{pmatrix}, \quad B = \begin{pmatrix} 0 \\ K_H \frac{T_z}{a_3} \\ \frac{K_H}{a_3} - K_H T_z \frac{a_2}{a_3^2} \end{pmatrix} \quad \text{and} \quad C = (1 \quad 0 \quad 0) \tag{5.12}$$

With this representation, reconstruction of the last two coordinates of the system state is necessary and requires an observer design. Finally, for a given output temperature set point $Y^r = T_{ref}$, the corresponding equilibrium in the state space is

$$U_r = \frac{1}{K_H} Y^r \quad \text{and} \quad X^r = \begin{pmatrix} Y^r \\ 0 \\ -\frac{T_z \hat{\theta}_1}{a_3} Y^r \end{pmatrix}$$

5.3.2 Simulation results

Simulation results for the feedback strategy are reported in Figure 5.1. For simplicity, we consider a given operating point for the heater (i.e. a constant gas velocity), which results in a constant delay of $D = 10$ s and constant coefficients $a_3 = 1560$, $a_2 = 9300$, $a_1 = 250$ and $K_H = 0.075$. The system is assumed to be initially at the origin $X(0) = [0 \quad 0 \quad 0]$ and is erroneously estimated as $\hat{X}(0) = [0 \quad 0.1 \quad 0.1]^T$. Finally, the delay is overestimated with $\hat{D} = 15$ s.

First, one can observe that the response time of the system is considerably improved by the feedback strategy. Second, the effect of the delay estimation error is particularly notable at the beginning of the observer response.

From a more general point of view, this behavior is consistent with that usually obtained for the design of a linear system observer.

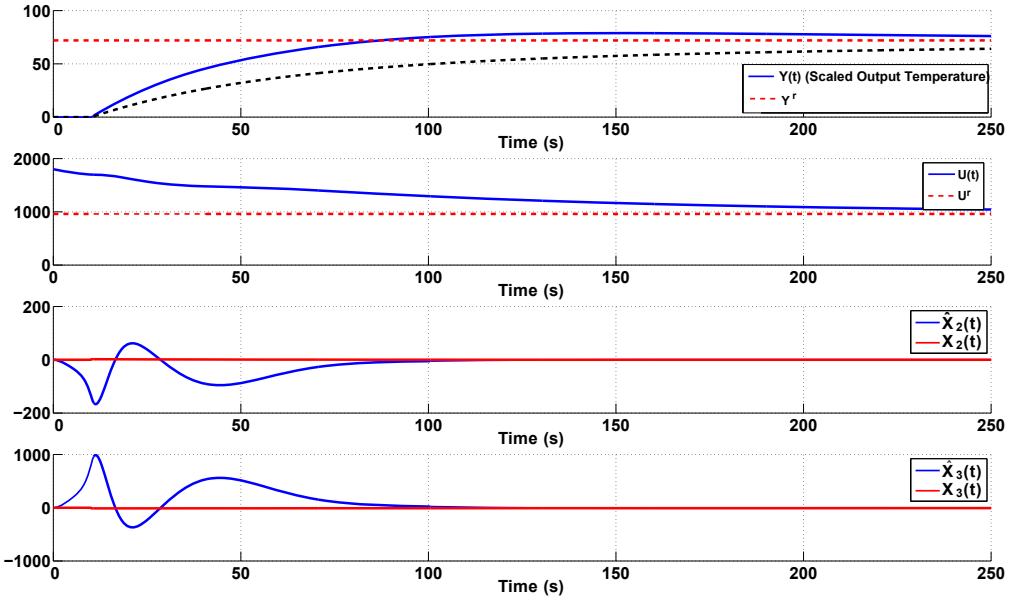

Figure 5.1: Simulation results for control of plant (5.11) represented in the form of (5.12). The plant is supposed to be initially at zero, namely $X(0) = [0 \quad 0 \quad 0]^T$, $u(.,0) = 0$; but if initially erroneously estimated with $\hat{X}(0) = [0 \quad 0.1 \quad 0.1]$. The constant input delay $D = 10$ s is overestimated with $\hat{D} = 15$ s. The controller gain K is chosen according to an LQR design, while the observer gain is constant at $L = [5 \quad -33 \quad 200]^T$.

Chapter 6

Input disturbance rejection

Chapitre 6 – Rejet de perturbation *Ce chapitre aborde la problématique du rejet de perturbation pour une loi de contrôle de type prédictif. Nous considérons seulement le cas simple d'une perturbation constante portant sur l'entrée et obtenons une loi d'adaptation de ce biais permettant la compensation robuste du retard de commande. Les résultats globaux de convergence asymptotique obtenus sont illustrés en simulation sur une dynamique de réchauffeur.*

Contents

In this chapter, we focus on compensation of a constant unknown bias acting on the system input. A number of studies have dealt with complex external disturbances for linear disturbances on delay systems [Pyrkin 10], even in a nonlinear context [Bobtsov 10]. Nevertheless, these works consider the delay value as known. The aim here is to give some directions to fill this gap by considering the simple case of a constant disturbance.

We consider the plant

$$\begin{cases} \dot{X}(t) = AX(t) + B[U(t-D) + d] \\ Y(t) = X(t) \end{cases} \tag{6.1}$$

where, compared to (2.15) we consider the plant as perfectly known and the system state X as measured.

6.1 Controller design

To reject the disturbance d, we introduce a dedicated estimate in the control law

$$\left\{ \begin{array}{ll} U(t) = & U_0(t) - \hat{d}(t) \\ U_0(t) = & U^r - KX^r + Ke^{A\hat{D}}X(t) + K\hat{D}\int_0^1 e^{A\hat{D}(1-x)}B\hat{u}_0(x,t)dx \end{array} \right. \tag{6.2}$$

and define the corresponding distributed actuator corresponding to the control prediction part U_0, namely, for $x \in [0,1]$ and $t \geq 0$, $u_0(x,t) = U_0(t + D(x-1))$, $\hat{u}_0(x,t) = U_0(t + \hat{D}(x-1))$, $\hat{e}_0(x,t) = \hat{u}_0(x,t) - U^r$ and $\tilde{e}_0(x,t) = u_0(x,t) - \hat{u}_0(x,t)$. The estimate $\hat{d}$ is chosen as

$$\dot{\hat{d}}(t) = \gamma_d \tau_d(t) \tag{6.3}$$

$$\tau_d(t) = \frac{\tilde{X}(t)^T PB}{b_2} - \hat{D}\int_0^1 (1+x)[\hat{w}_0(x,t) + A\hat{D}\hat{w}_{0,x}(x,t)]Ke^{A\hat{D}x}Bdx \tag{6.4}$$

Theorem 6.1.1

Consider the closed-loop system consisting of (6.1) *and the control law* (6.2) *with* (6.3)-(6.4)*. Define*

$$\Gamma(t) = |\tilde{X}(t)|^2 + \|e_0(t)\|^2 + \|\hat{e}_0(t)\|^2 + \|\hat{e}_{0,x}(t)\|^2 + \tilde{d}(t)^2 + \int_{t-D}^t \int_s^t \left[|\tilde{X}(r)|^2 + \|\hat{e}_0(r)\|^2 + \|\hat{e}_{0,x}(r)\|^2 \right] drds$$

Then there exist $\delta^* > 0$ and $\gamma^* > 0$ such that, provided that $|\gamma_d| < \gamma^*$ and $|\tilde{D}| < \delta^*$,

$$\forall t \geq 0\,, \quad \Gamma(t) \leq R\Gamma(0)\,,$$
$$\lim_{t\to\infty} X(t) = X^r \quad \textit{and} \quad \lim_{t\to\infty} U(t) = U^r$$

The previous theorem gives global asymptotic convergence (except for the delay estimation error, which is required to be sufficiently small). The disturbance estimate update law is chosen through a Lyapunov design, as in Chapter 3. It is inspired by the well-known result that an integral stabilizing controller for a linear system rejects any constant disturbance [Kailath 80]. The delay-free form of the system is stabilized by the $\tilde{X}$ term of update law (6.3)–(6.4), whereas the rest of the update law (6.4) accounts for the delay existence. The similarity between this update law and the one proposed in Chapter 3 is evident in (3.4)–(3.6) because the estimation errors in the two cases have a similar impact on the dynamics.

The main novelty is the introduction of a double integral term in the functional Γ. This term does not help to characterize the system state, as it is more or less redundant with the first one, but is useful in the Lyapunov analysis, as shown below. Besides, a limitation on the update gain (γ_d) is still present and has an impact on the integrator gain.

6.2 Convergence analysis

6.2.1 Error dynamics and Lyapunov analysis

Before working with a Lyapunov-Krasovskii functional, we introduce again a backstepping transformation of the actuator state

$$\hat{w}_0(x,t) = \hat{e}_0(x,t) - \hat{D}\int_0^x Ke^{A\hat{D}(x-y)}B\hat{e}_0(y,t)dy - Ke^{A\hat{D}x}\tilde{X}(t) \tag{6.5}$$

Using this transformation, (2.15) can be expressed as

$$\dot{\tilde{X}}(t) = (A+BK)\tilde{X}(t) + B\left[\tilde{e}_0(0,t) + \hat{w}_0(0,t)\right] + B\tilde{d}(t) + B\left[\hat{d}(t) - \hat{d}(t-D)\right] \tag{6.6}$$

In details, (6.6) can now be viewed as the result of four distinct factors:

- the stabilized dynamics (the $A+BK$-term);
- the mismatch between the delay and its estimate, namely $B\tilde{e}(0,t)$;
- the mismatch between the disturbance and its estimate, $\tilde{d}(t)$; and
- the delay effects over the disturbance rejection (non-synchronization between the estimate and the plant).

Now, define the following Lyapunov-Krasovskii functional

$$V(t) = \tilde{X}(t)^T P\tilde{X}(t) + \frac{b_2}{\gamma_d}\tilde{d}(t)^2 + b_1 D\int_0^1 (1+x)\tilde{e}_0(x,t)^2dx + b_2\hat{D}\int_0^1 (1+x)\hat{w}_0(x,t)^2dx$$
$$+ b_2\hat{D}\int_0^1 (1+x)\hat{w}_{0,x}(x,t)^2dx + b_3\int_{t-D}^t\int_s^t \left[|\tilde{X}(r)|^2 + \|\hat{w}_0(r)\|^2 + \|\hat{w}_{0,x}(r)\|^2\right]drds$$

Considering (6.5) and its inverse transformation

$$\hat{e}_0(x,t) = \hat{w}_0(x,t) + \hat{D}\int_0^x Ke^{(A+BK)\hat{D}(x-y)}B\hat{w}_0(y,t)dy + Ke^{(A+BK)\hat{D}x}\tilde{X}(t)$$

the actuators dynamics can be written as

$$\begin{cases} D\tilde{e}_{0,t}(x,t) = \tilde{e}_{0,x}(x,t) - \tilde{D}f(x,t) \\ \quad \tilde{e}(1,t) = 0 \end{cases}$$
$$\begin{cases} \hat{D}\hat{w}_{0,t}(x,t) = \hat{w}_{0,x}(x,t) - \hat{D}Ke^{A\hat{D}x}B\left[\tilde{e}_0(0,t) + \tilde{d}(t) + \hat{d}(t) - \hat{d}(t-D)\right] \\ \quad \hat{w}_0(1,t) = 0 \end{cases}$$
$$\begin{cases} \hat{D}\hat{w}_{0,xt}(x,t) = \hat{w}_{0,xx}(x,t) - \hat{D}^2KAe^{A\hat{D}x}B[\tilde{e}_0(0,t) + \tilde{d}(t) + \hat{d}(t) - \hat{d}(t-D)] \\ \quad \hat{w}_{0,x}(1,t) = \hat{D}Ke^{A\hat{D}}B\left[\tilde{e}(0,t) + \tilde{d}(t) + \hat{d}(t) - \hat{d}(t-D)\right] \end{cases}$$

where the function f is defined as

$$f(x,t) = \frac{\hat{w}_{0,x}(x,t)}{\hat{D}} + KB\hat{w}_0(x,t) + K(A+BK)e^{(A+BK)\hat{D}x}\tilde{X}(t)$$
$$+ \hat{D}\int_0^x K(A+BK)e^{(A+BK)\hat{D}(x-y)}B\hat{w}_0(y,t)dy$$

Taking a time derivative of V_4 and using suitable integrations by parts, one obtains

$$\begin{aligned}\dot{V}(t) &= -\tilde{X}(t)^T Q\tilde{X}(t) + 2\tilde{X}(t)^T PB[\tilde{e}_0(0,t) + \hat{w}_0(0,t)] + 2\tilde{X}(t)^T PB\left[\hat{d}(t) - \hat{d}(t-D)\right] \\ &+ \frac{2b_2}{\gamma_D}\tilde{d}(t)\left(\tau_d(t) - \dot{\hat{d}}(t)\right) + b_1\Big(- \tilde{e}_0(0,t)^2 - \|\tilde{e}_0(t)\|^2 - 2\tilde{D}\int_0^1 (1+x)\tilde{e}_0(x,t)f(x,t)dx\Big) \\ &+ b_2\Big(- \hat{w}_0(0,t)^2 - \|\hat{w}_0(t)\|^2 - 2\hat{D}\int_0^1 (1+x)Ke^{A\hat{D}x}B[\tilde{e}_0(0,t) + \hat{d}(t) - \hat{d}(t-D)]\hat{w}_0(x,t)dx\Big) \\ &+ b_2\Big(2\hat{w}_{0,x}(1,t)^2 - \hat{w}_{0,x}(0,t)^2 - \|\hat{w}_{0,x}(t)\|^2 - 2\hat{D}^2\int_0^1 (1+x)KAe^{A\hat{D}x}B \\ &\times [\tilde{e}_0(0,t) + \hat{d}(t) - \hat{d}(t-D)]\hat{w}_{0,x}(x,t)dx\Big) \\ &+ b_3\Big(- \int_{t-D}^t \left[|\tilde{X}(r)|^2 + \|\hat{w}_0(r)\|^2 + \|\hat{w}_{0,x}(r)\|^2\right]dr + D\left[|\tilde{X}(t)|^2 + \|\hat{w}_0(t)\|^2 + \|\hat{w}_{0,x}(t)\|^2\right]\Big)\end{aligned} \tag{6.7}$$

Furthermore, observing that $\hat{d}(t) - \hat{d}(t-D) = \gamma_d \int_{t-D}^t \tau_d(s)ds$ and the definition of τ_d in (6.4), Cauchy-Schwartz's inequality and Young's inequality can be applied to provide the following inequalities for the non-negative terms of (6.7)

$$\begin{aligned}&2\left|\tilde{X}(t)^T PB[\tilde{e}_0(0,t) + \hat{w}_0(0,t) + \hat{d}(t) - \hat{d}(t-D)]\right| \le \frac{\lambda_{min}(Q)}{2}|\tilde{X}(t)|^2 \\ &\qquad + \frac{4|PB|^2}{\lambda_{min}(Q)}[\tilde{e}_0(0,t)^2 + \hat{w}_0(0,t)^2] + \gamma_d M_1\int_{t-D}^t \left(|\tilde{X}(r)|^2 + \|\hat{w}_0(r)\|^2 + \|\hat{w}_{0,x}(r)\|^2\right)dr \\ &2\int_0^1 (1+x)|\tilde{e}_0(x,t)||f(x,t)|dx \le M_2\left(|\tilde{X}(t)|^2 + \|\tilde{e}_0(t)\|^2 + \|\hat{w}_0(t)\|^2 + \|\hat{w}_{0,x}(t)\|^2\right) \\ &2\hat{D}\left|\int_0^1 (1+x)Ke^{A\hat{D}x}B[\tilde{e}_0(0,t) + \hat{d}(t) - \hat{d}(t-D)]\hat{w}_0(x,t)dx\right| \\ &\qquad \le \|\hat{w}_0(t)\|^2/2 + M_3\tilde{e}_0(0,t)^2 + \gamma_d M_3\int_{t-D}^t \left(|\tilde{X}(r)|^2 + \|\hat{w}_0(r)\|^2 + \|\hat{w}_{0,x}(r)\|^2\right)dr \\ &2\hat{w}_{0,x}(1,t)^2 - \hat{w}_{0,x}(0,t)^2 \\ &\qquad \le M_4\tilde{e}_0(0,t)^2 + \gamma_d M_5\int_{t-D}^t \left(|\tilde{X}(r)|^2 + \|\hat{w}_0(r)\|^2 + \|\hat{w}_{0,x}(r)\|^2\right)dr \\ &2\hat{D}^2\left|\int_0^1 (1+x)KAe^{A\hat{D}x}[\tilde{e}_0(0,t) + \hat{d}(t) - \hat{d}(t-D)]\hat{w}_{0,x}(x,t)dx\right| \\ &\qquad \le \|\hat{w}_{0,x}(t)\|^2/2 + M_6\tilde{e}_0(0,t)^2 + \gamma_d M_6\int_{t-D}^t \left(|\tilde{X}(r)|^2 + \|\hat{w}_0(r)\|^2 + \|\hat{w}_{0,x}(r)\|^2\right)dr\end{aligned}$$

With these inequalities and choosing $b_2 \geq \frac{8|PB|^2}{\lambda_{min}(Q)}$, (6.7) yields

$$\begin{aligned}\dot{V}(t) \leq & -\frac{\lambda_{min}(Q)}{2}|\tilde{X}(t)|^2 - \frac{b_2}{2}\hat{w}_0(0,t)^2 - \left(b_1 - \frac{b_2}{2} - b_2(M_3+M_4+M_6)\right)\tilde{e}_0(0,t)^2 - b_1\left\|\tilde{e}_0(t)\right\|^2 \\ & - -\frac{b_2}{2}\left\|\hat{w}_0(t)\right\|^2 - \frac{b_2}{2}\left\|\hat{w}_{0,x}(t)\right\|^2 + b_1|\tilde{D}|M_2\left(|\tilde{X}(t)|^2 + \left\|\tilde{e}_0(t)\right\|^2 + \left\|\hat{w}_0(t)\right\|^2 + \left\|\hat{w}_{0,x}(t)\right\|^2\right) \\ & + b_3\left(D\left[|\tilde{X}(t)|^2 + \left\|\hat{w}_0(t)\right\|^2 + \left\|\hat{w}_{0,x}(t)\right\|^2\right] - \int_{t-D}^{t}\left[|\tilde{X}(r)|^2 + \left\|\hat{w}_0(r)\right\|^2 + \left\|\hat{w}_{0,x}(r)\right\|^2\right]dr\right) \\ & + \gamma_d\left(M_1 + b_2(M_3+M_5+M_6)\right)\int_{t-D}^{t}\left(|\tilde{X}(r)|^2 + \left\|\hat{w}_0(r)\right\|^2 + \left\|\hat{w}_{0,x}(r)\right\|^2\right)dr\end{aligned}$$

By choosing $b_1 > b_2\left(1/2 + M_3 + M_4 + M_6\right)$ and defining $M_7 = M_1 + b_2(M_3 + M_5 + M_6)$ together with

$$\begin{aligned}V_{0,1}(t) =& |\tilde{X}(t)|^2 + \left\|\tilde{e}_0(t)\right\|^2 + \left\|\hat{w}_0(t)\right\|^2 + \left\|\hat{w}_{0,x}(t)\right\|^2 \\ V_{0,2}(t) =& \int_{t-D}^{t}\left[|\tilde{X}(r)|^2 + \left\|\hat{w}_0(r)\right\|^2 + \left\|\hat{w}_{0,x}(r)\right\|^2\right]dr \\ \eta =& \min\left\{\lambda_{min}(Q)/2, b_1, b_2/2\right\}\end{aligned}$$

one obtains

$$\dot{V}(t) \leq -\left(\eta - b_3 D\right)V_{0,1}(t) + b_1|\tilde{D}(t)|M_2V_{0,1}(t) - (b_3 - \gamma_d M_7)V_{0,2}(t)$$

Consequently, if $b_3 = \gamma_d M_7$, and the update gain is (conveniently) chosen as $\gamma_d = \frac{\eta}{2DM_7}$, and if $|\tilde{D}| < \delta^* = \frac{\eta}{4b_1M_2}$, one concludes that

$$\forall t \geq 0\,, \quad \dot{V}(t) \leq -\frac{\eta}{4}V_{0,1}(t) \tag{6.8}$$

and finally that $\forall t \geq 0\,, \quad V(t) \leq V(0)$. This concludes the proof of Theorem 6.1.1.

6.2.2 Convergence result

To obtain the stability result stated in Theorem 6.1.1, we apply the same arguments as in Chapters 3 and 4. First, the stability result can be rewritten in terms of the functional Γ as: $\forall t \geq 0\,,\, \Gamma(t) \leq R\Gamma(0)$, with $R > 0$.

We conclude by applying Barbalat's Lemma to the variables $|\tilde{X}(t)|$ and $|\tilde{U}(t)|$. Integrating (6.8), from 0 to $+\infty$, one obtains that both signals are square integrable. Further, similar to the above considerations, the equations

$$\begin{aligned}\frac{d|\tilde{X}(t)|^2}{dt} =& 2\tilde{X}(t)^T\left[(A+BK)\tilde{X}(t) + B(\tilde{e}_0(0,t) + \hat{w}_0(0,t)) + B\tilde{d}(t) + B(\hat{d}(t) - \hat{d}(t-\hat{D}))\right] \\ \frac{d\tilde{U}(t)^2}{dt} =& 2\tilde{U}(t)\left[Ke^{A\hat{D}}\dot{X}(t) + K\int_0^1 e^{A\hat{D}(1-x)}B\hat{u}_{0,x}(x,t)dx - \dot{\hat{d}}(t)\right]\end{aligned}$$

together with (6.3)–(6.4) and the stability result give that both $d|\tilde{X}(t)|^2/dt$ and $d\tilde{U}(t)^2/dt$ are uniformly bounded for $t \geq \bar{D}$. The convergence result directly follows. The same arguments applied to $d\tilde{U}_0(t)^2/dt$ give the convergence of the prediction part of the control to U^r and of the disturbance estimate to the unknown disturbance.

6.2.3 Main specificities and other comments

The proof is similar to those given earlier. Here, as in Chapter 3, the disturbance estimate is chosen via a Lyapunov design. The main difference is the appearance of a de-synchronized term $\hat{d}(t) - \hat{d}(t-D)$ due to the additive form of controller (6.2), which requires introduction of a double integral term to treat this mismatch. Finally, it should be noted that the disturbance estimate converges to the unknown but constant disturbance.

6.3 Illustration: disturbance rejection for an air heater

In this section, we focus on the same illustrative example as in Section 5.3 (air heater). For convenience, we repeat the transfer function

$$G(s) = \frac{K_H(T_z s + 1)}{a_3 s^3 + a_2 s^2 + a_1 s + 1} e^{-Ds} \tag{6.9}$$

As previously, we consider a fixed operating point of the system that yields a constant delay $D = 10$ s and constant coefficients $a_3 = 1560$, $a_2 = 9300$, $a_1 = 250$ and $K_H = 0.075$. A state-space representation of the plant is (as before)

$$A = \begin{pmatrix} 0 & 1 & 0 \\ 0 & 0 & 1 \\ -\frac{1}{a_3} & -\frac{a_1}{a_3} & -\frac{a_2}{a_3} \end{pmatrix}, \quad B = \begin{pmatrix} 0 \\ K_H \frac{T_z}{a_3} \\ \frac{K_H}{a_3} - K_H T_z \frac{a_2}{a_3^2} \end{pmatrix} \quad \text{and} \quad C = (1 \quad 0 \quad 0)$$

We assume that a constant disturbance $d = 50$ impacts the input and that the delay is overestimated with $\hat{D} = 15$ s. We assume that the system is fully measured.

Finally, for a given output set point $Y = T_{ref}$, the corresponding references are

$$U_r = \frac{1}{K_H} Y^r \quad \text{and} \quad X^r = \begin{pmatrix} Y^r \\ 0 \\ -\frac{T_z \hat{\theta}_1}{a_3} Y^r \end{pmatrix}$$

Simulation results for the feedback strategy are provided in Figure 6.1. The system is considered initially at the origin $X(0) = [0 \quad 0 \quad 0]$ with $\hat{d}(0) = 0$.

Results are reported in Figure 6.1. First, one can observe that the disturbance bias is correctly estimated. which is compliant with the convergence of both the plant and the control law to their references. Second, the response time is slightly shortened compared to the simulation results proposed in Section 5.3. This is because the plant is fully measured in this example.

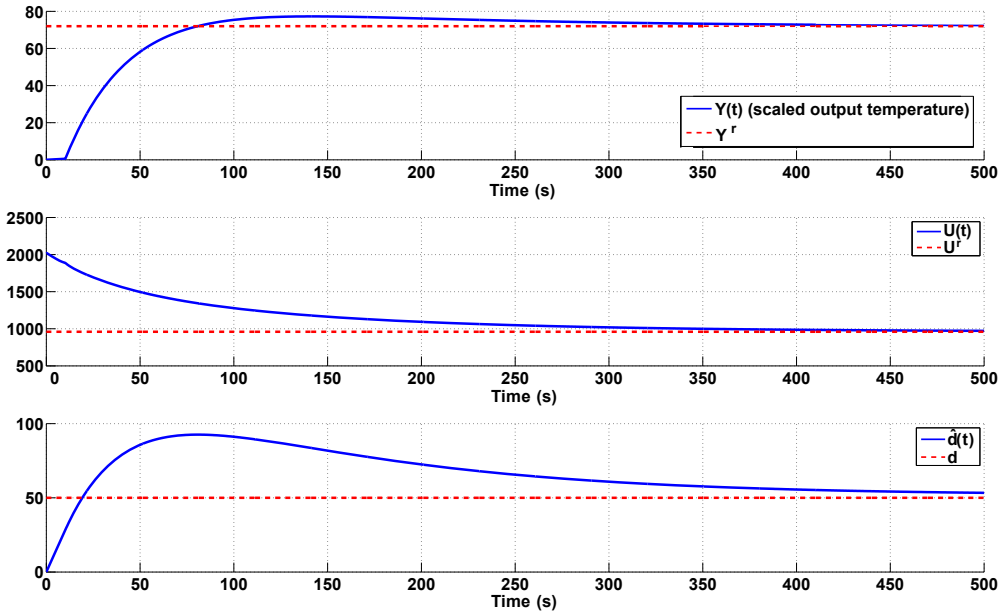

Figure 6.1: Simulation results for control of plant (6.9). The plant is initially at zero, namely $X(0) = [0 \quad 0 \quad 0]^T$, $u(.,0) = 0$, and impacted with a constant disturbance $d = 50$. The constant input delay $D = 10$ s is overestimated with $\hat{D} = 15$ s. The controller gain K is chosen according to an LQR design and the integrator gain is $\gamma_d = 0.039$.

Chapter 7

Case study of a Spark-Ignited engine: control of the Fuel-to-Air Ratio

Chapitre 7 – Contrôle de richesse sur moteur essence. *Dans ce chapitre, nous illustrons la polyvalence de la méthodologie adaptative générique proposée dans cette partie en réalisant plusieurs combinaisons des éléments présentés dans les chapitres précédents. Nous considérons ici le problème de la régulation de la richesse pour un moteur essence suralimenté à injection indirecte. Après avoir détaillé pourquoi l'asservissement de cette quantité à la stoechiométrie est essentiel au fonctionnement d'un moteur essence, nous présentons les stratégies usuelles de contrôle correspondante. En nous inspirant de ces stratégies, la boucle de rétroaction employée ici exploite le signal donné par une sonde à oxygène (sonde Lambda) dont l'emplacement dans la ligne d'échappement génère un retard de transport incertain. Nous présentons un modèle de dynamique validé sur banc moteur puis considérons deux stratégies différentes pour tenir compte du phénomène de mouillage de paroi inhérent au dispositif d'injection indirecte. Les performances des deux lois de contrôle distinctes obtenues sont illustrées par des essaus expérimentaux sur banc moteur.*

Contents

In this chapter, we present some practical combinations of the various elements proposed in the previous chapters. The considered application belongs to the field of gasoline engine control and is the control of the Fuel-to-Air Ratio (FAR).

Before detailing the different control strategies that were considered and tested experimentally on a test bench, we provide a background on internal combustion engines with a focus on the control architecture for Spark-Ignited (SI) engines.

7.1 Background on SI engine control and FAR regulation

There are two main classes of automotive engines, both of which generate torque by burning a mixture of air and fuel (and exhaust gases). These are: (1) compression ignition engines (also referred to as diesel engines), in which combustion is initiated by compressing the mixture inside the cylinder during the operating cycle; (ii) SI engines (gasoline engines) in which combustion is initiated by a correctly timed spark plug. The latter is the class of engines considered in this thesis.

7.1.1 SI engine structure

The general structure of as SI engine is shown in Figure 7.1. Details can be found in [Heywood 88]. The elements presented there can be be divided in three main subsystems:

- the *air path* which consists of the intake throttle, the turbocharger, intake and exhaust manifolds, valve actuators, and all the pipes. The air path feeds the cylinder with the correct amount of air (and burned gas) by providing appropriate thermodynamic conditions.
- the *fuel path* (mainly the injectors) is used to inject the appropriate amount of fuel into the combustion chamber. In modern SI engines, it is usually located within the cylinder (direct injection) but it can also be located in the intake pipe (port-fuel injection or indirect injection).
- the *ignition path*, which consists in the spark plug, aims at initiating the combustion.

In general, a throttle valve, located at the engine intake, controls the air flow through the intake manifold pressure (or, depending on the operating point via the turbocharger), while injectors are responsible for fuel injection. The air/fuel mixture inside the cylinder after the intake valve is closed is ignited by the spark plug and the combustion-generated

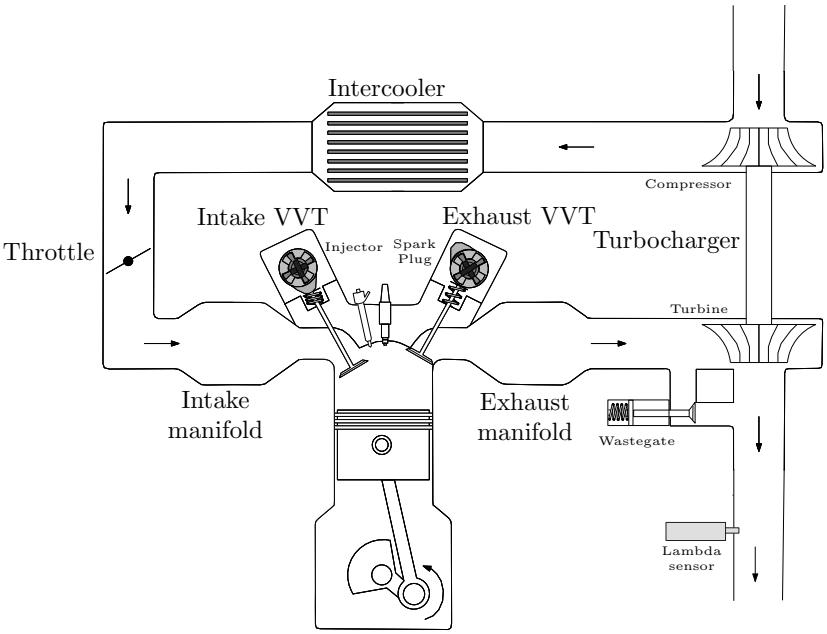

Figure 7.1: Schematic illustration of a turbocharged SI engine equipped with direct injection and VVT devices. An oxygen sensor (Lambda sensor) used for feedback control of the FAR is located in the exhaust line, downstream of the turbine and upstream of the three-way catalytic converter.

pressure in the combustion chamber pushes down the piston, which transmits energy to the crankshaft.

7.1.2 Stoichiometric operation

To meet standard requirements for emission of pollutants resulting from combustion, SI engines are equipped with a three-way catalytic (TWC) converter. This device, located in the engine exhaust, fulfills three simultaneous tasks for the three main concerned pollutant emissions: reduction of the nitrogen oxides (NO_x), oxidation of carbon monoxide (CO) and the oxidation of hydrocarbons (HC).

As these three reactions involve contradictory optimal combustion conditions (lean or rich environment), they occur most efficiently when the engine is operating near the stoichiometric point (see Figure 7.2). Outside of a narrow band around the stoichiometric composition, conversion efficiency decreases very rapidly [Kiencke 00]. In the context of ever-increasing requirements to reduce pollutant emissions and fuel consumption, accurate FAR control is then necessary.

FAR is defined as the ratio between the in-cylinder fuel mass m_f filling the cylinder at each stroke and the air mass aspirated into the cylinder m_{asp}. For convenience, the normalized ratio is commonly used

$$\phi = \frac{1}{FAR_S} \frac{m_f}{m_{asp}} \tag{7.1}$$

where FAR_S is the stoichiometric FAR value[1]. The aim of the control is then to maintain

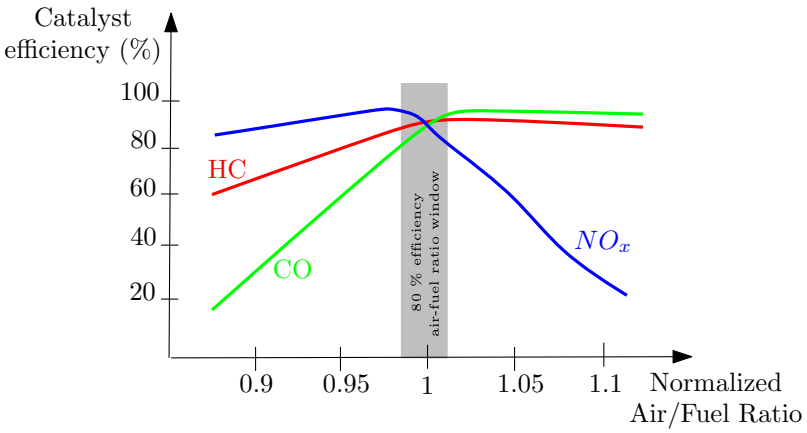

Figure 7.2: Three-way catalytic converter efficiency for a warm device.

ϕ as close as possible to unity.

7.1.3 Existing control strategy for the fuel path and air path

The necessity of maintaining a stoichiometric blend of fuel and air in the cylinder means that variations of the air path and fuel path have to be intimately correlated.

Because of the relative slowness of the air path compared to the fuel path, the produced torque can be considered as following the variations in air filling. Therefore, the air path of an SI engine is classically dedicated to the driver torque request and the fuel path is then adjusted. Correct coordination of the two paths is crucial to both torque generation and stoichiometry.

Aspirated air mass model

Over the years, numerous air path controllers have been designed (see [Das 08], [Van Nieuwstadt 00], or [Leroy 08] among others) and usually provide an aspirated air mass estimate m_{asp}^{est}. This estimate is then used to compute the set-point for the injected fuel mass. To account for the relative slowness of the air path and to obtain a correct synchronization of the two paths, a predictive technique may be used for this estimate (see for a detailed description [Chevalier 00]).

FAR control architecture

FAR management usually consists of a feedforward term, $m_f^{ff} = FAR_S m_{asp}^{est}$, associated with a feedback loop based on measurements by an oxygen sensor (a.k.a. Lambda sensor) located in the exhaust line [Di Gaeta 03]. Such an architecture is shown in Figure 7.3. Note that in this scheme, the regulated value is actually the measured signal ϕ_m, as discussed below.

In the following we pursue this generic approach, but simply propose an alternative feedback control to the usual carefully tuned PID. Before detailing this control design, we focus on the FAR dynamics to characterize the regulation problem under consideration.

[1] For a conventional SI engine, its value is around $\frac{1}{14.6}$.

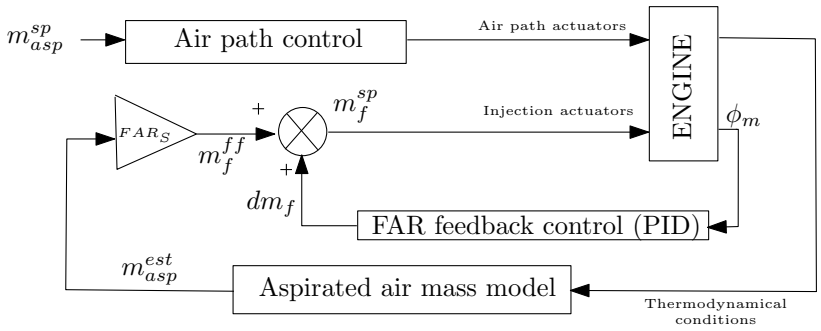

Figure 7.3: Classical general FAR control strategy. An aspirated air mass estimate is used to compute a fuel mass feedforward term. This term is completed by a feedback loop using the FAR measurement ϕ_m.

7.2 FAR dynamics

The closed-loop FAR strategy relies on a signal given by the Lambda Sensor, which is located in the exhaust line, downstream of the turbine and upstream of the catalyst. As the actuator (the injector, inside or near the combustion chamber) and the control variable (the exhaust FAR ϕ_m) are not co-located, the system dynamics naturally involves a transport delay [Kahveci 10].

As this delay originates from transportation of material, it is highly variable over the operating range of the engine[2]. This justifies the design of a prediction-based control law using the various elements proposed in the previous chapters. To identify the best components to use among the ones presented, we now detail an FAR model.

7.2.1 Transport delay and sensor dynamics

As pointed out in numerous studies (e.g. [Wang 06], [Guzzella 10], [Jankovic 11]), the dynamics of the sensor can be approximated by a low-pass transfer function, driven by a delayed input signal. In practice,

$$\tau_\phi \dot{\phi}_m(t) \quad = \quad -\phi_m(t) + \phi(t - D(t)) \tag{7.2}$$

where ϕ_m is the normalized FAR signal measured[3] and the intake FAR ϕ is defined in (7.1). Accounting for a static injection error δm_f and a transient aspirated air mass estimation error δm_{asp}, this expression can be reformulated as

$$\phi(t) = \frac{1}{FAR_S} \frac{1 + \delta m_f}{1 + \delta m_{asp}(t)} \frac{m_f^{sp}(t)}{m_{asp}^{est}(t)} = \frac{\alpha(t)}{FAR_S} \frac{m_f^{sp}(t)}{m_{asp}^{est}(t)} \tag{7.3}$$

where the errors δm_f and $\delta m_{asp}(t)$ are assumed proportional[4]. As a result, defining the control variable as $U(t) = \frac{1}{FAR_S} \frac{m_f^{sp}(t)}{m_{asp}^{est}(t)}$ in accordance with the previous considerations

[2]The delay variations are related to the gas speed. As the fresh air mass flow rate varies according to the engine speed and the torque request, this delay is also variable.

[3]The quantity measured by the oxygen sensor is the exhaust equivalent ratio $\phi_{exh} = m_{bg}/m_{exh}$, where m_{exh} is the exhaust gas mass and m_{bg} the exhaust burned gas mass, which can be related to the in-cylinder quantities as ϕ_m.

[4]These errors could also have been considered as additive and would have yielded the choice of another control design.

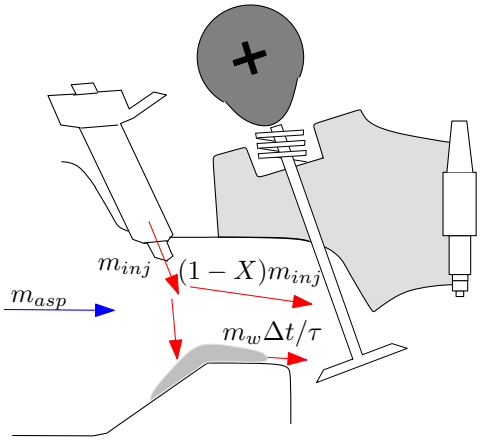

Figure 7.4: Model of the wall-wetting phenomenon that occurs for an indirect injection set-up.

(7.2) can be rewritten as

$$\tau_\phi \dot{\phi}_m(t) = -\phi_m + \alpha(t)U(t-D) \tag{7.4}$$

which is compliant with the general plant form given in (2.15).

Delay description

The delay D includes injection and combustion lags and the transport delay from the exhaust valve to the oxygen sensor:

$$D = D_{inj} + D_{burn} + D_{trans} \tag{7.5}$$

where the injection delay D_{inj} is the sum of computation duration and injection (including the sensor lag). The combustion delay D_{burn} depends on the timing of intake and exhaust valves. Finally, the transport delay D_{trans} depends on the gas velocity.

7.2.2 Wall-wetting phenomenon

In the case of indirect injection, the fuel injected in liquid form is not instantaneously vaporized in the intake manifold: a proportion X of the injected quantity constitutes a liquid fuel film on the intake manifold walls. The fuel mass entering the cylinder is then different from the injected mass. This well-known phenomenon is called wall-wetting (see [Hendricks 97], [Arsie 03]). It is represented in Figure 7.4 and described in terms of flows in [Aquino 81] as

$$\begin{cases} \dot{m}_w = XF_{inj} - \dfrac{m_w}{\tau} \\ F_f = (1-X)F_{inj} + \dfrac{1}{\tau}m_w \end{cases} \tag{7.6}$$

Of course, at steady-state, the fuel masses are equal, i.e. $F_f = F_{inj}$. At each stroke, the full mass admitted in the cylinder is $m_f = (1-X)m_{inj} + m_w\Delta t/\tau$. The parameters (τ, X) can be identified experimentally and depend mainly on the engine speed (and, less

significantly, on the fuel properties and on the intake manifold pressure and temperature). The set-point for the injected mass of fuel m_{inj}^{sp} can then be determined from the set-point for the in-cylinder mass of fuel m_f^{sp} and a (τ, X)- look-up table, by simply inverting this model.

7.2.3 Experimental model validation

Model (7.4) was validated on an experimental test bench. The engine under consideration in this section is a turbocharged 2L four-cylinder SI engine using indirect injection (Renault F4Rt).

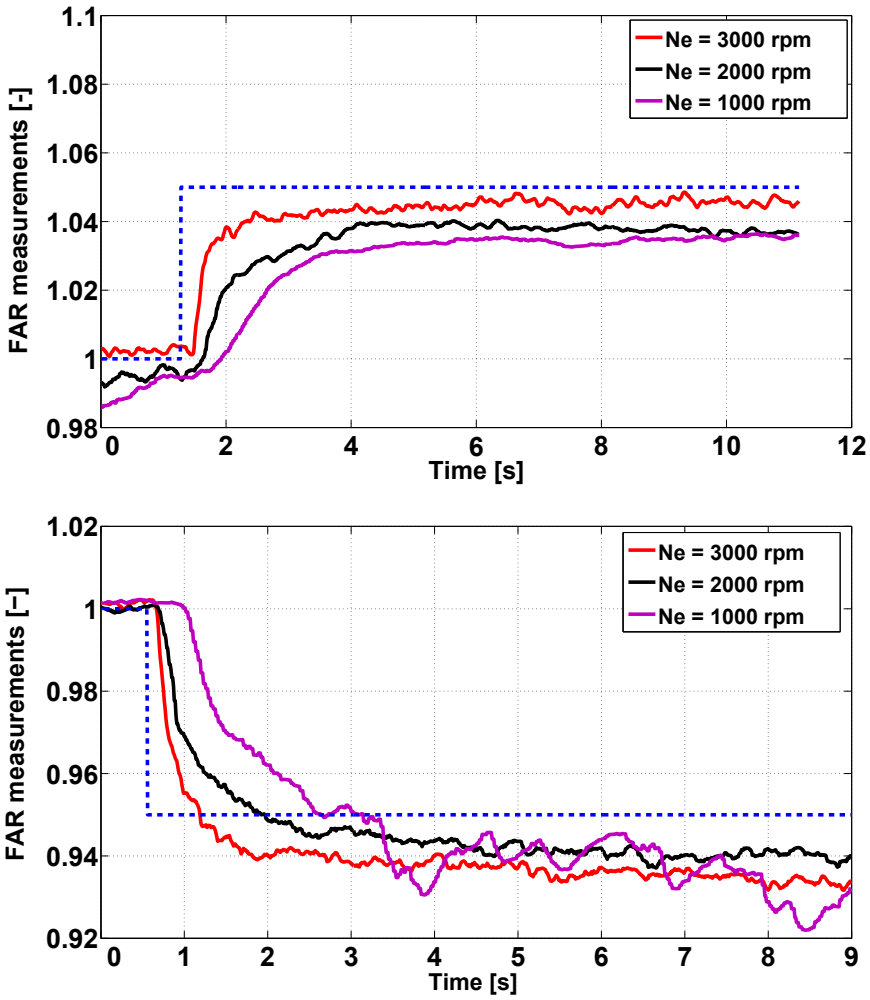

Figure 7.5: FAR open-loop dynamics for two different transients starting from the stoichiometric point: an increasing step (m_f^{sp} 5% greater) and a decreasing step (m_f^{sp} 5% lower). The torque is constant at 10 Nm and three different engine speed are considered, $N_e = 1000$, 2000 and 3000 rpm.

Figure 7.5 shows the open-loop FAR response to two different steps for m_f^{sp} corresponding to two different steps on the input U in (7.4), for different engine speed (1000, 2000 and 3000 rpm) and a low torque request (10 Nm). It is easy to see the occurrence of a delay that decreases with the engine speed and the occurrence of a time constant and a static gain that vary with the engine operating point.

Parameter	Unit	Operating range	Step size
Engine speed	rpm	800 and 1000 to 3500	500
Effective torque	Nm	50 to 200	50

Table 7.1: Test Bench Data.

The general dynamics is well captured by the input delay first-order system (7.4).

These experiments were conducted over a wide engine operating range (see Table 7.1) to identify the parameters τ_ϕ, α and D when possible. Figure 7.6 shows the results obtained, which can be interpreted as follows.

The error gain α

α aggregates various error factors, as defined in (7.3), including the in-cylinder air mass estimation error and the injection error. This term cannot be easily measured, as the error varies over the operating range and over time due to device ageing among other causes.

For example, it is evident from Figure 7.5 that, for a given engine speed and torque request, α varies with the FAR (which can be explained by variations in δm_{asp} depending on the injected fuel mass).

Therefore, this quantity is very uncertain, even if, as can be observed, its variability is relatively small ($\alpha \in [\underline{\alpha}, \bar{\alpha}] = [0.75; 1.25]$) and of low-frequency.

The time constant τ_ϕ

This constant represents the sensor dynamics, namely the time needed to fill the porous coating layers that protect the sensor electrodes. As depicted in Figure 7.6, it can be readily identified as a function of the aspirated air flow as

$$\tau_\phi = \frac{1}{a_\tau + b_\tau F_{air}} \tag{7.7}$$

where a_τ and b_τ are constant. From now on, we assume that we have accurate knowledge of τ_ϕ via (7.7).

The delay D

From (7.5), a simple representative parametrization of the delay is

$$D(N_e) = \frac{a_D}{N_e} \tag{7.8}$$

where a_D is constant and which is commonly used (see [Coppin 10]) but is an inaccurate approximation. Indeed, in Figure 7.6 substantial variations with the torque request are evident for a given engine speed. Nevertheless, for simplicity, we keep this approximation but consider the delay as relatively uncertain, even if it belongs to the interval $[\underline{D}, \bar{D}] = [100, 600]$ ms.

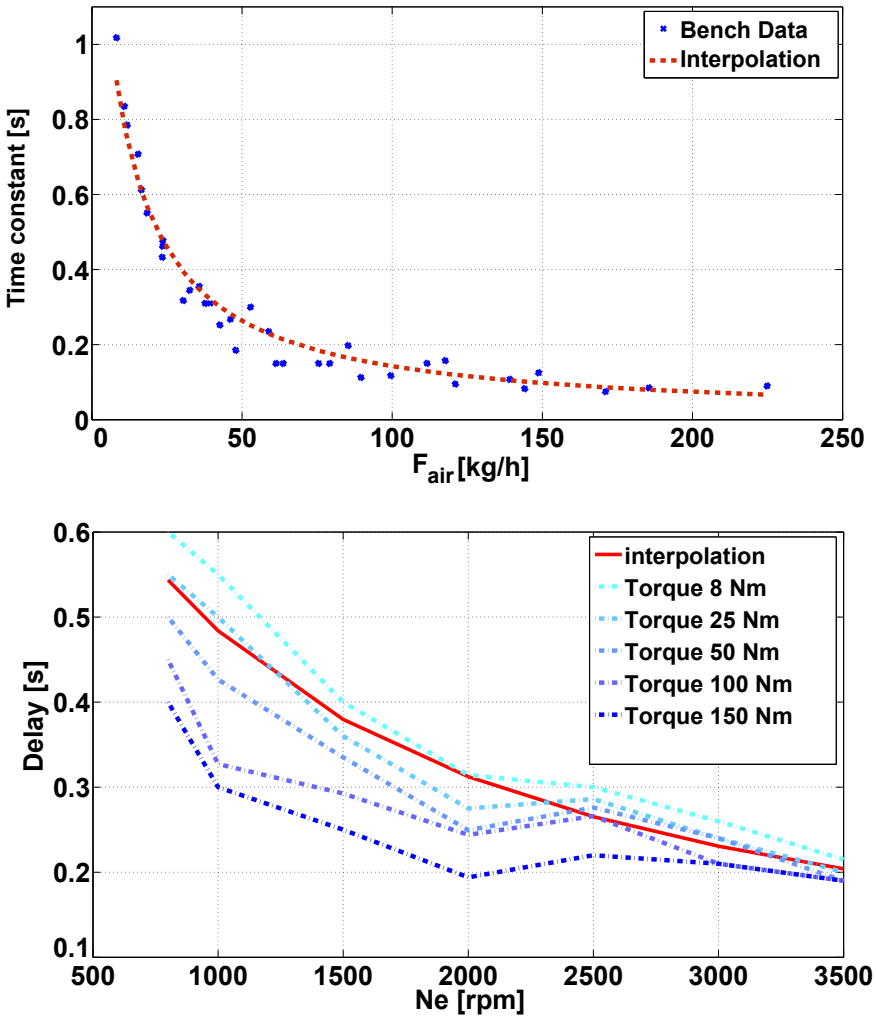

Figure 7.6: Observed time constant τ_ϕ and delay D variations over the engine operating range.

7.3 A first control design for scalar plant

From the previous considerations, one can summarize the FAR regulation problem by the control of the dynamics

$$\begin{cases} \tau_\phi \dot{\phi}_m(t) = -\phi_m(t) + \alpha U(t-D) \\ \tau_\phi = \tau_\phi(F_{air}) \\ \alpha = \alpha(N_e, F_{air}) \\ D = D(N_e, F_{air}) \end{cases} \tag{7.9}$$

with:

- an unknown gain $\alpha \in [0.75, 1.25]$ that varies with the operating point (and extremely slowly over time as it is mostly related to ageing); and
- an uncertain input time delay, estimated by $\hat{D} = \hat{D}(N_e) \in [\underline{D}, \bar{D}] = [100, 600]$ ms.

Then, for a given operating point, all the parameters are constant. Using the notations of (2.15), we define $X = \phi_m$, $\theta = \alpha$, $A = 1/\tau_\phi$ and $B(\alpha) = \alpha/\tau_\phi$. We note $\phi^r = 1$ the FAR set-point [5] and $U^r(\alpha) = \phi^r/\alpha$ the corresponding control reference.

The control goal is here to improve the transient performance by substantially decreasing the time response of the system. Therefore, compensation of the delay seems to be a promising way to achieve this objective.

This question falls directly into the scope of Theorem 3.1.1. Indeed, one can easily check that the required Assumptions 1-4 are fulfilled.

7.3.1 Controller equations

For a given operating point (N_e, F_{air}), we denote $\tau_\phi = \tau_\phi(F_{air})$ the corresponding time constant and arbitrarily set the controller gain as $K = -1$. Applying the control strategy presented in Theorem 3.1.1 with a constant delay estimate $\hat{D} = \hat{D}(N_e)$, we define the following.

Prediction control law

$$U(t) = \frac{\phi^r}{\hat{\alpha}(t)} + \phi^r - e^{-\hat{D}/\tau_\phi}\phi_m(t) - \hat{D}\frac{\hat{\alpha}(t)}{\tau_\phi}\int_0^1 e^{-\hat{D}(1-y)/\tau_\phi}\hat{u}(y,t)dy$$

Distributed input estimate

$$\begin{cases} \hat{D}\hat{u}_t(x,t) = \hat{u}_x(x,t) \\ \hat{u}(1,t) = U(t) \end{cases} \tag{7.10}$$

[5] except for a high load, for which it is useful to obtain a rich mixture ($\phi^r > 1$) to prevent knock.

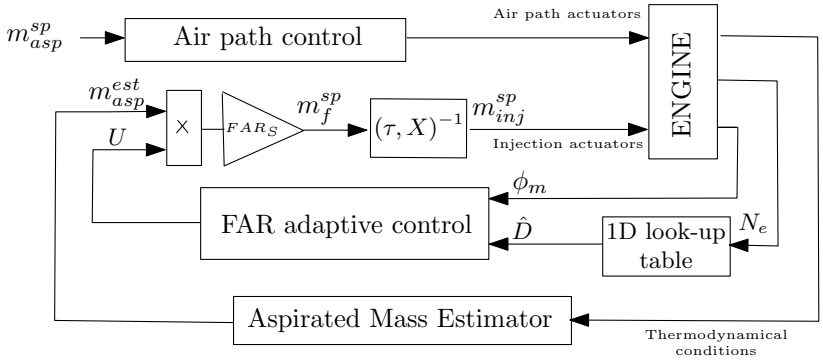

Figure 7.7: Proposed alternative FAR adaptive control strategy. Compared to Figure 7.3, the control U now takes into account the aspirated air mass estimation error and the injection error, using an estimate of the transport delay $\hat{D}$. An inverse wall-wetting model $(\tau, X)^{-1}$ was added to the architecture to account for indirect injection.

Transformed estimated distributed input

$$\begin{cases} \hat{w}(x,t) = \hat{e}(x,t) + \hat{D}\dfrac{\hat{\alpha}(t)}{\tau_\phi}\displaystyle\int_0^x e^{-\hat{D}(x-y)/\tau_\phi}\hat{e}(y,t)dy + e^{-\hat{D}x/\tau_\phi}(\phi_m(t) - \phi^r) \\ \hat{e}(x,t) = \hat{u}(x,t) - \dfrac{\phi^r}{\hat{\alpha}(t)} \end{cases} \tag{7.11}$$

Parameter update law

$$\begin{cases} \dot{\hat{\alpha}}(t) = \gamma\dfrac{\phi^r}{\hat{\alpha}(t)}h(t) & (7.12) \\ h(t) = \dfrac{\phi_m(t) - \phi^r}{b} + \dfrac{\hat{D}}{\tau_\phi}\displaystyle\int_0^1 (1+x)\left[\hat{w}(x,t) - \frac{\hat{D}}{\tau_\phi}\hat{w}_x(x,t)\right]e^{-\hat{D}x/\tau_\phi}dx & (7.13) \end{cases}$$

According to the local asymptotic stability result of Theorem 3.1.1, if the estimate $\hat{D}$ is close enough to the true delay D and if the initial conditions are chosen close enough to their corresponding reference or true value, then ϕ tracks ϕ^r and U tracks $\phi^r/\hat{\alpha}(t)$.

7.3.2 Transient control strategy

The range of variations of the delay and the parameter α over the entire operating space is sufficiently narrow so that the updated set-point lies in the vicinity of the current set-point at all times. Consequently, the previously presented controller (7.10)–(7.12) can be used in transient mode. No particular feedforward terms are needed.

In addition, it is possible to tune the transient behavior adjusting the gains γ and $-K$ to the operating point in a gain scheduling approach. This did not seem necessary in the following experimental test, in which the main objective was to validate the controller (its implementability and robustness assessment) and not to maximize its performances.

Figure 7.7 shows the general architecture of the adaptive control strategy.

7.3.3 Experimental results

Experimental set-up

All experimental results presented in this section were obtained for the engine described above. The set point for the in-cylinder fuel mass is related to that of the injected fuel mass through 2D look-up tables accounting for the wall-wetting phenomenon described above.

For this test, a PID controller tuned with Ziegler-Nichols rules [Ziegler 42] is used as a reference. For the proposed controller, the gains were chosen as $K = -1$ and $\gamma = 0.4$.

Torque trajectory at constant speed

To validate the proposed strategy, we consider an increasing torque variation at constant engine speed (1000 rpm), followed by a tip-out. The delay estimate corresponding to this engine speed is $\hat{D} = 390$ ms.

Figure 7.8 shows experimental results obtained on the test bench for the torque trajectory of Figure 7.8-(a).

Comparison of the performance of the controller to the reference PID in Figure 7.8-(c) reveals that the time response of the proposed controller is shorter for the first two steps of torque (2–12 s and 12–22 s). In addition, in the interval between 30 and 50 s, it is evident that convergence about the value $\phi^r = 1$ is tighter. This result is compliant with the corresponding set point for the in-cylinder fuel mass in Figure 7.8-(d), which is slightly higher for PID regulation.

More generally, there is slight but persistent de-synchronization between the PID controller and prediction-based results: the prediction-based feedback law still varies before the PID law. This is particularly evident in Figure 7.8-(d). This is because of the *anticipation* effect of our controller, tailored to deal with delay, which is its main advantage.

Figure 7.8-(e) shows the history of the estimator $\hat{\alpha}(t)$ throughout this experiment. Its behavior is well explained by the dynamics of the FAR tracking error

$$\tau_\phi \frac{d}{dt}[\phi_m(t) - \phi^r] = -(\phi_m(t) - \phi^r) + \hat{\alpha}(t)(u(0,t) - \frac{\phi^r}{\hat{\alpha}(t)}) + \tilde{\alpha}(t)u(0,t) \tag{7.14}$$

When FAR and control convergences have been obtained (i.e. when ϕ_m equals ϕ^r and U equals $\phi^r/\hat{\alpha}$), the estimate error $\tilde{\alpha}(t)$ is zero, which means that the estimate parameter $\hat{\alpha}(t)$ has converged to the unknown value α. This result (which unfortunately cannot be generalized to multi-parameter estimation in adaptive control [Ioannou 96]) is of great interest in the context of engine diagnosis (see [Ceccarelli 09]).

NEDC cycle

To test our controller under real representative driving conditions, experiments were conducted on a challenging part of the new European driving cycle (NEDC). This consists of one urban driving cycle (ECE) followed by an extra-urban driving cycle (EUDC). Results are reported in Figure 7.9.

In general, this demanding test yields similar conclusions. Tight convergence is obtained with the proposed strategy, particularly for a gear shift above 3 (corresponding to the time interval 250–600 s). The convergence value of $\hat{\alpha}$ obtained is indeed unique

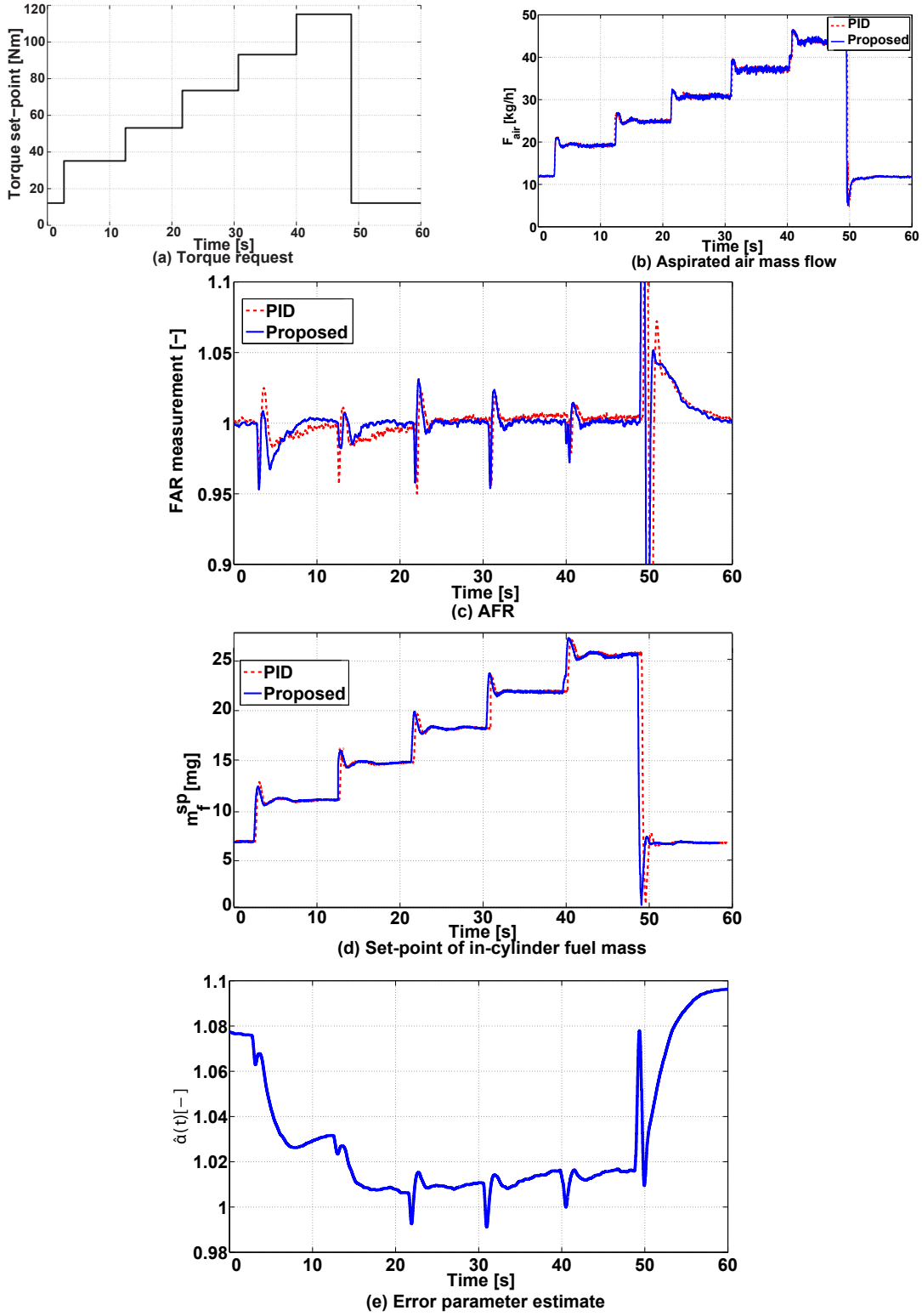

Figure 7.8: Test-bench results for a constant engine speed of 1000 rpm and the torque demand (a), for the proposed strategy (blue) and a tuned PID (red).

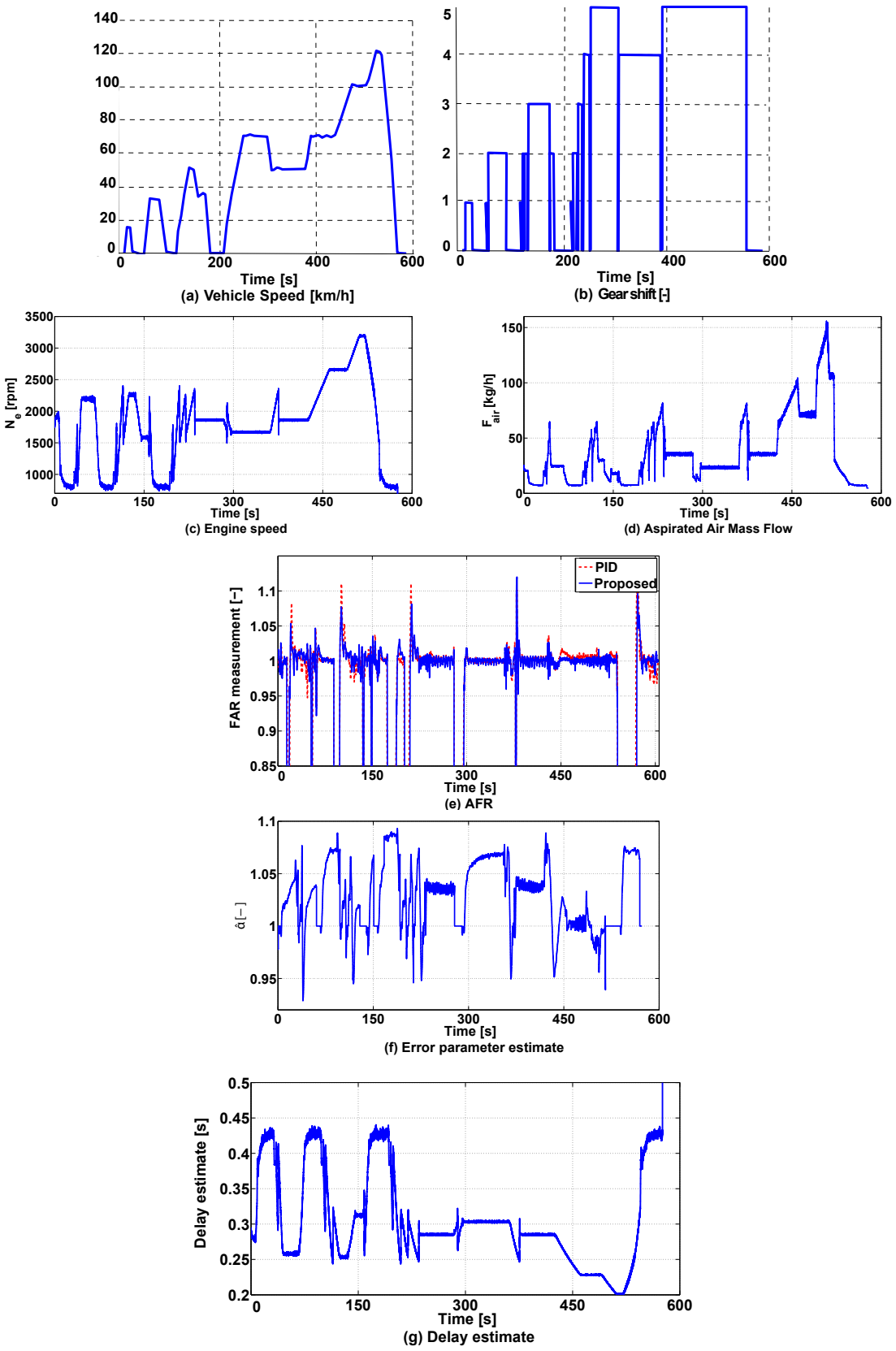

Figure 7.9: Test bench results during a normalized ECE (0–200 s) cycle and an EUDC (200–600 s) cycle, for the proposed strategy (blue) and a tuned PID (red).

for a given operating point: for example, around respectively 250 s and 425 s, the same operating point (N_e, F_{air})=(1800 rpm, 40 kg/h) is reached and $\hat{\alpha}$ converges around 1.04 each time. Interpreting α as a diagnosis information for the aspirated air charge model, one can see that it is globally overestimated ($\hat{\alpha}$ is globally greater than 1) except for high load where it is perfectly accurate (approx. 450 s).

More precisely, this test stresses the relevance of the proposed controller over a large range of operating points and under real driving conditions (injection shut-off corresponding to the sudden decrease in FAR in Figure 7.9(e)). Finally, Table 7.2 quantitatively summarizes the benefits of the proposed strategy for the two previous tests.

Test	Constant speed	NEDC
PID performance	0.0541	0.1622
Adaptive control performance	0.0464	0.1286
Relative gain compared with PID	14 %	20 %

Table 7.2: Performance comparison for the two controllers, measured as $\int_{\{t\,:\,\text{Injection ON}\}} \tilde{\phi}(t)^2 dt$.

7.4 Control design for the second-order plant induced by the wall-wetting phenomenon

In this section, we present an alternative design based on the complete dynamics. Taking explicitly into account the wall-wetting phenomenon leads to consideration of (stable) second-order dynamics with one zero.

7.4.1 Alternative model for indirect injection

We consider wall-wetting model (7.6), together with sensor dynamics (7.4). Taking a time derivative of (7.6) yields

$$\frac{dF_f}{dt} = (1-X)\frac{dF_{inj}}{dt} + \frac{1}{\tau}\left(XF_{inj} - \frac{m_w}{\tau}\right) = (1-X)\frac{dF_{inj}}{dt} + \frac{1}{\tau}(F_{inj} - F_f)$$

Then, taking a time derivative of (7.4) and using the previous equation, one obtains

$$\begin{aligned}
&\tau_\phi \frac{d^2\phi_m}{dt^2} + \frac{d\phi_m}{dt} = \frac{1}{FAR_S}\frac{d}{dt}\left[\frac{F_f(t-D)}{F_{air}(t-D)}\right] \\
&= \frac{1-\dot{D}}{FAR_S}\left[\frac{1}{F_{air}(t-D)}\left([1-X]\frac{dF_{inj}}{dt}(t-D) + \frac{1}{\tau}[F_{inj}(t-D) - F_f(t-D)]\right)\right. \\
&\left. - \frac{F_f(t-D)}{F_{air}(t-D)^2}\frac{dF_{air}}{dt}(t-D)\right]
\end{aligned}$$

As a result, using (7.4) again and taking into account the fact that the transient quantities $\frac{1}{F_{air}}\frac{dF_{air}}{dt}$ are negligible compared with the time scale $1/\tau$ and that the delay time

derivative is negligible compared to 1 (which are usual assumption, see [Orlov 06]), the last expression can be simplified to

$$\tau_\phi \frac{d^2\phi_m}{dt^2} + \left[1 + \frac{\tau_\phi}{\tau}\right] \frac{d\phi_m}{dt} + \frac{1}{\tau}\phi_m = \left[(1-X)\dot{v}(t-D) + \frac{1}{\tau}v(t-D)\right] \tag{7.15}$$

with $v = \frac{1}{FAR_S}\frac{F_{inj}}{F_{air}(t)} = \frac{1}{FAR_S}\frac{m_{inj}}{m_{asp}(t)}$. This is the dynamics that we consider in the following.

7.4.2 Dynamics analysis

As previously, we introduce proportional errors for both the injection process and the in-cylinder air flow estimation

$$v(t) = \frac{1}{FAR_S}\frac{1+\delta m_{inj}}{1+\delta m_{asp}}\frac{m_{inj}^{sp}}{m_{asp}^{est}(t)} = \alpha(t)\frac{1}{FAR_S}\frac{m_{inj}^{sp}}{m_{asp}^{est}(t)}$$

Defining the control variable as $U(t) = \frac{1}{FAR_S}\frac{m_{inj}^{sp}}{m_{asp}^{est}(t)}$, one obtains

$$\begin{cases} \tau_\phi\tau\ddot{\phi}_m(t) + (\tau_\phi+\tau)\dot{\phi}_m + \phi_m = \alpha(t)\left[\tau(1-X)\dot{U}(t-D) + U(t-D)\right] \\ \tau_\phi = \tau_\phi(F_{air}) \\ \alpha = \alpha(N_e, F_{air}) \\ D = D(N_e, F_{air}) \end{cases} \tag{7.16}$$

with:

- an unknown gain $\alpha \in [0.75, 1.25]$, that varies with the operating point (and extremely slowly over time due the ageing);
- an uncertain input time delay, estimated by $\hat{D} = \hat{D}(N_e) \in [\underline{D}, \bar{D}] = [100, 600]$ ms; and
- only one available measurement, ϕ_m.

The control goal is to improve the transient performances, as the system is stable. Therefore, compensation of the delay seems to be a promising way to achieve this objective.

To design such a controller, adaptation of the unknown parameter and observation are necessary. The resulting controller will then be a combination of the elements proposed in Chapters 3 and 5.

State-space representation

Defining the system state as $X \in \mathbb{R}^2$, the unknown plant parameter as $\theta = \alpha$ and the matrices

$$A = \begin{bmatrix} 0 & 1 \\ -\dfrac{1}{\tau_\phi\tau} & -\dfrac{1}{\tau_\phi} - \dfrac{1}{\tau} \end{bmatrix}, \quad B = \begin{bmatrix} 0 \\ \dfrac{\alpha}{\tau\tau_\phi} \end{bmatrix} \quad \text{and} \quad C = [1 \quad \tau(1-X)]$$

one can reformulate the problem as

$$\begin{aligned}\dot{X}(t) =& AX(t) + B(\theta)U(t-D)\\ Y(t) =& \phi_m(t) = CX(t)\end{aligned}$$

Defining the reference trajectories as $(X^r, U^r) = ([\phi^r \quad 0]^T, \phi^r/\alpha)$, we use the following prediction-based controller.

Controller design

Applying the certainty equivalence principle, we use various components for the control design based on the elements proposed in Chapters 3 and 5.

- **Control law**

$$U(t) = U^r(\hat{\theta}) - KX^r + K\left[e^{A\hat{D}}\hat{X}(t) + \int_0^1 e^{A\hat{D}(1-x)}B(\hat{\theta})\hat{u}(x,t)dx\right]$$

- **Observer**

$$\begin{aligned}&\dot{\hat{X}}(t) = A\hat{X}(t) + B(\hat{\theta})\hat{u}(0,t) - L(Y(t) - C\hat{X}(t))\\ &\forall x \in [0,1], \quad \hat{u}(x,t) = U(t + \hat{D}(x-1))\end{aligned}$$

- **Backstepping transformation**

$$\begin{aligned}&\forall x \in [0,1], \quad \hat{e}(x,t) = \hat{u}(x,t) - \frac{\phi^r}{\hat{\alpha}}\\ &\forall x \in [0,1], \quad \hat{w}(x,t) = \hat{e}(x,t) - \hat{D}\int_0^x Ke^{A\hat{D}(x-y)}B(\hat{\theta})\hat{e}(y,t)dy - Ke^{A\hat{D}x}\left[\hat{X}(t) - X^r\right]\end{aligned}$$

- **Update law**

$$\dot{\hat{\theta}}(t) = \gamma\left[\frac{(\hat{X}(t) - X^r)^T P(\hat{\theta})}{b} - \hat{D}K(\hat{\theta})\int_0^1 (1+x)[\hat{w}(x,t) + A\hat{D}\hat{w}_x(x,t)]e^{A\hat{D}x}dx\right]\begin{bmatrix}0\\ \frac{\phi^r}{\hat{\alpha}\tau\tau_\phi}\end{bmatrix}$$

In the spirit of the previous chapters, we foresee that the state X will asymptotically converge to the trajectory X^r and, equivalently, that the FAR will asymptotically converge to its set-point ϕ^r for any given operating point.

This control strategy is pictured in Figure 7.11.

7.4.3 Experimental results

Experiments were conducted on a test-bench for an atmospheric 1.4L four-cylinder SI engine (PSA ET3) to validate the proposed control strategy. The results obtained for torque variations at a constant engine speed are shown in Figure 7.10. The tuning parameters (feedback gain K, observer gain L and update gain γ) are constant over the whole operating range.

It is clear that good FAR convergence is obtained after each change in operating point and that the transient performance matches that of a PID controller.

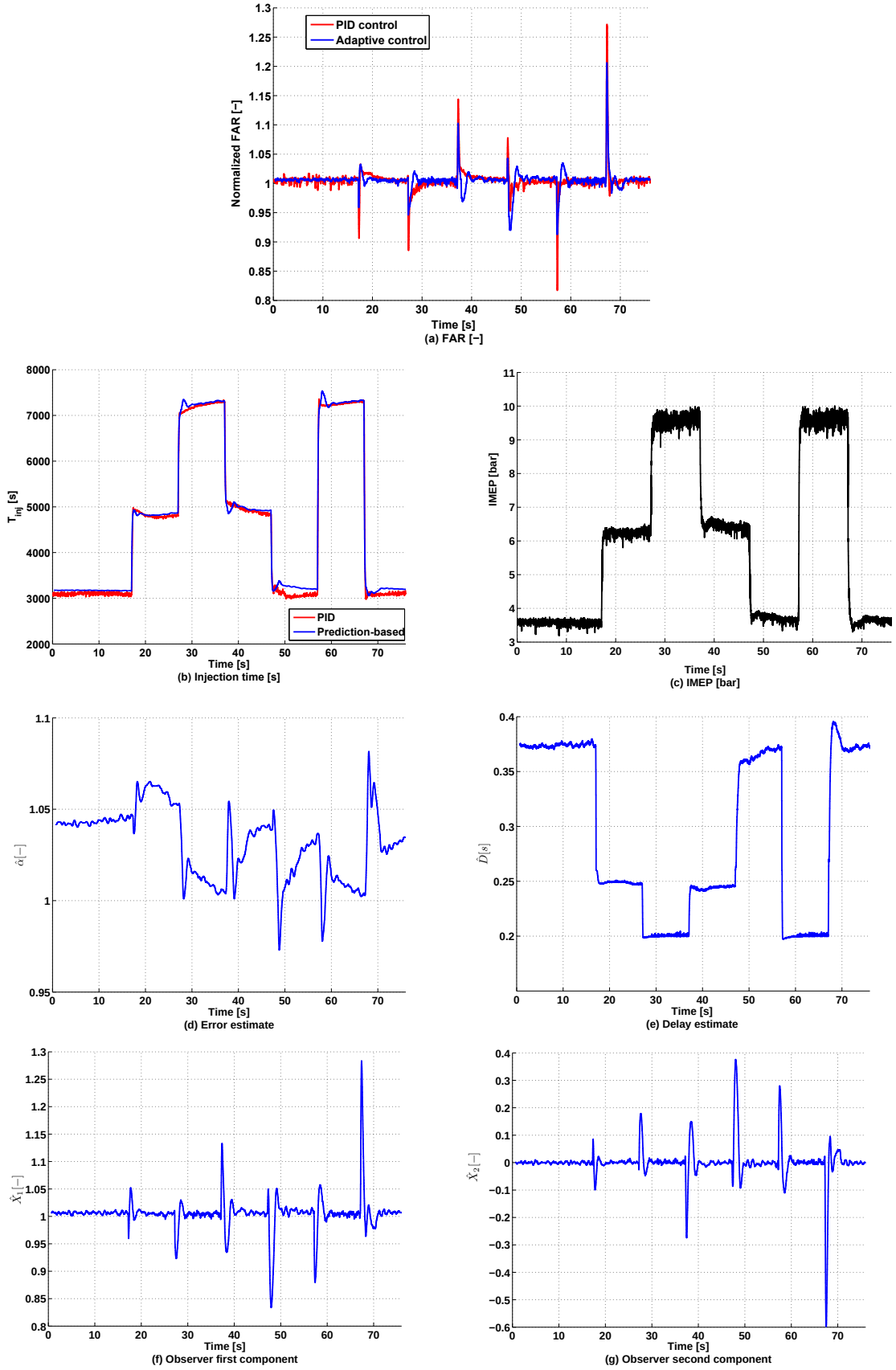

Figure 7.10: Test bench results for a constant engine speed $Ne = 2000$rpm for the torque variations picture in (c), for the proposed strategy (in blue) and for a PID controller (in red). The injection time represented in (b) characterizes the set-point for the injected mass.

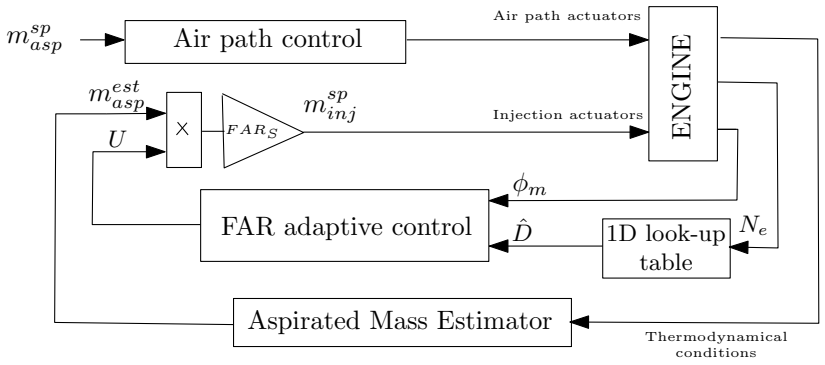

Figure 7.11: Proposed FAR adaptive control strategy for the second-order plant. Compared to Figure 7.7, the control U takes into account the wall-wetting model (τ, X) for indirect injection and compensates for it.

To emphasize the comparison between the classical PID controller and the prediction-based control proposed here, we focus on one particular transient occurring between 16 and 19 s, as shown in Figure 7.12. Three different phenomena occur:

- the aspirated air mass is underestimated during the transient, resulting in mis-synchronization of the fuel path and the air path. The injected fuel mass is computed based on the estimate $m_{asp}^{est} < m_{asp}$. Therefore, during this lag, the resulting intake FAR is $\phi = \frac{m_{asp}^{est}}{m_{asp}} < 1$. This generates the decrease measured between approximately 17.15 and 17.3 s;

- the air mass is still underestimated but, as the feedback loop is based on a prediction, the control anticipates the future important decrease of the FAR. Conversely, the PID simply uses the current FAR value and the computed input is therefore less aggressive. During this second phase, the FAR response of the PID is still decreasing while that of the prediction-based controller starts increasing up to unity; and

- in the last phase, the behavior of the two control laws is quite similar, even if the effect of the start of the transient is still evident.

The integral difference between the two responses during the transient is highlighted in gray in Figure 7.12.

While the first phase may be avoided by carefully designing a predicted aspirated air model (see [Chevalier 00]), the second phase will still occur. This is the main advantage of the proposed controller. The magnitude of this improvement is here accentuated by the mis-synchronization between the two paths, which would not reasonably be allowed on a commercial engine.

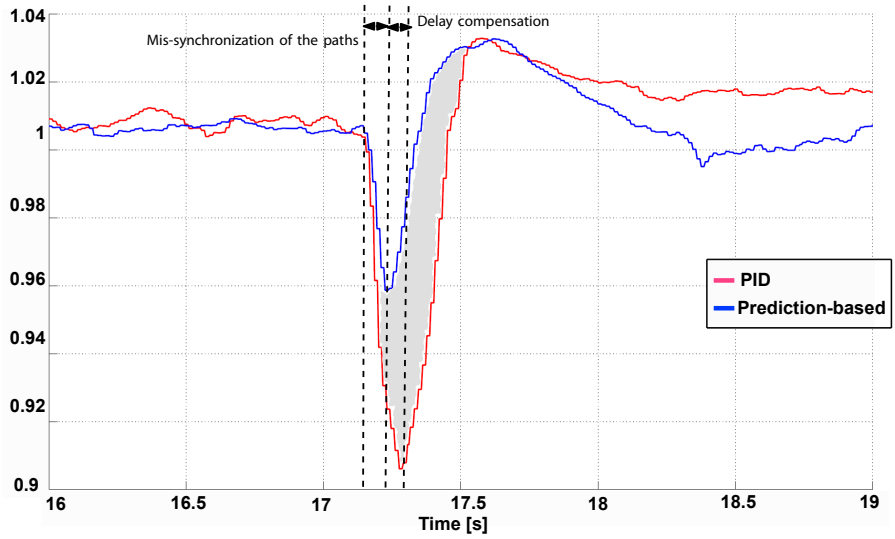

Figure 7.12: Magnification of the variation between 16 and 19 s. The FAR variations (top) originated by the torque request are partially compensated by a change in the injection timing (bottom).

Part II

Robust compensation of a class of time- and input-dependent input delays

Introduction

In this part, we address the problem of compensation-based regulation of a class of time- and input-dependent input delays.

As was detailed in Section 2.2, the key element for exact compensation of a time-varying delay is determination of the time window of the prediction. However, calculation of this time horizon requires knowledge of future variations of the delay to anticipate them. In the absence of any variations modeling, this approach is obviously unsuitable, as no information is available on the future delay.

In this part of the thesis, *robust compensation* is designed by using the current value of the delay as time horizon of prediction. The spirit of this approach is to consider the delay as slowly varying. It naturally calls for an extra assumption for the delay variations, which have to be sufficiently slow.

We go further in the analysis and consider the particular case of input-dependent delays. In this context, exact compensation may even result in an ill-posed problem. This is because of the reciprocal interactions between the control law and the delay, which yield a closed-loop dependence that is pictured in Figure 7.13. For this reason, we propose a two-step methodology for an input-dependent delay that disrupts this loop. First, following the previously mentioned robust compensation result, the delay derivative is required to be bounded. Second, this derivative is related to input fluctuations and to a small-gain condition for the feedback gain.

We formally prove an exponential stabilization result for a specific type of delay model, representative of a large class of flow process. This model involves an integral relation im-

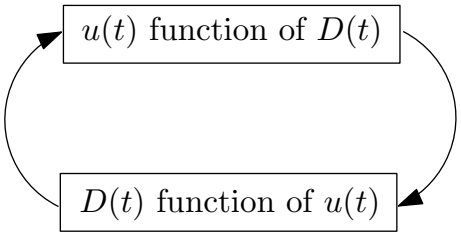

Figure 7.13: For an input-dependent delay, exact compensation of the delay involves the control law $u(t) = KX(r(t))$, where $r(t) = \eta^{-1}(t)$ with $\eta(t) = t - D(t)$. This control law depends on the current value of the delay, which itself depends on the current value of the control law, creating a circular scheme of dependency.

plicitly defining the delay in terms of the input history. Therefore, the delay is inherently time- and input-dependent.

This part is organized as follows. In Chapter 8, the mentioned model of transport delay is presented. Various delay systems, shown to be compliant with this model, are given. Then, in Chapter 9, practical use of this model is proposed, to estimate the transport delay occurring for a low-pressure exhaust burned gas recirculation loop on a SI engine. In Chapter 10, robust compensation of a general time-varying delay is designed, requiring that the delay variations are sufficiently slow. This condition is then further studied in the particular case of input-dependent delay belonging to the considered transport delay class. The merits of this result is then illustrated in Chapter 11 on a well-known time delay system, the temperature regulation of a shower (or bathtub).

Chapter 8

Examples of transport delay systems

Chapitre 8 – Quelques exemples de systèmes dynamiques avec retard de transport. *Ce chapitre détaille une famille particulière de retard variable dépendant de la commande. Le modèle considéré, représentant le retard comme la borne inférieure d'une équation implicite intégrale, est représentatif d'une large gamme de systèmes comprenant un transport de matière. Ce point est illustré ici par plusieurs modèles de systèmes à retard, certains du domaine du contrôle moteur.*

Contents

In this chapter, a particular class of time- and input-dependent delay model is introduced. This model is representative of a wide class of systems involving transport phenomena. To illustrate this point, we list a certain number of examples, most of them relative to SI engines, that entail a transport delay.

This class is then studied in Chapter 10, where sufficient conditions for robust stabilization are provided.

8.1 An implicit integral definition of transport delay

Consider a fluid flow with varying speed $v(t)$ through a pipe of length L. Following the Plug-Flow assumption [Perry 84], one can define the time t_{prop} of propagation through the pipe according to the integral equation[1]

$$\int_{t-t_{prop}}^{t} v(s)ds = L \tag{8.1}$$

[1]Formally, this integral equation can be directly obtained by studying the PDE $u_t + v(t)u_x = 0$ for $x \in [0, L]$ with $v(t) \geq 0$. Consider the new variable $w(t) = u(t, \int_\gamma^t v(s)ds)$ for a given constant $\gamma \leq t$, which satisfies $\frac{dw}{dt} = 0$. Therefore, $\forall t \geq 0\,, \quad w(t) = w(\gamma)$. By choosing $\gamma = t - D(t) \leq t$ such that $\int_{t-D(t)}^{t} v(s)ds = L$ which is the integral relation (8.1), one directly gets that the delay between the output and the input of the system is $D(t)$ as $u(t, L) = w(t) = w(t - D) = u(t - D(t), 0)$.

When one considers a delay D due to a transport phenomenon, it can then be defined through the lower bound of the integral

$$\int_{t-D(t)}^{t} \varphi(s, U(s))ds = 1 \tag{8.2}$$

where φ is a certain non-negative function that depends potentially on the manipulated variable U and potentially implicitly on time, gathering all other dependencies. For the simple example (8.1), one has $\varphi(s, U(s))) = v(s)/L$.

The delay modeled in (8.2) is well-defined:

- $D > 0$: as the function φ is non-negative, the lower bound of the integral has to be less or equal than the lower bound, i.e. $t - D(t) \leq t$.
- $\dot{D}(t) \leq 1$: this property is related to causality and guarantees that no back-flow occurs. Taking a time derivative of (8.2), one obtains

  $$\varphi(t, U(t)) - (1 - \dot{D})\varphi(t - D(t), U(t - D(t))) = 0$$

  or, equivalently,

  $$\dot{D} = 1 - \frac{\varphi(t, U(t))}{\varphi(t - D(t), U(t - D(t)))} \leq 1$$

  because the function φ is non-negative.

Furthermore, because φ is non-negative, the function $f : D \to \int_{t-D}^{t} \varphi(s, U(s))ds$ is strictly increasing and is therefore invertible. Consequently, one can easily compute the transport delay from it. This point is detailed in the next chapter.

We now describe a few examples of SI engine subsystems fitting into this class of models.

8.2 Fuel-to-Air Ratio

In Chapter 7, the FAR regulation problem for SI engines has been presented. As explained in Section 7.1.2, this ratio has to be kept as close as possible to the stoichiometric ratio. To do so, a feedback loop is typically used to coordinate the fuel path and the air path using a measurement given by a dedicated sensor in the exhaust line.

However, since the injector (i.e. the actuator) is located upstream of the intake line, a transport delay occurs. Further delays can be summed as

$$D = D_{inj} + D_{burn} + D_{trans}$$

where D_{inj} is the injection lag, D_{burn} is the combustion delay and D_{trans} is the transport delay from the exhaust valve to the oxygen sensor, which is represented in Figure 8.1. The transport delay can be expressed via the integral equation

$$\int_{t-D_{trans}}^{t} v_{bg}(s)ds = L_{ev\to\lambda}$$

where v_{bg} accounts for the burned gas velocity in the exhaust line and $L_{ev\to\lambda}$ is the pipe length from the exhaust valve up to the Lambda sensor.

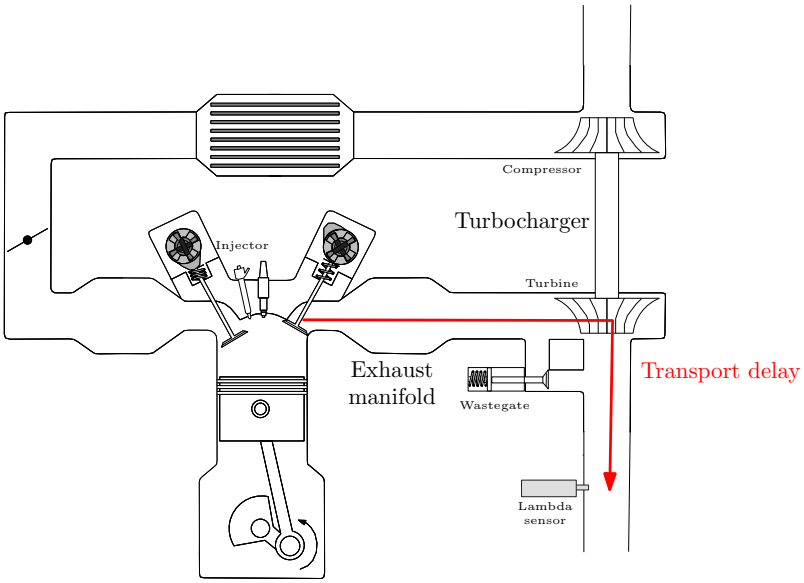

Figure 8.1: Schematic illustration of a turbocharged SI engine equipped with direct injection and VVT devices. In the formulation of the regulation problem of the Fuel-to-Air Ratio, a transport delay occurs because the Lambda sensor (measurement) is located downstream of the turbine (and upstream of the Three-Way catalyst) and the injector (actuator) is located near the combustion chamber.

For FAR regulation, the controlled variable does not interfere with the burned gas velocity v_{bg}. Therefore, the expression in 8.2, can be simplified with a varying input-independent delay,

$$\varphi(s, U(s)) = \varphi(s) = \frac{v_{bg}(s)}{L_{ev \to \lambda}}$$

However, because the gas speed is not measured, the last formula is not directly usable and requires some reformulation, like the one introduced in the next chapter (on a different topic).

8.3 Crushing-mill

In the survey article [Richard 03], a crushing mill system is described as an open problem in which the delay is inherently input-dependent.

This system is depicted in Figure 8.2. An input flow rate u_{in} of raw material enters the crushing mill and its size is reduced when the material is processed through the mill. Depending on the output size, the output flow of material u_{out} may be simply extracted if the size is small enough, or may be recycled over a rolling band of total length L and variable speed v_{rec}, which is controlled.

Then, the flow of recycled matter re-entering the mill depends on the material available on the rolling band and on its speed and is therefore delayed. Again, this delay is due to

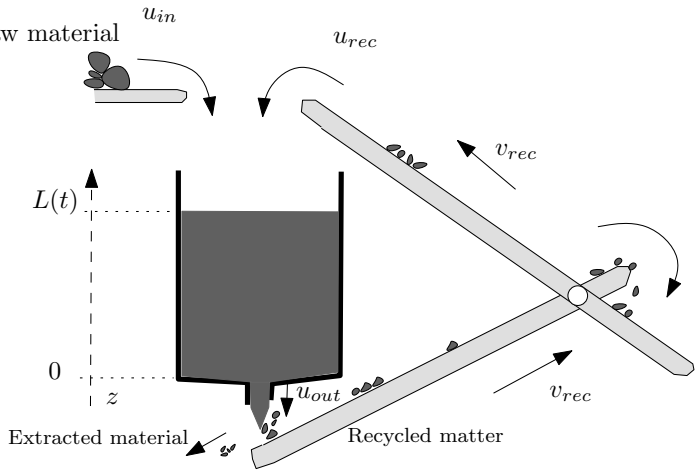

Figure 8.2: Schematic view of the crushing mill, with a variable conveyor speed $v_{rec}(t)$.

material transportation and can be simply expressed via the integral equation

$$\int_{t-D(t)}^{t} v_{rec}(s)ds = L$$

which follows the general form (8.2) with a function φ depending only on the manipulated variable

$$\varphi(s, U(s)) = \varphi(U(s)) = \frac{v_{rec}(s)}{L}$$

A complete model allowing to derive this equation is proposed in Appendix A. This model can be reasonably compared to the bath temperature regulation problem presented later and addressed in Chapter 11. It could be treated using a similar controller. Other examples of process systems that use such delay model can be found in [Chèbre 10, Barraud 06].

8.4 Catalyst internal temperature

We now consider a three-way catalytic converter (TWC) located in the exhaust line of a SI engine to treat pollutant emissions resulting from the combustion process. As the efficiency of this conversion strongly depends on the catalyst wall temperature, it is necessary to consider the thermal behavior of the system to obtain good performance. The model considered here is based on a one dimensional distributed parameter system, which is eventually recast into a linear delay system.

The system is pictured in Figure 8.3. Exhaust burned gas enter the monolith at $x = 0$ with a varying mass flow rate $F(t)$. Convective exchange with the wall occurs all along the monolith from $x = 0$ to $x = L$ yielding inhomogeneous distributed temperature profiles of the gas $T_g(x, t)$ and the catalyst wall $T_w(x, t)$[2]. Initially, when the catalyst is cold, no chemical reaction can occur and only the gas warms the monolith wall. Here, we show that the wall temperature dynamics of the catalyst can be modeled by a first-order plus delay equation, fed by the gas temperature at the inlet. The time-varying delay can be represented by a transport equation of the form (8.2).

[2]On the contrary, the axial conduction in the solid is not important and can be neglected, as previously demonstrated in [Vardi 68], [Young 76].

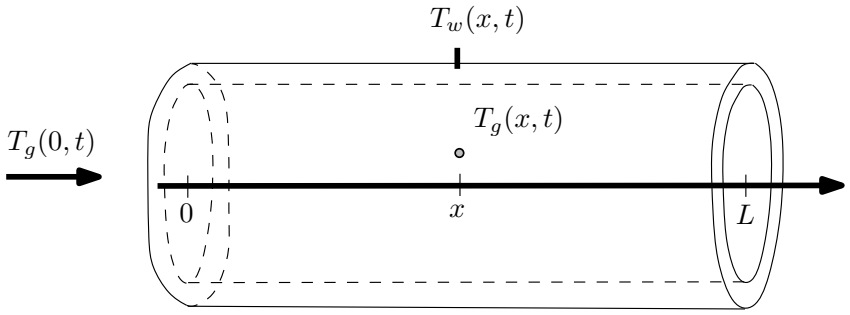

Figure 8.3: Schematic view of the distributed profile temperature inside a TWC, v being the wall temperature and w the temperature of the gas flowing through the catalyst.

Denoting $T_w(.,t)$ and $T_g(.,t)$ respectively the wall and gas temperatures, we consider a coupled linear infinite dimensional thermal dynamics

$$\begin{cases} \dfrac{\partial T_w}{\partial t}(x,t) = k_1(T_g(x,t) - T_w(x,t)) & (8.3) \\ F(t)\dfrac{\partial T_g}{\partial x}(x,t) = k_2(T_w(x,t) - T_g(x,t)) & (8.4) \end{cases}$$

where $F > 0$ is the varying gas mass flow rate and $k_1, k_2 > 0$ are given constants. More details about this model can be found in [Lepreux 10] [3].

By taking a spatial derivative of (8.3), a time-derivative of (8.4) and matching terms with (8.3)-(8.4), one obtains the decoupled equations

$$\begin{cases} F(t)\dfrac{\partial^2 T_w}{\partial x \partial t} = -k_2\dfrac{\partial T_w}{\partial t} - k_1 F(t)\dfrac{\partial T_w}{\partial x} \\ F(t)\dfrac{\partial^2 T_g}{\partial x \partial t} + \dot{F}(t)\dfrac{\partial T_g}{\partial x} = -k_2\dfrac{\partial T_g}{\partial t} - k_1 F(t)\dfrac{\partial T_g}{\partial x} \end{cases}$$

where the first equation defining T_w can be solved using a spatial Laplace transform (with p as Laplace variable) to get

$$\forall t \geq 0\,, \quad (F(t)p + k_2)\frac{d\hat{T}_w}{dt} = -k_1 F(t) p \hat{T}_w(p,t)$$

This scalar system can be solved as

$$\hat{T}_w(p,t) = \exp\left(-\left[\int_{t_0}^{t} \frac{k_1 F(s) p}{F(s)p + k_2} ds\right]\right)\hat{T}_w(p,t_0)$$

for every t_0 such that $t_0 \leq t$. A catalyst is a low-pass filter so it is relatively insensitive to high frequencies. Consequently, by considering only low spatial frequencies (i.e. $Fp << k_2$ for any gas flow F), the term below the integral can be substantially simplified. Taking into account this consideration and rewriting the resulting equation into the space domain, one obtains

$$\forall x \in [0, L]\,, \quad T_w(x,t) = T_w\left(x - \left[\int_{t_0}^{t} \frac{k_1}{k_2} F(s) ds\right], t_0\right)$$

[3] One point of importance to notice is that this model does not include the enthalpy originating from the chemical reactions inside the catalyst.

Formally, for any $x \in [0, L]$, one can define $D(x,t) \geq 0$ such that

$$\int_{t-D(x,t)}^{t} \frac{k_1}{k_2} F(s)ds = x \tag{8.5}$$

which is equivalent to the implicit integral equation (8.2). Consequently, the wall temperature at x is formally delayed by

$$\forall x \in [0, L], T_w(x,t) = T_w(0, t - D(x,t))$$

Besides, using (8.3) for $x = 0$, one can obtain that T_w satisfies a first-order plus delay model with respect to the inlet temperature $T_g(0,.)$.

This delay is indeed a transport delay, compliant with the form (8.2) in which the function φ does not depend on the input (the inlet gas temperature) but on an exogenous signal (the mass flow rate F) and is defined as

$$\varphi(s, U(s)) = \varphi(s) = \frac{k_1}{xk_2} F(s)$$

This delay can be computed from the information of the mass flow rate used for cylinder charge estimation and used for warm-up strategies, for example.

From the elements presented in this chapter, the frequent appearance in process and flow systems of a transport delay defined by an implicit integral relation of type (8.2) is clear. In the following chapter, we describe practical calculations to invert this relation to determine the delay. The system under study is the recirculation of burned gas in SI engines. In Chapter 10, methods to guarantee delay compensation are investigated, with a focus on the class of delay presented in this chapter.

Chapter 9

Practical delay calculation. A SI engine case study : Exhaust Gas Recirculation

Chapitre 9 – Cas pratique de calcul du retard de transport : recirculation de gaz brûlés sur moteur essence. *Ce chapitre détaille l'implémentation pratique du modèle implicite intégral de retard précédemment introduit. La vitesse distribuées des gaz, de dimension infinie et non mesurée, est reliée au débit massique par la loi des gaz parfaits. Cette dernière est utilisée sur une segmentation judicieuse de la ligne admission, réalisée en fonction des capteurs disponibles. Après quelques éléments introductifs, nous détaillons cette procédure ainsi que le modèle de dilution considéré qui est ensuite utilisé en boucle ouverte pour fournir un estimateur du taux de gaz brûlés admission. Des essais expérimentaux sur banc moteur mettent en exergue la pertinence de cet estimateur ainsi que la technique de calcul du retard employée.*

Contents

In this chapter, we present practical computations of a delay transport equation of type (8.2), as described earlier in Chapter 8, occurring on the low-pressure Exhaust Gas Recirculation (EGR) loop of a SI engine.

As emphasized in the previous chapter, because of the positivity of the integrand function φ, the function $f : D \mapsto \int_{t-D}^{t} \varphi(s, u(s))ds$ is strictly increasing and is therefore invertible. For a given history of φ, it is possible to calculate the delay D by successively evaluating the function f for increasing arguments, starting from 0, until the equation defining D is matched. Here, we present a case study for an SI engine for which the function φ is not directly known but related to measured signals (mass flow rates). Despite this difficulty, we show here that the delay can be computed and used, for example, to design an open-loop estimate.

This chapter is organized as follows. In a first section, some further elements of background on downsized SI engines are presented, especially on EGR, before focusing on the resulting transport delay which is the main specificity of this technology (compared to the one usually embedded in Diesel engines). We present a model of the intake burned gas rate dynamics, under the form of a LTV system with a time-dependent delay output. Implementation and test bench experimental results are provided.

9.1 Background on turbocharged SI engines and interest of EGR

Downsizing (reduction of the engine size) has appeared as the most efficient solution to reduce pollutant emissions of SI engines and, in turn, satisfy increasingly stringent environmental requirements. Downsized engines can reach high levels of performance and driveability, provided they are equipped with direct injection, turbocharger and Variable Valve Timing (VVT) actuators [Stefanopoulou 98].

A major control issue for such engines is prevention of the knock phenomenon, which is an undesirable self-ignition of the gaseous blend that occurs at high loads (see [Eriksson 99]). To address this issue, one strategy is to use EGR through a low-pressure circuit (see [Hoepke 12] or [Potteau 07]). A typical implementation is represented in Figure 9.1. In this recirculation configuration, burned gases are picked up downstream of the catalyst and mixed with fresh air upstream of the compressor. EGR is a valuable alternative to spark advance degradation, which is commonly considered to prevent knock[1]. The addition of exhaust gas to the gaseous blend leads to an increase of the auto-ignition delay: intermixing of the incoming air with recirculated exhaust gas dilutes the mixture with inert gas, increases its specific heat capacity and consequently lowers the combustion peak temperature. The net effect of EGR is therefore prevention of knock which leads to substantial improvements of overall combustion efficiency [Cairns 05].

However, EGR has some downside. During tip-outs (defined as a transient mode during which the torque demand is suddenly decreased), the presence of burned gases in the intake manifold, and later in the combustion chamber, seriously impacts the combustion process and may cause the engine to stall. Furthermore, EGR has strong interactions with simultaneously operating engine controllers such as stoichiometric FAR regulation [Jankovic 09]. To illustrate this point, Figure 9.2 shows a classic architecture for engine control with air path control, fuel path control and ignition path control. To counteract

[1]Furthermore, the latter solution leads to a substantial increase in the exhaust gas temperature, which is detrimental to the exhaust after-treatment devices. To counteract this phenomenon, the combustion mixture is often purposely made richer to decrease the exhaust temperature. Consequently, in addition to a higher fuel consumption, the catalyst efficiency is significantly reduced.

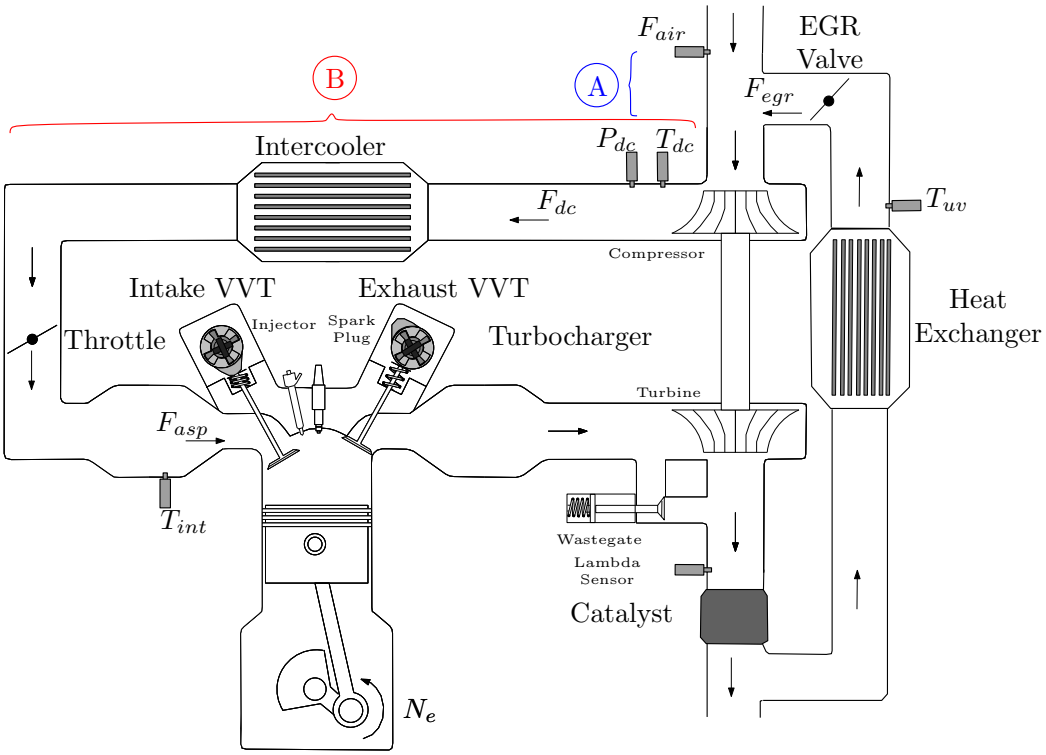

Figure 9.1: Scheme of a turbocharged SI engine equipped with direct injection, VVTs and a low-pressure EGR loop. Parts A and B of the intake line account for two different dynamics that are depicted in Figure 9.3.

the impact of intake burned gas, a solution would be to modify the feedforward action on the cascaded controllers (fuel path and ignition path controllers) based on a real-time estimate $\hat{x}$ of the intake burned gas rate.

However, it is not easy to obtain this estimate. First, no real-time sensor for this variable is embedded in real-world vehicles. The approach that we advocate is to substitute a model for such a sensor[2]. Second, for the low-pressure gas recirculation circuit considered, the amount of burned gases reintroduced is controlled by an EGR Valve, an actuator located upstream of the compressor. Consequently, the relatively long distance between the compressor and the inlet manifold leads to a large transport delay (up to several seconds depending on the engine specifications). Most importantly, this delay depends on the gas flow rate and therefore is time-varying (and partly input-varying, as emphasized below) to a large extent.

Comparison with Diesel EGR In the seemingly similar context of automotive Diesel engines, numerous solutions for the discussed control issues have been developed in the last decades (see for example [Ammann 03], [Van Nieuwstadt 00], [Zheng 04] and the references therein). However, none of these strategies includes any transport delay model, which is non-negligible for SI engines, as discussed. Indeed, besides using a low-pressure EGR circuit configuration (which substantially increases the transport lag compared to high-pressure configuration [Stotsky 02] [Lauber 02]), the combustion constraints for SI

[2]Other studies (see [Caicedo 12]) have investigated the potential of using a cylinder pressure sensor signal, but such sensors are not commercially used at present because of cost constraints.

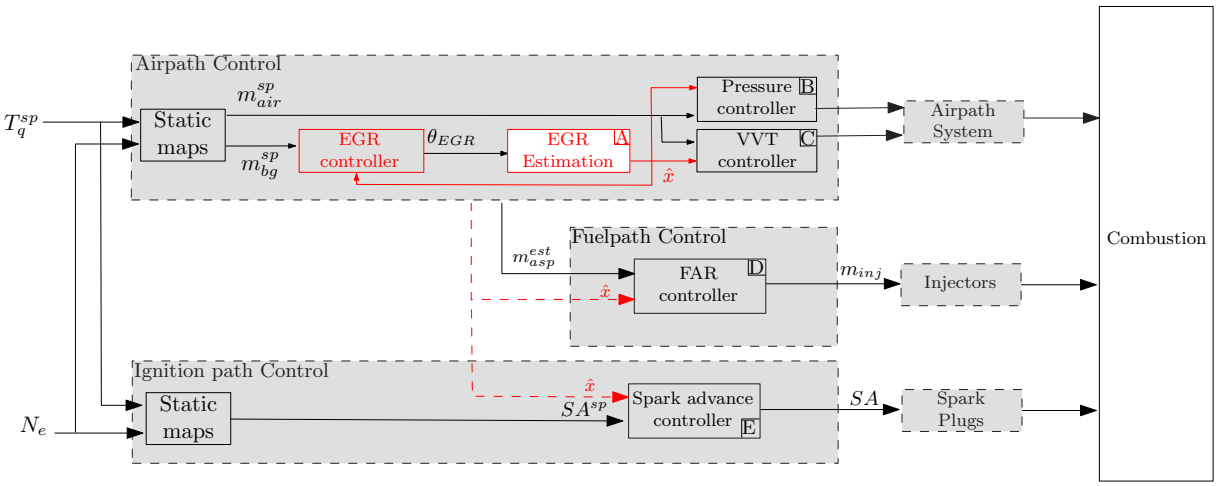

Figure 9.2: Classic architecture for SI engine control with elements relative to EGR shown in red. Block A contains the model proposed in this chapter. Blocks B and C are the low-level pressure and VVT controllers. Block D is the low-level FAR controller. Block E is the spark advance controller. $\hat{x}$, an estimate of the intake burned gas fraction, used as an extra feedforward term would bring a relevant mean of controllers coordination and be a source of valuable performances improvements.

engines significantly increase the magnitude of the delay:

1. first, SI engines require a stoichiometric FAR, which results in a fraction of burned gas close to unity in the exhaust line. Consequently, to obtain a given intake fraction of burned gas, the amount of exhaust burned gas to be reintroduced at steady state is substantially lower than for Diesel engines;

2. in contrast to Diesel engines, SI engines may operate at intake pressure less than atmospheric pressure (low loads). For this operating range, the steady-state gas flow rates are considerably less important. To illustrate this point, consider an idle speed operating point for both Diesel (intake manifold pressure $P_{int} = 1$ bar) and SI ($P_{int} = 0.2$ bar) engines. At fist order, thermodynamical conditions on the intake line (from the EGR valve down to the throttle) can be considered as similar for the two engines and the gas mass flow rates as proportional to the intake manifold pressure. Therefore, the propagation time is up to $\frac{1}{0.2} = 5$ times more important for the SI application.

Here, a model of the intake burned gas rate is presented, that explicitly accounts for the transport time-varying delay and its dependency on the history of gas flow rates in a way that compensates for thermal exchanges and induced changes in the gas velocity. The model is then used as a "software" sensor. The estimation is based on a practical delay calculation that was experimentally validated on a test bench. The estimate is then used to coordinate the controllers.

9.2 Modeling

Consider the air path of a turbocharged SI engine equipped with an intake throttle, a waste gate, dual independent VVT actuators and a low-pressure EGR loop, as depicted in Figure 9.1. Such a set-up is usually considered for downsized engines [Kiencke 00].

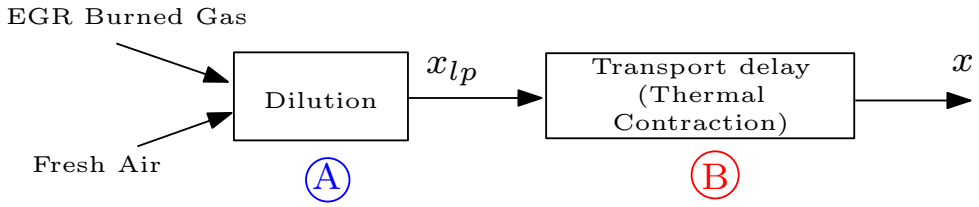

Figure 9.3: Scheme of the intake burned gas fraction dynamics.

Formally, the in-cylinder burned gas fraction x_{cyl} is defined as the ratio of the in-cylinder burned gas mass originating from the EGR loop m_{bg} to the total mass of gas in the cylinder volume ($m_{asp} = m_{air} + m_{bg}$)

$$x_{cyl} = \frac{m_{bg}}{m_{air} + m_{bg}}$$

Hereafter, this variable is considered equal to x the intake burned gas fraction [3].

9.2.1 Dilution dynamics and transport delay

Defining x_{lp} as the burned gas rate upstream of the compressor, the EGR dynamics can be expressed as

$$\dot{x}_{lp} = \alpha \left[-(F_{egr}(t) + F_{air}(t))x_{lp}(t) + F_{egr}(t) \right] \tag{9.1}$$
$$x(t) = x_{lp}(t - D(t)) \tag{9.2}$$

where $D(t)$, the transport delay between this ratio and the intake composition, can be implicitly defined by the integral equation

$$\int_{t-D(t)}^{t} v_{gas}(s)ds = L_P \tag{9.3}$$

where L_P is the pipe length from the compressor to the intake manifold and v_{gas} is the gas speed. (9.3) is in the form (8.2).

Comments Equation (9.1) is a balance equation for the volume downstream of the EGR valve, using the fact that the EGR circuit is totally filled with burned gas[4]. Depending on the engine set-up, the thermodynamics constant α in (9.1) is either measured or known. Following the proposed model, which is represented in Figure 9.3, the intake burned gas fraction is a first order dynamics with a transport delay.

For clarity, the approach used to model the mass flow rate variables in (9.1)–(9.3) is presented in Appendix C. We assume that these are known quantities.

To provide an implementable open-loop estimation of x based on the model (9.1)–(9.3), the delay D must be related to available measurements. This point is now addressed.

[3] In fact, this relation depends mainly on the VVT control strategy [Leroy 08]. We neglect this influence here for the sake of clarity.

[4] For SI engines, FAR is regulated to its stoichiometric value (see [Heywood 88]), which results in an exhaust burned gas fraction close to unity.

9.2.2 Transport delay description

Equation (9.3) implicitly determines the delay according to the gas speed along the intake line, which, besides being a distributed parameter, is not measured in practice. However, using the ideal gas law (as is classically done for engine gas flows, e.g. in [Heywood 88]), one can relate this variable to thermodynamic conditions and mass flow rates that are measured or modeled. The used relation is

$$\forall t \geq 0\,, \quad v_{gas}(t) = \frac{1}{S(x)} \frac{rT(t)}{P(t)} \left[F_{air}(t) + F_{egr}(t)\right]$$

where

- S is the current pipe area
- T, P are the current temperature and pressure values
- r is, as previously, the (common) ideal gas constant of both fresh air and burned gas

From this reformulation, it is clear that the delay can be implicitly expressed using the mass flow rates $F_{air}(t)$ and $F_{egr}(t)$[5]. Consequently, the delay variations depend on both the input (the EGR mass flow rate) and implicitly on time (via the fresh air mass flow rate and the pressure/temperature), which is compliant with the general form of (8.2). In practice, the total mass flow rate under the integral is estimated as $F_{air}(s) + F_{egr}(s) = F_{dc}(s)$ (a model of the mass flow rate F_{dc} being provided in Appendix C).

Thermal contraction of the gas occurs inside the intake cooler (Figure 9.1). This results in spatial variations in the gas velocity v_{gas}. To model this, we split the intake line into three main sections with cumulative transport delays D_1, D_2 and D_3 such that $D = D_1 + D_2 + D_3$. This decomposition is pictured in Figure 9.4. The three main sections are as follows:

- *downstream of the compressor to the intercooler:* here, the current pressure and the temperature are measured. We can use them to write

$$\int_{t-D_1(t)}^{t} \frac{rT_{dc}}{P_{dc}} F_{dc}(s)ds = V_1 \tag{9.4}$$

  where V_1 is the corresponding volume.

- *inside the intercooler:* considering boundary conditions, the pressure inside the intercooler can reasonably be assumed to be spatially constant and equal to the input pressure P_{dc}. We assume that the spatial profile of the internal temperature is affine with respect to the spatial variable, with measured boundary conditions T_{dc} and T_{int}, i.e. $T(x) = \frac{T_{int}-T_{dc}}{L_2}x + T_{dc}$ for any position $x \in [0, 1]$ inside the intercooler. Under this assumption, (9.3) yields

$$\int_{t-D_2(t)-D_1(t)}^{t-D_1(t)} \frac{r}{P_{dc}} F_{dc}(s)ds = S_2 \int_0^{L_2} \frac{dx}{T(x)} = \frac{V_2}{T_{int} - T_{dc}} \ln\left(\frac{T_{int}}{T_{dc}}\right) \tag{9.5}$$

  where L_2, S_2 and V_2 are the corresponding length, area and volume.

[5]In classical control architectures, the intake manifold pressure is regulated to provide a given in-cylinder mass of fresh air, regardless of the amount of recirculated burned gas. Therefore, these two mass flow rates can be considered as independent.

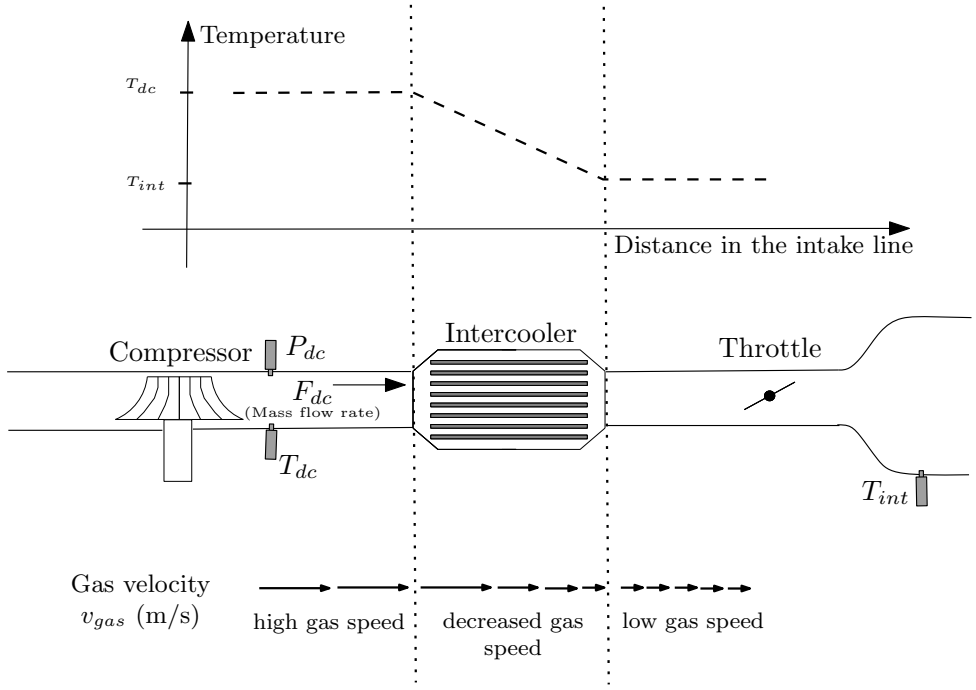

Figure 9.4: The intake line is split into three parts to account for spatial differences in the gas velocity. Along the line, the temperature decreases, which results in an increase in velocity that is analytically determined by the ideal gas low using measurements from temperature and pressure sensors located along the line.

- *downstream of the intercooler to the intake manifold:* here, the temperature is approximately equal to the intake manifold temperature, which yields

$$\int_{t-D_3(t)-D_2(t)-D_1(t)}^{t-D_2(t)-D_1(t)} \frac{rT_{int}}{P_{dc}} F_{dc}(s)ds = V_3 \tag{9.6}$$

  where V_3 is the corresponding volume.

Setting values for the intermediate volumes V_1, V_2 and V_3, one can calculate the delay in a very straightforward manner, solving (9.4), (9.5) and (9.6) sequentially. The transport delay is then simply deduced as $D(t) = D_1(t) + D_2(t) + D_3(t)$.

The numerical method for solving this problem is based on the observation that the term under the integral is strictly positive and that the integral is then a strictly increasing function of the delay D_i ($i \in \{1, 2, 3\}$) appearing in its lower bound. By simply sampling and evaluating the integral at increasing values of D_i starting from 0, one can obtain a numerical evaluation of the corresponding delay. All these calculations can be performed online[6].

9.2.3 Estimation strategy with practical identification procedure

An estimation strategy for the model above is summarized in Figure 9.5. Real-time temperatures and pressures measurements are used to determine the value of the delay.

[6]This approach is directly inspired of [Petit 98] and [Zenger 09] for modeling plug flows in networks of pipes problem.

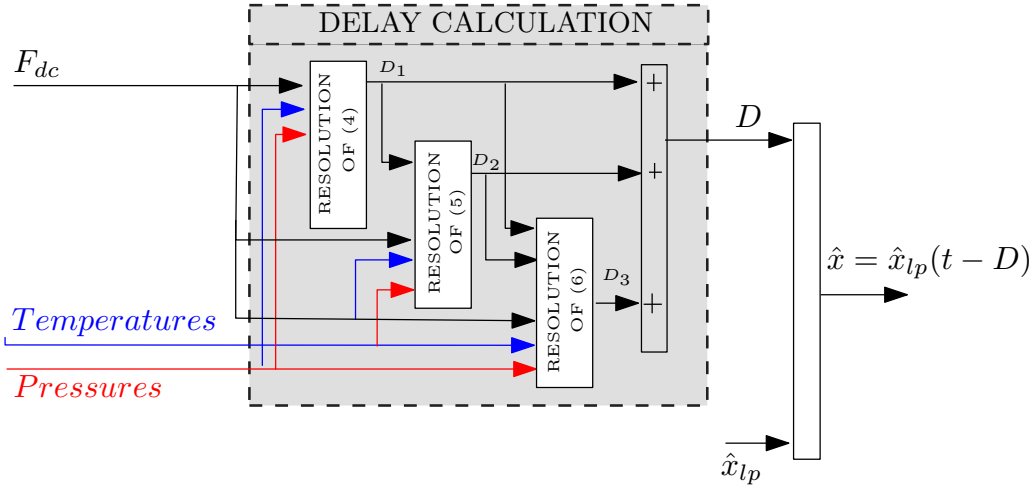

Figure 9.5: Strategy for proposed delay calculation for intake burned gas fraction estimate x. The implicit integral equations (9.4)–(9.6) can be numerically solved by sampling and calculating the integrals at increasing values of D_i starting from 0, which are real-time compliant calculations.

These informations are commonly available using (cheap) embedded sensors. Values for physical volumes (V_1, V_2 and V_3) can be used to calibrate the model.

It is worth noting that splitting of the intake line as proposed above was motivated mainly by the instrumentation available and in particular by the availability of temperature (and pressure) sensors. It can easily be adapted to any engine. In particular, if no temperature nor pressure sensors are available downstream of the compressor, they can be replaced by approximations using the intake values at the expense of slight updates of the volumes values in the fit. Indeed, the two pressures are sufficiently close and these equations are moderately sensitive to temperature. In such a case, the delay can be directly determined by one equation of type (9.4).

9.3 Experimental results

The proposed model (9.1)–(9.3) together with (9.4)–(9.6) was used as a "software" sensor and the estimate obtained was embedded into a real-time control target and used on a test-bench. The experiments aim at validating the model and in particular the delay modeling.

9.3.1 Experimental set-up and indirect validation methodology from FAR measurements

The engine under consideration is a Renault F5Rt 1.8L four cylinder SI engine with direct injection (see [Le Solliec 06] for details). The air path consists of a turbocharger controller with a waste gate, an intake throttle, an intercooler and a low-pressure EGR loop. This engine set-up is consistent with the scheme in Figure 9.1.

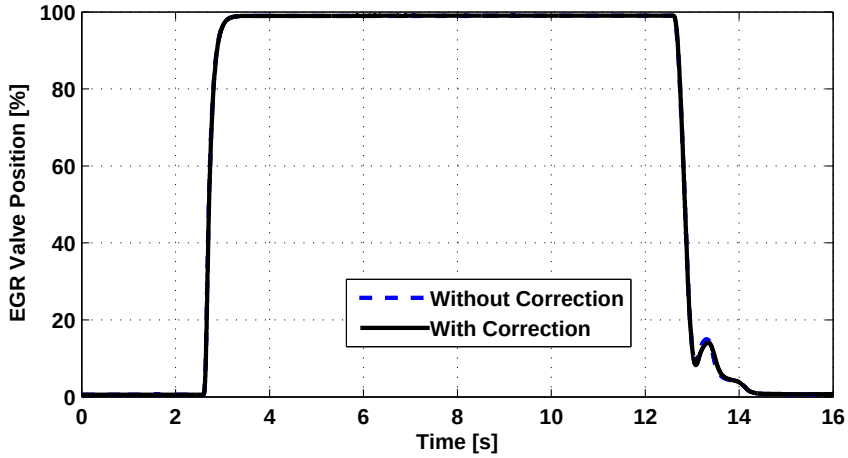

(a) EGR valve position

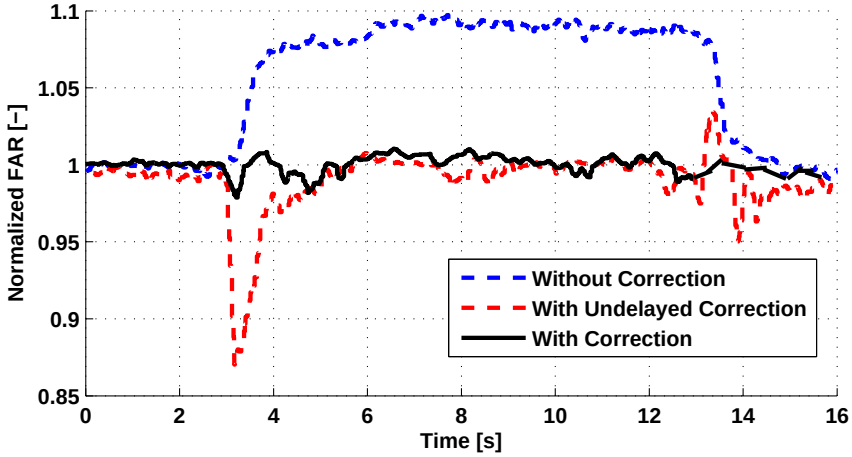

(b) Normalized FAR

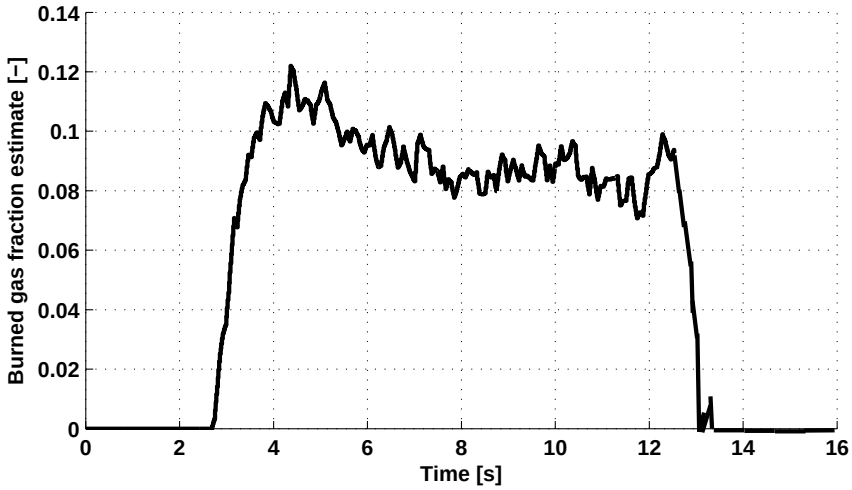

(c) Burned gas fraction estimate

Figure 9.6: Experimental results for constant engine speed ($N_e = 2000$ rpm) and torque request (IMEP = 8 bar). The EGR valve position is pictured in (a). Blue dotted curve: gas composition transient without estimation. Black curve: gas composition transient with estimation and feedforward correction.

To validate the proposed estimation strategy, since *no real-time information for the intake burned gas fraction is available* for this engine, we focus on the open-loop response of the FAR, which should be regulated to 1.

Here, the FAR is simply controlled by a feedforward strategy for the mass of fuel injected into the cylinder, namely

$$m_{inj} = FAR_{st} m_{air}$$

The additional feedback term that is commonly used is purposely omitted.

When no burned gas is recirculated, the in-cylinder air mass is accurately estimated using the model presented in Appendix (see [Leroy 09]), i.e. $m_{air} = m_{asp}$. When burned gas are reintroduced, one can formally write $m_{air} = m_{asp} - m_{bg} = m_{asp}(1 - x)$ and consequently estimate the in-cylinder air mass as $m_{asp}(1 - \hat{x})$, where $\hat{x}$ is the estimate of the intake burned gas fraction provided by the proposed model.

With this setup, it is possible *to qualitatively relate the FAR variations to the intake burned gas fraction*. Indeed, if the estimation is accurate, the normalized FAR remains close to unity and, in turn, one obtains an indirect validation of the intake burned gas rate estimation. Any offset reveals a steady-state estimation error while any temporary undershoot (or overshoot) reveals a mis-estimation of the delay.

9.3.2 First validation : variation of the amount of reintroduced EGR (constant delay)

The first scenario considered is variation of the amount of burned gas reintroduced for a given operating point. Two different operating points are considered, both at a constant engine speed $N_e = 2000$ rpm for a requested torque of 12.5 bar (Figure 9.7) and of 8 bar (Figure 9.6).

This scenario is of particular interest for validation as the intake mixture composition is the only parameter that varies.

Figure 9.7(c) and Figure 9.6(c) picture the intake burned gas fraction estimates corresponding to the EGR valve variations in (a). The corresponding delays are constant and are not reported.

With burned gas feedforward correction: $m_{air} = (1 - \hat{x})m_{asp}$ The corresponding normalized FAR evolution is pictured in black in Figure 9.7(b) and Figure 9.6(b). It is clear that, in both cases, the normalized FAR remains satisfactorily close to the unity. This behavior reveals a good fit between the real intake burned gas rate and the estimate provided in Figure 9.6(c).

For comparison, the FAR response for a burned gas fraction estimate computed neglecting the delay is also provided (red dotted curves). The mis-synchronization due to neglecting the delay leads to a transient overestimation of the burned gas fraction and consequently to a significant FAR undershoot. This stresses the importance of the delay in the burned gas rate dynamics and the relevance of the proposed model.

Without burned gas correction, i.e. considering $m_{air} = m_{asp}$ In this case, as the in-cylinder mass air is overestimated, the injected mass of fuel is too large. This results in

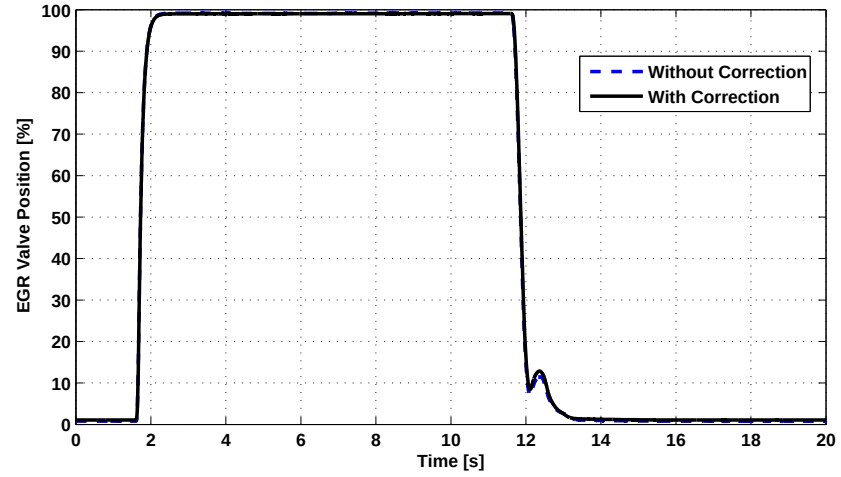

(a) EGR valve position

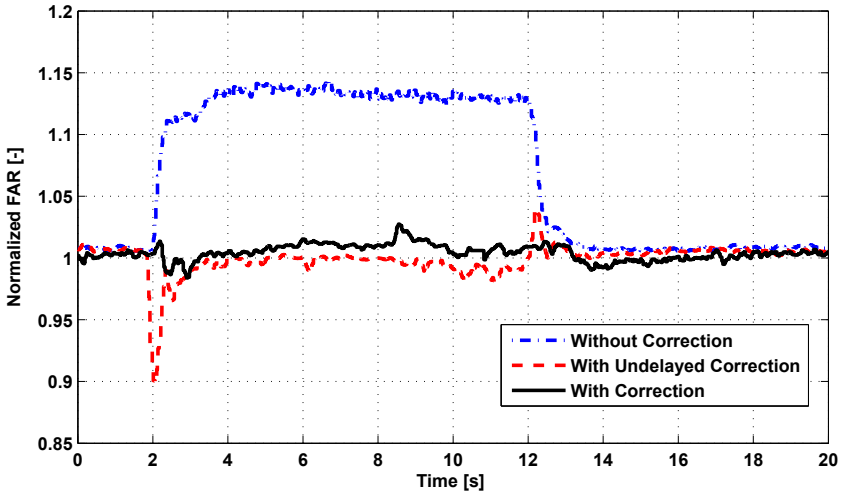

(b) Normalized FAR

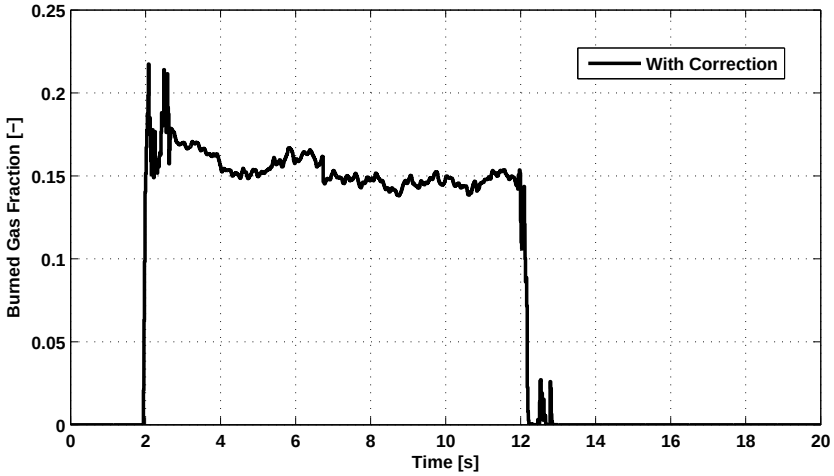

(c) Burned gas fraction estimate

Figure 9.7: Experimental results for constant engine speed ($N_e = 2000$ rpm) and torque request (IMEP = 12.5 bar). The EGR valve position is pictured in (a). Blue dotted curve: gas composition transient without estimation. Black curve: gas composition transient with estimation and feedforward correction.

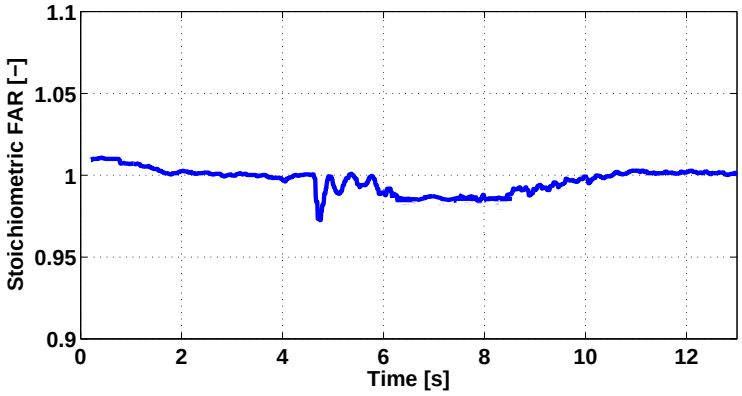

(a) Normalized FAR

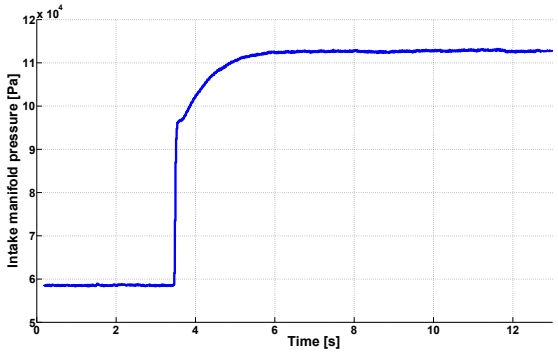

(b) Intake manifold pressure

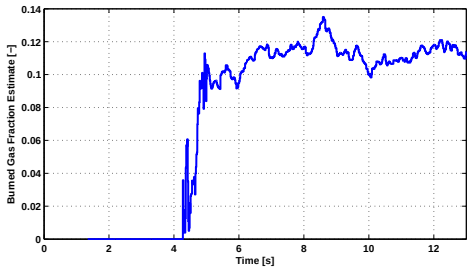

(c) Intake burned gas fraction estimate

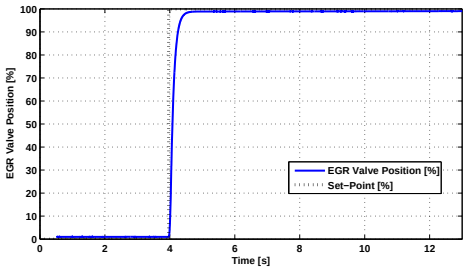

(d) EGR valve position

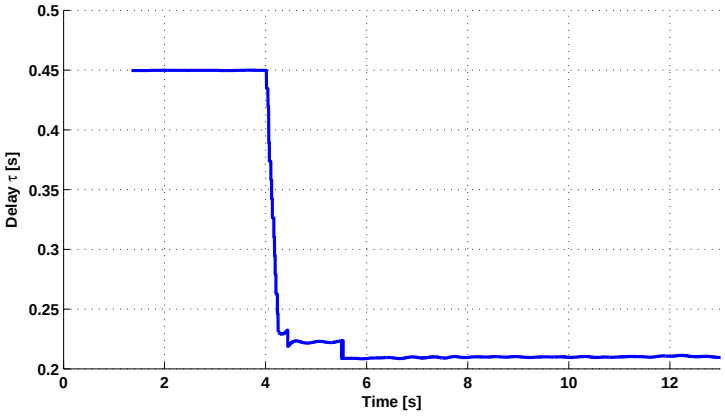

(e) Transport delay

Figure 9.8: Experimental results for constant engine speed ($N_e = 2000$ rpm) and a transient torque request (step from IMEP = 6 bar to 12.5 bar), resulting into a delay variation. The normalized FAR response pictured in (a) uses the intake burned gas fraction estimation pictured in (b), obtained with the on-line estimation of the delay (d).

both case in deviation of the normalized FAR, respectively to 1.14 and 1.09 (blue dotted curve in Figure 9.7 and Figure 9.6). A feedback control would reasonably eliminate this offset, but, since the FAR measurement obtained is delayed (see [Lauber 11] for a FAR dynamics details), an important overshoot would still be present.

9.3.3 Second validation : torque transients (varying delay)

The second scenario under consideration is a torque transient requested by the driver corresponding to a step from 6 bar to 12.5 bar. This tip-in is a typical driving situation leading to an increase in the in-cylinder air mass set point and consequently the total gas flow rate. Both the dilution dynamics in (9.1) and the delay vary during this transient.

The scenario also implies a variation of the EGR amount requested, as the initial operating point is low loaded and does not require any EGR. Without any dedicated control structure, we simply consider here the EGR valve position as either fully closed or fully open. Its variations are shown in Figure 9.8(c).

The calculated delay is shown in Figure 9.8(d). As the total mass flow rate increases during the transient, the delay gradually decreases, as expected.

Finally, as in the previous scenario, FAR remains close to unity. This validates the burned gas fraction estimate variations depicted in Figure 9.8(b).

Chapter 10

Robust compensation of a varying delay and sufficient conditions for the input-dependent transport delay case

Chapitre 10 – Compensation robuste d'un retard variable et conditions suffisantes pour une famille de retard dépendant de la commande. *Dans ce chapitre, nous proposons d'utiliser la valeur courante du retard comme horizon de prédiction dans le contrôle et prouvons que le retard est alors compensé de façon robuste pourvu que ses variations soient suffisamment lentes au cours du temps. Dans le cas d'un retard dépendant de la commande et défini par l'équation intégrale de transport faisant l'objet des chapitres précédents, nous montrons qu'une condition suffisante pour cela est une condition de petit gain portant sur le gain de rétroaction. Ce résultat est obtenu grâce à des propriétés de stabilité d'équations différentielles à retard (inégalités de type Halanay), obtenues par analyse de la dépendance implicite entre commande et variations du retard.*

Contents

In this chapter, the problem of robust compensation of a time- and input-dependent delay is addressed. We focus on the class of transport delays described in Chapter 8 and illustrated in Chapter 9.

We consider a potentially unstable LTI plant driven by a delayed input ϕ, where the

varying delay $D(t)$ is implicitly defined in terms of the input history by

$$\int_{t-D(t)}^{t} \varphi(s, U(s))ds = 1 \tag{10.1}$$

where the integrated variable φ is assumed to be strictly positive with a strictly positive lower bound. Therefore, the resulting transport delay $D(t)$ is well defined and, in particular, is upper-bounded. Our aim is to stabilize the plant over a given equilibrium set-point by a predictor-based feedback approach.

The main concern for compensation of a time-varying delay is the calculation of the prediction horizon, which involves future variations of the delay. The particular model of transport delay under study here does not allow prediction of future delay values. This is why only *robust compensation* is designed here, in which the prediction is simply calculated based on the current value of the delay.

We start our analysis with formulation of a general condition for the delay variation to achieve global exponential stabilization of the plant. We then focus on the particular case of a solely input-dependent delay and relate this condition to a small-gain condition for the feedback gain.

10.1 Robust compensation for time-varying delay

Theorem 10.1.1

Consider the closed-loop system

$$\dot{X}(t) = AX(t) + BU(t - D(t)) \tag{10.2a}$$

$$U(t) = K\left[e^{AD(t)}X(t) + \int_{t-D(t)}^{t} e^{A(t-s)}BU(s)ds\right] \tag{10.2b}$$

where $X \in \mathbb{R}^n$, U is scalar, the vector K is chosen such that $A + BK$ is Hurwitz, and $D : \mathbb{R}_+ \to [0, \overline{D}]$ is a time-differentiable function. Consider the functional

$$\Gamma(t) = |X(t)|^2 + \int_{t-D(t)}^{t} U(\theta)^2 d\theta + D(t)^2 \int_{t-D(t)}^{t} U'(\theta)^2 d\theta$$

There exists $\delta^* \in]0; 1[$ such that, provided

$$\forall t \geq 0\,, \quad |\dot{D}(t)| < \delta^*\,, \tag{10.3}$$

then there exist $R, \rho > 0$ such that

$$\forall t \geq 0\,, \quad \Gamma(t) \leq R\Gamma(0)e^{-\rho t}$$

and the plant (10.2a) *globally exponentially converges to the origin.*

Control law (10.2b) is a predictor directly inspired by the constant delay case and forecasts values of the state over a time window of varying length $D(t)$. *Exact compensation of the delay is not achieved with this controller.* For exact compensation, one would need

to consider a time window of length which exactly matches the value of the future delay, as in [Nihtila 91] and [Krstic 09a]. In detail, defining the delay operator $\eta(t) = t - D(t)$ and assuming that its inverse $r = \eta^{-1}$ exists and is available, exact delay-compensation is obtained according to the feedback law

$$U(t) = KX(r(t)) = K\left[e^{A(r(t)-t)}X(t) + \int_{t-D(t)}^{t} e^{A(r(t)-r(s))}BU(s)\frac{ds}{1-\dot{D}(r(s))}\right] \quad (10.4)$$

However, this requires to be able to predict the future variation of the delay via the function r, for which values over the time interval $[t - D(t), t]$ are necessary to calculate (10.4). This may not be practically achievable for an input-varying delay (more details are given in Section 2.2).

In this context, equation (10.3) can be interpreted as a condition for robust compensation achievement[1]. This condition means that if the delay varies sufficiently slowly, its current value $D(t)$ used for prediction is close enough to its future values, and the corresponding prediction is accurate enough to guarantee stabilization of the plant. In other words, one can easily observe that, assuming $\dot{D}(t) << 1$ (and consequently $r(t) - r(s) \approx t - s$) (10.2b) is a direct approximation of (10.4).

The main advantage of this prediction-based approach is that control law (10.2b) only requires knowledge of the current delay value and is therefore implementable provided the delay is known.

We now prove this theorem.

Proof: In the following, we use the Lyapunov tools presented in Section 2.4 to analyze the stability of input time-delay systems.

First, to extend these tools to the time-varying delay case, we introduce the distributed input $u(x,t) = U(t + D(t)(x-1))$, $x \in [0,1]$, so the plant (10.2a) can be rewritten as

$$\left\{\begin{array}{rcl} \dot{X}(t) & = & AX(t) + Bu(0,t) \\ D(t)u_t(x,t) & = & u_x(x,t) + \dot{D}(t)(x-1)u_x(x,t) \\ u(1,t) & = & U(t) \end{array}\right.$$

The input delay is now represented as a coupling with a transport PDE driven by the input and for which the convection speed varies both with space and time.

Pursuing the mentioned approach, we now define the following transformed distributed input

$$w(x,t) = u(x,t) - D(t)K\int_0^x e^{AD(t)(x-y)}Bu(y,t)dy - Ke^{AD(t)x}X(t) \quad (10.5)$$

This Volterra integral equation of the second kind is designed such that $w(1,t) = 0$, consistently with the control choice formulated earlier. The plant corresponding to (10.2a)–(10.2b) can then be expressed as

$$\left\{\begin{array}{rcl} \dot{X}(t) & = & (A+BK)X(t) + Bw(0,t) \\ D(t)w_t(x,t) & = & w_x(x,t) - \dot{D}(t)g(x,t) \\ w(1,t) & = & 0 \end{array}\right. \quad (10.6)$$

[1]Interestingly, a similar condition is often stated in Linear Matrix Inequality approaches, such as [Yue 05] for example, in which the delay is also assumed to be time-differentiable.

where the function g is defined as

$$\begin{aligned} g(x,t) =&(1-x)u_x(x,t) + D(t)K\left[Axe^{AD(t)x}X(t) + \int_0^x e^{AD(t)(x-y)}B(y-1)u_x(y,t)dy\right] \\ &+ D(t)K\int_0^x e^{AD(t)(x-y)}(I + AD(t)(x-y))Bu(y,t)dy \end{aligned}$$

For the Lyapunov analysis below, we also need the equation governing the spatial derivative of the transformed distributed input w_x

$$\begin{aligned} D(t)w_{xt}(x,t) =&w_{xx}(x,t) - \dot{D}(t)g_x(x,t) \\ w_x(1,t) =&\dot{D}(t)g(1,t) \end{aligned}$$

We can now start the Lyapunov analysis and introduce the following Lyapunov-Krasovskii functional

$$V(t) = X(t)^T PX(t) + b_1 D(t)\int_0^1 (1+x)w(x,t)^2dx + b_1 D(t)\int_0^1 (1+x)w_x(x,t)^2dx$$

where the symmetric matrix P satisfies the Lyapunov equation $P(A+BK) + (A+BK)^T P = -Q$ for a given symmetric definite positive matrix Q for which $\lambda_{min}(Q)$ is its minimum eigenvalue. After taking a time derivative of V, integrations by parts yield

$$\begin{aligned} \dot{V}(t) \leq& -\tilde{X}(t)^T Q\tilde{X}(t) + 2\tilde{X}(t)^T PBw(0,t) + b_1\left(-w(0,t)^2 - \|w(t)\|^2\right) + b_1\left(2w_x(1,t)^2\right. \\ &\left.-w_x(0,t)^2 - \|\hat{w}_x(t)\|^2\right) + |\dot{D}(t)|b_1\int_0^1 (1+x)[w(x,t)^2 + w_x(x,t)^2]dx \\ &+ 2b_1|\dot{D}(t)|\left|\int_0^1 (1+x)w(x,t)g(x,t)dx\right| + 2b_1|\dot{D}(t)|\left|\int_0^1 (1+x)w_x(x,t)g_x(x,t)dx\right| \end{aligned}$$

To bound the remaining positive terms, one can introduce the inverse transformation of (10.5)

$$u(x,t) = w(x,t) + D(t)K\int_0^x e^{(A+BK)D(t)(x-y)}Bw(y,t)dy + Ke^{(A+BK)D(t)x}\tilde{X}(t)$$

and its spatial derivative to obtain the following inequalities, using Young's and Cauchy-Schwartz's inequalities,

$$\begin{aligned} &2\left|\int_0^1 (1+x)w(x,t)g(x,t)\right|dx \leq M_1\left(|\tilde{X}(t)|^2 + \|w(t)\|^2 + \|w_x(t)\|^2\right) \\ &2w_x(1,t)^2 \leq M_2|\dot{D}(t)|^2\left(|\tilde{X}(t)|^2 + \|w(t)\|^2 + \|w_x(t)\|^2\right) \\ &2\left|\int_0^1 (1+x)w_x(x,t)g_x(x,t)\right|dx \leq M_3\left(|\tilde{X}(t)|^2 + \|w(t)\|^2 + \|w_x(t)\|^2 + w_x(0,t)^2\right) \end{aligned}$$

where M_1, M_2 and M_3 are positive constants, the expressions of which are omitted for sake of brevity. Using Young's inequality and the previous ones, defining $V_0(t) = |\tilde{X}(t)|^2 + \|w(t)\|^2 + \|w_x(t)\|^2$, it is straightforward to obtain

$$\begin{aligned} \dot{V}(t) \leq& -\frac{\underline{\lambda}(Q)}{2}|\tilde{X}(t)|^2 - \left(b_1 - \frac{2|PB|^2}{\underline{\lambda}(Q)}\right)w(0,t)^2 - b_1\|w(t)\|^2 - b_1\|w_x(t)\|^2 \\ &- b_1(1 - M_3|\dot{D}(t)|)w_x(0,t)^2 + b_1|\dot{D}(t)|(M_1 + M_2|\dot{D}(t)| + M_3 + 2)V_0(t) \end{aligned}$$

Consequently, choosing $b_1 \geq 2|PB|^2/\lambda_{min}(Q)$ and defining

$$\delta^* = \min\left\{\frac{\min\{\underline{\lambda}(Q)/2, b_1\}}{b_1(M_1+M_2+M_3+2)}, \frac{1}{M_3}, 1\right\} \tag{10.7}$$

we obtain the existence of a positive constant μ such that, provided $|\dot{D}(t)| < \delta^*, t \geq 0$,

$$\forall t \in \mathbb{R}_+, \quad \dot{V}(t) \leq -\mu V_0(t) \leq -\frac{\mu}{\max\left\{\bar{\lambda}(P), 2b_1\overline{D}\right\}}V(t)$$

Consequently, $V(t) \leq V(0)e^{-\frac{\mu}{\max\left\{\bar{\lambda}(P),2b_1\overline{D}\right\}}t}, \quad t \geq 0$. Finally, observing that there exist positive constant r_1, r_2, r_3 such that the following inequalities are fulfilled

$$\begin{aligned}
\|u(t)\|^2 \leq & r_1|X(t)|^2 + r_2\|w(t)\|^2 \\
\|u_x(t)\|^2 \leq & r_3|X(t)|^2 + r_4\|w(t)\|^2 + r_5\|w_x(t)\|^2 \\
\|w(t)\|^2 \leq & s_1|X(t)|^2 + s_2\|u(t)\|^2 \\
\|w_x(t)\|^2 \leq & s_3|X(t)|^2 + s_4\|u(t)\|^2 + s_5\|u_x(t)\|^2
\end{aligned}$$

one can obtain that, for any $t \geq 0$,

$$\frac{1}{\max\left\{\bar{\lambda}(P), 2b_1\right\}}V(t) \leq \Gamma(t) \leq \frac{\max\left\{1+\overline{D}r_1+\overline{D}r_3, r_2+r_4, r_5\right\}}{\min\{\underline{\lambda}(P), b_1\}}V(t)$$

which gives the existence of R and ρ. This concludes the proof. ■

Theorem 10.1.1 guarantees exponential convergence provided that variations in the delay are sufficiently slow. An expression of the bound δ^* on these variations is provided in (10.7). However, as it is obtained from a Lyapunov analysis, it is quite conservative and is not recommended for practical use. Nevertheless, this expression leads to the conclusion, at least according to the Lyapunov proof, that the faster the dynamics of the system, the smaller is this bound, which is expected. In particular, the constants M_1, M_2 and M_3 introduced above are then larger, which results in a smaller value of δ^*.

Second, it is also worth noticing that the bound δ^* indirectly depends on the absolute value of the feedback gain K. Indeed, one can show that M_2 is a linear function in $|K|$ and P and therefore b_1 also depend on $|K|$; a thorough study of (10.7) yields the conclusion that δ^* tends to zero as $|K|$ tends to zero and is constant as $|K|$ tends to $+\infty$.

When the delay depends on external variables (i.e. ϕ depends on s), it is not possible to go further to guarantee that condition (10.3) is fulfilled. We now investigate the case of a solely input-dependent delay, for which a more complete analysis can be performed.

10.2 Derivation of sufficient conditions for input-vary–ing delays

In this section, we consider the case of a purely input-dependent delay. Namely, with the formalism introduced in (10.1), we consider $\varphi(s, \phi(s)) = \phi(s)$ or, equivalently,

$$\int_{t-D(t)}^{t} \phi(s)ds = 1 \quad \text{with} \quad \phi(t) = \text{Sat}_{[\underline{u},+\infty[}(U(t)) \tag{10.8}$$

The variable ϕ should be understood in this context as a (normalized) flow rate. Therefore, the saturation operator is necessary to make the control law compliant with the positivity of the input variable. These elements are sketched in Figure 10.1.

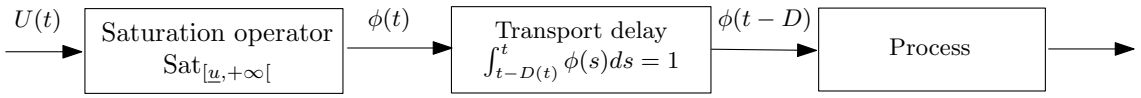

Figure 10.1: The addressed problem, in which the input is delayed by a transport delay that is input-dependent.

10.2.1 Problem statement

The plant under consideration in this section is the following linear one[2]

$$x^{(n)}+a_{n-1}x^{(n-1)}+\ldots+a_1\dot{x}+a_0x=b_0\phi(t-D(t)) \tag{10.9}$$

which we wish to stabilize over the equilibrium $x^r=b_0/a_0U^r$ with $U^r\geq\underline{u}>0$. To construct a prediction-based control law, we use Theorem 10.1.1 and focus on a general condition to guarantee that (10.3) holds, the form of which should be more compliant with practical control implementation. This leads to the formulation of Theorem 10.3.1 below.

With this aim in view, to use Theorem 10.1.1, we first formulate a state-space representation of this system as

$$\begin{cases}\dot{X}=AX(t)+B\phi(t-D(t))\\ \displaystyle\int_{t-D(t)}^{t}\phi(s)ds=1 \quad\text{with}\quad \phi(t)=\ \mathrm{Sat}_{[\underline{u},+\infty[}(U(t))\end{cases} \tag{10.10}$$

where

$$A=\begin{pmatrix}0&1&&0\\ \vdots&&\ddots&\\ 0&0&&1\\ -a_0&-a_1&\ldots&-a_{n-1}\end{pmatrix},\quad B=\begin{pmatrix}0\\ \vdots\\ 0\\ b_0\end{pmatrix} \tag{10.11}$$

and X^r is the state-space equilibrium corresponding to the original equilibrium x^r. For clarity, we make the following extra assumption for this state-space representation[3].

Assumption 6. *The system state X is assumed to be fully measured.*

According to the elements proposed in the previous section, we then consider the control law

$$U(t)=U^r+K\left[e^{AD(t)}X(t)+\int_{t-D(t)}^{t}e^{A(t-s)}B\phi(s)ds-X^r\right] \tag{10.12}$$

Following Theorem 10.1.1, we know that this control law achieves global exponential stability provided that $\dot{D}(t)<\delta^*$, $t\geq 0$ (with δ^* potentially depending on $|K|$). We now focus on a sufficient condition to fulfill the latter.

[2]Potential zeros can still be handled by a suitable choice of state-space representation and of the output vector.

[3]Addition of a state observer into this control law and the study of its compliance with the corresponding analysis are natural extensions of this work.

Reformulation of Condition 10.3 Taking a time derivative of (10.8) and defining the error variable $\varepsilon = \phi - U^r$ and using the fact that $\phi \geq \underline{u}$, one obtains

$$\dot{D}(t) = 1 - \frac{\varepsilon(t) + U^r}{\varepsilon(t - D(t)) + U^r} = \frac{\varepsilon(t - D) - \varepsilon(t)}{\varepsilon(t - D) + U^r} \leq \frac{2 \max |\varepsilon_t|}{\underline{u}}$$

where ε_t is the function defined by $\varepsilon_t : s \in [-\overline{D}, 0] \mapsto \varepsilon(t + s)$ and $\max \varepsilon_t$ is then defined on the interval $[-\overline{D}, 0]$. As a result, condition (10.3) is satisfied if

$$\forall t \geq 0\,, \quad \max |\varepsilon_t| < \frac{\underline{u}\delta^*(|K|)}{2} \tag{10.13}$$

This is the condition we aim at guaranteeing and on which we focus in the following. This requires an analysis of the dynamics of the variable ε.

10.2.2 Error dynamics, defined through the predictor-based control law

Preliminary result

To obtain the differential equation governing $\varepsilon = \phi - U^r$, we establish preliminary results for the successive derivations of this variable. In the following, $Z = X - X^r$ is the state tracking error.

Lemma 1. *If the actuator is unsaturated over the interval $[t - D(t), t]$, the control variable in* (10.25) *satisfies the following differential equations for $1 \leq m \leq n$*

$$\varepsilon^{(m)} - \sum_{l=1}^{m} K A^{l-1} B \varepsilon^{(m-l)} = f_Z^m(t) + f_\varepsilon^m(t) + (1 + \dot{D})^m K e^{AD} A^m Z + K \int_{t-D}^{t} A^m e^{A(t-s)} B \varepsilon(s) ds \tag{10.14}$$

with

$$\begin{cases} f_Z^1(t) = 0 \\ \text{for } 2 \leq m \leq n\,,\ f_Z^m(t) = \dfrac{d[(1 + \dot{D})^{m-1}]}{dt} K e^{AD} A^{m-1} Z + \dfrac{d}{dt}\left(f_Z^{m-1}(t)\right) \end{cases}$$

$$\begin{cases} f_\varepsilon^1(t) = \dot{D} K e^{AD} B \varepsilon(t - D) \\ \text{for } 2 \leq m \leq n\,,\ f_\varepsilon^m(t) = \dfrac{d}{dt}\left(f_\varepsilon^{m-1}(t)\right) + \left[(1 + \dot{D})^{m-1} - (1 - \dot{D})\right] \varepsilon(t - D) K e^{AD} A^{m-1} B \end{cases}$$

Furthermore, the sequences (f_ε^m) and (f_Z^m) satisfy the following properties:

- *for $2 \leq m \leq n$, f_ε^m is a polynomial function in $\varepsilon_t, \ldots, \varepsilon_t^{(m-1)}, \dot{D}, \ldots, D^{(m)}$ without constant nor first-order terms.*
- *assume that $1 + \dot{D} > 0$. Then, for $2 \leq m \leq n$, f_Z^m is a polynomial function in $\varepsilon_t, \ldots, \varepsilon_t^{(m-1)}$, $\dot{D}, \ldots D^{(m)}$ and $\frac{1}{1+\dot{D}}$, at least quadratic in the variables $\varepsilon_t, \ldots, \varepsilon_t^{(m-1)}$, $\dot{D}, \ldots D^{(m)}$.*

Proof: We start by observing that, when the actuator is unsaturated over the time interval $[t - D(t), t]$, the error system can be written following (10.10) and (10.12) as

$$\begin{cases} \dot{Z}(t) = AZ(t) + B\varepsilon(t - D(t)) & (10.15) \\ \varepsilon(t) = K\left[e^{AD(t)}Z(t) + \displaystyle\int_{t-D(t)}^{t} e^{A(t-s)}B\varepsilon(s)\right] & (10.16) \end{cases}$$

We now constructively establish the first result of this lemma by induction and successive substitutions.

Initial step: taking a time-derivative of (10.16) and using (10.15), one gets

$$\dot{\varepsilon}(t) = KB\varepsilon(t) + (1+\dot{D})Ke^{AD}AZ + \underbrace{\dot{D}Ke^{AD}B\varepsilon(t-D)}_{=f_\varepsilon^1(t)} + \underbrace{f_Z^1(t)}_{=0} + K\int_{t-D}^{t} Ae^{A(t-s)}B\varepsilon(s)ds$$

which gives (10.14) for $m = 1$.

Induction: assume that the property is true for a given $m \geq 1$. We now show that it also holds for $m+1$. Taking a time derivative of (10.14) for some $m \geq 1$ yields

$$\begin{aligned} \varepsilon^{(m+1)} - \sum_{l=1}^{m} KA^{l-1}B\varepsilon^{(m+1-l)} &= \frac{d}{dt}\left(f_\varepsilon^m(t)\right) + \underbrace{\frac{d}{dt}\left(f_Z^m(t)\right) + \frac{d(1+\dot{D})^m}{dt}Ke^{AD}A^mZ}_{=f_Z^{m+1}(t)} \\ &+ \dot{D}(1+\dot{D})^m Ke^{AD}A^{m+1}Z + (1+\dot{D})^m Ke^{AD}A^m\left[AZ + B\varepsilon(t-D)\right] + KA^mB\varepsilon(t) \\ &- (1-\dot{D})Ke^{AD}A^mB\varepsilon(t-D) + K\int_{t-D}^{t} A^{m+1}e^{A(t-s)}B\varepsilon(s)ds \end{aligned}$$

Rearranging terms, one obtains (10.14) for $m+1$. This gives the conclusion.

Second, the property of the sequence (f_ε^m) is straightforward using the definition of this sequence together with the fact that

$$(1+\dot{D})^{m-1} - (1-\dot{D}) = \sum_{l=1}^{m-1} \begin{pmatrix} n \\ l \end{pmatrix} \dot{D}^l + \dot{D}$$

Finally, to obtain the property for the sequence (f_Z^m), again, we reason by induction.

Induction: we assume that the property is true for a given $m \geq 2$. Then, using (10.14) for m, one can obtain

$$\begin{aligned} f_Z^{m+1}(t) &= \frac{d[(1+\dot{D})^m]}{dt}Ke^{AD}A^mZ + \frac{d}{dt}(f_Z^m(t)) \\ &= \frac{m\ddot{D}}{1+\dot{D}}\left[\varepsilon^{(m)} - \sum_{l=1}^{m} KA^{l-1}\varepsilon^{(m-l)} - f_Z^m(t) - f_\varepsilon^{m+1}(t) - K\int_{t-D}^{t} A^m e^{A(t-s)}B\varepsilon(s)ds\right] \\ &+ \frac{d}{dt}(f_Z^m(t)) \end{aligned}$$

Using the induction assumption jointly with the previous lemma, one can conclude that f_Z^{m+1} is a polynomial function in $\varepsilon_t, \ldots, \varepsilon_t^{(m)}, \dot{D}, \ldots, D^{(m+1)}, \frac{1}{1+\dot{D}}$, *at least quadratic* in $\varepsilon_t, \ldots, \varepsilon_t^{(m)}, \dot{D}, \ldots, D^{(m+1)}$.

Initial step: the same argument as that above applies for $m = 2$. ■

It is now possible to express the dynamics of ε in the following form.

Lemma 2. *Consider $t_0 \in \mathbb{R}$ and assume that the function ϕ is unsaturated for $t \leq t_0$ (or equivalently that $U(t) \geq \underline{u}\,, t \leq t_0$). Then the error variable $\varepsilon = U - U^r$ with U as defined in* (10.12) *satisfies the following differential equation for $t \leq t_0$*

$$\begin{aligned}\varepsilon^{(n)} + (a_{n-1}+b_0k_{n-1})\varepsilon^{(n-1)} + \ldots + (a_0 + b_0k_0)\varepsilon \\ = \pi_0(\varepsilon_t, \ldots, \varepsilon_t^{(n-1)}) + \pi_1\left(\dot{D}, \ldots, D^{(n)}, \varepsilon_t, \ldots, \varepsilon_t^{(n-1)}, \frac{1}{1+\dot{D}}\right)\end{aligned} \tag{10.17}$$

where the constants k_i are the coefficients of the feedback gain $K = [-k_0 \ldots - k_{n-1}]$ and π_0 and π_1 are polynomial functions satisfying the following properties:

- *there exists a class $\mathcal{K}_\infty$ function β such that*

$$|\pi_0(\varepsilon_t, \ldots, \varepsilon_t^{(n-1)})| \leq \beta(|K|) \max |E_t|$$

  with $E(t) = [\varepsilon(t) \quad \dot{\varepsilon}(t) \ \ldots \ \varepsilon^{(n-1)}(t)]^T$.

- *π_1 is at least quadratic in the variables $\varepsilon_t, \ldots, \varepsilon_t^{(n-1)}, \dot{D}, \ldots, D^{(n)}$.*

Proof: The dynamics matrix that we consider in (10.11) is of the companion type, so the Cayley-Hamilton theorem gives

$$A^n = -\sum_{i=0}^{n-1} a_i A^i$$

Therefore, the dynamics equation (10.14) for $m = n$ can be reformulated as

$$\begin{aligned}\varepsilon^{(n)} - \sum_{l=1}^{n} KA^{l-1}B\varepsilon^{(n-l)} = \\ f_Z^n(t) + f_\varepsilon^n(t) - (1+\dot{D})^m Ke^{AD}\sum_{i=0}^{n-1} a_i A^i Z + K\int_{t_D}^{t} A^n e^{A(t-s)}B\varepsilon(s)ds\end{aligned}$$

Using (10.14) for m ranging from 1 to $n-1$, one can replace the state-dependent terms in this last expression to obtain

$$\begin{aligned}\varepsilon^{(n)} - \sum_{l=1}^{n} KA^{l-1}B\varepsilon^{(n-l)} = \\ f_Z^n(t) + f_\varepsilon^n(t) - \sum_{m=0}^{n-1} a_m(1+\dot{D})^{n-m}\left[\varepsilon^{(m)} - \sum_{l=1}^{m} KA^{l-1}B\varepsilon^{(m-l)} - f_Z^m(t)\right. \\ \left. - f_\varepsilon^m(t) - K\int_{t-D}^{t} A^m e^{A(t-s)}B\varepsilon(s)ds\right] + K\int_{t-D}^{t} A^n e^{A(t-s)}B\varepsilon(s)ds\end{aligned}$$

In addition, using the Leibniz formula for the power $(1+\dot{D})^{n-m}$ together with the fact that

$$\sum_{l=1}^{n} KA^{l-1}B\varepsilon^{(n-l)} = -\sum_{l=1}^{n} b_0k_{n-l}\varepsilon^{(n-l)} + K\sum_{l=1}^{n} M_l\varepsilon^{(n-l)}$$

where the coefficients of the constant matrices M_l are polynomial functions of $a_0, \ldots, a_{n-1}$ and b_0, one can define

$$\pi_0(\varepsilon_t, \ldots, \varepsilon_t^{(n-1)}) = K \sum_{l=1}^{n} M_l \varepsilon^{(n-l)} + K \int_{t-D}^{t} A^n e^{A(t-s)} B\varepsilon(s) ds + \sum_{m=1}^{n-1} a_m \left[\sum_{l=1}^{m} K A^{l-1} B \varepsilon^{(m-l)} + K \int_{t-D}^{t} A^m e^{A(t-s)} B\varepsilon(s) ds \right] \quad (10.18)$$

$$\pi_1(\dot{D}, \ldots, D^{(n)}, \varepsilon_t, \ldots, \varepsilon_t^{(n-1)}) = f_Z^n(t) + f_\varepsilon^n(t) + \sum_{m=0}^{n-1} a_m (1+\dot{D})^{n-m} (f_Z^m(t) - f_\varepsilon^m(t)) - \sum_{m=1}^{n-1} a_m \left[\sum_{l=1}^{n-m} \begin{pmatrix} n-m \\ l \end{pmatrix} \dot{D}^l \right] \times \left[\varepsilon^{(m)} - \sum_{l=1}^{m} K A^{l-1} B \varepsilon^{(m-l)} - K \int_{t-D}^{t} A^m e^{A(t-s)} B\varepsilon(s) ds \right] \quad (10.19)$$

to obtain the dynamic (10.17). Finally, introducing

$$\beta(|K|) = |K| n \left[\sum_{l=1}^{n} |M_l| + |A|^{(n-1)} |e^{A\overline{D}} - 1||B| + \sum_{m=1}^{n-1} |a_m| \left[|A^{l-1}B| + |A|^{(m-1)} |e^{A\overline{D}} - 1||B| \right] \right] \quad (10.20)$$

which is a class $\mathcal{K}_\infty$ function, π_0 in (10.18) is such that

$$|\pi_0(\varepsilon_t, \ldots, \varepsilon_t^{(n-1)})| \leq \beta(|K|) \max |E_t|$$

with $E(t) = [\varepsilon(t) \quad \dot{\varepsilon}(t) \ldots \varepsilon^{(n-1)}(t)]^T$. Further, from (10.19) and using the properties of the sequences (f_ε^m) and (f_Z^m) stated in Lemma 2, π_1 is a polynomial function in the variables $\varepsilon_t, \ldots, \varepsilon_t^{(n-1)}, \dot{D}, \ldots, D^{(n)}$ and $\frac{1}{1+\dot{D}}$, that is *at least quadratic* in the variables $\varepsilon_t, \ldots, \varepsilon_t^{(n-1)}, \dot{D}, \ldots, D^{(n)}$. ■

10.2.3 Application of the Halanay-like Lemma 10.2.1 to the considered variable

The stability analysis performed here is based on the following DDE result that is established in Appendix B. We apply it to the dynamics obtained in the previous lemma to guarantee that the stability condition (10.13) holds.

Lemma 10.2.1

Let x be a solution of the n^{th} order DDE

$$\begin{cases} x^{(n)} + \alpha_{n-1}x^{(n-1)} + \ldots + \alpha_0 x = c\ell(t, x_t, \ldots x_t^{(n-1)}) \,, \; t \geq t_0 \\ x_{t_0} = \phi \in \mathcal{C}^0([-\overline{D}, 0], \mathcal{V}) \end{cases}$$

where the left-hand side of the differential equation defines a polynomial which roots have only strictly negative real parts, $c > 0$, ℓ is a continuous functional and $\mathcal{V}$ is a neighborhood of the origin for which ℓ satisfies the sup-norm relation

$$\forall t \geq t_0 \,, \quad |\ell(t, x_t, \ldots, x_t^{(n-1)})| \leq \max |X_t|$$

with $X = [x \quad \dot{x} \ldots x^{(n-1)}]^T$. Then there exists $c_{max} > 0$ such that, provided that $0 \leq c < c_{max}$, there exist $\gamma > 0$ and $r > 0$ such that

$$\forall t \geq 0 \,, \quad |X(t)| \leq r \, \max |X_{t_0}| e^{-\gamma(t-t_0)}$$

As shown in Appendix B, a constructive choice is $c_{max} = \frac{\underline{\lambda}(P)\underline{\lambda}(Q)}{2\overline{\lambda}(P)^2}$ and $r = \sqrt{\frac{\overline{\lambda}(P)}{\underline{\lambda}(P)}}$ for the couple (P, Q) of the Lyapunov equation corresponding to the asymptotically stable equation $x^{(n)} + \alpha_{n-1}x^{(n-1)} + \ldots + \alpha_0 x = 0$.

Lemma 3. *Consider the functional*

$$\Theta(t) = |X(t) - X^r| + \max_{[t-\overline{D}, t]} |U(s) - U^r| \tag{10.21}$$

and Q a symmetric definite positive matrix. Assume that, for a given $\epsilon \in (0, 1)$, there exists $k^* > 0$ such that

$$\beta(|K_0|) < (1 - \epsilon)\frac{\underline{\lambda}(P)\underline{\lambda}(Q)}{2\overline{\lambda}(P)^2} \quad \textit{with} \quad P(A + BK_0) + (A + BK_0)^T P = -Q \tag{10.22}$$

for any $K_0 \in \mathbb{R}^{1\times n}$ such that $|K_0| < k^*$, with β defined in (10.20)*. Then, there exists $\theta : \mathbb{R}_+ \mapsto \mathbb{R}_+$ such that for any $K \in \mathbb{R}^{1\times n}$ such that $|K| < k^*$ and $\Theta(0) < \theta(|K|)$, then*

$$\forall t \geq 0 \,, \quad |\varepsilon(t)| \leq \min \left\{ \frac{\underline{u}\delta^\star(|K|)}{2}, U^r - \underline{u} \right\}$$

which implies that condition (10.13) *is fulfilled.*

Proof: Assume for a moment that the function ϕ is unsaturated for $t \leq 0$. Therefore, dynamics (10.17) in Lemma 2 holds and is compliant with the framework of Lemma 10.2.1.

In details, first, the left-hand side of (10.17) is stable, as it represents the last line of the Hurwitz companion matrix $A + BK$. Second, by observing that

$$\dot{D} = \frac{\varepsilon(t - D) - \varepsilon(t)}{\varepsilon(t - D) + U^r}$$

one can obtain by induction that, for $m \geq 1$, $D^{(m)}$ is a polynomial function in $\varepsilon_t, \ldots, \varepsilon_t^{(m-1)}$, $\frac{1}{\varepsilon(t-D)+U^r}$ without terms of order 0 or 1. Therefore, π_1 is directly a polynomial function

of the variables $\varepsilon_t, \ldots, \varepsilon_t^{(n-1)}, \frac{1}{1+\dot{D}}$, that is *at least quadratic* in the variables $\varepsilon_t, \ldots, \varepsilon_t^{(n-1)}$. Finally, define

$$c\ell(t, \varepsilon_t, \ldots, \varepsilon_t^{(n-1)}) = \pi_0(\varepsilon_t, \ldots, \varepsilon_t^{(n-1)}) + \pi_1\left(\dot{D}, \ldots, D^{(n)}, \varepsilon_t, \ldots, \varepsilon_t^{(n-1)}, \frac{1}{1+\dot{D}}\right)$$

Observing that

$$\frac{1}{1+\dot{D}} = \frac{\varepsilon(t-D) + U^r}{2\varepsilon(t-D) - \varepsilon(t) + U^r}$$

and because π_1 is *at least quadratic*, it is possible to properly define a neighborhood of the origin $\mathcal{V}$ such that, for $\epsilon \in (0,1)$,

$$\left|\pi_1\left(\varepsilon_t, \ldots, \varepsilon_t^{(n-1)}\right)\right| \leq \epsilon c_{max} \max|E_t|$$

for E_t with values in $\mathcal{V}^{n-1}$ (and such that $1+\dot{D}(t) > 0$). Assume the existence of k^* such that the condition expressed in (10.22) is fulfilled. Therefore, by restricting $|K| < k^*$, $\beta(|K|) \leq (1-\epsilon)c_{max}$. Consequently, for $|K| \leq k^*$ and for $E_t([-\overline{D}, 0]) \subset \mathcal{V}^{n-1}$, one gets

$$\left|c\ell(t, \varepsilon_t, \ldots, \varepsilon_t^{(n-1)})\right| < c_{max} \max|E_t|$$

Therefore, Lemma 10.2.1 guarantees the existence of $r > 0$ and $\gamma > 0$ such that

$$\forall t \geq 0\,, \quad |E(t)| \leq r \max|E_0| e^{-\gamma t}$$

as long as the actuator ϕ is not saturated and that (10.17) applies. Yet, one can observe that a sufficient condition to ensure that the actuator is not saturated is $|\varepsilon(t)| \leq U^r - \underline{u}\,$, $t \geq 0$. Therefore, by choosing $\max|E_0| \leq \frac{1}{r}\min\left\{\frac{\underline{u}\delta^*(|K|)}{2}, U^r - \underline{u}\right\} =^{\Delta} \theta(|K|)$, one can ensure both that this condition is fulfilled for any $t \geq 0$ and that $|E(t)| \leq \frac{\underline{u}\delta^*(|K|)}{2}$, $t \geq 0$. In particular, the condition (10.13) is also fulfilled. This concludes the proof.

Finally, the choice $\max|E_0| \leq \frac{1}{r}\min\left\{\frac{\underline{u}\delta^*(|K|)}{2}, U^r - \underline{u}\right\}$ can be expressed in terms of Θ, judiciously redefining the function θ. ■

10.3 Sufficient conditions for robust compensation of an input-dependent delay

From the result finally obtained in Lemma 3, it is possible to gather the previous elements into the following result.

Theorem 10.3.1

Consider the closed-loop system

$$\begin{cases} \dot{X}(t) = AX(t) + B\phi(t - D(t)) & (10.23) \\ \int_{t-D(t)}^{t} \phi(s)ds = 1 \quad with \quad \phi(t) = Sat_{[\underline{u},+\infty[}(U(t)) & (10.24) \\ U(t) = U^r + K\left[e^{AD(t)}X(t) + \int_{t-D(t)}^{t} e^{A(t-s)}B\phi(s)ds - X^r\right] & (10.25) \end{cases}$$

where A and B are defined in (10.11), U is scalar, X^r is the state equilibrium corresponding to the original equilibrium x^r of plant (10.9) and U^r is the corresponding reference control. Consider the functional

$$\Theta(t) = |X(t) - X^r| + \max_{s\in[t-\overline{D},t]} |U(s) - U^r|$$

and Q a symmetric positive definite matrix. Assume that, for a given $\epsilon \in (0, 1)$, there exists $k^* > 0$ such that

$$\beta(|K_0|) < (1-\epsilon)\frac{\underline{\lambda}(P)\underline{\lambda}(Q)}{2\overline{\lambda}(P)^2} \quad with \quad P(A + BK_0) + (A + BK_0)^T P = -Q \qquad (10.26)$$

for any $K_0 \in \mathbb{R}^{1\times n}$ such that $|K_0| < k^*$, with β defined in (10.20) by A and B. Then, there exists $\theta : \mathbb{R}_+ \mapsto \mathbb{R}_+$ such that for any $K \in \mathbb{R}^{1\times n}$ such that $|K| < k^*$ and $\Theta(0) < \theta(|K|)$ the condition (10.3) is fulfilled and the plant exponentially converges to X^r.

The meaning of this result is not surprising : Theorem 10.1.1 requires that the delay varies sufficiently slowly, whereas the delay variations implicitly depend on the control input with a magnitude scaled by the gain K. Then, restricting the input variations by both choosing the feedback gain sufficiently small and the initial conditions close enough to the desired equilibrium seems like a natural solution. This is indeed the assumption formulated in Theorem 10.3.1.

The upper-bound k^* is defined through the assumption (10.26) which is worth being commented. The second part of this condition simply expresses that the feedback gain has to be compliant with stabilization; in other words, $A+BK$ is still required to be Hurwitz. Yet, the first part of the condition is more complex to investigate and the existence of a upper-bound k^* may not hold for any unstable plant[4]. This assumption is an obvious limitation of the proposed result, which should be investigated further in future works.

In particular, this result highlights the well known and long-standing necessity to *detune* the predictive controllers commonly used for delay systems.

[4]Conversely, the existence of k^* holds for a stable plant. Indeed, for a given matrix Q, one can obtain that $(1-\epsilon)\frac{\underline{\lambda}(P)\underline{\lambda}(Q)}{2\overline{\lambda}(P)^2}$ tends to a positive constant for $|K| \to 0$ (as P can be expressed ad $P = \int_0^\infty e^{(A+BK)^T t} Q e^{(A+BK)t} dt$ which is a continuous function of K [Rugh 96] and the (all real) eigenvalues of P can then be shown to be continuous with respect to K, using Rouché's Theorem for example [Miller 82]), while $\beta(|K|) \to 0$ by definition of the class $\mathcal{K}_\infty$ function β.

The approach proposed to address the problem of robust compensation of a linear system driven by a delayed input is based on a two-step methodology. First, the delay derivative must be bounded and, then, this derivative must be related to input fluctuations. Here, this approach was applied to a particular class of transport delays that are input-dependent (through an integral relation) using a Halanay-like inequality. The sufficient conditions obtained limit both the magnitude of the feedback gain and the initial conditions.

This approach may be applied to other equations defining the delay, but an accurate analysis for each type of dependence would be necessary. An example of such a study is given in the next chapter.

Chapter 11

Case study of the bath temperature regulation, as an input-dependent delay system

Chapitre 11 – Etude d'un système à entrée retardée en fonction de la commande : régulation de la température d'un bain. *Ce chapitre illustre les résultats théoriques du chapitre précédent sur un exemple classique des systèmes à retard, celui de la douche (ou du bain). Après avoir exposé brièvement le système considéré, nous commentons les résultats de simulation obtenus qui soulignent les nombreux avantages en termes de performance de notre approche par compensation robuste pour retard dépendant de la commande.*

Contents

In this chapter, at the light of a simple tutorial example, we illustrate the prediction-based controller for input-dependent input-delay proposed in Chapter 10. We focus on one of the simplest time-delay system example one can think of: the temperature regulation of the bath depicted in Figure 11.1, for which the non-negligible pipe holdups involved are directly correlated to the history of the input flow rates. Because of its relative simplicity and everyday occurrence, this example is often used to introduce time-delay systems in lectures [Zhong 06] and to illustrate some corresponding control challenges.

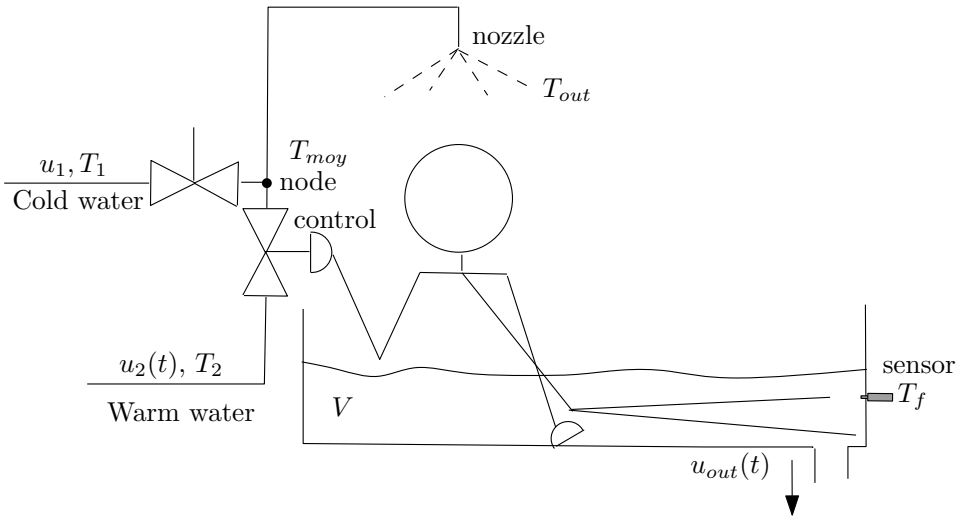

Figure 11.1: The studied shower and bathtub system.

After describing the system, we design a prediction-based control law based on the methodology presented in the previous section and illustrated by Theorem 10.3.1. The anticipation capabilities of the proposed controller are then illustrated using simulation results that report closed-loop performance.

11.1 Physical description and problem statement

Consider the bathtub system represented in Figure 11.1, where the water temperature (assumed to be homogeneous in the bath) is the result of mixing between a cold water source (flow rate u_1 and temperature T_1) and a warm source (u_2, T_2). For comfort, the user wishes to obtain a desired temperature T_{ref} without over- nor under-shoots as quickly as possible (namely, close to the minimum time introduced by the transport delay through the pipe).

For simplicity, we assume that the change of faucet position is immediate and that the cold flow rate is constant. Assuming that the position of the warm faucet is directly correlated to the flow rate through static relations, u_2 could then be considered as the input variable. Finally, we assume that the bath temperature T_f is available for measurement and that the bath volume is constant (i.e. $\forall t \geq 0,\ \ u_{out}(t) = u_1 + u_2(t)$).

11.1.1 Balance equations

Assuming that mixing at the node is instantaneous, the temperature at the node can simply be expressed as

$$T_{moy}(t) = \frac{u_1 T_1 + u_2(t) T_2}{u_1 + u_2(t)} \tag{11.1}$$

We neglect the heat transfer during flow transport from the node to the nozzle, namely

$$T_{out}(t) = T_{moy}(t - D(t)) \tag{11.2}$$

where $D(t)$ accounts for the varying transport delay implicitly defined by

$$V_P = \int_{t-D(t)}^{t} (u_1 + u_2(s))ds \tag{11.3}$$

where V_P is the pipe volume. Furthermore, considering the bathtub volume V as constant and using (11.2), a heat balance yields

$$\frac{d}{dt}(T_f) = \frac{u_1 + u_2(t)}{V} \left[-T_f(t) + T_{moy}(t - D(t))\right] \tag{11.4}$$

11.1.2 Constraints and control objective

Valve Position Both faucets have physical limitations and therefore the warm water flow rate is also bounded, i.e. $u_2 \in [0, \bar{u_2}]$.

Control objective The control objective is to have (11.4) track the given temperature T_{ref} as quickly as possible, taking into account the above constraints. To reach this goal, we develop a prediction-based control law by taking advantage of knowledge of the implicit delay variation law (11.3).

11.1.3 Link to the results of Chapter 10

The dynamics (11.4) under consideration is nonlinear. Therefore, Theorem 10.1.1 cannot be directly applied. For this reason, we present below a time-change that results in a linear form.

Second, the input in (11.4) is the average temperature T_{moy}. Therefore, the transport delay described in terms of the mass flow rates in (11.3) does not directly follow (10.8) because the integrated variable is not T_{moy}. However, this delay is still solely input-dependent[1] and the two-step methodology introduced above can still be applied. This is the purpose of the following section.

11.2 Problem normalization and control design

For clarity and without loss of generality, in this section we normalize the parameters introduced above as $T_1 = 0$, $T_2 = 1$, $u_1 = 1$, $V = 1$, $T_{ref} \in [0, 1[$ and denote by $u = u_2 \in [0, \bar{u}]$ the actual actuator.

11.2.1 Alternative system representation

To obtain a linear dynamic representation, we first introduce the following time-change

$$\tau = h_0(t) \triangleq \frac{1}{1 + \bar{u}} \int_0^t (1 + u(s))ds + \tau_0 \tag{11.5}$$

where $\bar{u}$ is a normalization factor chosen as $\bar{u} = \frac{T_{ref}}{1 - T_{ref}}$ and $\tau_0 \geq 0$ is a given constant. This leads to the alternative linear system

$$\frac{dX}{d\tau}(\tau) = (1 + \bar{u}) \left[-X(\tau) + T_{moy}(\tau - D_2(\tau))\right] \tag{11.6}$$

[1] In particular, it could be reformulated as $\int_{t-D(t)}^{t} \frac{u_1}{V_P} \frac{T_2 - T_1}{T_2 - T_{moy(s)}} ds = 1$.

where the alternative system state is defined as $X(\tau) = T_f(t)$ and a new delay is introduced as

$$D_2(\tau) = \tau - t + D(t) = \tau - h_0^{-1}(\tau) + D(h_0^{-1}(\tau)) \tag{11.7}$$

In this new time scale [2], (11.6) is a linear input delay system with constant parameters. Rewriting the alternative delay as $D_2(h_0(t)) = h_0(t) - t + D(t)$ and considering both (11.3) and (11.5), one can observe that this delay is still input-dependent, but in a much more complex way.

Before working with this representation, we need to make sure that (11.5)-(11.7) is well-posed in the sense detailed below.

(i) The function h_0 defined in (11.5) is a C^1 function, strictly increasing w.r.t. t. Therefore, it describes a diffeomorphism and in particular its inverse in (11.7) is well-defined.

(ii) One has to ensure that the delay D_2 is well defined, namely positive, whereby $\forall t \geq 0\,,\ \tau \geq t - D(t)$. This property is given by choosing τ_0 large enough compared to the upper bound of the delay $\bar{D} = V_P$.

(iii) h_0 is unbounded and then $\lim_{t\to\infty} T_f(t) = \lim_{\tau\to\infty} X(\tau)$ (if it exists). This allows direct translation of any asymptotic result obtained for the alternative plant (11.6) to the original (11.4).

11.2.2 Control law

The alternative plant (11.6) now directly fits in the framework of Theorem 10.1.1. Therefore, furthering this theorem, we use the controller

$$u(t) = Sat_{[0,\bar{u}]} \left\{ \frac{T_{moy}(t)}{1 - T_{moy}(t)}, \right\} \tag{11.8}$$

$$T_{moy}(t) = (1+k)T_{ref} - k\left[e^{-(1+\bar{u})D_2(t)} T_f(h_0^{-1}(t)) + (1+\bar{u}) \int_{t-D_2(t)}^{t} e^{-(1+\bar{u})(t-s)} T_{moy}(s) ds\right] \tag{11.9}$$

$$D_2(t) = t - h_0^{-1}(t) + D(h_0^{-1}(t)) \tag{11.10}$$

where the function h_0 is as defined in (11.5), and $\mathrm{Sat}_{[0,\bar{u}]}$ represents the usual saturation operator. Based on the elements presented in Theorem 10.1.1, this controller achieves global exponential convergence of the plant, provided that the following condition is fulfilled

$$\left| \frac{\partial D_2}{\partial \tau}(\tau) \right| < \delta^*(k) \tag{11.11}$$

We now investigate a sufficient condition to fulfill the latter.

[2] A different constant scale factor could be introduced in (11.5) to simplify the expression of (11.6) at the expense of later complexity in the analysis of closed-loop behavior.

11.2.3 Reformulation of the delay variations condition (11.11)

From (11.5) and (11.7), one can easily obtain an analytic expression of the partial derivative in (11.11)

$$\frac{\partial D_2}{\partial \tau}(\tau) = \frac{\partial D_2}{\partial \tau}(h_0(t)) = 1 - [1 - \dot{D}(t)]\frac{1+\bar{u}}{1+u(t)}$$

Furthermore, taking a time derivative of the implicit equation (11.3) with normalized data one obtains

$$1 - \dot{D}(t) = \frac{1+u(t)}{1+u(t-D(t))}$$

Substituting then yields

$$\left|\frac{\partial D_2}{\partial \tau}(\tau)\right| < \delta^* \Leftrightarrow \left|1 - \frac{1+\bar{u}}{1+u(t-D(t))}\right| < \delta^* \Leftrightarrow \frac{1+\bar{u}}{1+\delta^*} < 1+u(t-D(t)) < \frac{1+\bar{u}}{1-\delta^*}$$
$$\Leftrightarrow \frac{1-\delta^*}{1+\bar{u}} < 1 - T_{moy}(t-D(t)) < \frac{1+\delta^*}{1+\bar{u}}$$

Finally, exploiting the equilibrium relation between $\bar{u}$ and T_{ref}, this condition can be rewritten as the inequality

$$|T_{moy}(t-D(t)) - T_{ref}| < \delta^*(k)\frac{1}{1+\bar{u}} = \delta^*(k)(1-T_{ref}) \tag{11.12}$$

This is the condition we focus on in the following.

11.2.4 Derivation of a sufficient condition using an Halanay-like inequality

To analyze (11.12), we use the following stability result, directly inspired by the Halanay inequality reproduced in Appendix B, which also contains the proof of this result.

Corollary 1. *Consider a DDE of the form*

$$\left\{\begin{array}{rcl} \dot{x}(t) & + & ax(t) + bh(t,x_t) = 0\,, \quad t \geq t_0 \\ x_{t_0} & = & \phi \in \mathcal{C}^0([-\overline{D},0]) \end{array}\right. \tag{11.13}$$

where h is a continuous functional satisfying, on an open neighborhood $\mathcal{V}$ of the origin, the sup-norm relation

$$\forall x_t : [-\bar{D},0] \mapsto \mathcal{V}\,, \quad |h(t,x_t)| \leq \max|x_t| \tag{11.14}$$

Then if the initial value ϕ maps $[-\overline{D},0]$ to $\mathcal{V}$ and if $a \geq b \geq 0$, then there exists $\gamma \geq 0$ ($\gamma = 0$ if $a = b$ and $\gamma > 0$ otherwise) such that every solution satisfies

$$\forall t \geq t_0\,, \quad |x(t)| \leq \max|x_{t_0}|e^{-\gamma(t-t_0)} \tag{11.15}$$

This corollary can be used to establish the following intermediate lemma.

Lemma 4. *Consider a continuous real-valued f and a differentiable real-valued function ψ such that*

$$f(t) = -k\left[e^{-\alpha D(t)}\psi(t) + \alpha\int_{t-D(t)}^{t} e^{-\alpha(t-s)}f(s)ds\right] \tag{11.16}$$

$$\dot{\psi}(t) = \alpha\left[-\psi(t) + f(t-D(t))\right] \tag{11.17}$$

where $k > 0$ and $\alpha > 0$ are constant and $D : [0,\infty[\to [\underline{D}, \overline{D}](0 < \underline{D} < \bar{D})$ is a time-differentiable function such that

$$\forall t \geq 0\,, \quad |\dot{D}(t)| \leq \beta \max_{s\in[t-\overline{D},t]} |f(s)| \tag{11.18}$$

If there exists $t_0 \in \mathbb{R}$ s.t. $\forall t \in [t_0 - \bar{D}, t_0]|f(t)| < M/\beta$ with $M < 1$ and $\beta > 0$, then

$$\forall t \geq t_0\,, \quad |f(t)| < M/\beta$$

Proof: Taking the time derivative of (11.16) and using (11.17), one shows that f satisfies the following DDE

$$\dot{f}(t) + \alpha(1+k)f(t) = -\alpha\dot{D}(t)\left(f(t) + ke^{-\alpha D(t)}f(t-D(t)) + k\alpha\int_{t-D(t)}^{t} e^{-\alpha(t-s)}f(s)ds\right)$$

Then, defining $a = b = \alpha(1+k)$, $\mathcal{V} =]-M/\beta, M/\beta[$ and

$$h(t,x_t) = \frac{\dot{D}(t)}{1+k}\left[f(t) + k\left(e^{-\alpha D(t)}f(t-D(t)) + \alpha\int_{t-D(t)}^{t} e^{-\alpha(t-s)}f(s)ds\right)\right]$$

one can apply Corollary 1 using (11.18),

$$\begin{aligned}|h(x,t)| \leq & |\frac{\beta\max|f_t|}{1+k}\left(1 + k\left[e^{-\alpha D(t)} + 1 - e^{\alpha D(t)}\right]\right)\max|f_t| \leq \beta\max|f_t|^2 \\ & \leq \max|f_t| \text{ for } f_t : [-\overline{D}, 0] \mapsto \mathcal{V}\end{aligned}$$

and conclude that, $\forall t \geq t_0\,,\ f(t) \in \mathcal{V}$, i.e. $\forall t \geq t_0\,,\ f(t) < \frac{M}{\beta}$. ■

Theorem 2. *Consider the closed-loop system consisting of the plant* (11.4) *with the input delay defined through* (11.1)-(11.3) *and the control law* (11.8)–(11.10)*. There exists $k^* > 0$, potentially depending on the initial condition and the input past values over a time window of finite length, such that, for $k \in [0, k^*[$,*

$$T_f(t) \underset{t\to\infty}{\to} T_{ref}$$

Proof: Observing (11.8), we use Lemma 4 with $\alpha = 1 + \overline{u}$, $\psi(t) = T_f(h_0^{-1}(t)) - T_{ref}$ and $f = T_{moy} - T_{ref}$. Taking a time derivative of (11.5) evaluated at time $h_0^{-1}(t)$, one obtains $\frac{dh_0^{-1}(t)}{dt} = \frac{1+\overline{u}}{1+u(h_0^{-1}(t))}$ and it is clear that ψ satisfies

$$\begin{aligned}\dot{\psi}(t) &= \frac{dT_f}{dt}(h_0^{-1}(t))\frac{dh_0^{-1}(t)}{dt} = \left(1 + u(h_0^{-1}(t))\right)\left[-\psi(t) + f(h_0^{-1}(t) - D(h_0^{-1}(t)))\right]\frac{dh_0^{-1}(t)}{dt} \\ &= (1+\overline{u})\left[-\psi(t) + f(t - D_2(t))\right]\end{aligned}$$

	Notation	Value
Cold water temperature	T_1	20^o C
Warm water temperature	T_2	40^o C
Maximum flow rate	$\bar{u_2}$	0.25 L/s
Cold water flow rate	u_1	0.125 L/s
Pipe volume	V_P	6.3 L
Bath volume	V	100 L

Table 11.1: Bath parameters used for the simulation.

Consequently, we just need to study the alternative delay $D_2(t)$. Taking a time derivative of (11.7) and of the implicit relation (11.3), both evaluated at time $h_0^{-1}(t)$, one gets

$$\dot{D}_2(t) = 1 - \frac{d}{dt}[h_0^{-1}(t) - D(h_0^{-1}(t))] = 1 - \frac{1+\overline{u}}{1+u(h_0^{-1}(t) - D(h_0^{-1}(t)))}$$
$$= \frac{T_{moy}(t - D_2(t)) - T_{ref}}{1 - T_{ref}} = \frac{f(t - D_2(t))}{1 - T_{ref}}$$

Therefore, $|\dot{D}_2(t)| \leq \beta \max |f_t|$ with $\beta = \frac{1}{1-T_{ref}} > 0$ and f_t defined on $[-\overline{D}_2(t), 0]$. Furthermore, the previous results can easily be extended to the case in which the upper bound for the delay is time-varying and one can observe that $\delta^*(k) < 1$. Therefore, one deduces from Lemma 4 that for $t \geq t_0$, $|f(t)| < \delta^*(k)/\beta$ provided that $|f(t_0 + s)| < \delta^*(k)/\beta$, $s \in [-\overline{D}_2(t_0), 0]$ (where $\overline{D}_2(t_0)$ denotes the upper bound at time t_0). Then (11.12) is equivalent to the less restrictive condition

$$\max_{s \in [-\overline{D_2}(0), 0]} |T_{moy}(t) - T_{ref}| < \delta^*(k)(1 - T_{ref})$$

with $\overline{D_2}(0) = \overline{D} + \tau_0$. Finally, from (11.9), this condition is fulfilled provided $0 \leq k < k^\star$ with $k^\star > 0$. Finally, as the considered plant is stable, it is possible to choose k as small as desired and in particular into $[0, k^*[$. This concludes the proof. ■

Remark 3. *Comparing this result to that formulated in Theorem 10.3.1, it is worth noting that the condition required here only affects the magnitude of the feedback gain. This is because of the stability of the process under consideration. This is also the reason of the existence of k^*.*

11.3 Simulation results

In this section, we provide some simulation results. We compare our prediction-based controller to a "memoryless" controller using simple proportional feedback and to an open-loop controller.

The parameters of the bath system used for simulation are listed in Table 11.2.4. Our aim is to control the system from an equilibrium point at which the bathtub is filled only with cold water, namely $T_f(0) = 20^o$ C, to $T_{ref} = 30^o$ C. Figure 11.2 compares the three aforementioned strategies, with the same feedback gain $k = 10$ for the two closed-loop controllers. It is clear that both feedback strategies provide a significant

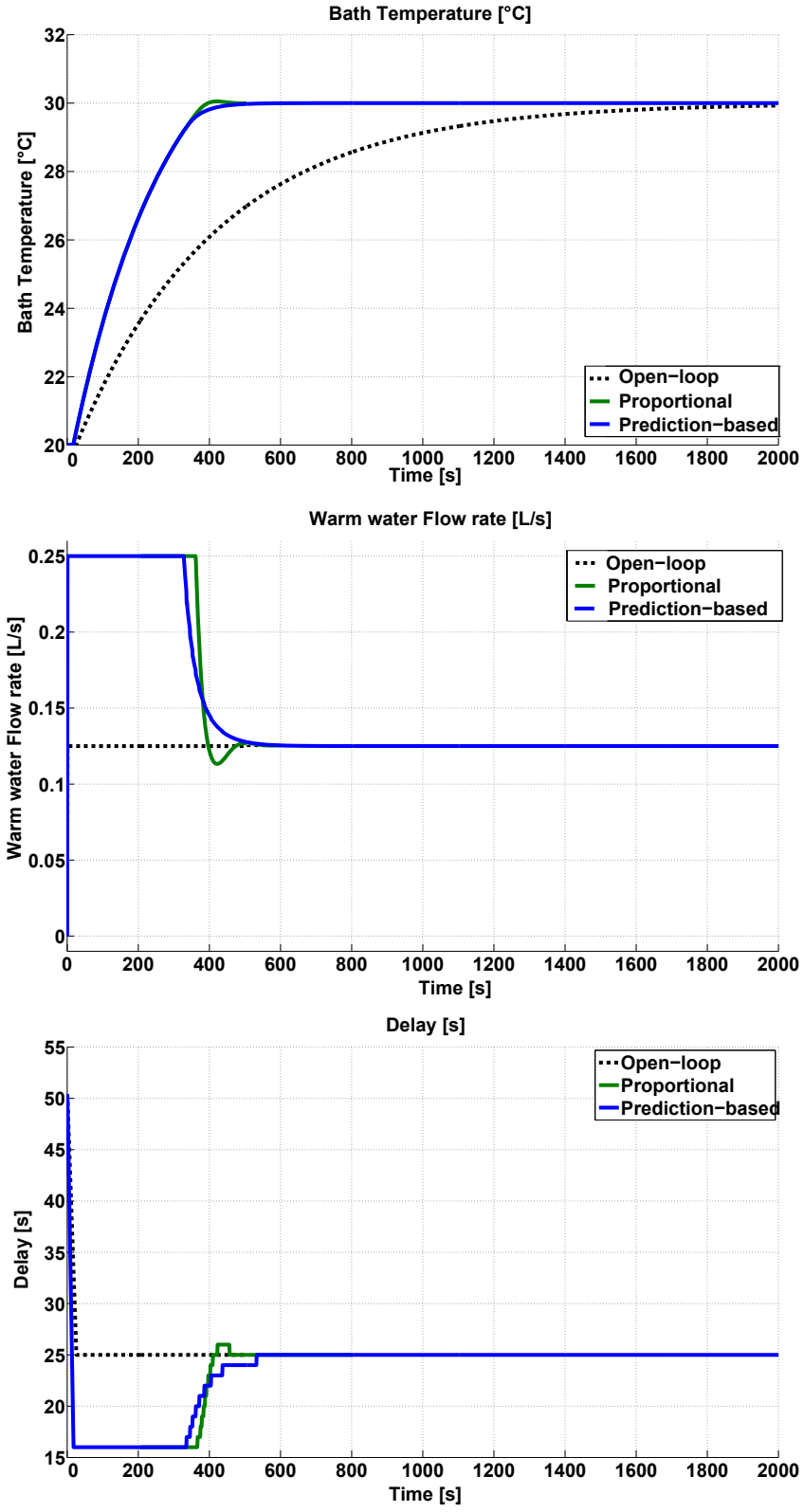

Figure 11.2: Stabilization of the bath temperature at the equilibrium $T_{ref} = 30^o$ C, starting from $T_f(0) = 20^o$ C respectively without feedback (black dotted) and with a gain $k = 10$ both for proportional (green curve) and prediction-based (blue curve) feedback.

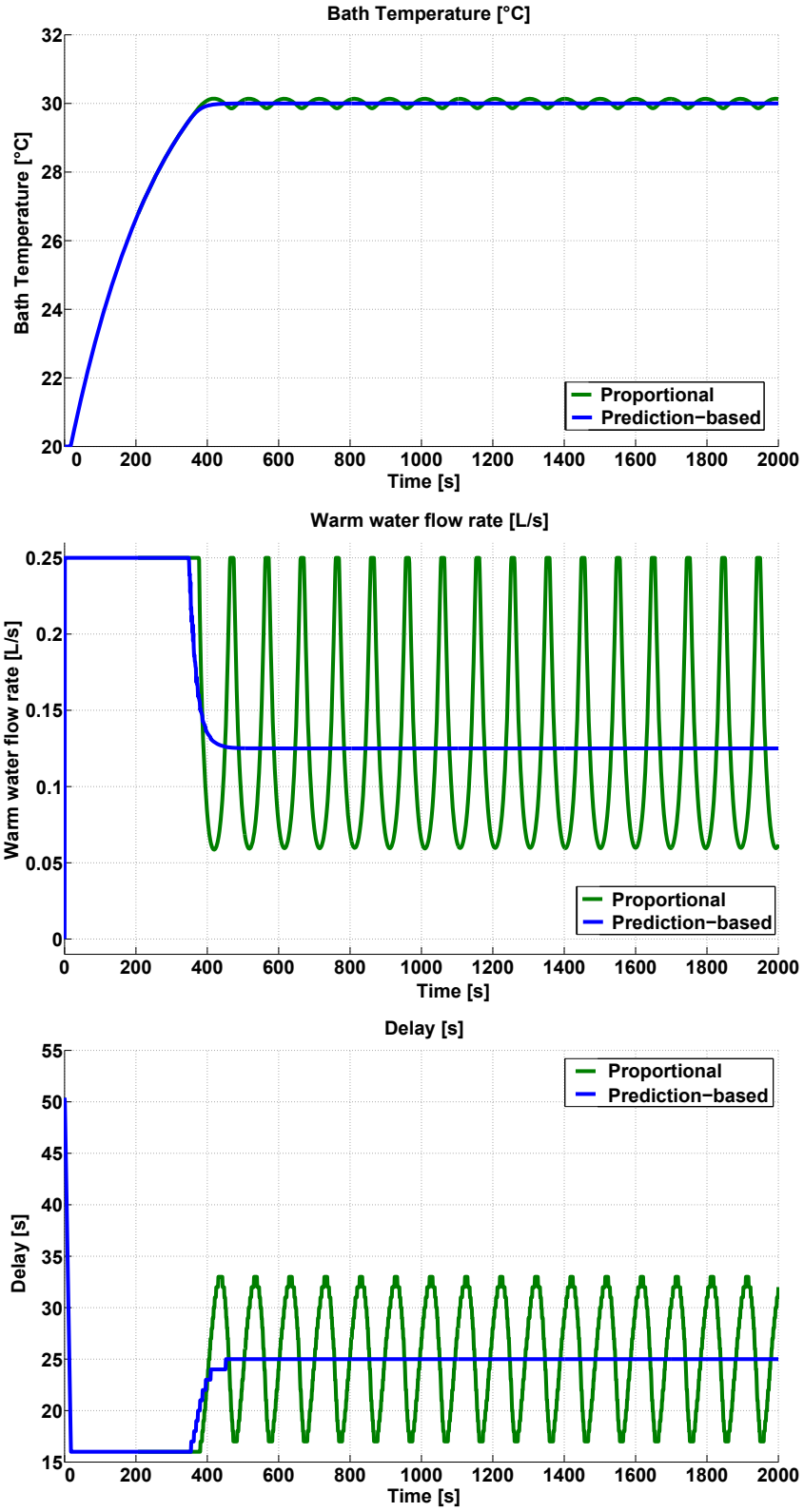

Figure 11.3: Stabilization of the bath temperature about the equilibrium $T_{ref} = 30^o$ C, starting from $T_f(0) = 20^o$ C for proportional (green curve) and prediction-based (blue curve) feedback, both with a gain of $k = 26$.

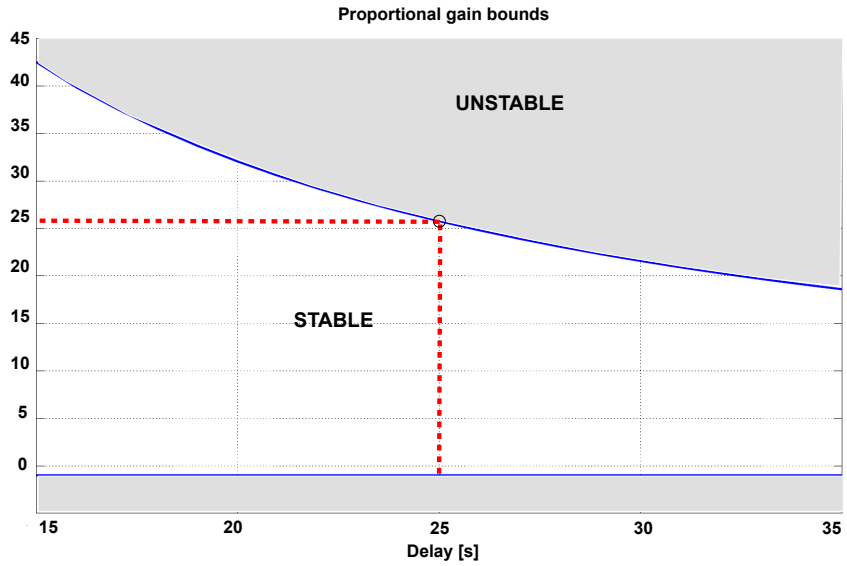

Figure 11.4: Stabilizing proportional gain k corresponding to (11.6) for a delay varying between 15 and 35 s. The maximum gain obtained for a 25-s delay is circled in red.

performance improvement over the open-loop strategy, as expected. In particular, the proposed controller favorably compares to a simple proportional controller in terms of output variations and overall effect. In detail, both controllers increase the warm water flow rate u, which results into a delay decrease (approximately 10 s shorter than with an open-loop strategy). Nevertheless, it is also evident that the proportional controller generates an overshoot and, as expected, has a later action compared to the prediction-based controller.

In light of this result, as the two feedback laws act quite similarly, it may be preferable to use the proportional feedback law, which is much easier to implement. However, the merits of the proposed prediction-based law are highlighted for increasing feedback gain k. Indeed, damped oscillations quickly appear for proportional control and the damping decreases as the gain increases. Finally, for a gain value $k = 26$, a limit cycle is reached and stabilization cannot be achieved, as observed in Figure 11.3. This can be easily interpreted by analyzing the characteristic equation of the closed-loop alternative system (11.6)

$$\Delta(\lambda) = \lambda + \frac{u_1 + \bar{u_2}}{V}\left(1 + ke^{-\lambda D_2}\right) = 0 \tag{11.19}$$

It is well known that the (infinite number of) characteristic roots of (11.19) are all located in the right-hand complex half-plane if and only if the following condition is satisfied [Silva 05]

$$-1 < k < \frac{V}{(u_1 + \bar{u_2})D_2}\sqrt{z_1^2 + \left(\frac{u_1 + \bar{u_2}}{V}\right)^2 {D_2}^2} \tag{11.20}$$

where z_1 is the unique solution of $\tan(z) = -\frac{V}{(u_1+\bar{u_2})D_2}z$ on the interval $(\pi/2, \pi)$. This range of variation is represented in Fig. 11.4, for a delay varying between 15 s and 35 s (corresponding to the range of the delay oscillations in Figure 11.3). The value of the

maximum stabilizing gain for a 25 s delay (the delay steady-state value of the operating point considered) is circled in red. As the proportional gain k increases from 25 to the critical value of 26, it is evident that the upper unstable region is reached, generating the behavior observed in Figure 11.3. Conversely, the prediction-based control still yields good performances for this feedback gain, as it is well-tuned. If the actuator were not saturated, one would reasonably expect improvements in the transient dynamics.

Finally, calculating the expression (10.7) of δ^* provided below, one obtains a scale of 10^{-6}, which would result here into a gain limitation around 10^{-7} as the initial error tracking of the bath temperature is 10^o C. This value is of course conservative, as underlined by the above simulation results.

Perspectives

To conclude this thesis, several possible future directions are sketched, which could benefit from the proposed work.

The robust compensation methodology presented in this thesis has been tested experimentally on various SI engine subsystems and particular attention was paid to a transport delay class, representative of a wide range of flow transportation processes. The proposed approach is expected to be relevant for other types of applications involving similar transport phenomena, especially in the process industry, e.g. blending in refineries, raw mix proportioning control in cement plants, polymerization reactor with long feed pipes, etc.

From a theoretical point of view, three natural paths could be explored. First, in the input-dependent delay compensation methodology proposed in the second part of the manuscript, the existence of an upper-bound limit for the feedback gain for any unstable plant would be worth further analysis ; this would reasonably involve elements of condition number theory for Lyapunov matrix equations. The compliance of this analysis with state observer design would also be worth being investigated. From the elements presented in the first part, this objective seems reachable but it is expected that the stability results would yield substantial calculations and require the initial state estimation error to be sufficiently small. Second, other delay defining equations could be considered as-well to ensure the generality of the obtained results. Third, the extension of the elements presented in this manuscript to some class of nonlinear systems (e.g. forward complete systems) would be worth being investigated.

Finally, an interesting question that remains open is the relevance of the approach proposed here for delayed measurements. Indeed, when the delay is time-varying, an output delay is not formally equivalent to an input-delay representation. Synchronization of data and models has long been a topic of importance for practitioners of observers and data fusion algorithms design. The potential application of delay compensation technique in this context is still to address.

Bibliography

[Adam 00] E. J. Adam, H. A. Latchman & O. D. Crisalle. *Robustness of the Smith predictor with respect to uncertainty in the time-delay parameter.* In Proceedings of the American Control Conference, volume 2, pages 1452–1457. IEEE, 2000.

[Ammann 03] M. Ammann, N. P. Fekete, L. Guzzella & A. H. Glattfelder. *Model-based control of the VGT and EGR in a turbocharged common-rail Diesel engine: theory and passenger car implementation.* SAE transactions, vol. 112, no. 3, pages 527–538, 2003.

[Angeli 99] D. Angeli & E. D. Sontag. *Forward completeness, unboundedness observability, and their Lyapunov characterizations.* Systems & Control Letters, vol. 38, no. 4, pages 209–217, 1999.

[Aquino 81] C. F. Aquino. *Transient A/F control characteristics of the 5 liter central fuel injection engine.* In SAE International Journal of Passenger Cars-Electronic and Electrical Systems. SAE International, 1981.

[Arsie 03] I. Arsie, C. Pianese, G. Rizzo & V. Cioffi. *An adaptive estimator of fuel film dynamics in the intake port of a Spark Ignition engine.* Control Engineering Practice, vol. 11, no. 3, pages 303–309, 2003.

[Artstein 82] Z. Artstein. *Linear systems with delayed controls: a reduction.* IEEE Transactions on Automatic Control, vol. 27, no. 4, pages 869–879, 1982.

[Barraud 06] J. Barraud. *Commande de procédés à paramètres variables.* PhD thesis, PhD thesis, École des Mines de Paris, 2006.

[Bekiaris-Liberis 12] N. Bekiaris-Liberis, M. Jankovic & M. Krstic. *Compensation of state-dependent input delay for nonlinear systems.* In Proc. of the American Control Conference, 2012.

[Bobtsov 10] A. A. Bobtsov, S. A. Kolyubin & A. A. Pyrkin. *Compensation of unknown multi-harmonic disturbances in nonlinear plants with delayed control.* Automation and Remote Control, vol. 71, no. 11, pages 2383–2394, 2010.

[Bresch-Pietri 09] D. Bresch-Pietri & M. Krstic. *Adaptive trajectory tracking despite unknown input delay and plant parameters.* Automatica, vol. 45, no. 9, pages 2074–2081, 2009.

[Bresch-Pietri 10] D. Bresch-Pietri & M. Krstic. *Delay-adaptive predictor feedback for systems with unknown long actuator delay.* IEEE Transactions on Automatic Control, vol. 55, no. 9, pages 2106–2112, 2010.

[Caicedo 12] M. A. R. Caicedo, E. Witrant, O. Sename, P. Higelin*et al. A high gain observer for enclosed mass estimation in a Spark Ignited engine.* In Proceedings of the 2012 American Control Conference, 2012.

[Cairns 05] A. Cairns & H. Blaxill. *The effects of combined internal and external exhaust gas recirculation on gasoline controlled auto-ignition.* SAE Technical Paper, 2005.

[Ceccarelli 09] R. Ceccarelli, P. Moulin & A. Sciarretta. *Model-based adaptive observers for intake leakage detection in Diesel engines.* In Proc. of the American Control Conference, pages 1128–1133. IEEE, 2009.

[Chèbre 10] M. Chèbre, Y. Creff & N. Petit. *Feedback control and optimization for the production of commercial fuels by blending.* Journal of Process Control, vol. 20, no. 4, pages 441–451, 2010.

[Chevalier 00] A. Chevalier, C. W. Vigild & E. Hendricks. *Predicting the port air mass flow of SI engines in air/fuel ratio control applications.* In SAE World Congress. SAE International, 2000.

[Coppin 10] T. Coppin, O. Grondin & N. Maamri. *Fuel estimation and air-to-fuel ratio control for flexfuel Spark-Ignition engines.* In 2010 IEEE International Conference on Control Applications (CCA), pages 555–560. IEEE, 2010.

[Das 08] H. B. Das & S. J. Dhinagar. *Airpath modeling and control for a turbocharged Diesel engine.* In SAE Technical paper. SAE International, 2008.

[Di Gaeta 03] A. Di Gaeta, S. Santini, L. Glielmo, F. De Cristofaro, C. Di Giuseppe & A. Caraceni. *An algorithm for the calibration of wall-wetting model parameters.* In SAE Technical Paper. SAE International, 2003.

[Eriksson 99] L. Eriksson. *Spark advance modeling and control.* PhD thesis, Linkĺoping University, May 1999.

[Evesque 03] S. Evesque, A. M. Annaswamy, S. Niculescu & A. P. Dowling. *Adaptive control of a class of time-delay systems.* Journal of Dynamic Systems, Measurement and Control, vol. 125, page 186, 2003.

[Guzzella 10] L. Guzzella & C. H. Onder. Introduction to modeling and control of internal combustion engine systems. Springer Verlag, 2010.

[Halanay 66] A. Halanay. Differential equations: stability, oscillations, time lags, volume 23. Academic Press, 1966.

[Hale 71] J. Hale. Functional differential equations. Springer, 1971.

[Hendricks 97] E. Hendricks. *Engine modelling for control applications : a critical survey.* Meccanica, vol. 32, pages 387–396, 1997.

[Henson 94] M. A. Henson & D. E. Seborg. *Time delay compensation for nonlinear processes.* Industrial & engineering chemistry research, vol. 33, no. 6, pages 1493–1500, 1994.

[Heywood 88] J. B. Heywood. Internal combustion engine fundamentals. McGraw-Hill New York, 1988.

[Hoepke 12] B. Hoepke, S. Jannsen, E. Kasseris & W. K. Cheng. *EGR effects on boosted SI engine operation and knock integral correlation.* SAE International Journal of Engines, vol. 5, no. 2, pages 547–559, 2012.

[Huang 95] C. T. Huang & Y. S. Lin. *Tuning PID controller for open-loop unstable processes with time delay.* Chemical Engineering Communications, vol. 133, no. 1, pages 11–30, 1995.

[Huang 97] H. P. Huang & C. C. Chen. *Control-system synthesis for open-loop unstable process with time delay.* IEE Proc-Control Theory Appl, vol. 144, no. 4, pages –, 1997.

[Ioannou 96] P. A. Ioannou & J. Sun. Robust adaptive control. Prentice Hall Englewood Cliffs, NJ, 1996.

[Ioannou 06] P. A. Ioannou & B. Fidan. Adaptive control tutorial. Society for Industrial Mathematics, 2006.

[Ivanov 02] A. Ivanov, E. Liz & S. Trofimchuk. *Halanay inequality, Yorke 3/2 stability criterion, and differential equations with maxima.* Tohoku Mathematical Journal, vol. 54, no. 2, pages 277–295, 2002.

[Jankovic 09] M. Jankovic & I. Kolmanovsky. *Developments in control of time-delay systems for automotive powertrain applications.* In Delay Differential Equations, recent advances and new directions, Balachandran, B. and Kalmar-Nagy, T. and Gilsinn D. E., pages 55–92. Springer Science, 2009.

[Jankovic 11] M. Jankovic & S. Magner. *Disturbance attenuation in time-delay systems - a case study on engine air-fuel ratio control.* In Proc. of the American Control Conference, 2011.

[Kahveci 10] N. E. Kahveci & M. Jankovic. *Adaptive controller with delay compensation for Air-Fuel Ratio regulation in SI engines.* In Proc. of the American Control Conference, pages 2236–2241. IEEE, 2010.

[Kailath 80] T. Kailath. Linear systems. Prentice-Hall Englewood Cliffs, NJ, 1980.

[Kiencke 00] U. Kiencke & L. Nielsen. Automotive control systems. Springer-Verlag, Berlin, 2000.

[Klamka 82] J. Klamka. *Observer for linear feedback control of systems with distributed delays in controls and outputs.* Systems & Control Letters, vol. 1, no. 5, pages 326–331, 1982.

[Kravaris 89] C. Kravaris & R. A. Wright. *Deadtime compensation for nonlinear processes.* AIChE Journal, vol. 35, no. 9, pages 1535–1542, 1989.

[Krstic 08a] M. Krstic. Boundary control of PDEs: a course on backstepping designs. Society for Industrial and Applied Mathematics Philadelphia, PA, USA, 2008.

[Krstic 08b] M. Krstic & A. Smyshlyaev. *Backstepping boundary control for first-order hyperbolic PDEs and application to systems with actuator and sensor delays.* Systems & Control Letters, vol. 57, no. 9, pages 750–758, 2008.

[Krstic 09a] M. Krstic. Delay compensation for nonlinear, adaptive, and PDE systems. Birkhauser, 2009.

[Krstic 09b] M. Krstic & D. Bresch-Pietri. *Delay-adaptive full-state predictor feedback for systems with unknown long actuator delay.* In Proceedings of the 2009 American Control Conference, pages 4500–4505, 2009.

[Kwon 80] W. Kwon & A. Pearson. *Feedback stabilization of linear systems with delayed control.* IEEE Transactions on Automatic Control, vol. 25, no. 2, pages 266–269, 1980.

[Landau 98] I. D. Landau, R. Lozano & M. M'Saad. Adaptive control. Springer London, 1998.

[Lauber 02] J. Lauber, T. M. Guerra & W. Perruquetti. *IC engine: tracking control for an inlet manifold with EGR.* SAE Transactions Journal of Passenger Cars: electronic and electrical systems, vol. 20, pages 913–917, 2002.

[Lauber 11] J. Lauber, T. M. Guerra & M. Dambrine. *Air-fuel ratio control in a gasoline engine.* International Journal of Systems Science, vol. 42, no. 2, pages 277–286, 2011.

[Le Solliec 06] G. Le Solliec, F. Le Berr, G. Colin, G. Corde & Y. Chamaillard. *Engine control of a downsized Spark Ignited engine : from simulation to vehicle.* In Proc. of ECOSM Conference, 2006.

[Lepreux 10] O. Lepreux. *Model-based temperature control of a Diesel oxidation catalyst.* PhD thesis, MINES Paristech, 2010.

[Leroy 08] T. Leroy, J. Chauvin & N. Petit. *Controlling air and burned gas masses of turbocharged VVT SI engines.* In Proc. of th 47th IEEE Conference on Decision and Control, pages 5628–5634, 2008.

[Leroy 09] T. Leroy, J. Chauvin, F. Le Berr, A. Duparchy & G. Alix. *Modeling fresh air charge and residual gas fraction on a dual independant variable valve timing SI engine.* SAE International Journal of Engines, vol. 1, no. 1, pages 627–635, 2009.

[Malisoff 09] M. Malisoff & F. Mazenc. Constructions of strict lyapunov functions. Springer, 2009.

[Manitius 79] A. Manitius & A. Olbrot. *Finite spectrum assignment problem for systems with delays.* IEEE Transactions on Automatic Control, vol. 24, no. 4, pages 541–552, 1979.

[Michiels 03] W. Michiels, S. Mondié & D. Roose. *Necessary and sufficient conditions for a safe implementation of distributed delay control laws.* In Proceedings of the joint CNRS-NSF workshop: Advances in control of time-delay systems, pages 1–4, 2003.

[Michiels 07] W. Michiels & S. I. Niculescu. Stability and stabilization of time-delay systems. Society for Industrial and Applied Mathematics, 2007.

[Miller 82] R. K. Miller & A. N. Michel. Ordinary differential equationsordinary1982miller. Academic Press, 1982.

[Mondié 01] S. Mondié, S. Niculescu & J. J. Loiseau. *Delay robustness of closed loop finite assignment for input delay systems.* In Proc. of the 3rd IFAC Conference on Time Delay Systems, Santa Fe, New Mexico, USA, 2001.

[Mondié 03] S. Mondié & W. Michiels. *A safe implementation for finite spectrum assignment: robustness analysis.* In Proc. of the 42nd IEEE Conference on Decision and Control , Hawaii, USA, 2003.

[Niculescu 01] S. I. Niculescu. Delay effects on stability: a robust control approach, volume 269. Springer Verlag, 2001.

[Niculescu 03] S. I. Niculescu & A. M. Annaswamy. *An adaptive Smith-controller for time-delay systems with relative degree n≥ 2.* Systems & Control Letters, vol. 49, no. 5, pages 347–358, 2003.

[Nihtila 91] M. T. Nihtila. *Finite pole assignment for systems with time-varying input delays.* In Proc. of the 30th IEEE Conference on Decision and Control, pages 927–928, 1991.

[O'Dwyer 00] A. O'Dwyer. *A survey of techniques for the estimation and compensation of processes with time delay*, 2000.

[Orlov 06] Y. Orlov, I. V. Kolmanovsky & O. Gomez. *On-line identification of SISO linear time-delay systems from output measurements: theory and applications to engine transient fuel identification.* In Proc. of the American Control Conference, page 6, 2006.

[Owens 82] D. H. Owens & A. Raya. *Robust stability of Smith predictor controllers for time-delay systems.* In Control Theory and Applications, IEE Proceedings D, volume 129, pages 298–304. IET, 1982.

[Palmor 80] Z. Palmor. *Stability properties of Smith dead-time compensator controllers.* International Journal of Control, vol. 32, pages 937–49, 1980.

[Palmor 96] Z. Palmor. *Time-delay compensation-Smith predictor and its modifications.* The control handbook, vol. 1, pages 224–229, 1996.

[Perry 84] R. H. Perry, D. W. Green & J. O. Maloney. Perry's chemical engineers' handbook, volume 7. McGraw-Hill New York, 1984.

[Petit 98] N. Petit, Y. Creff & P. Rouchon. *Motion planning for two classes of nonlinear systems with delays depending on the control.* In Proceedings of the 37th IEEE Conference on Decision and Control, pages 1007–1011, 1998.

[Polyanin 07] A. Polyanin & A. V. Manzhirov. Handbook of integral equations, volume 67. CRC Press, 2007.

[Potteau 07] S. Potteau, P. Lutz, S. Leroux, S. Moroz*et al.* *Cooled EGR for a turbo SI engine to reduce knocking and fuel consumption.* In SAE Technical Paper, pages 01–3978, 2007.

[Pyrkin 10] A. Pyrkin, A. Smyshlyaev, N. Bekiaris-Liberis & M. Krstic. *Output control algorithm for unstable plant with input delay and cancelation of unknown biased harmonic disturbance.* In Proc. 9th IFAC Workshop on Time Delay Systems, 2010.

[Richard 03] J.-P. Richard. *Time-delay systems: an overview of some recent advances and open problems.* Automatica, vol. 39, no. 10, pages 1667–1694, 2003.

[Rugh 96] W.J. Rugh. Linear system theory. Prentice-Hall, Inc., 1996.

[Silva 05] G. J. Silva, A. Datta & S. P. Bhattacharyya. PID controllers for time-delay systems. Birkhauser, 2005.

[Smith 57] O. J. M. Smith. *Closer control of loops with dead time.* Chemical Engineering Progress, vol. 53, no. 5, pages 217–219, 1957.

[Smith 59] O. J. M. Smith. *A controller to overcome dead time.* ISA Journal, vol. 6, no. 2, pages 28–33, 1959.

[Stefanopoulou 98] A. G. Stefanopoulou, J. A. Cook, J. W. Grizzle & J. S. Freudenberg. *Control-oriented model of a dual equal variable cam timing Spark Ignition engine.* Journal of Dynamic Systems, Measurement and Control, vol. 120, pages 257–266, 1998.

[Stotsky 02] A. Stotsky & I. Kolmanovsky. *Application of input estimation techniques to charge estimation and control in automotive engines.* Control Engineering Practice, vol. 10, no. 12, pages 1371–1383, 2002.

[Van Assche 99] V. Van Assche, M. Dambrine, J. F. Lafay & J. P. Richard. *Some problems arising in the implementation of distributed-delay control laws.* In Proceedings of the 38th IEEE Conference on Decision and Control, 1999., volume 5, pages 4668–4672, 1999.

[Van Nieuwstadt 00] M. J. Van Nieuwstadt, I. V. Kolmanovsky, P. E. Moraal, A. Stefanopoulou & M. Jankovic. *EGR-VGT control schemes: experimental comparison for a high-speed Diesel engine.* Control Systems Magazine, IEEE, vol. 20, no. 3, pages 63–79, 2000.

[Vardi 68] J. Vardi & W. F. Biller. *Thermal behavior of exhaust gas catalytic convertor.* Industrial & Engineering Chemistry Process Design and Development, vol. 7, no. 1, pages 83–90, 1968.

[Wang 06] D. Y. Wang & E. Detwiler. *Exhaust oxygen sensor dynamic study.* Sensors & Actuators: B. Chemical, vol. 120, no. 1, pages 200–206, 2006.

[Watanabe 81] K. Watanabe & M. Ito. *An observer for linear feedback control laws of multivariable systems with multiple delays in controls and outputs.* Systems & Control Letters, vol. 1, no. 1, pages 54–59, 1981.

[Watanabe 96] K. Watanabe, E. Nobuyama & A. Kojima. *Recent advances in control of time delay systems-a tutorial review.* In Proceedings of the 35th IEEE Decision and Control, 1996, volume 2, pages 2083–2089, 1996.

[Witrant 05] E. Witrant. *Stabilisation des systèmes commandés par réseaux.* PhD thesis, Laboratoire d'Automatique de Grenoble, 2005.

[Young 76] L. C. Young & B. A. Finlayson. *Mathematical models of the monolith catalytic converter.* AIChE Journal, vol. 22, no. 2, pages 343–353, 1976.

[Yue 05] D. Yue & Q. L. Han. *Delayed feedback control of uncertain systems with time-varying input delay.* Automatica, vol. 41, no. 2, pages 233–240, 2005.

[Zenger 09] K. Zenger & A. J. Niemi. *Modelling and control of a class of time-varying continuous flow processes.* Journal of Process Control, vol. 19, no. 9, pages 1511–1518, 2009.

[Zheng 04] M. Zheng, G. T. Reader & J. G. Hawley. *Diesel engine exhaust gas recirculation–a review on advanced and novel concepts.* Energy Conversion and Management, vol. 45, no. 6, pages 883–900, 2004.

[Zhong 06] Q. C. Zhong. Robust control of time-delay systems. Springer Verlag, 2006.

[Zhou 09] J. Zhou, C. Wen & W. Wang. *Adaptive backstepping control of uncertain systems with unknown input time-delay.* Automatica, vol. 45, pages 1415–1422, 2009.

[Ziegler 42] J. G. Ziegler & N. B. Nichols. *Optimum settings for automatic controllers.* Transactions on Automatic Control, vol. 5, no. 11, pages 759–768, 1942.

Notations and acronyms

Acronyms

Mathematical acronyms	
DDE	Delay Differential Equation
LTI	Linear Time Invariant
LTV	Linear Time Varying
PDE	Partial Differential Equation

Engine acronyms	
BGR	Burned Gas Rate
CI	Compression Ignition engine
CO	Carbon Monoxide
DOC	Diesel Oxidation Catalyst
ECE	Urban Driving Cycle
EGR	Exhaust Gas Recirculation
EUDC	Extra-Urban Driving Cycle
FAR	Fuel-to-Air Ratio
HC	Unburned Hydrocarbons
IMEP	Indicated Mean Effective Pressure
LP EGR	Low Pressure Exhaust Gas Recirculation
MAF	Mass Air Flow
NEDC	New European Driving Cycle
NO_x	Nitrogen oxides
PM	Particulate matter
SA	Spark Advance
SI	Spark Ignited
TDC	Top Dead Center
TWC	Three Way Catalytic converter
VVT	Variable Valve Timing

Function regularity classes and norms

$\mathcal{C}^0$	continuous functions
$\mathcal{C}^1$	continuously differentiable functions
$\|.\|$	Euclidean norm
$\mathcal{K}_\infty$	set of functions defined in $\mathbb{R}_+$ with values in $\mathbb{R}_+$, strictly increasing, taking the value 0 in 0 and tending to $+\infty$ in $+\infty$
Sat_I	saturation operator onto the interval I
Proj_Π	projector operator onto the convex set Π

$\|f(t)\| = \sqrt{\int_0^1 f(x,t)^2 dx}$, $f : (x,t) \in [0;1] \times \mathbb{R}_+ \to \mathbb{R}$

$\|f\|_\infty = \sup_{\hat{\theta}\in\Pi} |f(\hat{\theta})|$, $f : \Pi \to \mathbb{R}^l$ $(l \in \mathbb{N}^*)$

$|M| = \sup_{|x|\leq 1} |Mx|$, $M \in \mathcal{M}_l(\mathbb{R})$ $(l \in \mathbb{N}^*)$

$x_t : s \in [-\overline{D}, 0] \mapsto x(t+s)$ for $\overline{D} > 0$ and for a given function x. For any bounded function k defined on $[-\overline{D}, 0]$, a polynomial function $\pi\left(x(t_1), \ldots, x(t_{n-2}), \int_{t_{n-1}}^{t_n} k(t-s)x(s)ds\right)$ for $(t_1, \ldots, t_n) \in [t-\overline{D}, t]^n$ is denoted $\pi(x_t)$.

A polynomial function π in the variables $(x_1, \ldots, x_n, x_{n+1})$ is said to be *at least quadratic in* $x_1, \ldots, x_n$ iff, for any given x_{n+1}, the corresponding polynomial function $\pi_{x_{n+1}}$ defined as

$$\pi_{x_{n+1}}(x_1, \ldots, x_n) = \pi(x_1, \ldots, x_n, x_{n+1})$$

has no terms of order 0 or 1, e.g. $\pi = x_1^2 + x_1x_2x_3$ and $\pi = x_2x_1 + x_3x_1^2$ are both at least quadratic in (x_1, x_2) while $\pi = x_3 + x_3x_2^2$ is not.

Notations

Symbol	Description	Unit
dm_f	Feedback in-cylinder fuel mass set-point	mg/str
D_{burn}	Combustion duration	s
D_{inj}	Computation and injection duration	s
D_{trans}	Transport FAR delay	s
F	Gas mass flow rate	kg/s
F_{air}	Fresh air mass flow rate (upstream of the compressor)	kg/s
F_{asp}	In -cylinder mass flow rate	kg/s
F_{dc}	Mass flow rate downstream of the compressor	kg/s
F_{egr}	EGR mass flow rate through the EGR valve	kg/s
F_{egr}^{sp}	EGR mass flow rate set-point	kg/s
F_f	Mass flow rate of in-cylinder fuel	kg/s
F_{inj}	Mass flow rate of injected fuel	kg/s
F_{thr}	Mass flow rate through the throttle	kg/s
FAR_{st}	Stoichiometric Fuel-to-Air Ratio	-
L_P	Pipe length from the compressor down to the intake manifold	m
m_{air}	In-cylinder air mass	mg/str

Symbol	Description	Unit
m_{air}^{sp}	In-cylinder air mass set-point	mg/str
m_{asp}	Aspirated air mass	mg/str
m_{asp}^{est}	Estimated aspirated air mass	mg/str
m_{asp}^{sp}	Aspirated air mass set-point	mg/str
m_{bg}^{sp}	In-cylinder burned gas mass set-point	mg/str
m_{bg}	In-cylinder burned gas mass	mg/str
m_{exh}	Exhaust Gases Mass	mg/str
m_f	In-cylinder fuel mass	mg/str
m_f^{ff}	Feed-forward in-cylinder fuel mass set-point	mg/str
m_f^{sp}	In-cylinder injected fuel mass set-point	mg/str
m_{inj}	Injected mass of fuel	mg/str
m_w	Liquid fuel wall mass	mg
$L_{ev\to\lambda}$	Pipe length from the exhaust valve up to the Lambda sensor	m
N_e	Engine Speed	rpm
P_{atm}	Atmospheric pressure	Pa
P_{dc}	Pressure downstream of the compressor	Pa
P_{dt}	Pressure downstream of the turbine	Pa
P_{dv}	Pressure downstream of the EGR valve	Pa
p_{int}	Intake manifold pressure	Pa
P_{uv}	Pressure upstream of the EGR valve	Pa
r	Specific ideal gas constant	J/kg/K
SA^{sp}	Spark Advance set-point	CAD
S_{valve}	EGR valve effective area	m^2
T_1, T_1	Cold and warm bath sources temperature	K
T_{dc}	Temperature downstream of the compressor	K
T_f	Bath homogeneous temperature	K
T_g	Distributed gas temperature inside the catalyst	L
T_{int}	Intake manifold temperature	K
T_{moy}	Fluid temperature at the node	K
T_{ref}	Bath temperature set-point	K
T_{uv}	Temperature upstream of the EGR valve	K
T_R	Distributed resistance temperature	K
T_w	Distributed wall temperature	K
u_1, u_2	Cold and warm bath source flow rate	m^3/s
v_{bg}	Burned gas speed	m/s
v_{rec}	Conveyor belt speed	m/s
v_{gas}	Gas velocity	m/s
V_{dc}	Volume downstream of the compressor	m^3
V_{int}	Intake manifold volume	m^3
V_P	Pipe volume of the bath system	m^3
X	Ratio of un-vaporized fuel	-
x	Intake burned gas fraction	-
x_{cyl}	In-cylinder burned gas fraction	-
x_{lp}	Burned gas fraction upstream of the compressor	-
x_{sp}	Intake burned gas rate set-point	-
α	FAR error	-
δm_f	Fuel injection error	-

Symbol	Description	Unit
δm_{asp}	Aspirated air mass estimation error	-
ΔP	Differential pressure at the EGR valve	Pa
γ	Heat capacity ratio	-
θ_{egr}	EGR valve position set-point	%
θ_{egr}^{sp}	EGR valve position	%
τ	Wall-wetting time constant	s
τ_ϕ	Fuel-to-Air Ratio dynamic time constant	s
ϕ	Normalized Fuel-to-Air Ratio	
ϕ_m	Normalized Fuel-to-Air Ratio signal given by the Lambda sensor	-
ϕ^r	Fuel-to Air Ratio set-point	-

Appendix A

Modeling of some delay systems

A.1 Air Heater Model

Here we describe the design of a temperature model for an air heater, as shown in Figure A.1. This system is often used on experimental test benches to simulate changes in atmospheric conditions and to account for various disturbances of the intake air temperature.

Fresh air enters and flows through the air heater, where it is heated by an electrical resistance but also exchanges with the monolith wall. This yields spatially distributed temperature profiles for the air heater wall $T_w(x,t)$, the gas $T_g(x,t)$, and the resistance $T_R(x,t)$, as pictured in Figure A.2. Axial conduction in the solid is not important and can be neglected.

Thermal balance equations for the wall, the gas and the resistance give the following set of coupled PDEs

$$\begin{cases} \dfrac{\partial T_w}{\partial t}(x,t) = k_1(T_g(x,t) - T_w(x,t)) & \text{(A.1)} \\ \dfrac{\partial T_g}{\partial t}(x,t) + v(t)\dfrac{\partial T_g}{\partial x}(x,t) = k_2(T_w(x,t) - T_g(x,t)) + k_3(T_R(x,t) - T_g(x,t)) & \text{(A.2)} \\ \dfrac{\partial T_R}{\partial t}(x,t) = k_4(T_g(x,t) - T_R(x,t)) + k_5\phi(t) & \text{(A.3)} \end{cases}$$

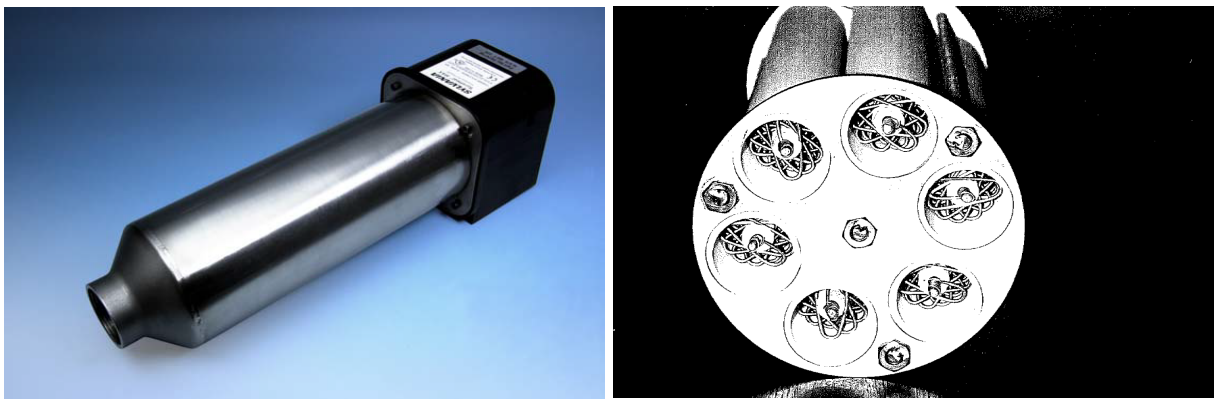

Figure A.1: Photograph of the air heater and a transversal view of the system.

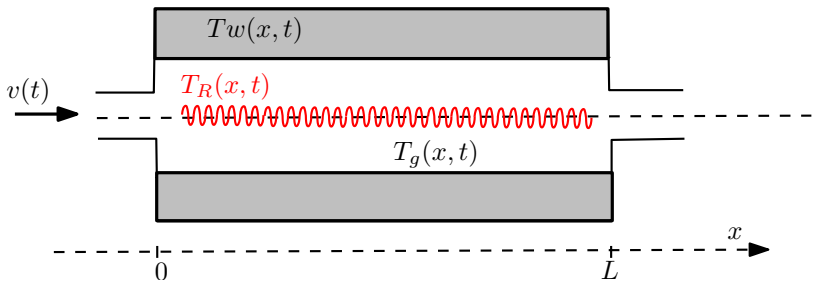

Figure A.2: Schematic view of thermal exchanges.

where ϕ denotes the ohmic heat generation, which is assumed to be spatially homogeneous; the intermediate positive constants involved can be explicitly expressed in terms of physical constants.

In the previous model, conduction within the wall and the gas storage were neglected compared to the convection phenomena.

We are interested in the transfer from the ohmic heat generation ϕ to the output gas temperature $T_g(L,t)$. To do so, in the following, we perform an operational calculus analysis of the previous infinite-dimensional model and exploit the low-pass filter property of the air heater.

A.1.1 Reduced model

In the Laplace domain, (A.1) and (A.3) can be rewritten as

$$\begin{aligned}\hat{T}_w(x,s) =& \frac{k_1}{s+k_1}\hat{T}_g(x,s)\\ \hat{T}_R(x,s) =& \frac{k_4}{s+k_4}\hat{T}_g(x,s) + \frac{k_5}{s+k_4}\hat{\phi}(s)\end{aligned}$$

Then, (A.2) can be reformulated as

$$v(t)\frac{d\hat{T}_g}{dx}(x,s) = -\left(s+k_2+k_3-\frac{k_1k_2}{s+k_1}-\frac{k_3k_4}{s+k_4}\right)\hat{T}_g(x,s) + \frac{k_3k_5}{s+k_4}\hat{\phi}(s)$$

Solving the resulting (spatially) ordinary differential equation yields

$$\begin{cases}\hat{T}_g(L,s) =& \exp\left(-\frac{L}{v}f(s)\right)\hat{T}_g(0,s) + \frac{k_3k_5}{(s+k_4)f(s)}\left(1-\exp\left[-\frac{L}{v}f(s)\right]\right)\hat{\phi}(s)\\ f(s) =& s\frac{s^2+s(k_1+k_2+k_3+k_4)+k_1k_3+k_2k_4+k_1k_4}{(s+k_1)(s+k_4)}\end{cases}$$

As an air-heater is a low-pass filter, it is almost non-sensitive to high frequencies and one can efficiently use a first-order Padé approximation to simplify this last expression. In other words, as f tends to zero for low frequencies, one can write

$$1-\exp\left(-\frac{L}{v}f(s)\right) \approx \frac{L/v\, f(s)}{1+L/2v\, f(s)}$$

and consequently obtain

$$\begin{aligned}\frac{\hat{T}_g(L,s)}{\hat{\phi}} \approx & \frac{L}{v}\frac{k_3k_5}{(s+k_4)(s+\frac{L}{2v}f(s))} \\ = & \frac{L}{v}\frac{k_3k_5(s+k_1)}{(s+k_1)(s+k_4)+\frac{L}{2v}s(s^2+s(k_1+k_2+k_3+k_4)+k_1k_3+k_2k_4+k_1k_4)}\end{aligned}$$

which is a transfer function with one zero and three poles, all in the right-half plane.

Accounting for the input delay Because of communication lags and the fact that the electrical devices are not located directly at the inlet of the air heater, a time lag occurs. This can be represented as follows

$$D = D_{trans} + D_{comm}$$

where D_{trans} if the transport dead time, which is inversely proportional to the gas speed v, and the transmission delay D_{comm} can be considered as constant.

Finally the transfer of the air heater is given the following equations

$$\boxed{\begin{aligned}&\frac{\hat{T}_g(L,s)}{\hat{\phi}} = \frac{K(T_zs+1)e^{-Ds}}{a_3s^3+a_2s^2+a_1s+1} \\ &\text{where} \\ &K=\frac{k_3k_5L}{k_4v}, \quad T_z=\frac{1}{k_1}, \quad D=\frac{\alpha}{v} \\ &a_3=\frac{\beta}{v}, \quad a_2=\gamma+\frac{\delta}{v} \quad \text{and} \quad a_1=\varepsilon+\frac{\zeta}{v}\end{aligned}} \tag{A.4}$$

In this model, the gain, the (stable) poles and the delay can be considered as functions of the varying gas speed which is not perfectly measured (uncertain).

A.1.2 Validation using experimental data

To validate the proposed model, experimental tests were conducted on a test bench under various operating conditions to identify the parametrization constants in (A.4).

Figure A.3 compares the resulting modeled temperature to experimental data gas mass flow rate of 12 kg/h and 54 kg/h. Several points can be observed. First, the long response time of the (stable) plant stresses the need for a closed-loop controller to improve transient performances. Second, the occurrence of an input delay is notable, but it is relatively small compared to the response time of the system. Finally, the overall trends are well captured by the proposed model.

In particular, the parameter values for a mass flow rate of 54 kg/h are those used for illustration purposes in Chapter 5 and Chapter 6. Details regarding possible control design are given in these chapters.

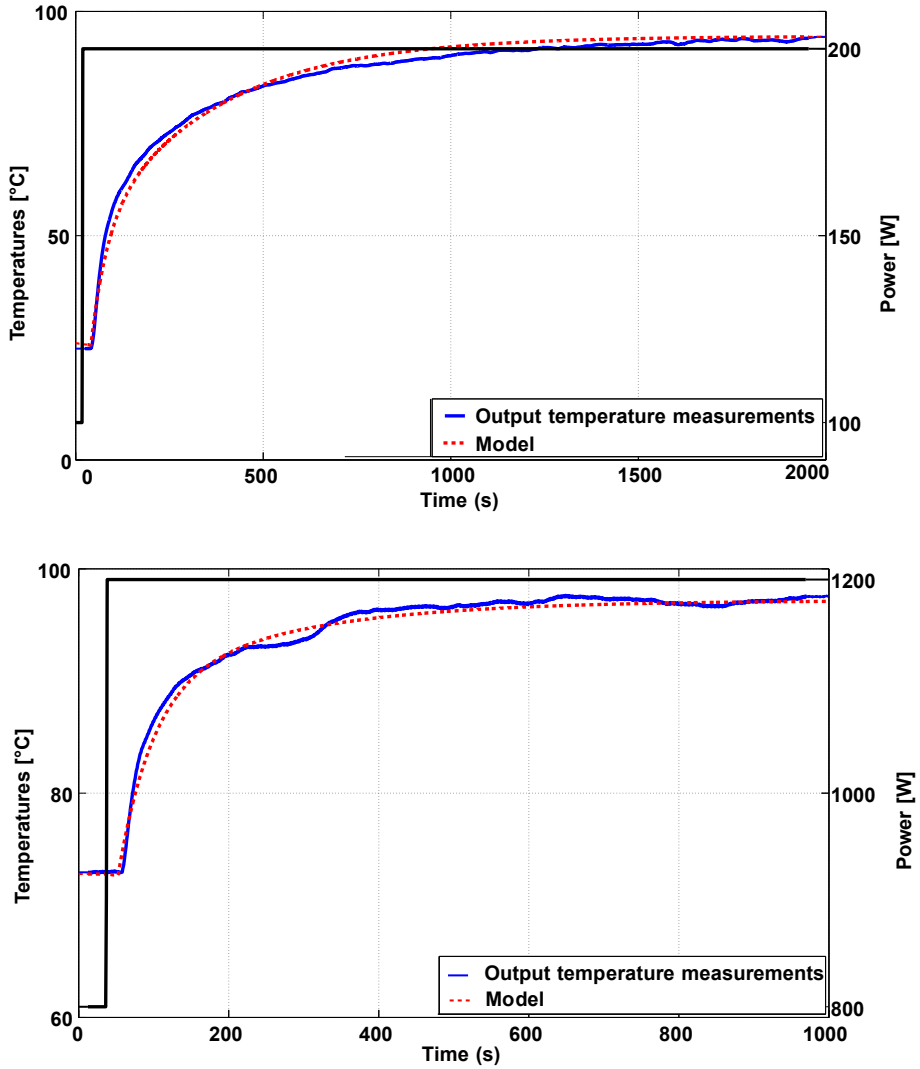

Figure A.3: Output gas temperature corresponding to a step of electrical heat (in black). The proposed model (red) is compared to experimental data (blue) for gas speed of 12 kg/h (top) and 54 kg/h (bottom).

A.2 Crushing mill

We consider the crushing mill pictured in Figure 8.2 and inspired from the example proposed in [Richard 03]. The task of this mill is to reduce the size of raw elements entering the process. We describe a model of this delayed system using the elements presented in Chapter 8.

The size of a volume V of N elements is defined as

$$y = \frac{V}{N}$$

The aim of the control design is to reduce the output size down to a critical value y_{lim}. We first propose an infinite-dimensional model, and then a finite-dimensional lumped model. Notations are listed in Table A.2.1.

A.2.1 PDE model

Distributed size profile into the mill

The size of elements into the mill satisfies the following parabolic PDE

$$\frac{\partial y}{\partial t}(x,t) - v_{CM}\frac{\partial y}{\partial x}(x,t) = -\eta y(x,t) \tag{A.5}$$

where $v_{CM} = \frac{u_{out}}{A} > 0$ is the uniform and constant propagation speed of the material inside the crushing mill and $\eta > 0$ is the size decay rate. This equation can be simply solved as

$$\forall x \in [0, L(t)], \quad y(x,t) = y(L(t-\delta(x,t)), t-\delta(x,t))e^{-\frac{\eta}{v_{cm}}[L(t-\delta(x,t))-x]}$$

in which the time-varying propagation time δ is implicitly defined as $\delta(x,t) = \frac{L(t-\delta(x,t))-x}{v_{CM}}$, because the speed of propagation v_{CM} is constant. Finally, a simple flow balance gives variations of the level L

$$\dot{L}(t) = \frac{u_{int} + u_{rec} - u_{out}}{A}$$

Recirculated matter flow

The output is recirculated only if the final size is greater than the critical value y_{lim}, i.e.

$$w(0,t) = \begin{cases} y(0,t) & \text{if} \quad y(0,t) > y_{lim} \\ 0 & \text{otherwise} \end{cases}$$

Boundary condition

Following the definition of the size introduced above, one can express the input elements size as a weighted average of the input flows

$$y(L,t) = \begin{cases} y_{in} & \text{if} \quad u_{rec} = 0 \\ \dfrac{u_{int}(t) + u_{rec}(t)}{\frac{u_{in}}{y_{in}} + \frac{u_{rec}}{y_{rec}}} & \text{otherwise} \end{cases}$$

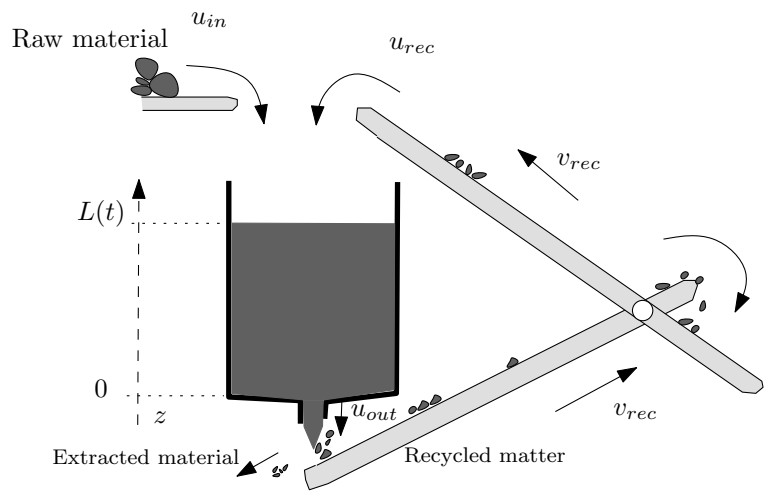

Figure A.4: Schematic view of the crushing system considered.

Table A.1: Variables used in the crushing mill model

A	Equivalent area of the mill
L	Height of the mill
L_{rec}	Height of the tread mill
u_{in}	Input flow rate
u_{out}	Output flow rate
u_{rec}	Input recirculated flow rate
v_{CM}	Propagation speed into the mill
v_{rec}	Speed of the tread mill
$w(z,t)$	Distributed size of the elements over the tread mill
$y(x,t)$	Distributed size into the mill
y_{in}	Size of the input product
δ	Time of propagation through the mill
η	Crushing efficiency of the mill

where the recirculated flow and size are related to the past values of the output conveyor belt speed and size via a delay

$$u_{rec}(t) = u_{out}(t)\frac{v_{rec}(t)}{v_{rec}(t - D(t))} \quad \text{and} \quad y_{rec}(t) = w(0, t - D(t))$$

This delay can be defined through the following implicit integral equation of the conveyor belt speed

$$\int_{t-D(t)}^{t} v_{rec}(s) = L_{rec}$$

A.2.2 Lumped model

In this section, we focus on the design of an average model that satisfies a more simple dynamics than the one presented above. With this aim, we define the average size as

$$Y(t) = \frac{1}{L(t)} \int_0^L e^{-\eta x} y(x, t) dx$$

Taking a time derivative of this quantity, using (A.5) and using integration by parts, one can show that this variable satisfies

$$\begin{aligned}\dot{Y}(t) =& -\frac{\dot{L}(t)}{L(t)} Y(t) + \frac{\dot{L}(t) + v_{CM}}{L(t)} e^{-\eta L} y(L, t) - \frac{v_{CM}}{L(t)} y(0, t) \\ =& -\frac{u_{in} + u_{rec}(t) - u_{out}}{V(t)} Y(t) + \frac{u_{in} + u_{rec}(t)}{V(t)} e^{-\eta L} y(L, t) - \frac{u_{out}}{V(t)} y(0, t)\end{aligned}$$

By approximating $y(0, t) \approx Y(t)$ and defining the input composition as $y_{in}(t - D(t)) = e^{-\eta L} y(L, t)$, the dynamics of the average variable Y can be rewritten as

$$\dot{Y}(t) = \frac{u_{in} + u_{rec}(t)}{V(t)} \left[-Y(t) + y_{in}(t - D(t))\right]$$

From this, the link to the bath model presented in Chapter 11 is obvious. Therefore, a similar control strategy can be reasonably applied.

Appendix B

Proof of Halanay-type stability results for DDEs

The DDE stability results used in Chapter 10 are instrumental to derive sufficient conditions for delay compensation. Here, we prove these results.

As before, a function x_t is defined over a given interval $[-\overline{D}, 0]$ (with $\overline{D} > 0$) as $x_t(s) = x(t+s)$ for a given function $x \in \mathcal{C}([-\overline{D}, 0], \mathbb{R})$ and $t \in \mathbb{R}$.

We first recall the original Halanay inequality[1]. Its proof can be found for example in the original paper [Halanay 66] and is also given in [Ivanov 02].

Lemma B.0.1

(Halanay inequality) Consider a positive, continuous, real-value function x such that, for some $t_0 \in \mathbb{R}$,

$$\dot{x}(t) \leq -ax(t) + b \max x_t\,, \quad t \geq t_0$$

with $a \geq b \geq 0$. Then there exists $\gamma \geq 0$ such that

$$\forall t \geq t_0\,, \quad x(t) \leq \max x_{t_0} e^{-\gamma(t-t_0)}$$

B.1 Extension to first-order scalar DDE stability

A straightforward extension of the Halanay inequality is stated below. This relies on a maximum property applied to a functional in the equation second-term. This property enables us to relate the dynamics considered to the aforementioned inequality, but is quite demanding. Therefore, we also propose a local version of this result.

[1] More precisely, in [Halanay 66], this result is stated for $a > b > 0$.

Lemma B.1.1

Consider a DDE of the form

$$\begin{cases} \dot{x}(t) & + & ax(t) + bh(t, x_t) = 0\,, \quad t \geq t_0 \\ x_{t_0} & = & \psi \in \mathcal{C}^0([-\overline{D}, 0], \mathbb{R}) \end{cases} \tag{B.1}$$

where the continuous functional h satisfies the sup-norm relation

$$|h(t, x_t)| \leq \max |x_t|$$

Then if $a \geq b \geq 0$, there exists $\gamma \geq 0$ ($\gamma = 0$ if $a = b$ and $\gamma > 0$ otherwise) such that every solution of (B.1) *satisfies*

$$\forall t \geq t_0\,, \quad |x(t)| \leq \max |x_{t_0}| e^{-\gamma(t-t_0)} \tag{B.2}$$

Proof: Consider x a non-trivial continuous solution of (B.1)[2], which satisfies the inequality

$$\frac{d|x(t)|}{dt} + a|x(t)| \leq b \max |x_t| \quad \text{provided } |x(t)| \neq 0$$

Following the proof of [Halanay 66], define $y(t) = ke^{-\gamma(t-t_0)}$, with $k > 0$ and γ chosen such that y satisfies the corresponding differential equation[3]

$$\dot{y}(t) = -\,ay(t) + b \max y_t\,, \quad t \geq t_0$$

We now define the difference $z = y - |x|$, which is a continuous function; we are interested in its sign change. We choose $k > \max |x_{t_0}|$ to ensure that $z(t_0) > 0$ for $t \in [t_0 - \overline{D}, t_0]$. Since the function z is continuous, we define

$$t_1 = \inf \{t > t_0 | z(t) = 0\} \in \mathbb{R} \cup \{\infty\}$$

Assume that $t_1 < \infty$. Then $|x(t_1)| = y(t_1) > 0$ by the analytic expression of y. By continuity, there exists an open set $]a_1, b_1[$ such that $t_1 \in]a_1, b_1[$ and $|x(t)| > 0$ for $t \in]a_1, b_1[$. Consequently, z is continuously differentiable on $]a_1, b_1[$ and satisfies

$$\forall t \in]a_1, b_1[\,, \quad \dot{z}(t) + az(t) \geq b\,(\max y_t - \max |x_t|)$$

Then $\dot{z}(t_1) \geq \max y_{t_1} - \max |x_{t_1}| > 0$ by the definition of t_1. However, one has

$$\dot{z}(t_1) = \lim_{t \to t_1^-} \frac{z(t) - z(t_1)}{t - t_1} = \lim_{t \to t_1^-} \frac{z(t)}{t - t_1} \leq 0 \text{ as } z(t) \geq 0 \text{ on } [t_0, t_1]$$

We finally conclude that $t_1 = \infty$. Then $\forall t \geq t_0\,, z(t) > 0$ and

$$\forall \epsilon > 0 \quad \forall t \geq t_0 \quad |x(t)| < (\max |x_{t_0}| + \epsilon) e^{-\gamma(t-t_0)}$$

which gives the result. ■

We now state a local version of the previous lemma.

[2] The continuity (and even more) is obtained by assuming ϕ smooth enough.

[3] $\gamma \geq 0$ is the unique solution on $[0, \infty[$ of $a - \gamma = be^{\gamma \overline{D}}$.

Corollary B.1.1

Consider a DDE of the form

$$\begin{cases} \dot{x}(t) &+& ax(t) + bh(t, x_t) = 0\,, \quad t \geq t_0 \\ x_{t_0} &=& \psi \in \mathcal{C}^0([-\overline{D}, 0], \mathcal{V}) \end{cases} \tag{B.3}$$

where h is a continuous functional satisfying, on an open neighborhood V of the origin, the sup-norm relation

$$\forall x_t : [-\bar{D}, 0] \mapsto \mathcal{V}\,, \quad |h(t, x_t)| \leq \max|x_t| \tag{B.4}$$

If the initial value ψ has values in $\mathcal{V}$ and if $a \geq b \geq 0$, then there exists $\gamma \geq 0$ ($\gamma = 0$ if $a = b$ and $\gamma > 0$ otherwise) such that every solution satisfies

$$\forall t \geq t_0\,, \quad |x(t)| \leq \max|x_{t_0}| e^{-\gamma(t-t_0)} \tag{B.5}$$

Proof: The essence of the proof is similar to that of Lemma B.1.1. Consider again a non-trivial solution x such that $x_{t_0} : [-\overline{D}, 0] \mapsto \mathcal{V}$ and $y(t) = ke^{-\gamma(t-t_0)}$ s. t.

$$\dot{y}(t) = -\,ay(t) + b \max y_t \text{ for } t \geq t_0$$

and $z = y - |x|$ with $z(t_0) > 0$.

Define again $t_1 = \inf\{t > t_0 | z(t) = 0\} \in \mathbb{R} \cup \{\infty\}$. If $k > \max|x_{t_0}|$ and $k \in \mathcal{V}$ (k always exists as $\mathcal{V}$ is an open set by assumption), one can ensure that $x(t) \in \mathcal{V}$ for $t \in [t_0, t_1]$ from the fact that $y(t) \in \mathcal{V}$, for $t \in [t_0, t_1]$. Then $\forall t \geq t_0 \quad z(t) > 0$ and the result directly follows. ■

B.2 Stability analysis for scalar DDEs of order n

Lemma B.2.1

Let x be a solution of the n^{th} order DDE

$$\begin{cases} x^{(n)} + \alpha_{n-1}x^{(n-1)} + \ldots + \alpha_0 x = c\ell(t, x_t, \ldots x_t^{(n-1)})\,, \; t \geq t_0 \\ x_{t_0} = \psi \in \mathcal{C}^0([-\overline{D}, 0], \mathcal{V}) \end{cases}$$

where the left-hand side of the differential equation defines a polynomial which roots have only strictly negative real parts, $c > 0$, ℓ is a continuous functional and $\mathcal{V}$ is a neighborhood of the origin for which ℓ satisfies the sup-norm relation

$$\forall t \geq t_0\,, \quad |\ell(t, x_t, \ldots, x_t^{(n-1)})| \leq \max|X_t|$$

with $X = [x \quad \dot{x} \ldots x^{(n-1)}]^T$. Then there exists $c_{max} > 0$ such that, provided $0 \leq c < c_{max}$, there exist $\gamma > 0$ and $r > 0$ ($r = 1$, $c_{max} = \alpha_0$ if $n = 1$) such that

$$\forall t \geq 0\,, \quad |X(t)| \leq r \max|X_{t_0}| e^{-\gamma(t-t_0)}$$

Proof: The idea is to use the scalar result of Corollary B.1.1. Define the scalar-valued function $m(t) = X^T P X$, where P is the symmetric positive definite matrix solution of the Lyapunov equation $A^T P + PA = -Q$ for some given symmetric positive definite matrix Q and A_0 is the companion matrix

$$A_0 = \begin{pmatrix} 0 & 1 & & \\ \vdots & & \ddots & \\ 0 & & & 1 \\ -\alpha_0 & -\alpha_1 & \dots & -\alpha_{n-1} \end{pmatrix}$$

Taking a time derivative of m, one can obtain

$$\begin{aligned} \dot{m}(t) =& - X^T(t) Q X(t) + 2X(t)^T P \begin{pmatrix} 0 \\ \vdots \\ 0 \\ c\ell(t, x_t, \dots, x_t^{(n-1)}) \end{pmatrix} \\ \leq& - \frac{\underline{\lambda}(Q)}{\overline{\lambda}(P)} m(t) + 2c\overline{\lambda}(P)|X(t)||\ell(t, x_t, \dots, x_t^{(n-1)})| \end{aligned}$$

Then,

$$\dot{m}(t) + \frac{\underline{\lambda}(Q)}{\overline{\lambda}(P)} m(t) \leq \frac{2c\overline{\lambda}(P)}{\sqrt{\underline{\lambda}(P)}} \sqrt{m(t)} |\ell(t, x_t, \dots, x_t^{(n-1)})|$$

Defining $a = \frac{\underline{\lambda}(Q)}{\overline{\lambda}(P)}$ and $b = 2c\frac{\overline{\lambda}(P)}{\underline{\lambda}(P)}$ and

$$h(t, m_t, \dots, m_t^{(n-1)}) = \sqrt{\underline{\lambda}(P)} \sqrt{m(t)} |\ell|$$

which satisfies the following over the neighborhood $\mathcal{V}$

$$|h(t, m_t, \dots, m_t^{(n-1)})| \leq \sqrt{m(t)} \max \sqrt{m_t} \leq \max m_t$$

Applying Corollary B.1.1, one can conclude that, if m_{t_0} has values in $\mathcal{V}$ and if $a > b$, then there exists $\gamma > 0$ such that

$$\forall t \geq t_0 \,, \quad m(t) \leq \max m_{t_0} e^{-\gamma(t-t_0)}$$

or

$$\forall t \geq t_0 \,, \quad |X(t)| \leq \sqrt{\frac{\overline{\lambda}(P)}{\underline{\lambda}(P)}} \max |X_{t_0}| e^{-\gamma(t-t_0)/2}$$

Finally, the condition $a > b$ can be reformulated as $c < \frac{\underline{\lambda}(P)\underline{\lambda}(Q)}{2\overline{\lambda}(P)^2} = c_{max}$ which concludes the proof. ■

Appendix C

Low-Pressure EGR control

Here we describe the design of an open-loop estimate of the intake burned gas rate and a control strategy that exploits this estimate. The open-loop estimate is computed based on the delay calculation procedure presented in Chapter 9. Details on the architecture of low-pressure EGR systems and this issue involved are also presented in Chapter 9.

Two different engine set-ups are considered here. The first set-up uses a sensor of the intake air mass flow rate while the second set-up assumes that a differential pressure sensor is located at the EGR valve. Experiments on a test bench underline the relevance of the proposed control strategy.

C.1 Dilution dynamics and transport delay

Defining x_{lp} as the burned gas rate upstream of the compressor, the EGR dynamics can be expressed as

$$\begin{cases} \dot{x}_{lp} = \alpha \left[-(F_{egr}(t) + F_{air}(t)) x_{lp}(t) + F_{egr}(t) \right] & \text{(C.1)} \\ x(t) = x_{lp}(t - D(t)) & \text{(C.2)} \end{cases}$$

The delay $D(t)$ between the ratio upstream of the compressor and the intake composition can be implicitly defined by the following integral equation

$$\int_{t-D(t)}^{t} v_{gas}(s) ds = L_P$$

where L_P is the pipe length from the compressor to the intake manifold and v_{gas} is the gas speed.

Following the presented model (C.1)–(C.2), the intake burned gas fraction is the result of first order dynamics coupled with a transport delay.

Open-loop estimation of the intake manifold burned gas rate proceeds in two steps:

- open-loop estimation of the low-pressure burned gas ratio, designed below; and
- estimation of the transport measurement delay, exploiting the integral form above and the perfect gas law. This step is presented in Chapter 9.

C.2 Flow rate model and corresponding low-pressure burned gas estimate

To compute an open-loop estimation of (C.1), mass flow rate information is needed. We first provide a model of the gas mass flow rate downstream of the compressor before describing its use in design of the burned gas ratio estimate.

C.2.1 In-cylinder and downstream compressor mass flow rates

We use the model of in-cylinder gas mass presented in [Leroy 09] to define mass flow rates. In this model, F_{asp} is represented as a function of the engine speed N_e, the manifold pressure P_{int} and the intake and exhaust VVT actuators positions. Using the ideal gas law, this flow rate is dynamically related to flow rates through the throttle and downstream of the compressor according to

$$F_{thr} = F_{asp}(N_e, P_{int}, VVT) + \frac{V_{int}}{rT_{int}}\dot{P}_{int} \tag{C.3}$$

$$F_{dc} = F_{thr} + \frac{V_{dc}}{rT_{dc}}\dot{P}_{dc} \tag{C.4}$$

where $r = r_{air} = r_{bg}$ is the (common) ideal gas constant. The variables used in these two last equations are either known or measured.

C.2.2 Low-pressure burned gas ratio model

Only the mass flow rate F_{egr} remains to be modeled in (C.1). We distinguish two cases, depending on the sensors used.

Intake mass air flow sensor Neglecting the mis-synchronization of the flows signals, we simply write (with a projection operator forcing the flow rate to be zero when the valve is closed)

$$\hat{F}_{egr}(t) = \text{Proj}_{\theta_{egr}>0}\{F_{dc}(t) - F_{air}(t)\} \tag{C.5}$$

The low-pressure burned gas ratio can then be estimated as the solution of the dynamics

$$\dot{\hat{x}}_{lp} = \alpha[-F_{dc}(t)\hat{x}_{lp}(t) + \hat{F}_{egr}(t)]$$

correctly initialized to zero when the EGR valve is closed. In this last equation, the constant α is known.

Differential pressure sensor The EGR mass flow rate can be assumed as sub-critical and modeled as [Heywood 88]

$$\begin{cases} F_{egr} = S_{valve}\psi(P_{uv}) & \text{(C.6)} \\ \psi(P_{uv}) = \dfrac{P_{uv}}{\sqrt{RT_{uv}}}\left(\dfrac{P_{atm}}{P_{uv}}\right)^{1/\gamma}\sqrt{\dfrac{2\gamma}{\gamma-1}\left(1-\left(\dfrac{P_{atm}}{P_{uv}}\right)^{\frac{\gamma-1}{\gamma}}\right)} & \text{(C.7)} \end{cases}$$

where S_{valve} is the effective opening area of the EGR valve, P_{uv} is the upstream valve pressure, obtained from atmospheric pressure and differential pressure sensor measurements

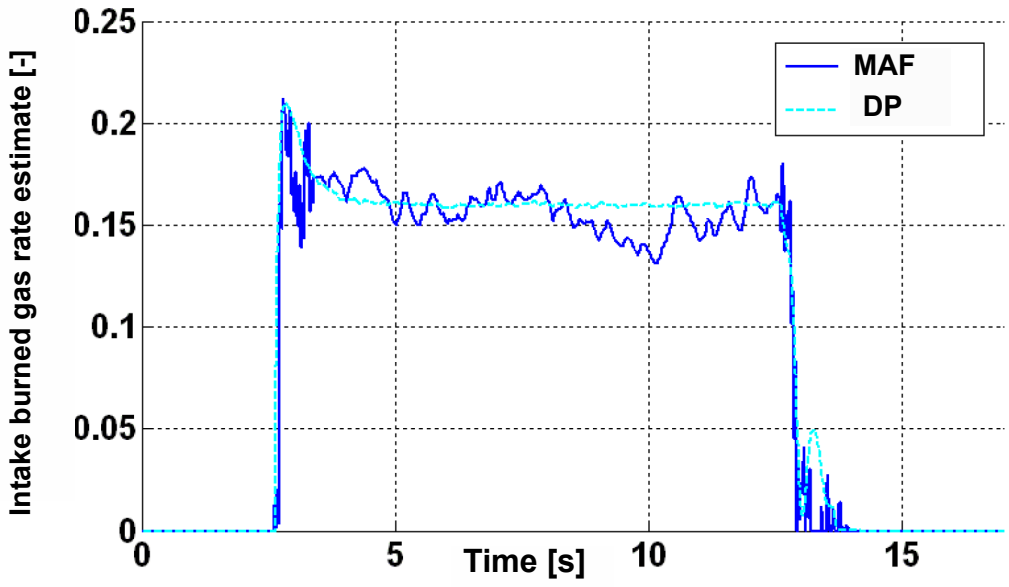

Figure C.1: Intake burned gas ratio estimate obtained with a MAF sensor (in cyan) and with a differential pressure sensor (in blue) for a given operating point (engine speed 2000 rpm and intake manifold pressure 1.2 bar).

(ΔP, which gives $P_{uv} = \Delta P + P_{atm}$) and γ is the ratio of specific heat. The effective area is itself statically related to the angular position of the actuator.

In practice, an alternative linearized model may be needed to account for the potential low values of the differential of pressure ΔP, which result into a pressure ratio P_{atm}/P_{uv} close to the unity.

Because the constant α is known, an estimate of the low-pressure burned gas rate is then simply

$$\dot{\hat{x}}_{lp} = \alpha[-F_{dc}(t)\hat{x}_{lp}(t) + F_{egr}(t)] \tag{C.8}$$

C.2.3 Experimental validation of the intake burned gas estimate

For experiments, the proposed estimation strategy was embedded into a real-time control target and tested on a test-bench. The aim of the experiments was to validate both model (C.1)–(C.2) and the corresponding estimation strategy presented above.

Experimental results are presented in Section 9.3, where the low-pressure estimate is not presented. These estimates are pictured in Figure C.1. In both instrumentation cases, the accuracy of the intake burned gas ratio is highlighted by the experimental results provided in Section 9.3.

C.3 Low-pressure burned gas rate control

The model (C.1)-(C.2)is an output-delay system, where the delay is time-varying. Consequently, due to this particular form, we propose here to directly control the low-pressure intake-burned gas rate x_{lp}, through a feedforward approach. This approach is based on steady-state pressure profile considerations.

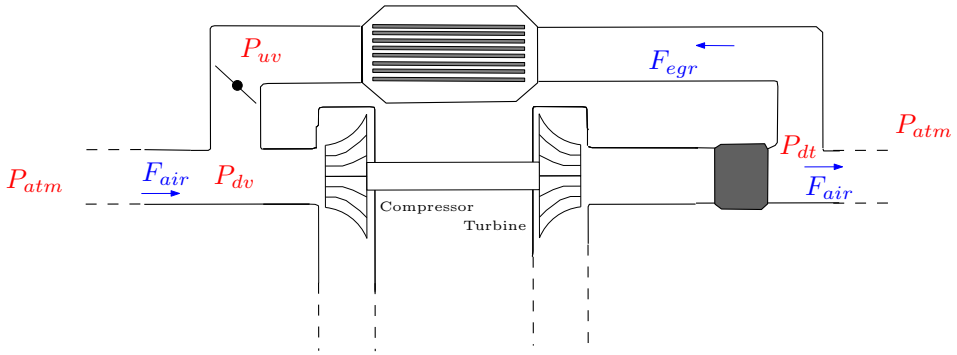

Figure C.2: Schematic view of the pressures and mass flow rates involved in the head losses balances.

C.3.1 Head losses balance at steady-state

At steady-state, first-order head losses balances of, respectively, the intake line, the exhaust line and the EGR circuit yield

$$\begin{aligned} P_{atm}^2 - P_{dv}^2 &= f_1(F_{air}) \\ P_{atm}^2 - P_{dt}^2 &= f_2(F_{air}) \\ P_{dt}^2 - P_{uv}^2 &= f_3(F_{egr}) \end{aligned}$$

Namely, the pressure drops along the considered pipe segments are simply written at first order as functions of the flowing mass flow rate, neglecting mainly the temperature influence.

Matching the terms involved in these three equations and writing a first-order approximation give the steady-state relation expressed in terms of the burned gas rate set-point x_{sp}

$$\Delta P = P_{uv} - P_{dv} = g(F_{air}, F_{egr}) = g(F_{air}, x_{sp})$$

This relation is then exploited to provide a feedforward control strategy.

C.3.2 EGR mass flow rate set-point and corresponding low-order control law

From there, considering the EGR mass flow rate model (C.6)-(C.7), one can directly obtain the following EGR valve set-point

$$\begin{aligned} F_{egr}^{sp} &= x_{sp} F_{dc} \\ \theta_{egr}^{sp} &= S_{valve}^{-1} \left(\frac{F_{egr}^{sp}}{\psi(g(P_{atm} + g(F_{air}, x_{sp})))} \right) \end{aligned}$$

where the total gas mass flow downstream of the turbine F_{dc} is modeled in (C.4) and the function ψ in (C.7). The function S_{valve} is a known 1D-look-up table which characterizes the EGR valve and is invertible. Correspondingly, the EGR valve set-point can be compactly expressed under the form

$$\theta_{egr}^{sp} = g(F_{air}, x_{sp}) \tag{C.9}$$

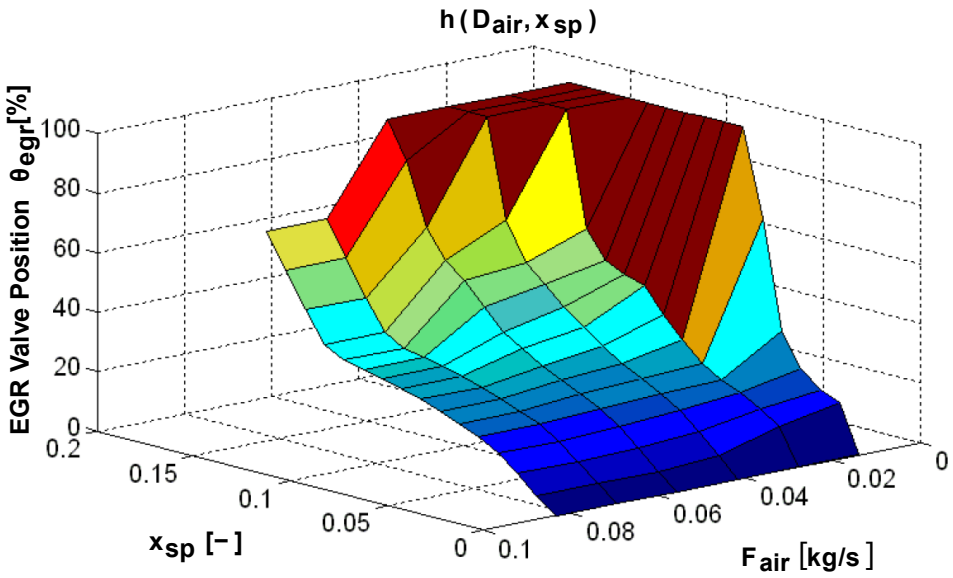

Figure C.3: Schematic view of the pressures and mass flow rates involved in the head losses balances.

Experiments were conducted at test-bench to identify this function g which is pictured in Figure C.3 for the operating range of the considered engine (Renault F5Rt).

To account for the potential inaccuracies of this map, or modifications due e.g. to devices aging, the final employed control law includes an integral error of the estimate low-pressure burned gas rate

$$\theta_{egr}^{sp} = g\left(F_{air}, x_{sp} + k_I \int_0^t [x_{sp} - \hat{x}_{lp}(s)]ds\right) \tag{C.10}$$

C.3.3 Experimental results

To validate the proposed control law, experiments were conducted at test bench. Figure C.4 reports the results corresponding to a torque transient from 8 bar to 12 bar occurring after $t = 2$s. As in Chapter 9, the engine under consideration is a Renault F5Rt $1.8L$ four cylinder SI engine with direct injection, and an air path consisting in a turbocharger, an intake throttle, an intercooler and a low-pressure EGR loop. For this engine, *no real-time information of the intake burned gas fraction is available* and therefore no data is provided here. Yet, the validity of the proposed estimates has been highlighted by the open-loop response of the FAR (see Chapter 9 for details).

Figure C.4(a) consists in the intake burned gas rate estimates obtained respectively with (C.9) (in blue) and with (C.10) (in red), compared with an intake burned gas rate trajectory (in black) obtained as a delay version of the low-pressure trajectory (black dotted). One can observe on Figure C.4(c) that the main contribution of the control law is achieved by the feedforward term (C.9). Yet, the action of the integral term added in (C.10) is decisive to track the given reference as it is noticeable in Figure C.4(a). It is worth noticing that the torque transient, indirectly represented in Figure C.4(b) with the intake pressure variations, is particularly challenging and that the obtained performances are therefore representative of the ones that could be expected on real driving conditions.

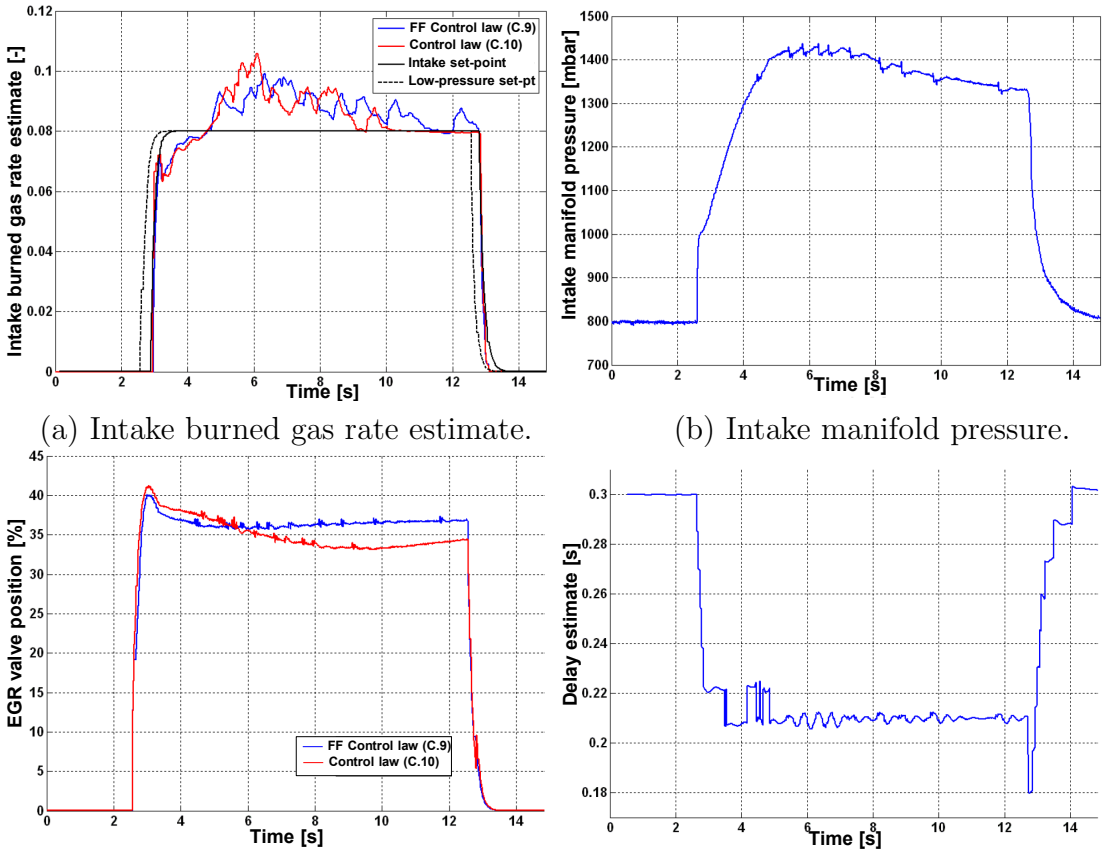

(a) Intake burned gas rate estimate.

(b) Intake manifold pressure.

(c) EGR valve position.

(d) Delay estimate.

Figure C.4: Torque variation (IMEP step from 8 bar to 12 bar) for a constant engine speed of 2000 rpm, resulting into an intake burned gas rate set-point change. The EGR valve control is realized for both control laws (C.9) and (C.10).

Commande robuste de systèmes à retard variable. Contributions théoriques et applications au contrôle moteur.

Résumé: Cette thèse étudie la compensation robuste d'un retard de commande affectant un système dynamique. Pour répondre aux besoins du domaine applicatif du contrôle moteur, nous étudions d'un point de vue théorique des lois de contrôle par prédiction, dans les cas de retards incertains et de retards variables, et présentons des résultats de convergence asymptotique. Dans une première partie, nous proposons une méthodologie générale d'adaptation du retard, à même de traiter également d'autres incertitudes par une analyse de Lyapunov-Krasovskii. Cette analyse est obtenue grâce à une technique d'ajout de dérivateur récemment proposée dans la littérature et exploitant une modélisation du retard sous forme d'une équation à paramètres distribués. Dans une seconde partie, nous établissons des conditions sur les variations admissibles du retard assurant la stabilité du système boucle fermée. Nous nous intéressons tout particulièrement à une famille de retards dépendant de la commande (retard de transport). Des résultats de stabilité inspirés de l'ingalité Halanay sont utilisés pour formuler une condition de petit gain permettant une compensation robuste. Des exemples illustratifs ainsi que des résultats expérimentaux au banc moteur soulignent la compatibilité de ces lois de contrôle avec les impératifs du temps réel ainsi que les mérites de cette approche.

Mots clés: Systèmes à retard, systèmes à paramètres distribués, contrôle moteur, ajout de dérivateur, control adaptatif, analyse de Lyapunov, contrôle robuste, équations différentielles à retard

---

Robust control of variable time-delay systems. Theoretical contributions and applications to engine control.

Abstract: This thesis addresses the general problem of robust compensation of input delays. Motivated by engine applications, we theoretically study prediction-based control laws for uncertain delays and time-varying delays. Results of asymptotic convergence are obtained. In a first part, a general delay-adaptive scheme is proposed to handle uncertainties, through a Lyapunov-Krasovskii analysis induced by a backstepping transformation (applied to a transport equation) recently introduced in the literature. In a second part, conditions to handle delay variability are established. A particular class of input-dependent delay is considered (transport). Halanay-like stability results serve to formulate a small-gain condition guaranteeing robust compensation. Illustrative examples and experimental results obtained on a test bench assess the implementability of the proposed control laws and highlight the merits of the approach.

Keywords: Time-delay systems, distributed parameter systems, engine control, backstepping, adaptive control, Lyapunov design, robust control, delay differential equations

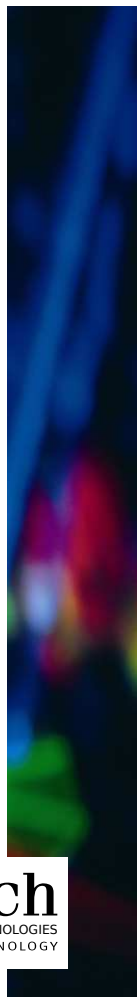

MINES ParisTech

ParisTech
INSTITUT DES SCIENCES ET TECHNOLOGIES
PARIS INSTITUTE OF TECHNOLOGY